APRIL 2017

Ph.D in Civil Engineering

IHSAN TAHA KADHIM

UNIVERSITY OF GAZİANTEP

GRADUATE SCHOOL OF

NATURAL & APPLIED SCIENCES

PROPERTIES OF SELF-COMPACTING RECYCLED AGGREGATE CONCRETE AND ITS IMPACT ON STRUCTURAL BEHAVIOR OF COMPOSITE TUBE COLUMNS

Ph.D THESIS

IN

CIVIL ENGINEERING

BY

IHSAN TAHA KADHIM

APRIL 2017

Properties of Self-Compacting Recycled Aggregate Concrete and its Impact on Structural Behavior of Composite Tube Columns

Ph.D. Thesis

in

Civil Engineering

University of Gaziantep

Supervisor

Assoc. Prof. Dr. Esra METE GÜNEYİSİ

by

Ihsan Taha KADHIM

April 2017

REPUBLIC OF TURKEY
UNIVERSITY OF GAZİANTEP
GRADUATE SCHOOL OF NATURAL & APPLIED SCIENCES
CIVIL ENGINEERING DEPARTMENT

Name of the thesis: Properties of Self-Compacting Recycled Aggregate Concrete and Its Impact on Structural Behavior of Composite Tube Columns

Name of the student: Ihsan Taha KADHIM

Exam date: 06.04.2017

Approval of the Graduate School of Natural and Applied Sciences

Prof. Dr. Ahmet Necmeddin YAZICI
Director

I certify that this thesis satisfies all the requirements as a thesis for the degree of Doctor of Philosophy.

Prof. Dr. Abdulkadir ÇEVİK
Head of Department

This is to certify that we have read this thesis and that in our opinion it is fully adequate, in scope and quality, as a thesis for the degree of Doctor of Philosophy.

Assoc. Prof. Dr. Esra METE GÜNEYİSİ
Supervisor

Examining Committee Members:	Signature
Prof. Dr. Mustafa GÜNAL	------------------------
Prof. Dr. Hanifi ÇANAKCI	------------------------
Assoc. Prof. Dr. Esra METE GÜNEYİSİ	------------------------
Assoc. Prof. Dr. Kasım MERMERDAŞ	------------------------
Assist. Prof. Dr. Volkan KALPAKCI	------------------------

I hereby declare that all information in this document has been obtained and presented in accordance with academic rules and ethical conduct. I also declare that, as required by these rules and conduct, I have fully cited and referenced all material and results that are not original to this work.

Ihsan Taha KADHIM

ABSTRACT

PROPERTIES OF SELF-COMPACTING RECYCLED AGGREGATE CONCRETE AND ITS IMPACT ON STRUCTURAL BEHAVIOR OF COMPOSITE TUBE COLUMNS

KADHIM, IHSAN TAHA

Ph.D. in Civil Engineering

Supervisor: Assoc. Prof. Dr. Esra METE GÜNEYİSİ

April 2017

176 Pages

This thesis mainly consists of two parts. First part covers the material characterization of recycled aggregate self-compacting concrete in terms of fresh, mechanical and fracture responses; while the second part of the thesis presents the research results on the structural behavior of the axially loaded steel tube columns filled with such concretes. Study parameters included single and combined uses of recycled fine and coarse aggregates, substitution levels, compressive strength of concrete core, cross section slenderness (D/t ratio) and yield strength of steel tube. To this aim, the hardened concrete properties were evaluated in terms of compressive strength, splitting tensile strength, static modulus of elasticity and net flexural strength. Failure mechanism of the notched concrete beams was also monitored via three-point bending test to observe the ductility level with respect to the fracture parameters. The statistical analysis based on GLM-ANOVA was also performed to assess the significance of the test parameters. Furthermore, comparison and code assessment for the axial load carrying capacity of the recycled aggregate concrete filled steel tube composite columns were studied by using four different design code equations (American Concrete Institute (ACI), Eurocode 4 (EC 4), Architecture Institute of Japan (AIJ) and Chinese Design Code for Steel-Concrete Composite Structures (DL/T)).

Keywords: Concrete filled steel tube column; Fracture characteristics; Load carrying capacity; Mechanical property; Recycled aggregate concrete.

ÖZET

GERİ KAZANILMIŞ AGREGALI KENDİLİĞİNDEN YERLEŞEN BETONUN ÖZELLİKLERİ VE KOMPOZİT TÜP KOLONLARIN YAPISAL DAVRANIŞLARINDAKİ ETKİSİ

KADHIM, IHSAN TAHA

Doktora Tezi, İnşaat Mühendisliği Bölümü

Tez Yöneticisi: Doç. Dr. Esra METE GÜNEYİSİ

Nisan 2017

176 Sayfa

Bu tez temel olarak iki kısımdan oluşmaktadır. İlk kısmı, geri kazanılmış agrega ile üretilen kendiliğinden yerleşen betonun taze, mekanik ve kırılma tepkileri açısından malzeme özellikleri, ikinci kısmı ise, bu tür beton dolgulu çelik boru kompozit kolonların eksenel yük altındaki yapısal davranışları üzerine araştırma sonuçlarını içermektedir. Çalışma parametreleri, geri kazanılmış ince ve iri agregaların yalnız ve beraber farklı oranlarda kullanımı, beton çekirdeğin basınç dayanımı, kesit narinliği (D/t) oranı ve çelik tüpün akma dayanımından oluşmaktadır. Bu amaçla, sertleşmiş beton özellikleri, basınç dayanımı, yarmada çekme dayanımı, elastisite modülü ve net eğilme dayanımı açısından değerlendirilmiştir. Kırılma parametrelerine göre süneklik seviyesini gözlemlemek için çentikli beton kirişlerde üç noktalı eğilme deneyi yapılmıştır. Test parametrelerinin önemi GLM-ANOVA'ya dayanan istatistiksel analiz kullanılarak değerlendirilmiştir. Ayrıca, geri kazanılmış agregalı beton dolgu çelik boru kompozit kolonların eksenel yük taşıma kapasitesi dört farklı tasarım kodu (Amerikan Beton Enstitüsü (ACI), Avrupa Yönetmeliği olan Eurocode 4 (EC 4), Japonya Mimarlık Enstitüsü (AIJ) ve Çelik Beton Kompozit Yapılar için Çin Tasarım Kodu (DL/T)) denklemi kullanılarak incelenmiştir.

Anahtar kelimeler: Beton dolgulu çelik boru kompozit kolon; Kırılma özellikleri; Yük taşıma kapasitesi; Mekanik özellik; Geri kazanılmış agregalı beton.

To My Family

ACKNOWLEDGEMENTS

In the name of Allah, the Most Benevolent, the most Merciful. First of all, I wish to record immeasurable gratitude and thankfulness to the One and The Almighty Creator, the Lord and Sustainer of the mankind and universe, in particular. It is only through His mercy and help that this work could be completed, and it is ardently desired that this little effort be accepted by Him to be of some service to the cause of humanity.

I would like to take this opportunity to express my gratitude to my advisor Assoc. Prof. Dr. Esra METE GÜNEYİSİ for her constant guidance and encouragement. Special thanks to the University of Gaziantep for the real support and the laboratory facilities. I will not forget to thank Assoc. Prof. Dr. Erhan GÜNEYİSİ and Prof. Dr. Mehmet GESOĞLU; for their encouragement, support, advice and caring about my work.

Further, special thanks to Research Asst. Hatice Öznur ÖZ, who was directly or indirectly involved in the process of producing this research report, for her generous assistance. To all my friends, for their support and giving me a suitable environment to study, and for the nice and useful moments I spent with them.

TABLE OF CONTENTS

LIST OF TABLES

LIST OF FIGURES

Page

LIST OF SYMBOLS/ ABREVIATIONS

a	Notch depth of the beam
A	Cross sectional area of the sample
Ac	Cross-sectional area of concrete
ACI	American Concrete Institute
AIJ	Architectural Institute of Japan
AISC	American Institute of Steel Construction
As	Cross-sectional area of steel tube
Asc	Area of composite section
ASR	Alkali-silica reaction
B	Width of the beam
B, C	Constant factors used in DL/T code
CCs	Conventional concretes
CDW	Construction and demolition waste
CFST	Concrete filled Steel Tube
CH	Hydrated lime; Ettringite
CMOD	Crack mouth opening displacement
COV	Coefficient of variations
CSH	Calcium silicate hydrate
D	Outer diameter of the column
Dc	Diameter of the concrete core
DF	Degrees of freedom
DL/T	Chinese Design Code for Steel-concrete Composite Structures
e	Eccentricity of loading
E	The static modulus of elasticity
Ec	Modulus of elasticity of concrete
Ec1	Modulus of elasticity of concrete (normal weight concrete)

Ecm	Secant elastic modulus of concrete
EC4	Eurocode 4
(EI)eff1	Effective stiffness of composite section
(EI)eff2	Effective flexural stiffness for calculation of relative slenderness
Es	Modulus of elasticity of steel
FA	Fly ash
fc, fcu	Mean cube compressive strength
fc'	Compressive strength of standard concrete cylinders ($\Phi 150\times 300$mm)
fck	characteristic strengths of the concrete
FPZ	Fracture process zone
fflex	Net flexural strength
fst	Splitting tensile strength
fscy	Nominal yielding strength of the composite section
fy	Yield stress of steel
g	Gravitational acceleration
GF	Fracture energy
GGBFS	Ground granulated blast furnace slag
h	Height of the cylinder
HPC	High performance concrete
HRWRA	High range water reducer agents
HSC	High strength concrete
ITZ	Interfacial transition zone
Ke	Correction factor=0.6
kic	Critical stress intensity factor
L	Length of the column
LEFM	Linear elastic fracture mechanics
Ic	Moment of inertia of concrete core
lch	Characteristics length
Ik	Effective length of a CFST column
Is	Moment of inertia of steel tube
LVDT	Linear variable displacement transducer
m	Mass of the beam

MEU	Ministry of environment and urbanization
MK	Metakaolin
n	Number of data samples
N	Rotational speed
NA, NAs	Natural aggregates
NCAs	Natural coarse aggregates
N_{cr}	The elastic critical force for the relevant buckling mode
NFAs	Natural fine aggregates
NFM	Nonlinear fracture mechanics
N_{PIR}	The characteristic value of the plastic resistance
Nu, Pu	Ultimate axial load carrying capacity
Pmax	The ultimate load
R	correlation coefficient
Ri	The vane radius
Ro	The outer container radius
RA, RAs	Recycle aggregates
RAC	Recycle aggregate concrete
RASCC	Recycle aggregate self-compacting concrete
RCA, RCAs	Recycle coarse aggregates
RCD	Roller compacted concrete for dam
RCA+RFA	Both grade of recycle aggregate
RFA, RFAs	Recycle fine aggregates
S	Span of the beam
SCC, SCCs	Self-compacting concretes
SCRACs	Self-compacting recycle aggregate concretes
SD	Standard deviation
SF	Silica fume
SIF	Stress intensity factor
SSD	Saturated surface dry condition
SP	Superplasticizers
t	Time, Thickness of steel tube
T	Torque

T_{500mm}	Time required to reach 500 mm slump flow
U	Length of the beam
V	The slope of the line
W	Width of the beam
W0	Area under load-deflection curve
w/b	Water/binder ratio
w/c	Water/cement ratio
WFM	Work-of-fracture method
y	Yield torque
Y	Intercept of the line with torque axis
τ	Shear stress
τ_o	Yield stress
μ	Plastic viscosity
γ'	Shear rate
δs	The specified deflection of the beam
ξ, η	Confinement factor
ηa, ηao	Factors related to the confinement of steel tube
ηc, ηco	Factors related to the confinement of concrete
$\bar{\lambda}$	Relative slenderness

CHAPTER I

INTRODUCTION

1.1 General

Aggregate, which is one of the most significant raw materials used in concrete sector, is produced annually by about 7 tons per person in Europe and by about 4 tons in Turkey. Aggregate in worldwide takes its place as first rank with 58% of the mine production (Öztürk et al., 2007). Hence, the global concrete industry consumes approximately 10 billion tons of aggregates annually. The global consumption after 2010 for natural aggregates (NAs) has been in the range of 8-12 billion tons (Tsung et al., 2006). Moreover, every year over 1 billion ton of construction and demolition waste (CDW) is generated worldwide (Amnon, 2004; Mehta, 2002). Thereby, managing and controlling CDW are the biggest challenge in our country and worldwide. Hence, 13-29% of the CDW is obtained from the solid wastes in urban areas; this ratio may increase to 50% especially in the case of natural disasters such as an earthquake (Öztürk, 2005). Previously, almost all materials which are used in the construction industry were entirely virgin and natural; thus, all wastes from demolished buildings were disposed in landfills and partially in unauthorized places. Consequently, CDW caused environmental and visual pollution as well as large quantity of concrete wastes generated from construction works, modifications, repairs, retrofits and demolishing of structures (Gesoğlu et al., 2004; Safiuddin et al., 2011).

It is crucial to reuse and recycle CDW in order to reduce the environmental pollution and to restrict the consumption of limited natural sources. Therefore, the effective use of these wastes provides interesting economic and environmental aspects. In some parts of the world, the number of production facilities and pilot plants are constructed to produce RAs from concrete wastes. Moreover, standards, guidelines and a lot of researches are published in the literature relating with the use of recycled

CDW (Öztürk, 2005; Öztürk, 2009). The utilization of RAs (created from processing CDW) in new construction has become more significant over the last two decades.

Indeed, the interest in using RAs has developed because there is depletion in the NAs resources; also, alternative aggregates for concrete are needed. In effect, the long distance between the sources of NAs and construction sites and scarceness of aggregate in metropolitan environments force the constructors to find out substituting materials via recycled ones. On the other hand, the removal and disposal of recycled materials such as old concrete often present an environmental problem and that usually occurs in urban environments (Grdic et al., 2010). Thereby, significant ecological problems in urban areas might be expected due to the removal and disposal of CDW. Moreover, it can diminish the environmental pollution and reduce the huge consumption of NAs in construction through recycling wastes materials as RAs (Safiuddin et al., 2011). Thus, recycling is deemed as the best method to improve the environment, not only through reducing the use of virgin aggregate but also by minimizing the landfills. Recycling of CDW can provide a cost-effective method for the construction industry (Kamal et al., 2013).

In Turkey, CDW is mainly generated from developing and modernizing cities, urban renewal plans and risk of earthquake. Hence, about 6-7 million houses are planned to be destroyed and re-built in the forthcoming 20 years according to Ministry of Environment and Urbanization (MEU); thereby, about 500 million tons of CDW are estimated to be generated (MEU, 2013). Therefore, MEU supports the project that defining criteria of recycling and reusing CDW. Actually, the recycling of CDW is important in point of protecting environment, saving the cost of landfilling as well as the lack of land for waste disposal and preservation of NAs resources (Poon et al., 2007).

The lack of codified provision does not signify a prohibition on the use of RAs. Although the European standard for the specification of concrete did not include any provisions for the use of RAs in concrete, the British Standard (BS EN 206-1, 2000; BS 8500-2, 2002) permits the use of RAs. However, provide additional requirements to allow using RAs in concrete. These conditions includes maximum masonry content, level of fine materials, asphalt content, sulfate content, *etc*. In effect, RAs are mainly use in low utility applications such as non-structural or non-bearing partitions. Nowadays, intermediate utility applications such as foundations for building and roads are conducted via utilizing these aggregates. However, with very limited extent, it used in high utility applications such as for elements of buildings or structural layers of roads. Actually, expand the use of RAs is strongly related with the improvement occurred in the quality of this aggregate, which is results from good demolition practice; also, it related with the recycling process itself like sieving and separation. Recently, improved the aggregates quality are available and noticeable at prices competitive to NAs. Nonetheless, utilizing RAs in concrete are still less than ambitious because the negative impression formed when low quality cement and aggregate were used; also, because the restrictions imposed by standards (Dhir, 2001).

Therefore, there is a need for reform the unfavorable impression, which is relatively prevalent for a long time, to increase the use of RAs in concretes. In Turkey, the production of NAs, for both grade of aggregate, is deemed to be high compare to other country referring to high exhaustion of natural sources. As depicted in Figure 1.1, the marginal percentage of reused and/or recycled material can be observed not only in Turkey but also in other parts around the world (UEPG, 2013).

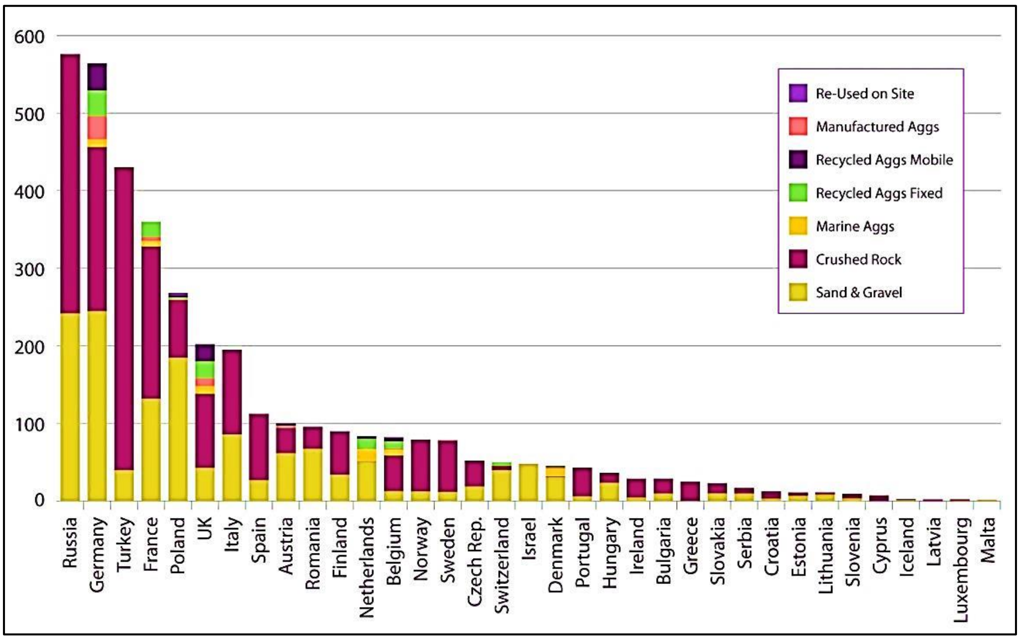

Figure 01.1 Aggregates production (in millions of tons) in 2012 (UEPG, 2013)

In effect, the most effective way to change the passive impression is to increase the performance characteristics of the RAs, which can be achieved via incorporation of other materials like mineral and chemical admixtures to substitute or supplement those conventionally used materials in concrete mixes. Figure 1.2 shows the percentage of consumed RAs around the world (UEPG, 2008).

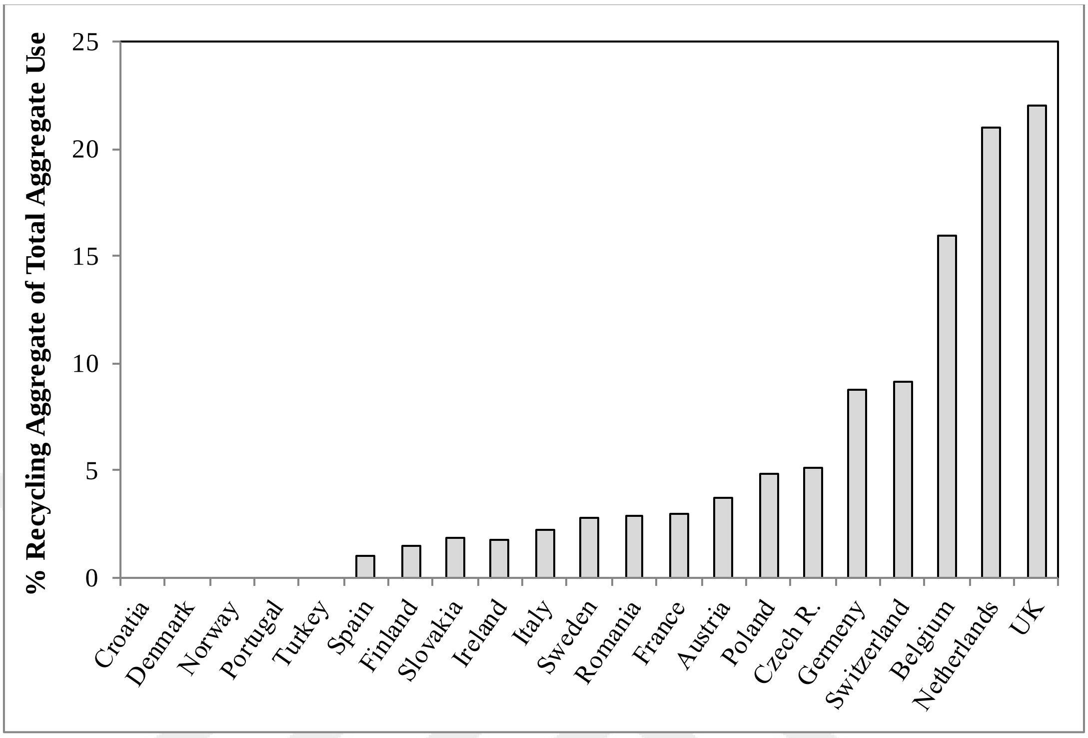

Figure 1.2 Percentage of consumption of RAs according to various countries (UEPG, 2008)

Recently, the world's attention to recycling seemed growing and a comprehensive tendency to maintain the environment by reducing the consumption of non-renewable natural resources like concrete had been spread. In USA, 1800 construction and demolition waste storing plants and 3500 recycling plants are exists; also, 25% of CDW in Europe recycled (Öztürk, 2005). Likewise, in Hong Kong, a pilot plant produced 240000 tons of high quality RAs in 2003 (Raoa et al., 2007). Similarly, about 30 million tons of CDW was recovered by the plants in Taiwan and it was used in the rehabilitation of damaged structures (Huang, 2002). In this regard, the total CDW production and quantities recovery are summarized in Table 1.1 (Klee, 2009).

Table 1.1 Total CDW production and recovery of some countries (Klee, 2009)

Country	CDW (Million tone)	Recovery CDW (Million tone)	Recovery CDW (%)
Australia	14	8	57
Belgium	14	12	86
Canada	N/A	8 (recycled concrete)	N/A
Czech Republic	9 (Include 3 of concrete)	1 (recycled concrete)	45
England	90	46	50-90
France	309	195	63
Germany	201	179	89
Ireland	17	13	80
Japan	77	62	80
Netherlands	26	25	95
Norway	N/A	N/A	50-70
Portugal	4	Minimal	Minimal
Spain	39	4	10
Switzerland	7 (Incl. 2 of concrete)	2	Near 100
Taiwan	63	58	91
Thailand	10	N/A	N/A
USA	317 (Incl. 155 of concrete)	127 (recycled concrete)	82

1.2. Motivations for the Research: Recycling and Concreting Aspects

Recycled aggregates are result from the processing of materials previously used in construction. Generally, it can be classified into two main categories (Wrap, 2007):

- RAs come predominantly from crushed concrete waste
- RAs resulted from the field of CDW materials such as brick-based and asphalt-based aggregate.

The level of contamination in the second category, which is particularly derived from asphalt pavements, is usually medium to high; thereby, it significantly affects the performance of produced concrete. Hence, the second type of aggregates is often used for secondary applications and it has little interest for utilize in concrete. Moreover, the use of this category in concrete actually conflict with the limitation and provisions set in standards such as BS 8500-2 (2002). In this standard, the maximum contaminant material level hinders the use of this aggregate and might be face a rejection by the public and the concrete industry especially in places where there is an abundance of proven NAs. With these limitations, it is most unlikely that concrete suppliers would be able to accept this type of RAs for concrete mixes. For this, this study mainly focus on the utilization of RAs resulted from crushing old concrete masses, which is contains little or no contamination, and produced in a recycling plant. In effect, the major concern leading to the limited use of RAs in concrete always related with the performance issues. Hence, identify the possible sources of weakness of RAs is the essential factor affecting in maximize the use and value of RA in concrete construction as well as structural applications; these are summarized in Figure 1.3.

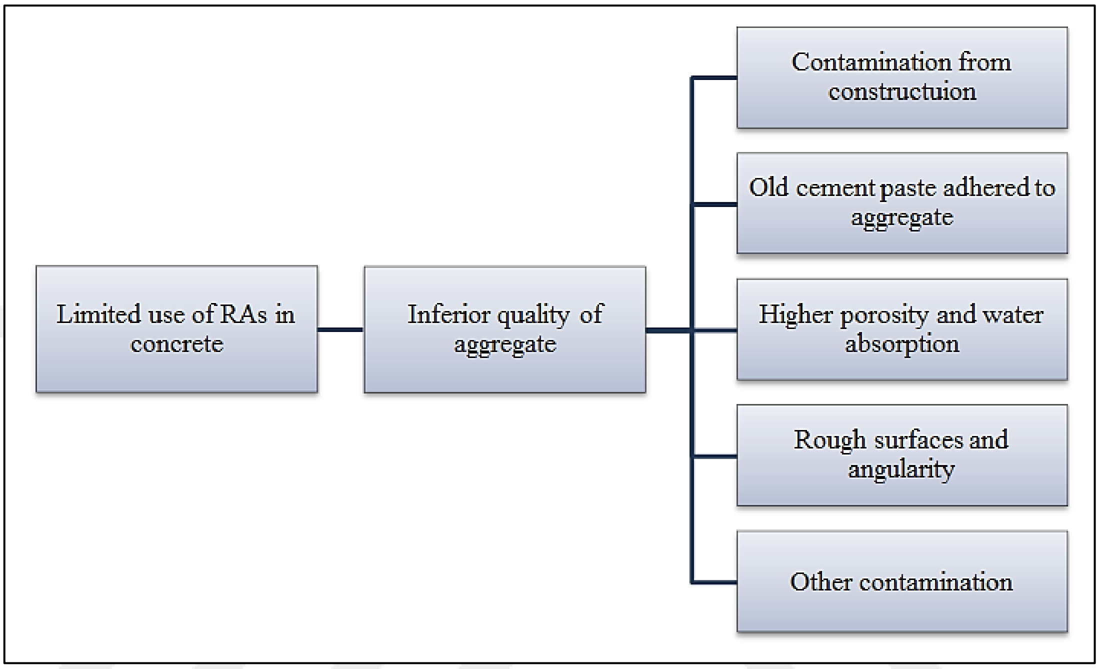

Figure 1.3 Sources of weakness of RAs (Wrap, 2007)

1.3 Use of RAC in Composite Columns and Practical Application in Structures

In general, recycle aggregate concrete (RAC) manufactured via replace NAs with aggregate comes by crushing, washing, grading and blending old concrete and/or CDW materials. For this, the mechanical properties as well as durability aspects of this concrete expect to be lower than in conventional concretes (CCs). Indeed, drawbacks such as low elastic modulus and load carrying capacity recorded for RAC (Wang et al., 2013). These shortcomings limit the usage of RAC in structural applications such as columns, slabs and beams (Topçu and Şengel, 2004; Wang et al., 2013; Chen et al., 2010; Tam et al., 2014). However, RAC seemed well appreciated in the term of low brittleness, low density as well as good thermal insulation (Katz, 2003; Topçu and Şengel, 2004). In this regard, plenty number of previous research emphasized that performance of RAC descends as high as the increase of RA replacement level. However, the axial capacity of RAC elements record little decrease compare with corresponding CCs elements; moreover, RCA still behaves well enough to resist the earthquake attack even with high levels of RA.

In structural construction, the consequences of RAC weakness need to be minimized as much as possible. For this, concrete filled steel tubes (CFST) seem to be suitable choice to enhance the inferior properties of RAC; in which it confine and protect concretes by outer steel tube. Thereby, inherent disadvantages of RAC will significantly decrease or eliminate leading to entire use of the merits of RAC simultaneously. In recent years, the uses of concrete filled steel tubular (CFST) columns are widely increasing for multiple construction members. The field of using RAC in CSFT structural elements seems promising in the future because of it's good features. However, the shortage of information related with the behavior of RAC in structures restricts the deployments of these concretes particularly in composite columns. In the composite columns, the combination between steel tube and concrete core provide combined advantages because the strengths of confined concrete considerably increase due to surrounding by steel as well as preventing or delaying the inward buckling of the steel tube via presence of concrete core (Jegadesh and Jayalekshmi, 2015). The utilizing of RAC as core concrete in a steel tube enhance its properties particularly mechanical aspects due to the confinement of surrounding steel tube. Moreover, the formwork of concrete eliminates due to border it by steel tube; thus, reduces the time of construction (Lu and Zhao, 2010). For this reasons, the field of CFST columns spread to cover new sectors such as bridges, subways and tall buildings (Tsuda et al., 1995; Chen and Chen, 1973; Zeghiche and Chaoui, 2005; Lin, 1998). In this regard, according to the shape of CFST column cross-section, there are several types of the column such as regular section, section with reinforcement, section with double skin tube and encased section as shown in Figure 1.4 (Gore and Kumbhar, 2014). Furthermore, practical application of such column systems in structure is illustrated in Figure 1.5. As seen in Figure 1.5, circular CFST column were used in different types of building (Schnider et al., 2004). Another example for the use of CFST column in a steel-concrete composite column structure is given in Figure 1.6 (Han et al., 2014).

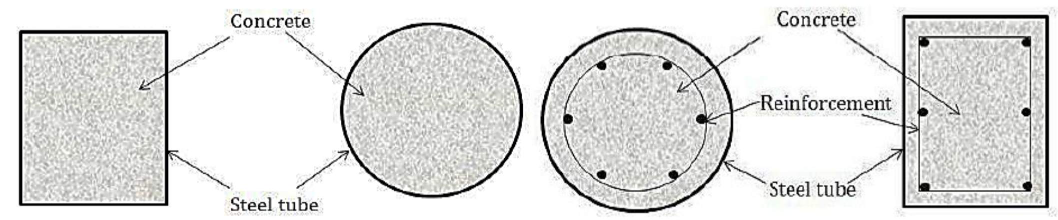

(a) Regular CFST section (b) CFST section with reinforcement

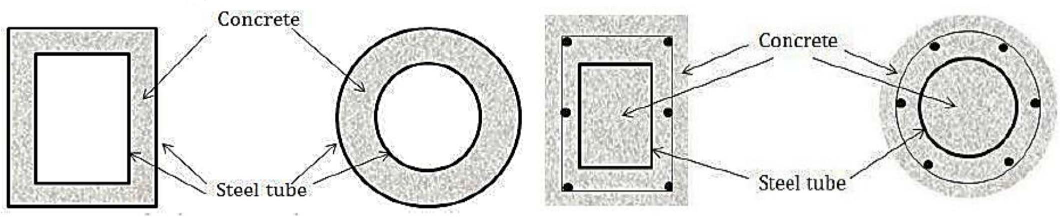

(c) Concrete filled double skin tube (d) Concrete encased CFST section

Figure 1.4 Types of CFST composite columns (Gore and Kumbhar, 2014)

(a) Field-fabricated CFT joint (b) Bent plate closure on girder web.

(c) Shop-fabricated CFT joint (d) Girder connection for shop joint

Figure 1.5 Practical application of circular CFST column (Schnider et al., 2004)

Figure 1.6 Steel-concrete composite column structure (Ruifeng building in Hangzhou - China) (Han et al., 2014)

Several previous studies compared the performance of CFST columns filled by RAC and CCs to evaluate the meaning of usage this type of concretes (Yang and Ma, 2013; Konno et al., 1997, Xiao et al., 2006; Yang and Han, 2006). The results of aforesaid studies revealed that there is similarity or only slight difference between the performance of RAC and CCs composite columns in bond performance and failure modes aspects. However, the fact that RAC have lower elastic modulus and compressive strength as well as high shrinkage and creep than normal concrete cannot overlook. For this, the structure member filled by RAC expected to exhibit slight low stiffness and bearing capacity as well as inferior performance of durability. In this regard, Konno et al. (1997) reported that the progress of fracture of CFST columns filled by RAC was faster than that of the confined CCs composite columns; in which fc' of RAC varied from 30 to 38 MPa and 35 MPa for normal concrete. However, the bearing capacity of RAC column was enough in quantity to be utilized though its stiffness. Beside foreside study, Konno et al. (1998) concluded that the deformational behavior of RAC column was similar to that of NAs columns. Moreover, the authors stated that it can be predict the stiffness of composite columns via consideration of the Young’s modulus of RAC, which it was lower than that of CCs.

1.4. Research Objectives

The concept of sustainable development in the structural engineering and concrete community need to widely separate and reach fully conviction that these concepts should be go in harmony, particularly with new orientation of the concrete or composite element production. Hence, utilize of RAs in new construction, with an extreme possible limit, becoming a necessity more than a luxe. The concrete member production field is deemed as one of the most likely feasible ways to use RAs. For this and to be more specifically, the main objective of this research is to dispel the fears of using RAs in the production of concrete and concrete filled steel tube (CFST) columns for the purposes of structural applications. However, it can be listed the objectives of this research below:

- Prepare a comprehensive study that deals with sourcing, production, impedimenta and use of RAs in concrete and concrete filled steel tube members.
- Study the influence of RAs on the properties of produced SCCs and investigates it's fundamental properties such as fresh and mechanical aspects.
- Investigate the fracture properties of SCCs produced with and without RAs and compare the differences to generate an overview about the fracture performance of RA concrete.
- Theoretically investigate the possibilities of using recycle aggregate self-compacting concrete (RASCC) as concrete core for the composite CFST columns as well as evaluated the axial load capacity (Pu) of CFST columns and applied it according to various design codes.

Through mineral and chemical material assistance, the successful production of RA concrete could lead to large-scale use of these aggregates for various structural applications. Moreover, rather than limiting the use of RAs in low value uses, it could be investigate enlarge the utilizing of this aggregate in new fields and concretes. Indeed, the encouraging fresh, strength and fracture performance of RA concrete also could be strengthen the belief of producing good properties concrete from these aggregate. Furthermore, the application of RA concrete in composite columns was performed and the ultimate capacity of such composite columns subjected to axial loading were computed based on different design codes such as ACI-318R, 2005, AIJ, 1997& 2001, DL/T, 1999 and Eurocode 4, 2004; then convenient comparisons are conducted between results in order to evaluate the most suitable code for the selected steel-concrete composite members.

1.5. Significance of the Study

Nowadays, due to increased amount of RAs around the world as a result of developing in crushing technologies, there is global trend to enlarge the use of RAs in new construction for economic and environmental reasons. Inasmuch the increased volumes of CDW and industrial by-products such as slag and SF, it is considered very useful to exploit these abundant materials in producing good quality concrete. Thereby, RA concrete can be competed the equivalent NAs concrete in many concrete applications. Recently, concrete techniques are widely improved, which can be allow to add a value to our knowledge and expand the use of these wastes. Moreover, in the recent days, considerable attentions have been observed about the performance and usability of structural members produced with RA concrete. For this, the effect of using concrete with RAs on the axial capacity of the composite columns is studied in details within the scope of this thesis.

1.6. Structure of the Thesis

The thesis consists of five chapters summarized as follows:

- **Chapter 1**: presents an introduction to this study and briefly provides basic information about CDW, RAs and SP in concrete. The environmental benefits come from the disposal of these materials and the advantages of using these wastes in new concrete and in new structural member such as CFST columns were briefly discussed. The motivations of the study, and briefly reviews some important issues which were deemed essential prerequisites to everyone dealing with recycling and RAs in concrete and CFST columns. As well as, the objectives and the significance of the study were clearly stated.
- **Chapter 2**: presents a literature review and overall background information regarding of use RAs in new concrete, particularly in SCCs. A brief background on recycling of old concrete and its contamination, which usually

exist in RAs, is given. Moreover, differences between RAs and NAs and classification of RAs were also extensively reviewed. The significance and economics of recycling CDW as well as it's processing and properties and use of RAs in structural members are briefly discussed in this chapter. Moreover, general review of recycle aggregate concrete filled steel tube (CFST) columns was presented as well as previous literatures studies related with this topic.

- **Chapter 3**: in this chapter, the methodology followed in this study was demonstrated. The properties and characteristics of materials used in this study were also described as well as materials test results were presented and discussed. Thus, the procedure and the main hypotheses and equations of tests on fresh and hardened SCCs are described. It is worth mentioning that the formulation explicated from four different design codes (Eurocode 4, ACI, AIJ, DL/T) are used and presented to predict the ultimate axial capacity of CFST columns.
- **Chapter 4**: presents results of tests conducted on the SCCs produced by utilizing NAs and/or RAs. The requirements and testing methods used to ensure production of this type of concrete were reviewed and reported. Moreover, the effect of incorporating SF and effect of water to binder ratio (w/b) ratio on the fresh, hardened and fracture properties of concretes were reported and evaluated. List of results and figures are presented and discussed; also, an analytical study via visual inspection of variance (GLM-ANOVA) was performed to assess the statistical significance of the experimental test parameters on the characteristics of SCCs. The results of theoretical comparisons and code assessment for the predicted axial load carrying capacity (Pu) of the concrete filled steel tubular (CFST) short columns as well as proper relations and proposed formulas extracted from study were presented.
- **Chapter 5**: The conclusions of experimental and theoretical study are reported in this chapter.

CHAPTER II

LITERATURE REVIEW AND BACKGROUND

2.1 Introduction

Concrete, which is the most consumed material in the world after water, often uses a considerable amount of non-renewable resources (Arezoumandi et al., 2014). Hence, in volume terms, concrete is the most widely used and manufactured material with nearly 2-2.5 tons produced annually for each living person. In effect, concrete has been described as the fundamental construction material (Neville, 2003; Domone and Illston, 2010). Concrete is defined as a blend of cement, water, fine and coarse aggregate, which aggregate bind together via chemical reaction (hydration) occurred between the cement and water.

In general, concrete wastes are delivered to the landfill sites for disposal; however, due to increase the charges of landfill as well as environmental reasons and because of the scarcity of NAs, aggregate derived from concrete wastes is growing interest in construction industry. In effect, while the construction industry grows, the effect of this growing on environment proportionally increased with time due to the large quantities of natural materials and energy used by the construction industry (Tam et al., 2006). Unfortunately, the construction industry consumes about 20-50% of all material resources from nature; hence, the effect of the construction industry on environment can be summarized as (Margarido, 2015):

- Using huge quantities of construction and demolition waste (CDW)
- Increase the emission of CO2, which result an increase in greenhouse gases.
- Water, air, noise and visual pollution.
- Consumption non-renewal and energy resources.
- Exhausting non-compensable natural resources.

Recently, the environmental protection becomes very important issue around the world. Therefore, the regulation related with CDW, which affected seriously environment, was made by the countries (Tam et al., 2006). The developing countries pressed to find solutions about these growing wastes through economic, social and environmental methods. Thus, localized sources scarcity, landfill and aggregate taxes, long transportation distances and increase landfilling costs are the part of problems need to be solved (Topçu and Günçan, 1995; European Commission Report (ECR.), 1999; Frondistou, 1977). The construction industry tried to determine the strategies to reduce the effect of CDW on the environment. Therefore, the identified the life cycle of the natural sources shown in Figure 2.1 can help to get a better understanding for this problem.

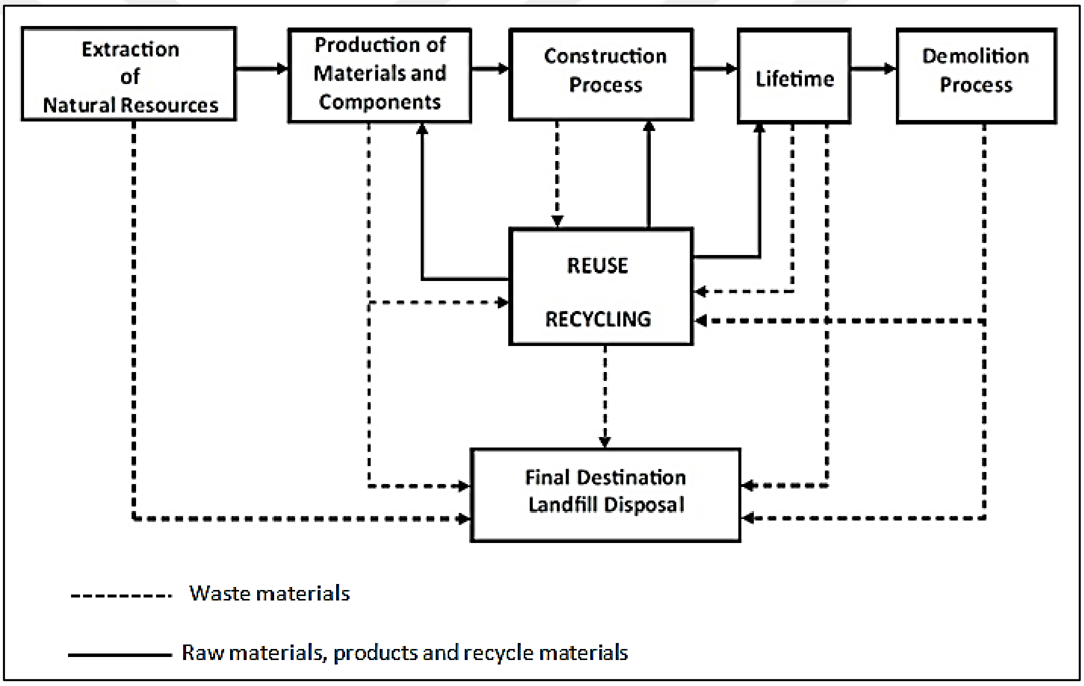

Figure 2.1 The life cycle block diagram of construction industry (Margarido, 2015)

2.2 Recycled Aggregate (RAs)

In the last two decades, the concept of recycling has gradually begun to get popular, particularly for concrete. Hence, there is a dramatically increased in the attention towards the environmental effect of construction and sustainable development. Moreover, concrete usually has much to offer on this regard because it has features of diminishing the depletion of natural resources, inert, durable and recyclable. In general, RAs are manufactured via re-processing of waste materials where CDW represents the largest source of wastes. In Australia, concrete is representing about 81% of the total volume of CDW. For this, recycling these wastes is the best way to minimize materials generated from construction activities.

Japan, with 100 % recycling of the wastes, are leading the countries in the field of recycling waste materials used in new construction applications. Similarly, in Hong Kong, about 14 million tons of CDW materials were generated from construction activities each year. Previously, these materials were dumped normally in the landfill sites and treated as waste debris. Nowadays, better ways to manage CDW were explored to drive better environmental sustainability (Nik, 2005). Created from CDW, RAs can be classified as hard inert materials ranging from broken concrete, rocks, bricks *etc*. from demolition sites. Moreover, RAs can originate from excavated materials which it comes from foundation work sites and material generated from the road maintenance works.

2.2.1. Use of RAs in New Concrete

In 1940s, the studies on recycling of concrete waste were initiated in Russia by Glushge; then; number of experimental investigations has been carried out in the following years (Xiao et al., 2006). Since, a large scale use of RAs in concrete has been reported after the Second World War in Germany (DeVenny, 1999). During the war, a large amount of destroyed and extremely damaged structures had to be demolished and the product reused in different applications. At the end of 1955, a total of 11.5 million m^3 of recycled materials was produced in Germany (Khalaf and DeVenny, 2004). In other parts of Europe, RAs had been used for different rudimentary applications at that time.

Worldwide, the use of RAs in new concrete is limited by standards and codes of practice. In UK, a protocol for RAs in new concrete permits the use of only up to 20% by mass. Similarly, in Hong Kong, only in low grade (grade 20 or less) concrete it is legal to use 100% coarse RAs, while only 20% by mass in high grade concrete (Nik, 2005). Also in Holland, at 1994 it was permitted and admitted that the use of 20% RAs by mass results in little difference in the properties of fresh or hardened concrete (DeVries, 1996). Hence, the increase in the use of RAs in construction become a desire and ambition a governments around the globe. In Germany, since

1991, the aim of recycling RAs created from CDW material in concrete has been set at 40% (Nik, 2005). Thus, a similar trend can be observed in Japan and USA where the RAs were used in concrete and asphalt pavements to build new roads and their associated concrete works.

Presently, BS 8500-2 (2002) provides a basis for the use of RAs in concrete as well as BS EN 12620 (2002). It deals with the properties of NAs, fillers and manufactured or RAs for use in concrete. However, to date statistics showed that only a small amount of RAs are used in high utility applications; and that is probably due to existing provisions and restrictions. In many applications, which are listed below, good quality NAs were extensively used in variety and unnecessarily cement based products like (Wrap, 2007):

- Building masonry bricks and blocks.
- Paving blocks and road kerbs.
- Concrete paving units and slabs (Cast in situ and pre-cast).
- Non-structural concrete walls and partitions.
- Pipe bedding material.
- Capping, piling mats, and sub-base layers in housing development.
- Road sub-base sidewalks and footpaths.
- Soil improvement, gabions, erosion control, general and engineered backfilling.
- Low grade concrete for different concrete structures.

Indeed, significant amounts of NAs could be saved if suitable RAs were used for these applications instead.

2.2.2. Contaminations in RAs

Impurities of RAs are the major factors which restrict the expansion of using this aggregate in the concrete industry. Unless removed, contaminants present in the original material will be passed on to the new concrete; thus, it could cause a harmful effect on strength and durability performance. For this, contaminants should be removed before crushing process of CDW. Indeed, materials such as glass and timber could be removed to obtain good quality materials from recycling sites (Buck, 1973; Collins, 1993). Moreover, other impurities like ferrous origins can be removed off by use of a large magnet or by being hand-picked while it passes through a conveyor belt. The most common contaminants usually found in RAs are old cement paste, residue asphalt, gypsum, chlorides and sulphates, organic materials and glass. According to BS 8500-2 (2002), the limits imposed on RAs composition are listed in Table 2.1.

Table 02.1 The recycled aggregates requirements according to BS 8500-2 (2002)

Property	Maximum Percentage (by mass)
Masonry content	10.0
Fines content	3.0
Lightweight materials content (density < 1000 kg/m^3)	1.0
Asphalt content	10.0
Other foreign materials (*e.g.* glass, wood plastics, metals *etc.*)	1.0
Acid-soluble sulphates SO_3	1.0

2.2.3. Classification of RAs

Unlike the RAs derived from old roads, aggregate produced from CDW are usually irregular in shape and content because the rubble is collected from various sources; moreover, the properties of this aggregate are unlikely to be consistent. Thereby, it is difficult to utilize these aggregates in the production of new concrete (BRE, 1992). Nevertheless, more cleanly aggregates are lead to more strong concrete (Amnon, 2004). Relevantly, BS 8500-2 (2002) classified RAs into two major classes:

- Class I: for aggregate derived from crushed concrete.
- Class II: for the aggregate produced from processed CDW, where the conditions are based on the composition of RAs.

According to Mulheron (1988), RAs can be classified into four main categories illustrated in Table 2.2. However, due to the lack of a well-defined and unified recycling process, there is a huge variation in materials produced from different recycling operations. Indeed, Operators cannot produce acceptable recycled products in conformity with standards; also, consumer confidence would remain low until changed this situation. Therefore, under these conditions, classification of recycled products seems unlikely to be possible. In the same regard, notable classification based on the maximum allowable values for impurities in RAs was introduced by RILEM (1994) and it displayed in Table 2.3. According to this classification RAs were classified into three groups:

- Group I: for aggregates produced from concrete masonry debris.
- Group II: for aggregates derived from concrete debris.
- Group III: the aggregate consists of debris from above two groups and more than 80% of NAs.

Table 0.2 The main categories of RAs (Mulheron, 1988)

	Categories	Descriptions
1	Crushed demolition debris	Sorted and screened crushed brick and/or concrete.
2	Clean graded mixed debris	Little or no impurities crushed brick and/or concrete.
3	Clean graded brick	Little or no impurities crushed brick containing stone or concrete (less than 5%).
4	Clean graded concrete	Little or no impurities crushed concrete containing stone or brick (less than 5%).

Table 0.3 Classification of RAs for concrete (RILEM, 1994)

Mandatory requirements	Conditions and Units	Type of aggregate		
		1	2	3
Dry density of particle	Minimum/(kg/m^3)	1500	2000	2400
Water absorption	Maximum (%)	20	10	3
The content of material with density < 2200 kg/m^3	Maximum (%)	-	10	10
The content of material with density < 1800 kg/m^3	Maximum (%)	10	1	1
The content of material with density < 1000 kg/m^3	Maximum (%)	1	0.5	0.5
Foreign materials content (glass, bitumen, *etc.*)	Maximum (%)	5	1	1
Metals content	Maximum (%)	1	1	1
Organic material content (%)	Maximum (%)	1	0.5	0.5
Filler content (< 0.063 mm) (%)	Maximum (%)	3	2	2
Sand content (< 4 mm) (%)	Maximum (%)	5	5	5
Sulphate content (%)	Maximum (%)	1	1	1

In order to overcome current barriers and concerns, which are restrict the applications and use of RAs in concrete, the study undertaken by Wrap (2007) studied the adoption of alternative method for classification of RA concrete. Hence, three main classes were proposed from accomplished study (Wrap, 2007):

- Class A: wide range utilizing of RA concrete including marine environments.
- Class B: concrete produced through combined NAs and RAs to use it for moderate exposure conditions.
- Class C: RA concrete subject to the mildest exposure conditions.

In the same regard, Vivian and Tam (2007) classifies RAs into grades depending on some properties as shown in Table 2.4; in which the highest quality recorded for Grade A whilst grade G represent the lowermost rank.

Table 0.4 Classification of RAs (Vivian and Tam, 2007)

Properties	Grades						
	A	B	C	D	E	F	G
Particle density(kg/m^3)	> 2.5	2.49-2.4	2.39-2.3	2.29-2.2	2.2-2.1	2.1-2	< 2
Water absorption (%)	< 1.0	1.1-3.0	3.0-5.0	5.1-7.0	7.1-9.0	9.1-10	> 10
Flakiness index (%)	< 8.0	9.0-16	17-22	23-28	29-34	35-40	> 40
10% fines value (kN)	> 150	149-120	119-110	109-100	99-80	79-50	<50
Impact value (%)	< 20	21-23	24-26	27-28	29-31	32-35	> 35
Chloride content (%)	< 0.01	0.02-0.03	0.03-0.05	0.05-0.1	0.1-0.5	0.5-1	> 1
Sulphate content (%)	< 0.01	0.02-0.03	0.03-0.05	0.05-0.1	0.1-0.5	0.5-1	> 1

2.2.4. Significance of Recycling

When the buildings are demolished, the resulting material is either through down in landfill sites or reused in new applications. Hence, by-products and waste demolitions materials are created from several sources. In effect, always there is need for renovation, rehabilitation, demolition, and rebuilding; thereby, CDW will result inevitably. Furthermore, rejected concrete, concretes resulted from not satisfying code requirements, delayed casting and tested concrete are also creating CDW. As shown in Figure 2.2, CDW can be deemed as renewable material; this leads to interpret the lifecycle of materials used in construction by four-step closed-loop (Gilpin et al., 2004). In the last two decade, the environment has become a major concern worldwide putting more responsible for the need to increase the waste recycling and reduces the disposal in landfill sites. For instant, in UK about 85% of the total waste was going to landfill under the Kyoto protocol. Moreover, to avoid the dumping of CDW in landfills, there is an economic incentive which it support the reclamation of recycled aggregates in construction (Gilpin et al., 2004).

The extraction process of NAs normally accompanied with many environmental impacts such as loss of usual countryside landscape, noisiness, blasting sound and vibration, visual disturbance and spread of dust. So, to decrease these problems and in the same time meet the demand of aggregate, more recycled materials should be recycle (Sherwood, 1995; Speare, 1995). In effect, high quality aggregates like granite, limestone, basalt and dolomite are used in for many low-value applications and/or utilize in unnecessarily and low-strength requirements applications. Instead of these valuable materials, RAs can be used. In many places worldwide, NAs have already become exhausted and in short supply; therefore, new sources of aggregate for different construction employment were required. There is a need for further development and researches deals with incorporation of RAs and use it in high-value applications including structural concrete elements. Moreover, the properties of RA concrete must be enhanced to meet the performance requirements and criteria of modern concrete.

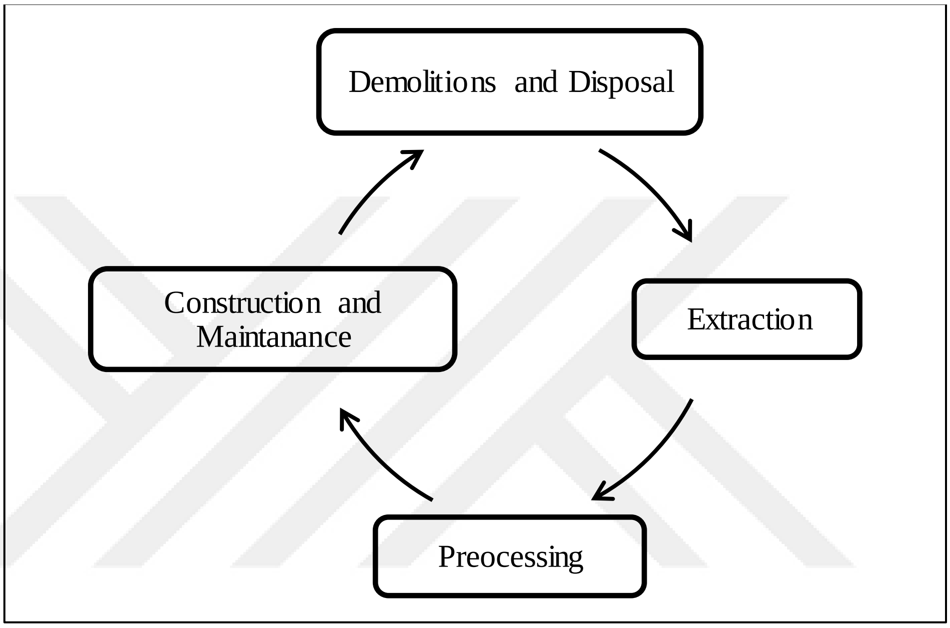

Figure 0.2 Life cycle of construction materials (Gilpin et al., 2004)

2.2.5. Economics of Recycling

When RAs is considered, the decision of using natural or recycle materials must be taken according to the cost of each type of construction elements. In effect, conditions like client opinion, transportation costs, taxes, quality of materials and its performance, availability of landfill sites and the concrete producer experience significantly effect on this decision. In each construction site, there is a cost to transport CDW to the specific landfill site. Sometimes the transporting cost as well as landfill taxes is more expensive than recycle CDW and take it to recycling site. Thus, RAs cost's relatively less per tons than aggregate extracted from primary resources (Gilpin et al., 2004).

Moreover, the screening and sorting of materials at the demolition source is also an economic factor. Indeed, there are other economic costs, which need to be account when the comparison has done between natural and recycle aggregate. For both types of aggregates, the transportation costs are economic crucial factor. Likewise, there is a potential further cost emerge from using additives materials, particularly with RAs, which it also should be considered. Indeed, the most important factor is the environmental cost and exhaustion the NAs from their source which it can never be replaced. The visual disturbance comes from extraction process would also create noise, dust, and vibration. However, for the production of RAs, these factors could be relevant. In UK, legislatives force further tax for the use of virgin aggregates to encourage the usage of RAs and to meet the growing in the aggregate demand which it ranged by 421-490 million tons/year in 2011 (Webb, 1999). Whereas, only 10% of total used aggregate were derived from recycled sources in 1991. So, the landfill tax regulations were introduced at 1996 to decrease the amount of waste going to landfill.

2.2.6. Construction and Demolition Waste (CDW)

Due to the growth of population and the flourishing of construction activities, CDW is steadily increasing worldwide. Conversely with natural resources, demolished waste can be deemed as a renewable source of materials due to the need for innovation, rebuilding, demolition and refurbishment. Nowadays, the prevailing trend is to convert all kind of wastes into environmentally friendly materials; thus, every possible technique should be taken to put these materials in a useful uses. In this regard, in UK approximately 333 million tons of wastes annually generated; including 107 million tons of CDW (about 32% of total waste). Annually, when CDW combined with wastes comes from mining and quarrying, industrial and dredged material, it rises to 80% of total waste in UK. Hence, it is one of the major sources of waste materials. Indeed, the main sources of waste are the construction industry (Defra, 2008). Indeed, a quantity of this size is worrying and alarming (Figure 2.3).

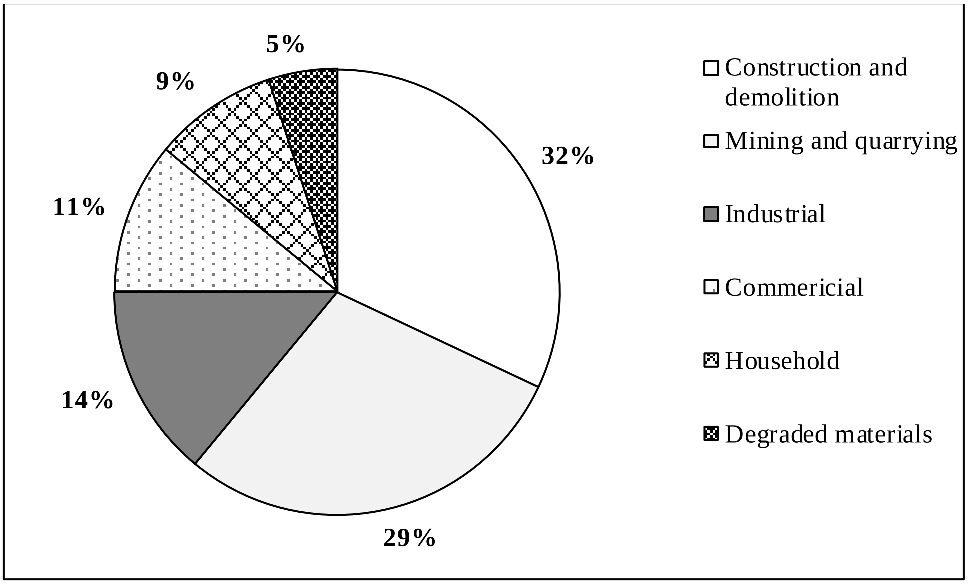

Figure 2.3 Estimated annual waste quantities in UK (Defra, 2008)

In the European Union , about 500 kg CDW for each capita was produced; moreover, the construction industry create about 50% of total waste and consumes about 50% of the produced natural materials (Nik, 2005). Hence, approximately half of the produced CDW is currently recycled and used as RAs; indicate that the sheer scale of CDW is equal to that of the aggregates used in construction (Wrap, 2007). In particular, 90% of the CDW was recycled to use it for inferior applications like filler materials. Whereas, each year only 10% of concrete waste was being crushed, sorted, sieved and added to manufacture new concrete. It is worth mentioning that the utilization of high-grade RA concrete has been discouraged due to the lack of suitable regulations (Collins, 1993).

Although the NAs appeared to be economically viable and are easily available at acceptable prices, the environmental implications are unfortunately negative because it means more depletion of natural resources, increased disposal of CDW, damage to natural landscapes due to quarrying and more landfill and disposal sites creating. Hence and due to the increased demand on new-build, the amount of CDW is expected to considerably increase in quantities and in price during few next years. Therefore, encourage recycling of waste will be the most suitable choice to meet this increment (Crawford, 2007). It is estimated that the annual generation of CDW waste in European Union could be as much as 450 million tons per annum. Actually, in Germany, Holland and Denmark, recycled material is generally cheaper than natural materials and less in cost than disposal (Akash et al., 2007). Therefore, most European Union countries aim to reach the range of 50% to 90% recycling materials since it was an average of 28% of all CDW in the late of 1990s (ECR., 1999). The situation is even more serious in other countries depending on it's technical development and in countries when the availability of natural construction materials is scarce. Since, recycling wastes in new concrete is likely to be the best option even though if the difficulties are presented.

Generality, almost waste materials produced by demolished structures are disposed of by dumping in un-authorized places which is causing environmental problems. Moreover, all kinds of CDW derived from good quality aggregate, rocks and quartz fine aggregate can be safely dumped especially in large open unused spaces. In very limited situations, CDW were used in rural and countryside farms roads to improve it's poor quality. Furthermore, the high transportation cost of CDW lead to dump in landfill sites located inside urban areas and then it will create space problem in addition to the environmental concern. Therefore, to preserve environment and to save the energy and cost, it is crucial to start recycling and re-use of CDW. However, the recycling of CDW is not easy to accept by client and construction industry unless appropriate legislations enforced it. Every year, staggering figure of discard concrete has reached to landfills and it is estimated to double this number within 10-15 years. Thereby, there is a desperate need to maximize the usage of RAs come from CDW in constructions. The performance of RA concrete needs to be improved to satisfy the requirements of the concrete industry which in turn contribute reducing energy consumption, maintaining natural resources and make concrete a more “green” material.

2.2.6.1. Processing of CDW

In general, the crushing process equipment and their correspondent accessories used in CDW crushing are similar to those commonly used in the crushing process of natural rock aggregate. However, the production site incorporates various types of crushers, screens, conveying belts, and sorting devices for dry-wet removal of other materials. Over the last two decade, recycling equipment has considerably developed and its advances and features are ranging from simple to very sophisticated. Moreover, the portable and fixed facilities crushing equipment are available in the market at accepted cost. For this, the number of recycling projects is readily increasing worldwide. As an example in Hong Kong illustrated in Figure 2.4, the major parts of modern steady recycling site are displayed (Fong and Jaime, 2002). Basically, CDW materials are crushed to produce granular materials of smaller particle size. Thus, the contamination content and the purposed application of RAs are the main factors controlling the degree of processing required.

In general, recycling plant basically consist of (Fong and Jaime, 2002):

- Primary sorting facility, crushers (*i.e.* primary and secondary).
- Contamination removal facilities (*i.e.* magnetic tools to separate metals, air knives and manual sorting belts).
- Removal services (heavy duty trucks and tractors).
- Stockpiles and storage areas.

Figure 0.4 The steady recycling facility (Fong and Jaime, 2002)

2.2.7. Adhered Mortar of RAs

In general, RAs contain not only the original aggregates, but also hydrated cement paste clinging to the surface of these aggregates; thus, make the paste of RAs more porous. For this, the density of the RAs is lower than NAs; also, the water absorption ability is higher than counterpart of NAs because the higher porosity of RA leads to higher water absorption capacity as well as increase the porosity of produced concrete (Grdic et al., 2010; Kou and Poon, 2009; Panda and Bal, 2013). Hence, the old mortar (adhered with aggregate) is often prone to entice more water than the

NAs. Therefore, compared with virgin aggregate, water absorption capacity of RAs usually observed high percentages; as well as, the size of RAs particles also effect on the absorption capacity. For example, the absorption capacity is about 3.7% for size 4-8 mm RAs, and about 8.7% for the 16-32 mm sizes; while, it is only 0.8-3.7% respectively for NAs (Hansen, 1983). Accordingly, RAs are characterized as a type of concrete aggregates with higher porosity and water absorption, lower density and mechanical strength compared to concrete contain NAs. As a consequence, it is crucial to prepare a convenient mix design to ensure obtaining the desired qualities for RA concrete (Kou and Poon, 2009; Güneyisi et al., 2014; Tsung et al., 2006; Panda and Bal, 2013; Grdic et al., 2010).

In effect, the adhered mortar at the surface of RAs exhibit lower specific gravity, bulk density and saturated surface dry (SSD) density. Conversely, it reveals high values of water absorption and abrasion resistance measured by Los Angeles test (Hansen and Narud, 1983; Ravindrajah and Tam, 1985; Buck, 1977; Modani and Mohitkar, 2014). Indeed, the most notable of these differences is the highly increase in water absorption. The amount of cement paste adhering to the aggregate particles surface cause an increase in the absorption capacity of RAs (Tavakoli and Soroushian, 1996-a). Further, the wide use of RAs in concrete restricted due to the high shrinkage and high water absorption of these aggregate (two to three times that of NAs). Hence, these drawbacks largely caused by the old mortar/cement paste adhered to the surface of RAs (Modani and Mohitkar, 2014; Hansen, 1986).

As depicted in Figure 2.5, the additional ITZ is the old layer locating between the parent aggregate and old adherent cement mortar (Modani and Mohitkar, 2014). Thus, the amount of old mortar clinging to natural grains mainly depends on the particles size of crushed RAs. Indeed, the quantity of adhered mortar increases whenever the aggregate size is decrease. At smaller size of the aggregate, the volume of adhered mortar proportionally increases. Therefore, recycle fine aggregates (RFAs) would often contain more adhered mortar and have higher absorption capacity. However, the utilization of RFAs for new concrete is usually avoided due to its higher absorption capacity and due to high shrinkage value for produced concrete (Hansen, 1996).

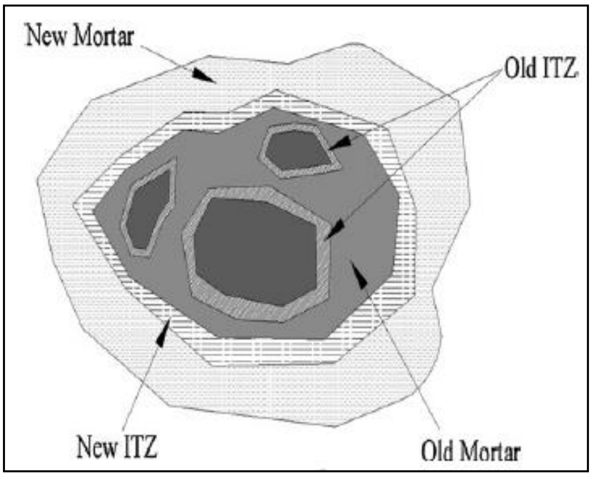

Figure 02.5 Microstructure of recycle aggregate particle (Modani and Mohitkar, 2014)

2.2.8. Factors Contributing to Performance of Structural RA Concrete

2.2.8.1. Water to Cement Ratio

It is crucial to know that the major factor effecting on the strength of concrete is the water to cement (w/c) ratio, or more precisely water to binder (w/b) ratio. It is well known that whenever w/c ratio increases, the resulted concrete would be in inferior quality at all ages; also, it significantly effects on fresh properties as well as hardened of concrete. Hence, the effect of w/c ratio on the fresh properties of concrete limits the usage of low- strength concrete, but incorporating of SP could remedy for this situation. In effect, high water content will make the concrete more workable, but in the same time it will supplant a voids and/or small pores inside the concrete matrix; then, it produced weak cement as well as weak and cellular ITZ. In low grade mixes, the initiation and propagation of micro-cracks as well as voids spread inside the concrete matrix are commonly lead to decrease the concrete strength. Therefore, concrete with a low w/c ratio is stronger in strength because it is less permeable than high w/c mixes; moreover, the lack in cracks and voids results more durable concretes. In this regard, Kou and Poon (2009) emphasized that the compressive strength of RA concrete increased by 40% when the w/c ratio dropped from 0.55 to 0.4. However, for high replacement levels of RAs, only minor difference in strength was recorded (Thomas et al., 2013).

2.2.8.2. Use of Admixtures

Mineral admixtures are incorporated in order to enhance the concrete performance, particularly in the durability aspects via decrease the permeability of produced concrete. In effect, the mineral admixture are primarily characterized by high quantities of reactive silica like fly ash (FA), GGBFS, SF, rice hull ash and metakaolin (MK). Inside the concrete matrix, the hydration reactions began directly when water is added to cement. Later, a gel of calcium silicate hydrate (CSH) and hydrated lime (CH) are formed in hydrated Portland cement system and it called "Ettringite". The ettringite formed as a product of the reaction between calcium sulfate and calcium aluminate. In effect, CSH is like glue binds the contents of concrete each other and gives the concrete it's strength and durability. In contrast, CH is brittle crystals which it gather up the surface of aggregate particles and rebar resulting a weakened in the matrix. When a source of additional reactive silica is added, it will react with CH to form more CSH and then supply more strength inside the matrix. However, several studies showed that concrete mixes incorporating pozzolans materials like SF were tend to require higher dosages of SP; thereby, enhance the workability of concrete (Mazloom et al., 2004; Hassan et al., 2000). It is worth mentioning that SF is an expensive admixture compared to other mineral admixtures; this could have an obstructive impact on the overall cost of concrete.

The chemical admixtures like SP start to use in the beginning of 1960s and it became a milestone in concrete technology (Malhotra, 1997). Previous findings proved that the use of high quantities of reactive silica material, besides chemical admixtures, could be beneficial to concrete performance. Moreover, the whole range of concrete properties can be enhanced especially in the aspects of durability like heat of hydration and drying shrinkage (Dhir, 1998). The enhancement in the concrete properties attribute to the porosity reduction of mortar matrix. Hence, this reduction strengthen the pore structure of concrete which is enhances the interlocking with the aggregate (Hassan et al., 2000). However, the concrete suffered from a higher rate of slump loss related with the use of SP especially if "traditional sulfonated naphthalene formaldehyde base" admixtures are used (Dhir et al., 1998; Liu et al., 2000).

Water-reducers materials like SP are commonly used in modern concrete and it traditionally known in a different name such as superfluidizers, superfluidifiers, super water-reducers, superplasticizers and high range water-reducers. The most advantage of SP is the increase of workability for low w/c ratio concrete. In effect, it makes the mixtures more workable and more suitable to cast especially in congested reinforcement and inaccessible areas, complex shuttering and deep sections. From this point of view, the invitations of self-compacting concretes (SCCs) are started as well as other related concrete types. Indeed, when SP admixtures are used, cement grains get catch on all available water to complete the hydration process. It is well known that in SCCs mixes, the water is very limited due to the much denser cement matrix than in ordinary concrete. Thereby, there is no excess water to be entrapped in the concrete matrix to produce further voids and pores or to migrate into the surface causing a bleeding in the mixture and forming microscopic ruts. Thus, both high quality cement paste and chemical bond results a higher compressive strength (Malhotra, 1997).

2.2.8.3. Blending of RAs and NAs

Typically aggregate occupied about 60-70% by volume of concrete matrix, so it form a considerable volume of concrete. In effect, aggregate contributes in the strength of concrete when the strength of the paste matrix is relatively low as well as it considered as cheap filler. In concrete matrix, three phases of failure can be occurred. The aggregate phase is one of the failure types which are happened when the aggregate is weaker than other phases (the cement paste and ITZ) (Neville, 2006). Indeed, cracks start to form and propagate across the aggregate grains when the concrete section is overloaded. Moreover, cracks are significantly reduced or stopped whenever encountered by strong aggregate (Karihaloo, 1995). Hence, weak and crisp aggregate are not expected to produce good concrete. The previous experience showed that, if low quality of RAs blends with a proven quality NAs it will result a better resultant concrete and improved the quality of aggregate mixture. However, Niro et al. (1998) reported that the improvement in the cube strength was less than 10% due to the blending of natural and recycled aggregates. Moreover, tensile strength and elasticity modulus were found to follow the same trend of strength improvement. In the study of Niro et al. (1998), the strength of RA concrete are far below similar NAs concrete. Therefore, it is necessary to blend RAs and NAs in different proportions and use high strength cement type to attain a satisfactory strength of RA concrete.

2.2.9 Physico-Mechanical Properties of RA concrete

2.2.9.1 Compressive Strength

In addition to other factors, the type of coarse aggregate, particularly it's mineralogy, has significant influence on physico-mechanical properties. With a similar mix proportions and under the same conditions, it was reported that different NAs have yielded different concrete properties. For instant, in limestone aggregate, the bond between cement paste and aggregate was stronger than gravel due to interfacial interlocking effects (Aïtcin and Mehta, 1990). The quality of RAs is more variable than NAs even for aggregates produced from the same source of CDW; therefore, the potential to develop different concrete properties is most likely high for RA concrete. The study presented by Tavakoli and Soroushian (1996-a) reported that RA concrete showed lower compressive strength than that of CCs for similar w/c ratio; while the strength is high for low w/c concrete. Likewise, at 100% RCAs concrete, about 20-30% extra cement content need to be utilized in order to achieve similar NAs concrete compressive strength (Etxeberria et al., 2007). According to Hansen and Narud (1992), about 5- 15% extra cement was required to obtain the same compressive strength of NAs concretes for 100% RCAs and RFAs concrete, respectively. Hence, the reduction in the strength due to utilizing RAs is more significant in the weaker concrete mix than the strong mixtures (Tabsh and Abdelfalah, 2009). However, RA concrete could reveal 2/3 of the required mechanical properties compared with NAs concrete with acceptable level of workability and durability (Vivian and Tam, 2007).

Aforementioned, the adhered mortar attached at the surface of the aggregate deemed as the main problem restricted the utilizing of RAs in concrete. Indeed, the old cement paste close fitting in parent aggregate grains plays an essential role to indicate the strength of produced concrete as well as the performance of concrete in the term of permeability and durability aspects (Hansen, 1985; Dae and Han, 2002; Etxeberria et al., 2007). It is well known that the amount of old mortar attached in the particles of RAs increases whenever the maximum size decreased; thereby, the compressive strength will be affected according to the size of RAs (Padmini et al., 2009). However, the un-hydrated cement adherent on the RAs may increase the long-term strength or at least compensate the potential reduction in strength due to the weakness of RAs (Khatib, 2005; Bordelon et al., 2009; Dhir et al., 1999). It was reported that the stuck adhered mortar adversely effect in the RA concrete for low w/b ratio mixes; while it does not effect in high w/b ratio mixes (Otsuki et al., 2003). However, RAs produced no significant adverse effect (about 8.5-12.2% decrease) on the compressive strength of SCCs (Alam et al., 2013; Safiuddin et al., 2011-a; Grdic et al., 2010; Bairagi and Kishore, 1993). Results of Khaldoun (2007) followed the aforesaid studies, which is the compressive strength of RA concrete was about 90% of that of NAs concrete; also, the rate of strength development and workability for both concretes was too close. Similarly, number of researchers' results can be summarized below for the percentage of decreasing in compressive strength.

- 45% for 100% replacement RAs (Yamato et al., 2000)
- 40% for 100% replacement RAs (Bairagi and Kishore, 1993)
- 25% for 100% replacement RAs (Amnon, 2003; Etxeberria et al., 2007)
- 24% for 100% replacement RAs (Ishiguro and Stanzl-Tschegg, 1995)
- 8- 24% for 100% replacement RAs (Ravindrarajah and Tam, 1985)
- 5-40 % for 100% replacement RAs (Hansen and Narud, 1992)
- 14-32% for 100% replacement RAs (B.C.S.J, 1978)
- 12.3% for 100% replacement RAs (Wang et al., 2013)
- 9% for 100% replacement RAs (Ravindrarjah et al., 2000)
- 13% for 100% replacement of RCAs (Gomez-Soberon, 2002)
- 23.5% for 100% replacement of RCAs (Topçu and Şengel, 2004)
- 22% for 100% replacement of RCAs (Kou et al., 2011-b)
- 20% for 100% replacement of RFAs (Kou and Poon, 2009)
- 36% for 100% replacement of RFAs (Khatib, 2005)
- 8% for 100% replacement of RFAs (Evangelista and DeBrito, 2010)
- 5% for 30% replacement of RFAs (Zega and DiMaio,2011)

Moreover, Salmon and Paulo (2004) replaced 20% of NAs by RAs derived from old concrete or masonry. The authors concluded that the RA concrete revealed most likely similar or sometimes better performance than CCs. However, this conclusion is agreed with the recommendations stated by RILEM, TC 121 DRG (1994). Also, Etxeberria et al. (2007) emphasized this assumption that RA concrete made with 25% of RCAs revealed similar mechanical properties of NAs concrete. Recently, the results of Dhir (1998) referred that there was limited effect on the properties of RA concrete due to using 20% by mass of aggregate. Moreover, the incorporation of SF in RA concrete produced similar strength properties of equivalent NAs concrete (Gonzalez and Martinez, 2008).

2.2.9.2 Tensile Strength

Mainly, due to the inferior properties of RAs, which it make the aggregate and/or the produced concrete cellular and more porous; the splitting tensile strength of RA concrete is lower than CCs (Ravindrarajah and Tam, 1985; Evangelista and DeBrito, 2010; Kou and Poon, 2009). Several previous studies investigate the effect of RAs in the concrete compare to equivalent NAs; thus, literatures reported that the splitting tensile strength of RA concrete lower than that of CCs by:

- 20% for 100% replacement RAs (Ravindrarajah and Tam,1985)
- 10% for 100% replacement RAs (Ajdukiewicz and Kilszczewicz, 2002)
- 18.8% for 70% replacement RAs (Solyman, 2005)
- 5-40 % for 100% replacement RAs (Hansen and Narud, 1992)
- 9-12% for 100% replacement of RCAs (Kou and Poon, 2009)
- 20% for 100% replacement of RCAs (Thomas et al., 2013)
- 23% for 100% replacement of 100% RFAs (Evangelista and DeBrito, 2010),
- 30% for 100% replacement of RFAs (Evangelista and DeBrito, 2007),
- 7% for 30% replacement of RFAs (Zega and DiMaio, 2011)

In contrast to other mechanical properties, several researchers claimed that tensile strength of RA concrete might be similar or better than that of CCs (Tavakoli and Soroushian, 1996-a; Sagoe et al., 2001; Etxeberria et al. 2007). Moreover, Kou et al. (2011-b) emphasized that the presence of SF in the concrete enhance the tensile strength results of RAs due to strengthen the bonding between the new cement paste and aggregate; thus, improve ITZ region. However, Gonzalez and Martinez (2008) showed that addition of SF did not improve the tensile strength or modulus of elasticity.

2.2.9.3 Modulus of Elasticity

The properties of aggregates, particularly RAs, significantly affected on the elasticity of concretes which is often lower than that of CCs (Neville, 2006). In general, due to large amount of old mortar adheres on the surface of RAs the modulus of elasticity of RA concrete is always lower than that of corresponding CCs, especially when the fine grade of RAs are used (Hansen and Narud, 1992; Etxeberria et al., 2007). The modulus of elasticity for RA concrete represent about 50-70% of the total elasticity of normal concrete (Akash et al., 2007). Moreover, whenever the RAs replacement level increase, concretes revealed lower value of elasticity (Khatib, 2005). Indeed, the modulus of elasticity is somewhat negatively affected by RAs (Hansen and Narud, 1992; Corinaldesi and Moriconi, 2009). Research indicates that the elastic modulus of RA concrete is less than NAs concrete by about 30%; attaining equal compressive strength (Katharina, 1997). In similar way, the reduction percentage was 12% (Andreas and Rühl, 1989), 15% (Gerardu and Hendriks, 1985), 45% (Jianzhuang et al., 2005) and 16% (Etxeberria et al., 2007) dependent on the level of RAs replacement. Other researcher’s results can be listed below:

- 10-40 % for 100% replacement RAs (Hansen and Narud, 1992)
- 20 % for 100% replacement RAs (Topçu and Günçan, 1995)
- 13% for 100% replacement RAs (Ishiguro and Stanzl-Tschegg, 1995)
- 45% for 100% replacement of RCAs (Xiao et al., 2005)
- 19% for 100%replacement of RFAs (Khatib, 2005)
- 18.5% for 100% replacement RFAs (Evangelista and De Brito, 2010)
- 7% for 30% replacement of RFAs (Zega and DiMaio, 2011)

It is worth mentioning, the given examples shown notable variation of strengths and stiffness of RA concrete; this behavior could be attributed to the inconsistency of properties of the RAs used by various investigators. However, the magnitude of elastic modulus comparatively high for RA concrete produced with coarse recycled aggregate and natural sand (RILEM, 1992). In the study of Bairagi and Kishore (1993), the reduction in modulus of elasticity for RA concrete was about 10-40%; while the creep and shrinkage were increased by 30-50% and 20-70%, respectively. However, Khaldoun (2007) reported that only slight difference (3%) can be noted in the modulus of elasticity results of RA concrete compare to reference concrete.

The modulus of elasticity was significantly affected by the w/c ratio used to produce concrete. It was reported that, for 100% replacement of RCAs, the decrease in w/b ratio from 0.55 to 0.40 results an increase in the modulus value by approximately 12% (Kou and Poon, 2009). Also, Frondistou (1977) reported that for 100% RA concrete, up to 40% decrease in the modulus of elasticity recorded at relatively higher w/c ratio (0.75) concretes; moreover, insignificant decrease registered at low w/c ratio (0.55) concretes. Nevertheless, the decrease in the concrete performance can be mitigated through different approaches like the processing of RAs, which is play a decisive role in determining the strength and durability of concrete (Reddy et al., 2013; Pereira et al., 2012; Kou and Poon, 2011-b). Also, the treated RAs can be a reliable alternative of NAs in construction, particularly for non-structural or lower level application (Safiuddin et al., 2011-b; Tsung et al., 2006).

2.2.9.4 Stress-Strain Relationship

It is well known that the area under the ascending and descending portion of the stress-strain curve provide measurement of the ductility as well as toughness of concrete, respectively. While, the peak of the curve could be represent the value of compressive strength of concrete. Naturally, when the concrete structures subjected to dynamic loading such as earthquakes, fatigue and impact loading the descending part become essential and influential (Jianzhuang et al., 2005). In effect, several previous study revealed that the replacing of RAs have a significant effect on the stress-strain relations through the rate of strain increasing is faster than applied stress, particularly at higher ratios (Bairagi and Kishore, 1993). Hence, Jianzhuang et al. (2005) produced typical set of stress-strain curves for the RA concrete at the same above mentioned replacements level. The authors claimed that the stress–strain relationship for RA concrete was quite similar to equivalent of NAs. As revealed in Figure 2.7, the substitution of RAs leads to a marked change in the response of stress–strain, which is summarized by following points:

- The ductility of the concrete, which is described by the descending portion of the stress-strain curve, was significant decrease whenever RA content increase. Moreover, the slope of descending branch of the curves is also decreasing.

- The peak strain (strain at peak stress) of RA concrete was lower than that of NAs concrete; then it increased whenever the percentage of RAs were increase. It was reported that for a 100% RAs replacement level, the peak strain was increased by 20%.

- RAs used in this study were slightly more deformable than NAs. Indeed, the strain at peak stress can be estimated as 0.0019 for NAs concrete while it is only 0.0022 for equivalent RAs.

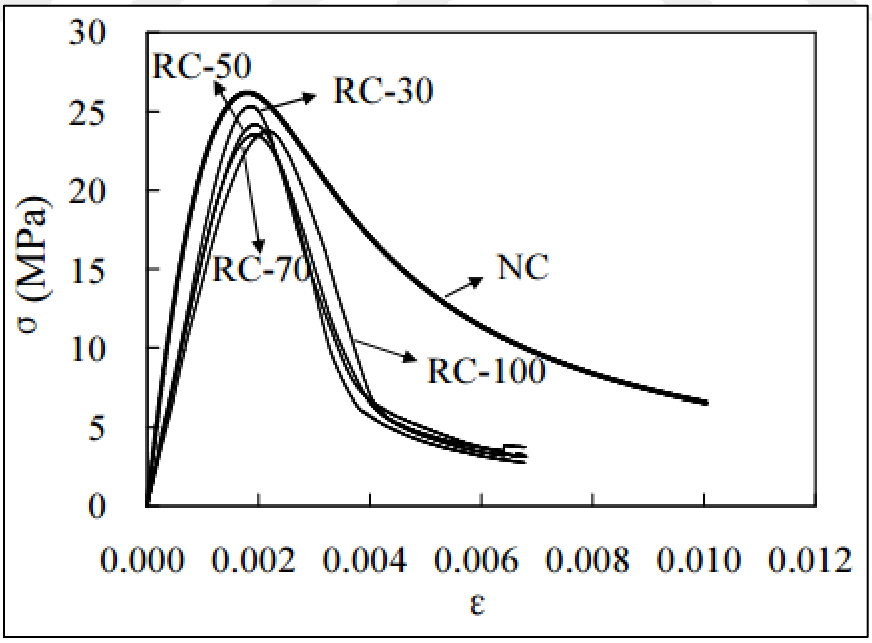

Figure 2.6 Stress–strain relationship of RA concrete at various replacement levels (Jianzhuang et al., 2005)

(Note: as example, RC30 refer to the concrete with 30% RAs and so on)

According to Khaldoun (2007), the peak strain in RA concrete was 5.5% greater than in NAs concrete. However, several previous studies reviewed that the shape of the stress-strain relationship of RA concrete is very similar to counterpart of NAs concrete. For this, RA concrete structures can be theoretically designed in similar way of NAs concrete structures. However, in particular case when strain at peak stress is shown to be excessive, an extra partial safety factor might need to be incorporated into the design process when RA concrete is going to be used in structural concrete.

In general, the shear strength of concrete indicated via the resistance of coarse aggregate for shearing stresses (Wang et al., 2013). Hence in most cases, RAs are relatively weaker than NAs and yielded low shear strength. For NAs concrete, shear cracks initiate in the cement matrix and around the coarse aggregate particles (Angelakos et al., 2001). In this regard, Wang et al. (2013) stated that in high strength concrete (HSC), the matrix is stronger than equivalent CCs and then the formed crack surface becomes smoother because shear cracks pass through the matrix as well as aggregate. Although limited data are available on commercial RAs, it is believed that the behavior and properties of RA concrete in which aggregates were derived from CDW could be different for fresh and hardened properties. Fong and Jaime (2002) estimated that the performance of RAs derived from recycling facility was more consistent than aggregates produced from CDW. However, the strength of the source concrete has small influence on the properties of RA concrete (Khaldoun 2007; Wrap, 2007).

2.3. Fracture Mechanics

2.3.1. General

Fracture mechanics deals with the field of cracks propagation in materials. The solid mechanics analytical methods are employed to compute the driving force on a crack. The resistance of material to crack is evaluating via experimental solid mechanics (Griffith, 1921). Hence, this science investigates the strain and stress around the cracks. In homogeneous materials, cracks propagate as perpendicular direction to maximum tensile stress counter to heterogeneous materials; when it prone to follow the path of the weakest material. In general, the shape of crack potentially will be high irregular when the stress intensity factor (SIF) is almost uniform. The irregularities will stimulate the cracks to slowly growing to a simple shape as well as smoothed out. Hence, due to the relation between SIF and critical energy release rate of the material, the field of fracture mechanics is promising with a great possibility to apply it in the concrete structural design (Bažant, 1998; Shah et al., 1995; Karihaloo, 1995; Van Mier, 1997; Bažant, 2002). In effect, to improve the mechanical performance of materials, fracture mechanics deemed as an important technique in the modern materials science. The physics of stress and strain of materials particularly applies to find the defects of microscopic crystallographic inside the materials and to predict the microscopic mechanical failure of bodies.

Recently, fracture mechanics has reached to the stage which it can be used in the engineering design to avoid the sudden brittle failure of materials such as concrete. Indeed, the properties of materials significantly affected on the mechanical behavior of all materials used in structures. The compressive strength theory is considered in the designing of concrete in application; whilst, the brittleness of materials is neglected. Hence, the brittleness of concrete indicates the determination of the fracture parameters (Akçay, 2007). Generally, fracture mechanics deals with the propagation of a crack and it's interaction with other interfacial cracks. Moreover, it deals with places, formation and state of affairs of failure.

Mainly, there are two theory developed to describe the failure mechanisms, nonlinear fracture mechanics (NFM) and linear elastic fracture mechanics (LEFM). It is well known that the theory of LEFM can be applied in brittle and homogenous materials such as glass but it not efficient for heterogeneous or quasi-brittle materials like concrete; so, NFM deemed as modified state of LEFM (Taşdemir et al., 1999). The introduction of LEFM by Griffith, for homogeneous and brittle materials consider as a turning point for the fracture mechanics theory. Whilst the fundamental initiation of fracture mechanics science conducted by (Kaplan, 1964). In effect, the study of Kaplan, (1964) deemed as the first successful application of fracture mechanics theories accomplished in concrete. The author also pointed out that a LEFM theory is no longer valid to describe the fracture mechanisms for heterogeneous materials like concrete because of the existence of fracture process zone (FPZ). In effect, FPZ is based on assumption that the stress approach infinity at the crack tip (Kaplan, 1961; Mindess and Diamond, 1982; Karihaloo, 1995; Tasdemir and Karihaloo, 2001).

Also, the essential contributions of Orowan and Irwin were based on developing LEFM theory for the case of non-brittle materials (Irwin, 1957).

Until it reaches to the maximum stress, stress–strain curve for a brittle materials are linearly elastic. At maximum stress point, the crack catastrophically initial and propagates leading to failure (Figure 2.9-a). For concrete which is considered as quasi-brittle material, non-linearity essentially exists before the maximum stress is reached (f_y-f_t). However, the mechanisms of deformation are not fully understood after the region of proportional limit (f_y). Firstly, micro-cracks are initiated and distributed randomly leading to localize it into a macro-crack at specific point before the peak stress (Figure 2.9-b). After the attainment of the maximum load, macro-crack critically propagates; also, strain or tension softening could monitored via steady-state propagation of this crack. Under a closed-loop displacement-controlled testing condition, the displacement during the post-peak stage occurred through opening of major cracks. Thus, the tail region of strain softening (CD) is induced by the aggregate interlock and other frictional effects. Thereby, the deformation increases whenever tensile capacity decreased (area of BCD); then, it leads to an increase in the fracture surface area. The practical application of LEFM in concrete is limited and all cement-based materials different behave from these theories (Alaee, 2002). It is worth mentioning that only quasi-brittle material exhibits this kind of behavior (Khalaf and DeVenny, 2004; Murthy et al., 2009).

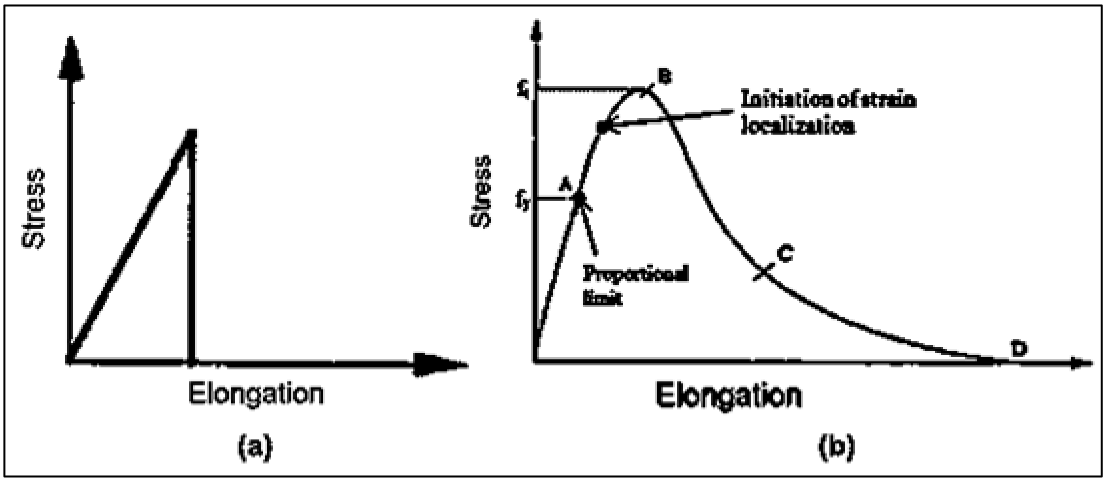

Figure 0.7 The relationship of stress-displacement in tensile state for (a) brittle and homogenous materials (b) non-linear elastic material (Karihaloo, 1995; Murthy et al., 2009)

In effect, FPZ can be defining as the zone where the material undergoes softening damage (tearing). The FPZ significantly influence the fracture behavior of concrete. The plastic flow fracture in concrete and rock occurred next to non-existent and non-linear zone; also, it is quite small and entirely rolled by FPZ. Actually, when the variation along the structure thickness or width is neglected, commonly such materials become quasi-brittle. The inelastic fracture response may be taken into account because the cohesive pressure acting on the crack faces. Indeed, the cohesive pressure occurred due to the presence of FPZ.

In this regard, Figure 2.10 represents the FPZ in linear, non-linear elastic and non-linear quasi-brittle material (concrete) as well as the modeling of materials with LEFM (Karihaloo, 1995; Dugdale, 1959; Bažant, 2002). Actually, Figure 2.10 (b) and (c) represent this model with non-linear plastic and non-linear quasi-brittle fracture mechanics, respectively. Since, (L) letter shown in figure denote to linear elastic material; while, (N) and (F) denote to non-linear material and fracture behavior, respectively (Karihaloo, 1995). Hence, over years, several literatures have been conducted to modify the theory of LEFM and make it applicable for concrete; also, to introduce the theories of NFM. The main differences between the above-mentioned concepts are briefly depicted in Figure 2.10.

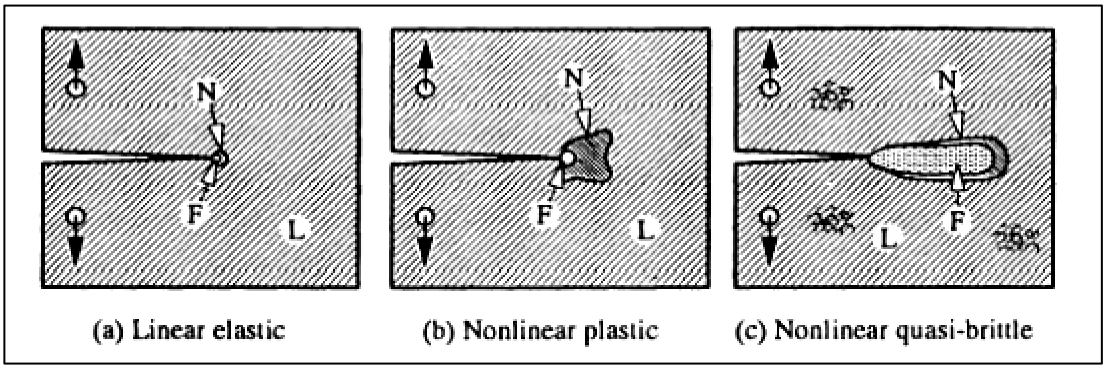

Figure 2.8 Main FPZ modeling with (a) linear elastic fracture mechanics (b) Ductile-brittle (metals) (c) Quasi-brittle (concrete) (Karihaloo 1995)

In order to evaluate the fracture aspects of concrete, the proposed predominant fracture mechanics models based approaches are:

- Model of fictitious crack (Hillerborg, et al., 1976)
- Model of crack band (Bažant and Oh, 1983)
- Size effect law (Bažant, 1984)
- Model of two parameter fracture (Jenq and Shah, 1985)
- Model of effective crack (Nallathambi and Karihaloo, 1990)
- Concepts of boundary effect and local fracture energy distribution (Hu and Wittmann, 2000; Duan et al., 2003)
- Size effect law, two parameter and fictitious crack model (RILEM, 1985)

2.3.2 Fracture Mechanics of RA Concretes

Predominantly, the strength of concrete indicates the quality of concrete and its potential performance and use as an acceptance criterion. However, the measuring of conventional strength parameters such as compressive or tensile strength will not ensure the performance of the concrete structure owing to interaction of pre-existing cracks, the material behavior and geometry of the structure. Hence, the fracture parameters of concrete can present more description of the potential load-carrying capacity of the material in a given structural system (Shah et al., 1995; Bažant and Planas, 1998). Unfortunately, the fracture performance of RAs has not been fully explained in the literature yet; thus; this field can provide further knowledge about the material performance when it use for concrete systems (Bordelon et al., 2008). In RA concrete, almost all fracture parameters recorded lower values than equivalent of NAs concrete. Indeed, the reasons for this probably inasmuch to:

i. The crack needs not to bypass the abundant stiff and hard NAs and select flat path through the material. Moreover, the fracture surfaces of RA concrete specimens are flatter in shape and less tortured than those of CCs specimens. Hence, less grain boundary fractures along aggregates may be observed on RA concrete fracture surfaces. The energy consumption owing to "aggregate bridging" behind the crack tip is reduced as well as the energy needed to create new fracture surface; so that, the resulting fracture energy is reduced.

ii. Aggregates in RA concrete do not have as high fracture resistances as NAs. Therefore the FPZ in front of the crack tip is small; which in addition leads to less energy consumption during crack propagation (Ishiguro and Stanzl-Tschegg, 1995). Furthermore, in the literature of Topçu and Günçan (1995), stress–strain diagram of RA concrete with different replacement level (0%, 30%, 50%, 70% and 100%) was prepared. The result revealed that whenever RAs amount increased, the strength, toughness, elastic modulus, elastic and plastic energy were decreased.

The application of fracture mechanics to RA concrete is still in early stage, particularly for SCCs and other modern concretes. However, plenty of literature investigates the effect of RAs on the fracture and failure characteristics of concrete. Bordelon et al. (2008) examined the fracture behavior of paving concrete made with RCAs, natural coarse aggregates (NCAs) and a blend of both aforementioned aggregates. Moreover, discrete structural fibers were added to each concrete mixture to compare it in accordance with fracture behavior of the CCs mixtures. Thus, several previous researches concluded that RCAs concrete mixtures must be modified by blending them with NAs or adding discrete structural fibers in order to attain similar tensile strength and fracture properties of NAs concrete. The total fracture energy of a RCAs concrete mixture was also improved by 53% by blending it with NCAs. Finally, the fracture behavior of RCA concrete with 0.2% volume fraction of synthetic macro-fibers was similar to NAs concrete for the same fiber dosage; also, for blended of NAs and RCAs concrete. In this regard, Reis and Jurumenha (2011) investigate the fracture behavior of polymer concrete and effect of RAs on the results. In that study, the concrete manufactured via recycled foundry waste in substitution of virgin aggregate. RAs were contaminated with polymer resin from the mold. The results revealed that the use of recycled foundry sand significantly effect on the fracture properties of produced concrete. Moreover, it was reported that utilizing recycled sand might increase the fracture toughness of concrete; whilst, fracture energy was keep unchanged. The authors reached a conclusion that recycled sand might be a good alternative as traditional aggregate. Likewise, the study conducted by Arezoumandi et al. (2014) investigates the effect of different replacement level of RCAs (0, 30, 50, 70, and 100%) on the fracture properties of produced concrete. Results of this study revealed that high replacement level of RCAs mixtures yielded low values of fracture energy. Moreover, aforesaid study plotted the relationship between fracture energy and compressive strength results based on the fracture energy data available in the study of Bažant et al. (2002). Hence, general trend can be notice that fracture energy increase whenever compressive strength increase.

In order to enable the propagation of crack, there are three modes of applying a force (Figure 2.9):

I. Opening crack mode (mode I); tensile stress normally subjected on the crack plane.

II. Sliding crack mode (mode II); shear stress parallel subjected to the crack plane as well as perpendicular to the crack forehead.

III: Tearing crack mode (mode III); shear stress parallel subjected to the crack plane as well as parallel to the crack forehead.

Ishiguro and Stanzl-Tschegg (1995) studied Mode- I fracture behavior of RA concrete. In this study, the authors derived the fracture parameters as well as plotted the softening diagram from the load-displacement curves. The results referred that fracture energy (G_F) and compressive strength of RA concrete was only represented 60 and 76% of equivalent NAs concrete.

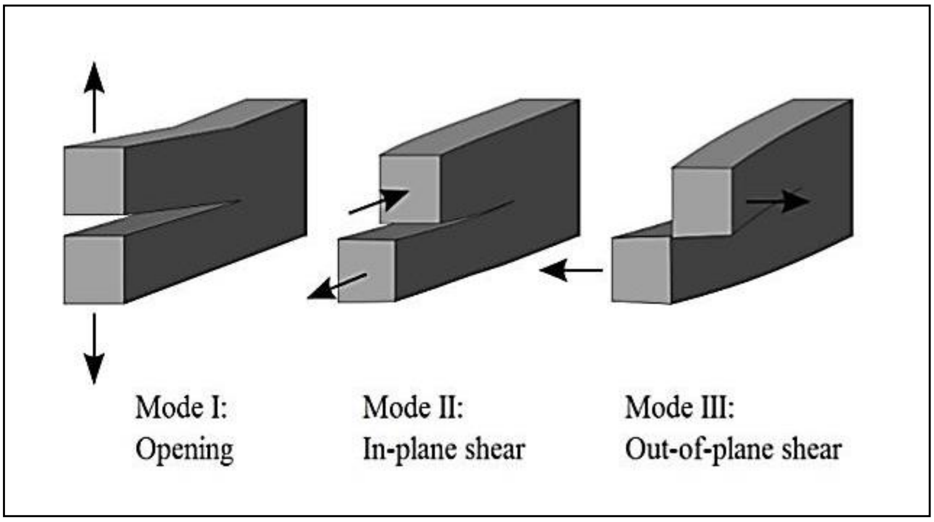

Figure 0.9 Fundamental modes of failure (Karihaloo, 1995)

2.4. Self-Compacting Concretes for Structural Application

2.4.1. General

In construction industry, self-compacting concretes (SCCs) are an innovative concrete which is able to flow under its own weight and completely fill the formwork while it preserving homogeneity even in the presence of packed steel reinforcement. SCCs can flow through and fill the gaps between the reinforcements and corners of molds without need of compaction or vibration (Okamura and Ouchi, 2003). Originally developed to compensate a growing shortage of skilled labor, SCCs has proved beneficial environmentally and economically as well as designing aspects due to a number of factors, such as (EFNARC, 2005):

- Reduced the levels of noise via no need to vibration
- More Safe for environment
- More fast in construction
- Reduce the workers and manpower of the construction site.
- Good surface finishes
- More easy for placing of concrete
- Enhance the durability aspects for concrete
- More free in design and difficult architecture shapes.
- More Thin concrete sections

In CCs, skilled workers need to reach sufficient compaction to make high durable concrete structures. Hence, the lack of skilled construction workers leads to decrease in the quality of construction work. So, the employment of SCCs deemed as a best solution to produce high quality concrete regardless of the quality of construction work. This type of innovative concrete can penetrate into each formwork corner simply with no need to vibration and totally via its own weight (Figure 2.10).

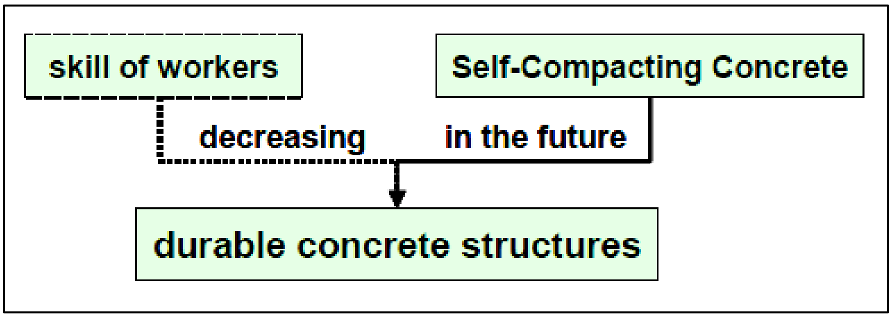

Figure 2.10 Requirements for SCCs (Okamura and Ouchi, 2003)

In Japan 1988, SCCs prototype was completed and performed satisfactorily tests concerning with heat of hydration, shrinkage and durability aspects, densities and other properties (Ozawa et al., 1989). Thus, Aitcin named this concrete as HPC and referred the high durability of concrete due to low water-cement ratio (Gagne et al., 1989). Since then the term HPC has been used to describe high durability concrete. Later, it changed into "self-compacting high performance concrete" (Okamura and Ouchi, 2003). In order to achieve self-compatibility in concrete, sufficient segregation resistance between mortar and aggregate are necessary as well as good deformability for paste and/or mortar (Figure 2.11 and 2.12). For this, Okamura and Ozawa utilize SP in order to decrease water-powder ratio and aggregate content (Okamura and Ouchi, 2003).

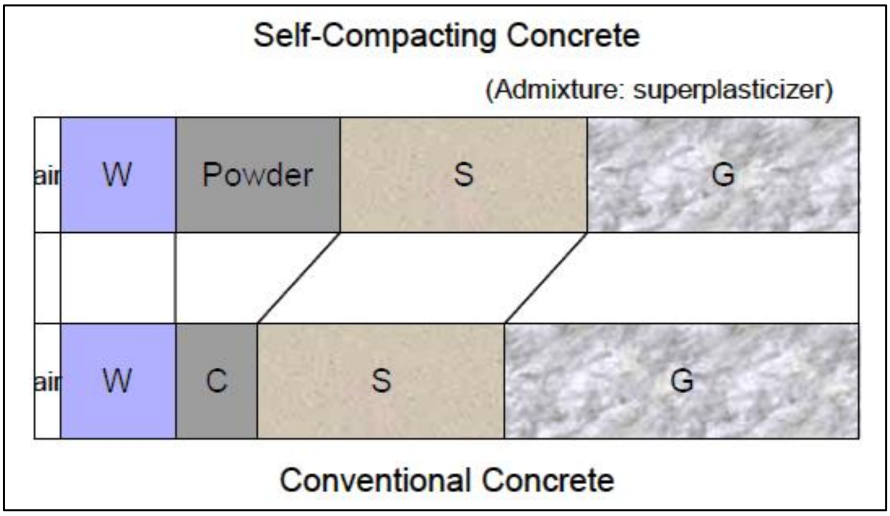

Figure 0.11 Mix-proportioning for CCs and SCCs (Okamura and Ouchi, 2003)

(Note: W,C,S,G denote to water, cement, sand and gravel, respectively)

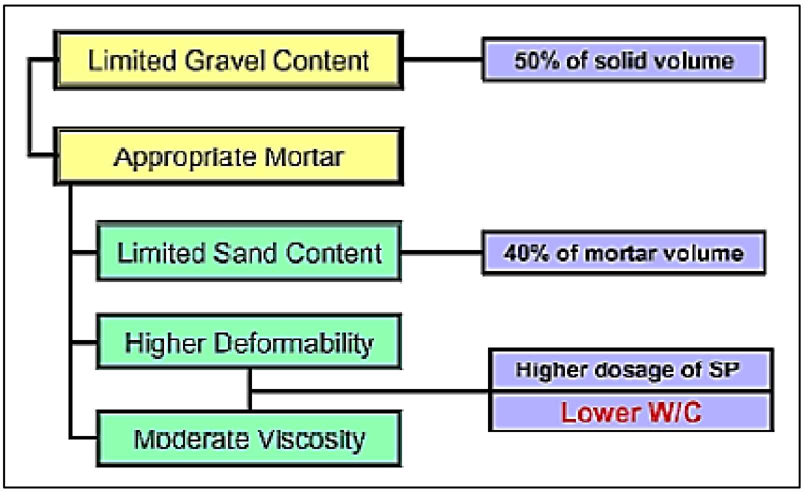

Figure 2.12 Methods to achieve SCCs (Okamura and Ouchi, 2003)

To avoid the blockage occurred in normal concrete, the intense energy consumption induced by coarse aggregate content must be restricted to depressed levels. In this regard, mix-proportioning of SCCs are depicted in Figure 2.13 compared with CCs and roller compacted concrete for dam (RCD) concrete. Obviously, the aggregate content, which requires vibrating compaction, is smaller than CCs.

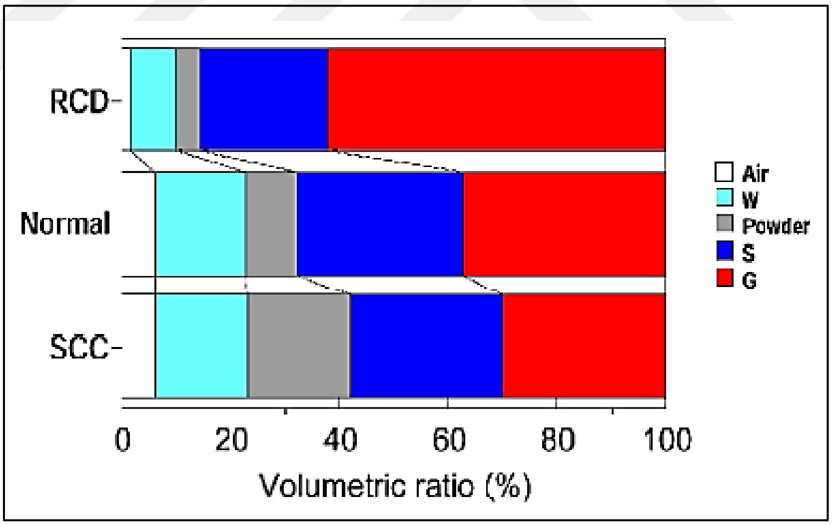

Figure 2.13 Mix proportioning of SCCs compared with other types of concrete (Okamura and Ouchi, 2003)

It is crucial to mention that concrete mix can be classified as SCCs if it fulfilled three requirements, which is recommended by ERNARC (2005) and RILEM technical committee (2006):

- **Filling ability**: the ability of concrete to complete the filling of formwork as well as encapsulate and penetrate into the steel reinforcement network.

- **Passing ability**: the ability of concrete to passing through narrow openings and enclosed spaced of formwork (such as the areas of packed reinforcement and other obstacles) without the concrete blockage caused by interlock aggregate particles.
- **Resistance to segregation**: the ability of concrete to reserve the homogeneity throughout mixing, casting and transportation; moreover, preserver high fluidity without aggregate blockage.

In the other hand, previous literatures such as Grdic et al. (2010) define the filling ability and stability of SCCs by four key characteristics. In effect, the passing ability of concrete, flowability, segregation resistance and viscosity are the most characteristics should be presence in concrete to consider it as SCCs. Hence, the desired properties are reached via adding the chemical additives to the concrete such as SP. In most frequently, SP combined with other types of admixtures such as minerals in order to modify the viscosity; the viscosity of concrete could be enhanced through adding mineral additive-powder (ERNARC, 2005; Okamura and Ouchi, 2003). In this regard, several test methods have been employed in order to characterize the properties of SCCs. According to ERNARC (2005), there is no single or multiple (combination) of methods has achieved to the universal approval. Therefore, more than one test should be conducted for each mix design to evaluate the parameters of workability. Test methods for different parameters are tabulated in Tables 2.5.

Table 0.5 List of test methods for workability properties of SCCs (ERNARC, 2005)

Property	**Test**
Filling ability	Abrams cone Slump flow
	V- funnel
	T50cm slump flow
	L- box
	U- box
	Fill- box
	Orimet
Passing ability	J- ring
Segregation resistance	V- funnel at $T_{5minutes}$
	GTM screen stability test

2.4.2. Self-Compacting Recycle Aggregate Concretes (SCRACs)

In modern day, high workable and as durable as possible versatile concrete demands are rose significantly, particularly for infrastructural needs. Since, the development of SCCs meets these requirements and has proven the significance of this concrete ever since its inception. Hence, the practice of disposing CDW as landfills has changed because of the environmental and economic implications of it. The aggregate used in preparation of old concrete was deemed as inert materials and it is possibly an exploitable resource. For example, in North America and European Union, the concrete waste represents about 50% of total CDW (Reddy et al., 2014). Therefore, exploiting the concrete waste seems a correct selection; where the search for sustainable concrete can be initiated without problem. In general, the basic components of SCCs are similar to those of CCs, in which traditional aggregates such as gravel or crushed stone and river or mining sand used in this concrete. The aggregates as coarse and fine grade are occupy 55–60% of the SCCs volume as well as play an essential role in evaluating the workability, strengths and durability of concrete (Okamura and Ouchi, 2003). Further, the aggregate has a considerable effect on the cost of SCCs. Therefore, less expensive aggregates with satisfactory properties are generally desirable to use in SCCs. Beside the multiple benefits of RAs previously mentioned before, these aggregate can be represent a perfect alternative to meet the environmental requirements as well as to face the scarcity of natural sources particularly in the recent decade. Hence, the use of RAs in SCCs will contribute not only finding a solution for the disposal problem caused by the concrete wastes but also reduce the demand for natural sources; in addition, reduce the environmental impact due to the harvesting and processing of virgin aggregates.

Recently, several researchers had produced SCCs using RAs as partial and full replacements of NAs. These aggregate was used with and without treatment, particularly the aggregate surface treatment. Pioneer work in the field of using RA concrete as structural material was in normal concrete not in SCCs (Limbachiya, 2004). Moreover, several prospects of using RAs in certain different requirements of concrete were also investigated (Tavakoli and Soroushian, 1996-a; Topçu and Guncan, 1995). In these literatures, a decrease in the mechanical properties was revealed in all produced concretes due to using RAs; likewise, the percentage of reduction directly proportional with the amount of these aggregate (Topçu and

Guncan, 1995). Aforementioned, the extent and method of recycling as well as using industrial by products like FA and SF influenced the properties of consequent concrete (Montgomery, 1998; Kou et al., 2011-a). For this, the improvement and enhance the quality of RAs were the major goal for researchers (Ravindrarajah and Collins, 1998). In this regard, Nishio et al. (1998) tested a reinforced concrete column and wall structure produced by SCCs and RFAs derived from dry crushed rock. Afterward, fresh and mechanical properties have been measured at 28 and 91 days; then the following conclusions were revealed that the segregation increased whenever flow distance with increased. Also, compare with CCs, lower values of modulus and higher shrinkage recorded for SCRACs and special care in placing is required to achieve the homogeneity in concrete. Moreover, the drying shrinkage did not lead a deleterious cracking of this concrete. Grdic et al. (2010) studied the properties of SCCs when RCAs obtained from crushed concrete are used. For this, 0%, 50% and 100% substitution percentage of RCAs was used to produce SCRACs. The results revealed that there was slight difference between the properties of CCs and RCAs concrete; also, RCAs can successfully be employed to produce SCCs. In the same regard, Panda and Bal (2013) presented a study of the influence of different amounts of RCAs obtained from CDW (about 25 years old) on the properties of SCCs and compared the results with CCs containing 100% NAs. In that study, NCAs is partially replaced with RCAs by a percentage 10%, 20%, 30% and 40%. Then, the strength properties of produced concrete are investigated. The experimental results indicate that the strength of SCCs decreased whenever RAs replacement ratios were increased. Also, the study recommends SCCs marginally achieves required compressive strength up to 30% replacement of RCAs.

Kou and Poon (2009) used both grade of RAs to produce SCCs and tested it for fresh and hardened properties. The researchers produced three different SCCs mixtures with 100% RCAs as well as different levels of RFAs as a substantial of NAs; while cement content keep constant for concrete. Also, Fonseca et al. (2011) investigate the effect of curing conditions on the performance of RCAs concrete. In addition to strength properties, the analyzing of study include abrasion resistance of SCRACs. In the same context, Salkhordeh et al. (2011) prepared two series of SCCs with 100% RCAs and different percentages of RFAs (0%, 20%, 40%, 60%, 80% and 100%). In this study, the cement content was kept constant at 350 kg/m3, while w/b ratio were

0.50 and 0.45 for series I and II, respectively. Moreover, Nano-Silica was added by 10% of cement weight to enhance the compressive strength of produced concrete. The results revealed that it can be easily produced proper SCCs from RAs; also the adding of Nano-silica to the concrete enhanced the strength properties of it.

Safiuddin et al. (2011-a) used RAs as partial and full replacements of NAs to produce SCCs and investigate the fresh properties of the produced concrete. The replacement level of RAs was 0%, 30%, 50%, 70%, and 100% by weight of NAs. Likewise, w/b ratio and high range water reducer agents (HRWRA) dosage were kept the same dosage for all concretes. The results indicated that SCCs with 30% and 50% RAs were possessed adequate segregation resistance, filling ability and passing ability. Thus, it can be utilize RCAs (more than 50% NCAs) to produce SCCs with no effect on the fresh properties of concrete.

2.5 Composite Columns

2.5.1 General

Eurocode 4, 2004 design code classified composite columns into encased sections (partially or fully) and concrete filled tubes (rectangular and circular), see Figure 2.14. The design code formulas apply for composite columns and composite compression members.

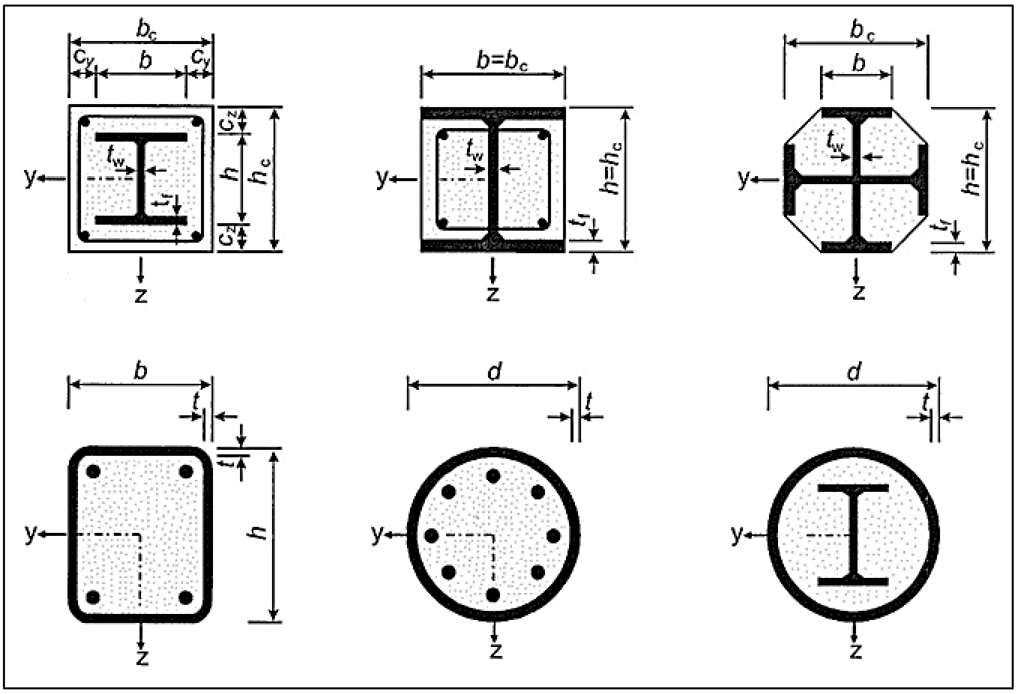

Figure 2.14 The typical cross-sections of composite columns (Eurocode 4, 2004)

The concrete encasement columns either full or partial encased to enhance the performance of the structural core via increase the stiffening; thus, increase the resistance of columns against local and overall buckling (Ketema, 2005). Indeed, columns encased by concrete have one or more rolled steel sections inside the steel structural (Figure 2.15). In this regard, concrete filled steel tube columns also available in multiple steel hollow tube shapes (square, rectangular, circular, etc). As shown in Figure 2.16, the transverse and longitudinal steel reinforcement could reinforce the columns.

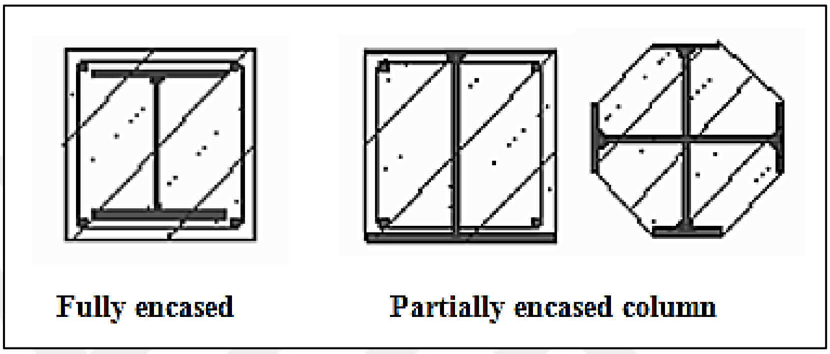

Figure 2.15 Fully and partially concrete encased columns (Ketema, 2005)

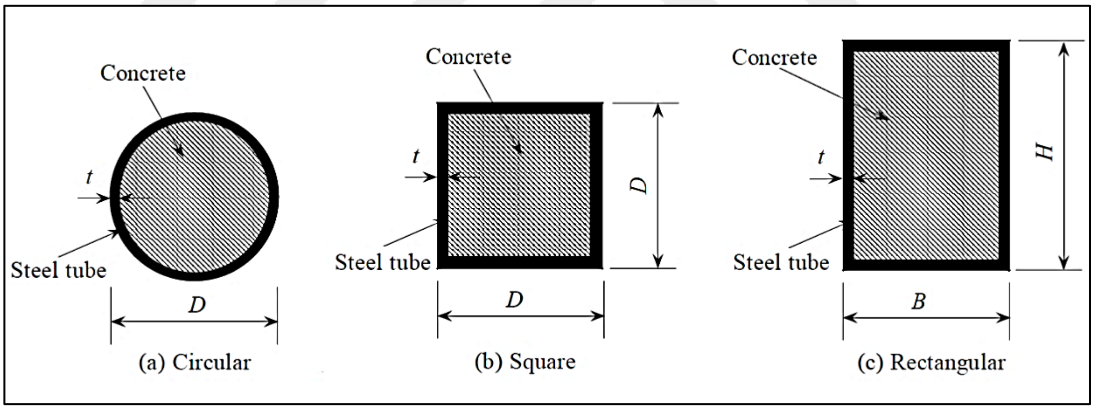

Figure 0.16 The types of concrete-filled steel tube columns (Lu and Zhao, 2010)

In general, Concrete Filled Steel Tube (CFST) structural element consists of concrete (plain or reinforced) in the core restricted by steel tube forming a kind of steel-concrete structures. The wide spread of CFST structure, particularly in columns, attributes to the combined advantages of steel and concrete together. Indeed, the strengths of confined concrete considerably increase due to surrounding it by steel tube; also, the inward buckling of the steel tube is delayed or prevented via presence of concrete core (Jegadesh and Jayalekshmi, 2015). Steel tube not only contributes to the strength of element but also borders the concrete, which eliminates the formwork of concrete; thus, reduces the time of construction (Lu and Zhao, 2010). Hence, the term "composite column" or CFST includes any compression member in which steel and concrete contribute to the strength of structure; where the element of steel acts compositely with concrete (Darshika et al., 2014). One of the first uses of CFST columns in the construction of skyscraper SEG Plaza can be seen in Figure 2.17. In this construction circular CFST column having steel grade of Q345 and infill concrete grade C60 were utilized (Han et al., 2014).

Figure 2.17 SEG Plaza skyscrapers in Shenzhen (Han et al., 2014)

The remarkable increase in the axial load capacity (Pu) of CFST columns leads to reducing the cross-section area of elements as well as the distinct performance of earthquake-resistant characteristics (static and dynamic) (Güneyisi et al., 2016). Therefore, the usage of CFST columns expands to include various structure types such as tall buildings, bridges and subway platforms, etc. (Tsuda et al., 1995; Chen and Chen, 1973; Zeghiche and Chaoui, 2005; Lin, 1998). In CFST columns, concrete core represents 75-98 % of total cross-section area. For this, concrete is a pivotal factor controlling the strength of the output columns. Hence, the determination of concrete type must take into account multiple design considerations as well as the availability of concrete materials. In this regard, recycle aggregate concrete (RAC) could offer a reasonable choice to using it in the field of CFST columns particularly in countries where the natural materials are exhausted (Kou and Poon, 2009). Beside the economic aspects, RAC represents a perfect way to improve the environment via minimizing the concrete waste generated from construction activities (Poon et al., 2007; Safiuddin et al., 2011-b). Indeed, waste recycling is important because it decreases the pollution of nature and it also helps to reuse energy production procedure (Safiuddin et al., 2011-a)]. In effect, the scarcity of natural materials in metropolitan environments as well as the long distance between the source of materials and construction sites compels constructors to substitute the natural aggregate (NA) by the recycled materials (Grdic et al., 2010). In the case of natural disasters such as earthquakes, about 50% of the construction and demolition waste is obtained from solid wastes in urban areas compared with 13-29% in normal situations (Mehta and Monteiro, 2006). Hence, recycling of old concrete and demolition waste can provide a cost-effective method for the construction industry and engineering practice.

2.5.2 Ultimate Load Capacity of CFST Columns under Axial Compression

In effect, theoretical analysis and experimental investigation of maximum load capacity of CFST columns have a significant role in the research and engineering practices. For this, several numbers of studies (theoretical and/or experimental) related with the field of circular CFST columns were conducted in the last few years (Lu and Zhao, 2010; O'Shea and Bridge, 1994; Goode, 1997; Saisho et al., 1999; Giakoumelis and Lam, 2004; Sakino and Hayashi, 1991; Han et al., 2005). Previous literatures investigated the strength aspects as well as D/t ratios of circular CFST columns and/or stub columns. For short CFST columns, the failure occurred either in compressive yielding of steel or crushing of concrete core; while the local buckling occurred in high (D/t) ratio columns (Zeghiche and Chaoui, 2005). Hence, the engineering properties such as diameter-to-thickness (D/t) ratio, length, confining coefficient and slenderness of columns are deemed as crucial and critical (O'Shea and Bridge, 1994; Ghasemian and Schmidt, 1999). For this, literatures with different D/t ratios and combinations of various material properties were conducted and investigated. In effect, Goode (2007) documented a series of databases and compiled 1819 concrete-filled steel (CFT) tests in order to conduct comparison of these databases of circular CFT stub columns. The author also compared the results with Eurocode 4 and concluded that it can be use the results of this code design with confidence and good agreement with test results. Further, the average ratio of Test/EC4 results recorded 1.11. The author suggest that EC4 limitation on concrete strength could be safely extended to fc' = 75 MPa (Figure 2-18).

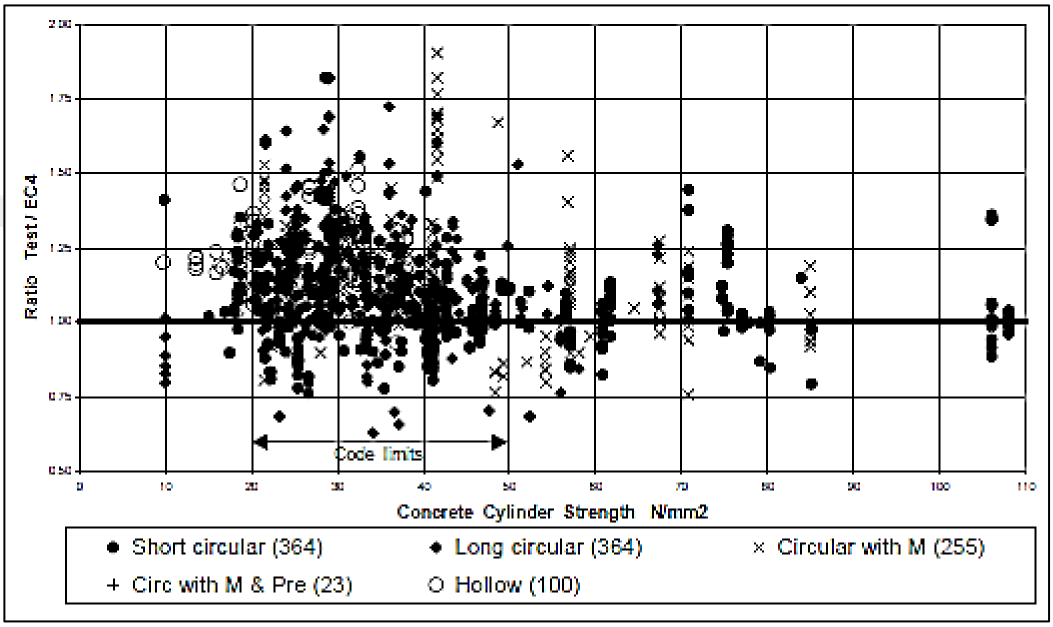

Figure 0.18 The average ratio of Test/EC4 results vs. the strength of concrete of Circular section columns (Goode, 2007)

In similar way, Güneyisi et al. (2016) compared 314 comprehensive experimental data samples extracted from previous studies and prepared a data set for testing the proposed model. The authors predict model by means of gene expression programming (GEP) and compare it with the available models presented in multiple design codes as well as some existing empirical models proposed by several previous researchers. As shown in Figure 2-19, the results of the study revealed that the GEP model was much better than the available formulae (design codes and previous study), yielding higher correlation coefficient and lower error. Moreover, the proposed model exhibit fully satisfactory accuracy to be used for estimation of predicted Pu value; hence, correlation coefficients (R) recorded 0.999 and 0.989, for training and testing databases, respectively.

Lu and Zhao (2010) summarized a total of 250 experimental data of axial load capacity (Pu) for tube CFT stub columns published in previous studies. The authors applied the design codes (ACI, AISC, AIJ, Eurocode 4, DL/T) as well as existing empirical models proposed by previous researchers to calculate Pu value of circular CFT stub columns. The empirical models proposed by authors provided an efficient representation of the ultimate axial strength of circular CFST stub columns; even for high yield strength of steel tube. Moreover, the study suggested limiting values of essential engineering properties such as yield strength of steel tubes, the compressive strength of concrete (fc'), effective length and diameter-to-thickness ratio (D/t) of stub columns. The author believed that the proposed empirical models can easily use by engineers to predict Pu values of CFST stub columns for multiple engineering designs.

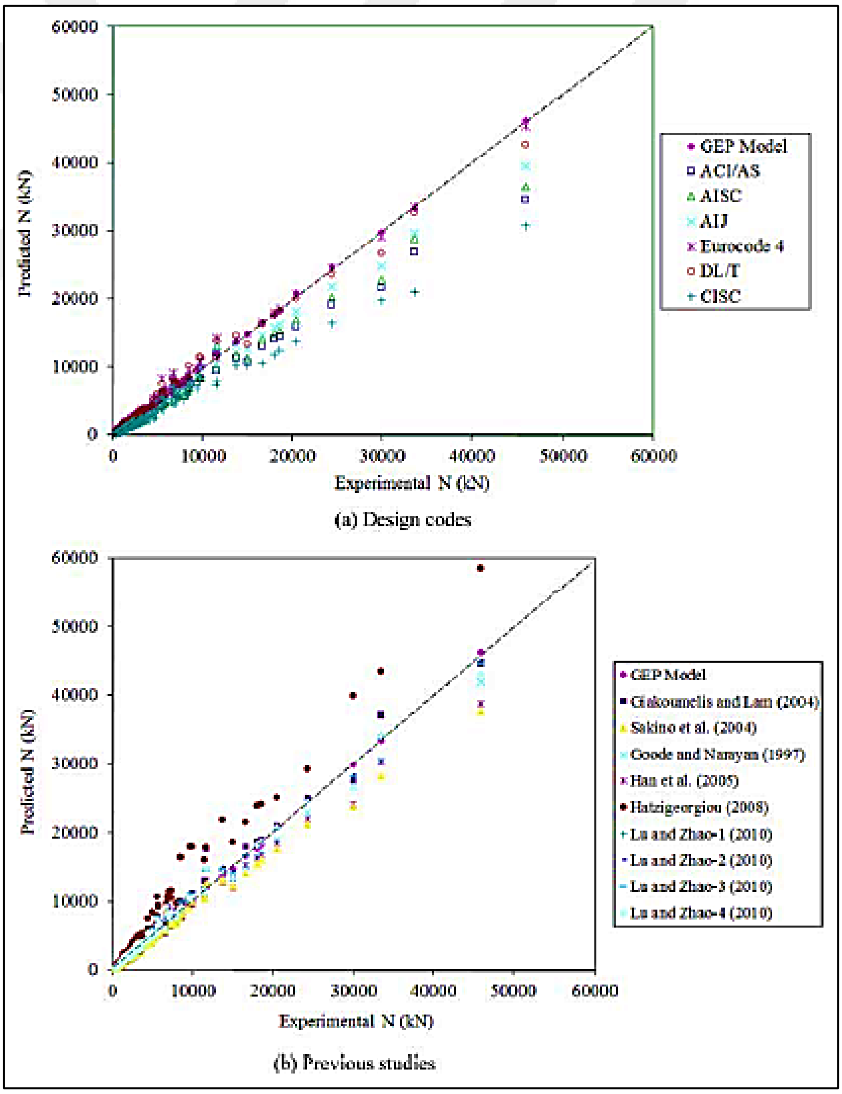

Figure 2.19 The proposed GEP model compared with existing models presented in (a) design codes and (b) previous studies (Güneyisi et al., 2016)

2.5.3 Properties of Recycled Aggregate CFST Structural Members

The aforesaid literatures were undertaken to investigate the structural behavior of steel tube columns filled with CCs. Limited research has been conducted to investigate the effect of RASCC on the predicted axial capacity of CFST columns. Moreover, the studies dealing with full RAs replacement level are also limited. In this regard, Dong et al. (2013) prepared an experimental study to investigate the structural behavior of normal and recycled aggregate CFST columns. The authors employed 22 specimens to investigate the effect of several engineering parameters such as tube condition (square or circular, hollow or solid), concrete type (CCs or RAC) and full wrapping or partial wrapping strengthening arrangements. The study concluding revealed an interesting results that the Pu of for steel tubes filled with RAC showed slightly higher values than corresponding columns filled with CC. The results also indicated that both reinforcing arrangements enhance Pu strength compared with control column, and that the full wrapping arrangement is much more effective than the partial wrapping one. As shown in Figure 2.20, the theoretical study provided and compared the bearing capacity of the composite columns with the experimental results.

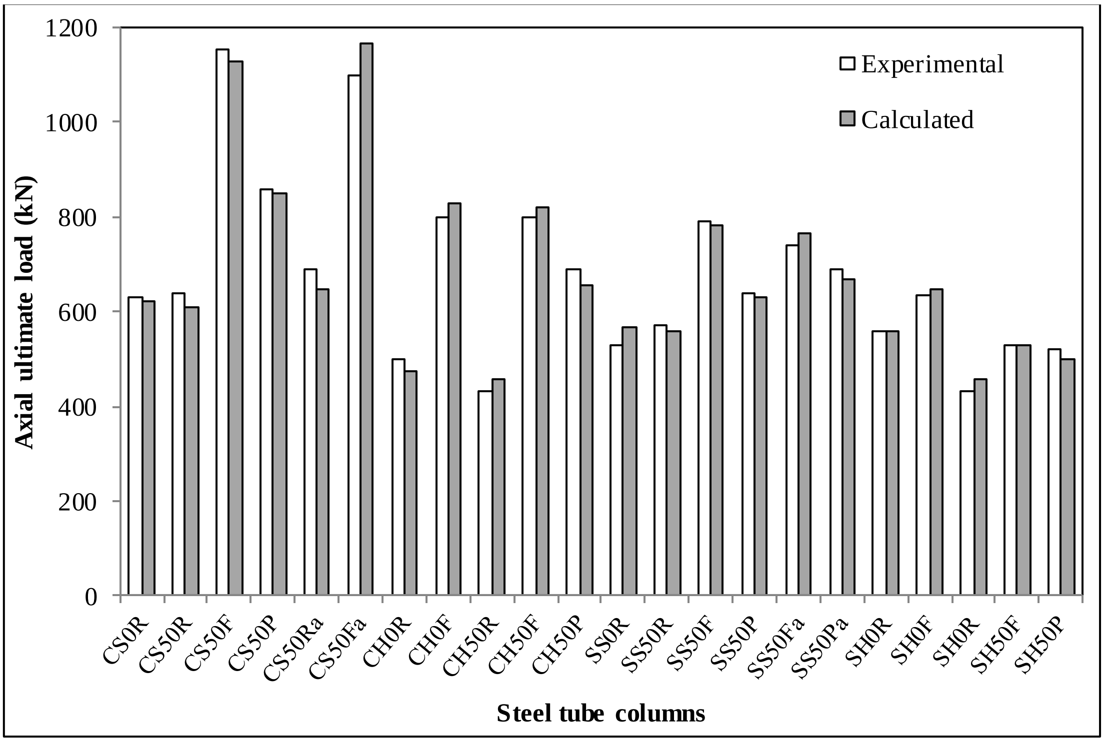

Figure 2.20 The results of Pu vs. experimental results for all CFST columns (Dong et al., 2013)

In the study of Wang et al. (2015), 39 CFST stub columns filled by RAC were prepared and investigated for compressive performance under axial loading. The authors yielded several engineering variables to conducted study; variables such as RAs replacing level, origin of RAs, As/Ac ratio as well as the strength of RAC. The mechanical properties of stub columns filled by RAC showed less scatter results due to the presence of steel tubes. Moreover, about 10% reduction percentage observed for compressive strength of CFST columns filled by RAC. As depicted in Figure 2.21, the RAC source slightly affected the ultimate axial load of CFST columns (Nu). The CFST columns with RAs extracted from two different sources approximately the same axial capacity; about 0.9% variation in Pu was seen. In addition, it was found that the ultimate capacity of the specimens which it filled by concrete strength of 50 MPa was 29% higher than those specimens filled by 35 MPa concrete strength.

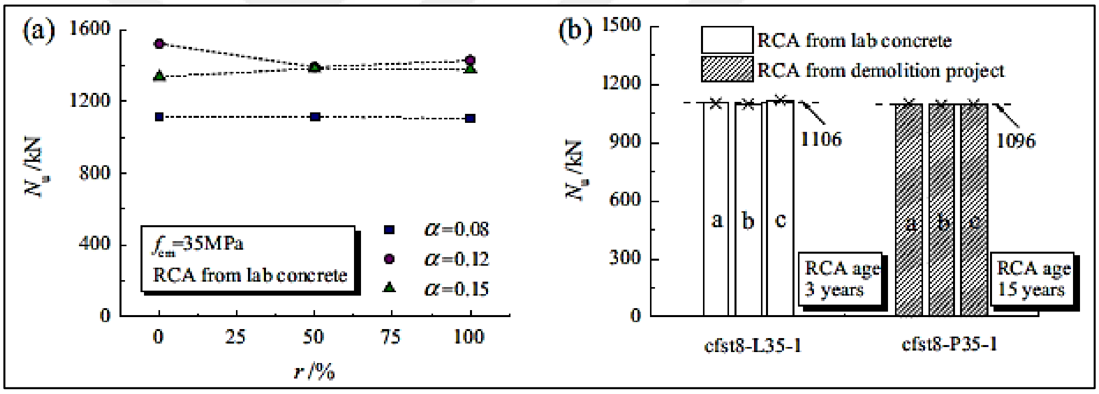

Figure 2.21 The ultimate load performance according to (a) replacement level of RAC (b) sources of RCA (Wang et al., 2015)

Yang and Han (2006) reported that the typical failure modes of RAC columns were similar to those of CFST columns filled with CC; however, RAC columns revealed slightly low results in term of Pu and ductility. The authors experimentally tested total of 40 specimens (30 stub columns and 10 beams) with several parameters like RAs replacement level, circular or square columns section. The main objectives of the study are to investigate the effect of RAs on the compressive and flexural behavior of CFST members filled by RAC. The study emphasized that RAs replacement ratios (0-50%) had no effect on the failure process of the specimens. However, when the applied load reaches 60 ~70% of the ultimate strength, lines became visible at the end of the tube. Moreover, the behavior of CFST filled by RAC is similar to the corresponding columns filled by NAs concrete in the term of compressive and flexural strengths. The values of ultimate strength increase by the range of 1-5% and 2.4-9.4% for the CFST specimens with RAC containing 25% and 50% RAs, respectively. Further, the ranges are 2.2- 5.4%, and 4.8- 9.1% for elastic modulus property (Figure 2.22).

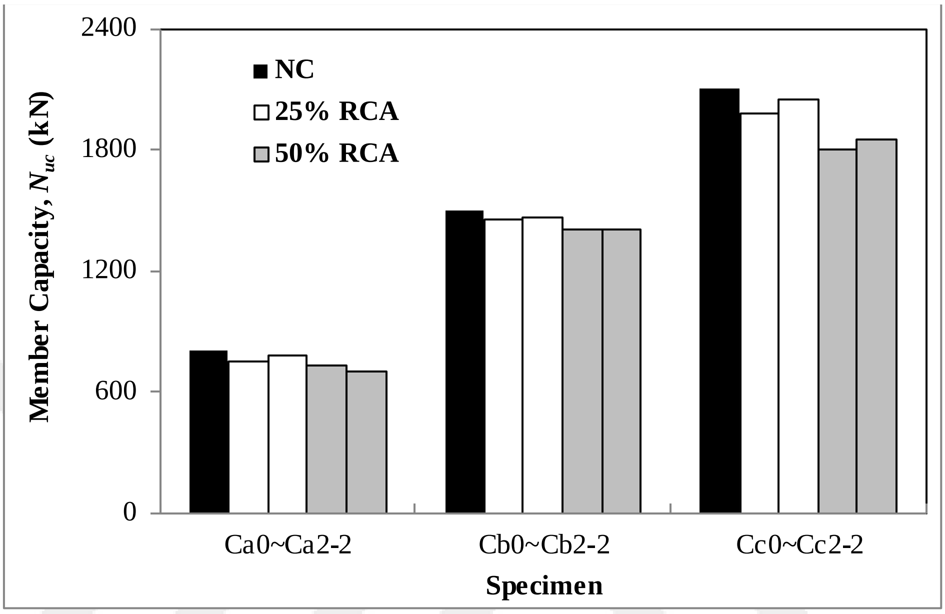

(a)

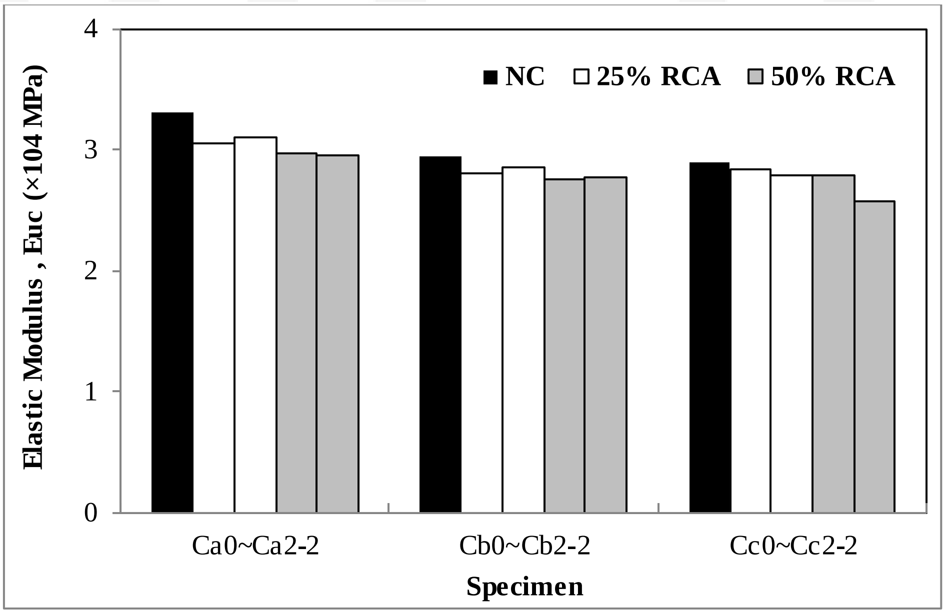

(b)

Figure 2.22 The effect of RAs replacement level on the (a) ultimate strengths (b) elastic modulus of stub columns (Yang and Han, 2006)

Konno et al. (1997) concluded that the ultimate strength of composite column filled by RAC was smaller than those of the confined CC columns; further, the fractures progressed faster. However, Chen et al. (2010) stated that the failure process of RAC was similar to CC filled-circle steel tube columns. In this study, 22 specimens employed to test the mechanical behavior of circular RAC composite columns with multiple parameters such as RAs replacement levels as well as steel confine coefficient. The authors conclude that CFST columns filled by RAC are similar in failure patterns to ordinary concrete-filled steel tube column; in which shear failure occurred in tested columns and the failure patterns like "waist drum-shaped" (Figure 2.23). Moreover, the peak stress slightly increased whenever RAs replacement level increase. The study results revealed that the bearing capacity and the peak strain of CFST columns filled by RAC increased at high steel confined coefficient.

In effect, Yang and Ma (2013) tested 28 specimens of RAC filled stainless steel tube (FSST) stub columns and beams (14 stub columns and 14 beams). The specimens were circular and square cross section area; while the RAs replacement levels were 0, 25%, 50% and 75% for both fine and coarse aggregate grade. The authors observed the failure patterns of CFST specimens and concluded that the replacing level of RAs had little influence on the failure pattern up to and beyond the bearing capacity of the specimens (Figure 2.24). Furthermore, FSST of square specimens had more buckling positions compared with circular section; this behavior was due to the worse confinement of square tube to core concrete. The study revealed that FSST filled by RAC stub columns have stable load-deformation responses and good deformation-resistant ability; further, the performance of RAC as concrete core generally enhanced due to the confinement of the outer stainless steel tube.

Figure 0.23 The failure patterns of CFST specimen columns (Chen et al., 2010)

Figure 2.24 The failure patterns of CFST specimen columns (a) Circular section. (b) Square section. (Yang and Ma, 2013)

CHAPTER III

RESEARCH METHODOLOGY

3.1 Introduction

In this thesis, the experimental and computational studies were considered. In the first part of the study, the experimental program includes an investigation the mechanical and fracture properties of SCCs made with RAs as fine and coarse grade. For this, the program conducted in two stages; firstly, manufacturing RAs via casting CCs and then crushed and sieve it. Secondly, the production of the self-compacting recycled aggregate concretes (SCRACs) was first tested for fresh properties (slump flow, T_{500} mm time, V-funnel time, L-box). Thereafter, SCRACs were tested for mechanical aspects such as compressive and splitting tensile strengths as well as modulus of elasticity. The fracture parameters test was also employed to observe the ductility as well as the brittleness level of concrete.

The second part of the study encompasses the possible use of RA concrete in the composite columns and it's effect on the axial capacity of such columns. For this, four widely used design codes, namely American Concrete Institute (ACI), Eurocode 4 (EC 4), Architecture Institute of Japan (AIJ) and Chinese Design Code for Steel-Concrete Composite Structures (DL/T) were taken into account.

3.2 Materials

In this study, ordinary Portland cement (CEM I 42.5 R), corresponding to TS EN 197-1 (2002) was utilized to prepare all SCRACs specimens produced in this study. The used cement had specific gravity and Blaine fineness of 3.15 g/cm^3 and 394 m^2/kg, respectively. The chemical components of cement are shown in Figure 3.1. While, the physical properties illustrated in Table 3.1.

Ground granulated blast furnace slag (GGBFS) used in the present study was supplied from Iskenderun cement production factory. The utilized slag had a specific gravity and Blaine fineness of 2.79 g/cm^3 and 418 m^2/kg, respectively. The chemical components of GGBFS are also shown in Figure 3.1. While, physical properties given in Table 3.1. Furthermore, silica fume (SF) utilized in the present study was supplied from Norway; it had a specific gravity and specific surface area 2.35 g/cm^3 and 324 m^2/kg. In Figure 3.1 and Table 3.1, the chemical composition as well as physical characteristics of SF is provided.

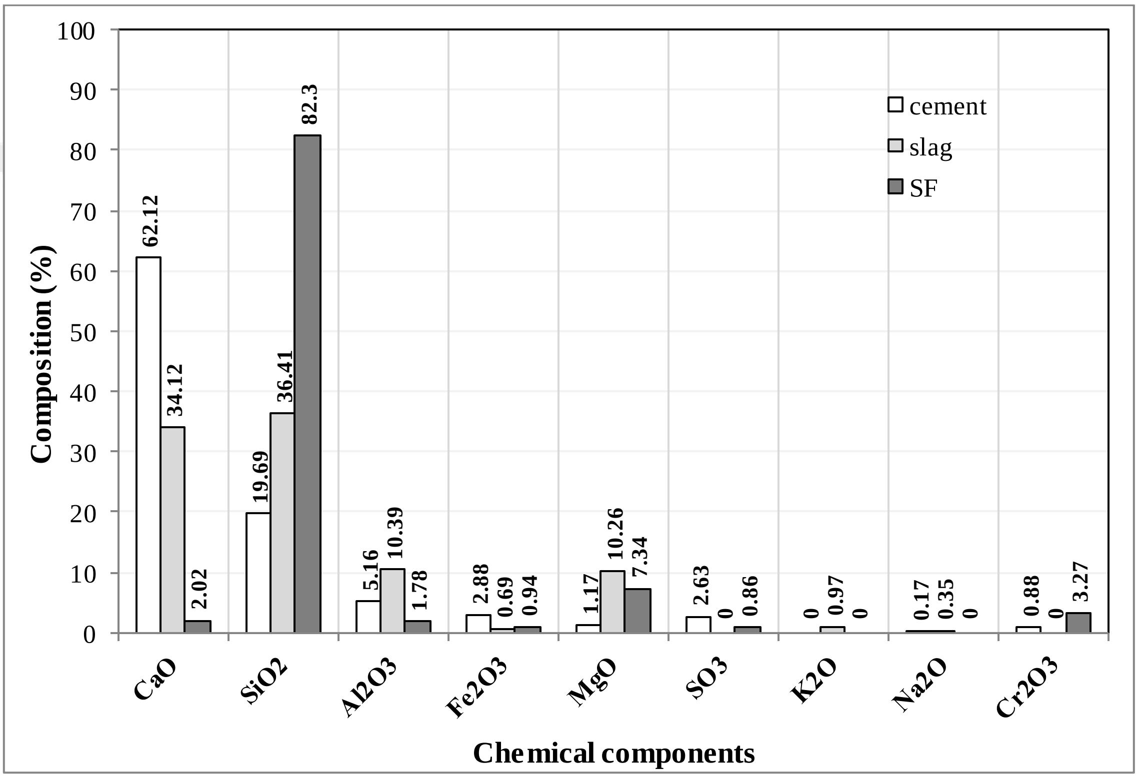

Figure 0.1 Chemical compositions of cement, slag and SF

Table 3.1 Physical characteristics of cement, slag and SF

Physical properties	Cement	Slag	SF
Loss of ignition	0.87	1.64	1.21
Specific gravity (g/cm^3)	3.15	2.79	2.35
Blaine Fineness (m^2/kg)	394	418	324

High range water reducing agents (HRWRA) used in the present study had a specific gravity of 1.07 kg/l; the properties of HRWRA are presented in Table 3.2. Natural aggregates (NFAs and NCAs) were used together with recycled aggregate (RFAs and RCAs) for producing SCCs. Hence, NFAs and NCAs were replaced by RFAs and/or RCAs, respectively to produce 16 SCCs mixtures. In this regard, crushed sand NFAs had specific gravity and fineness modulus of 2.42 g/cm^3 and 2.38, respectively; while, maximum size of 16 mm NCAs had a specific gravity and fineness modulus of 2.73 g/cm^3 and 5.61, respectively. Sieve analysis and physical characteristics of NAs are tabulated in Table 3.3; moreover, aggregate grading in accordance with TS 706 (2009) curve are shown in Figure 3.2.

Table 3.2 Characteristics of High Range Water Reducing Agents (HRWRA)

Properties	HRWRA
Name	Glenium 51
Color tone	Dark brown
Condition	Liquid
Specific gravity (kg/l)	1.07
Chemical description	Modified polymer
Recommended dosage	1-2% (% binder content)

Recycle aggregates (RAs) were manufactured through two stages; the first stage was conducted by producing CCs with strength approximately equal to 20 MPa. The second stage contained crush concrete and sieved to separate it into a fine and coarse aggregate. The physical characteristics of RAs as well as sieve analysis are summarized in Table 3.3. Similar to NAs, the grading of RAs compatible with TS 706 EN 12620 (2009) grading curves are graphically illustrated in Figure 3.2. Moreover, the physical characteristics of the RAs and NAs were determined according to ASTM C127 (2007). Thus, RFAs used in study with size between (0.25-4) mm, specific gravity and 24-hour absorption was 2.11 g/cm^3 and 17.94%, respectively. While, RCAs was with size between (4-16) mm, specific gravity and 24-hour absorption were 2.37 g/cm^3 7.39%, respectively. As shown in Figure 3.3, both RFA and RCA were used in SSD condition to prevent early slump loss of SCCs.

Table 3.3 Physical characteristics of NAs and RAs

Sieve size (mm)	Natural aggregate		Recycled aggregate	
	NFA	NCA	RFA	RCA
16	100	100	100	100
8	100	41.4	100	38.2
4	100	0	97.7	0
2	56.8	0	65.9	0
1	35.0	0	42.3	0
0.5	22.7	0	26.3	0
0.25	16.4	0	17.4	0
Fineness modulus	2.7	5.6	2.5	5.62
Absorption (%)	2.1	0.5	10.9	7.4
Specific gravity	2.42	2.72	2.11	2.37

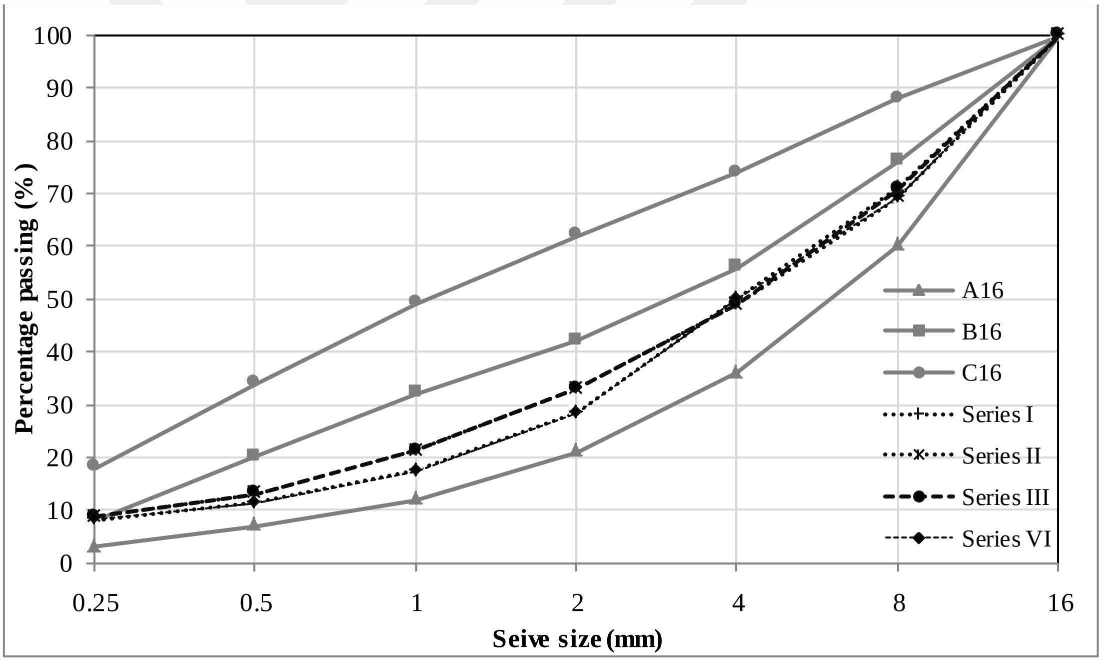

Figure 0.2 Aggregate grading for Series I, II, III and VI mixes

Figure 3.3 RCAs and RFAs in SSD condition

3.3 Mixture Proportioning and Casting

In order to produce SCRACs mixtures, 16 different mixes were prepared via replacing NCAs and/or NFAs by RCAs and/or RFAs, respectively. The mixes were scheduled as four series. Series I mix included 100% NAs, while Series II mixes included RCA and NFA. Series III was made with NCAs and RFAs. Finally, Series IV was produced with 100% RAs (RFAs+RCAs). Each series mentioned above consisted of four mixes. The first and second mixes had a binder content of 570 kg/m^3 and a w/b ratio of 0.30, while, the third and fourth mixes were designed with binder content and w/b ratio of 480 kg/m^3 and 0.43, respectively. In all mixes the GGBFS was used as a replacement for 25% of the total binder content. The volume fractions as well as mix proportion concretes are listed in Table 3.4 In this study, mix codes were determined according to the mixture composition. For example, 0.3RCA100RFA0SF10 indicates that the concrete is design with w/b of 0.30, the RCAs content of 100%, RFAs content of 0% and SF content of 10%.

In effect, RAs previously immersed in water for at least 30 minutes to conduct the SSD condition and to overcome the extreme absorption ability of this aggregate (Gesoğlu, 2004; Gesoğlu, 2007; Gesoğlu, 2012; Güneyisi, 2012). Meanwhile, concretes were mixed in a 20 L capacity pan mixer; further, the mix process follow the procedure of ASTM C192 (2007). Concrete casting sequence started with mixing the saturated surface dry RAs with the binder for one minute and was followed by incorporating NCAs and/or NFAs in the mixer. After homogenizing of the aggregates and the binder for 30 s, HRWRA was added to the mix via dissolving it in the mixing water; moreover, the adding process conducted in two parts to avoid segregation of the contents. Later, concretes were mixed for 3 minutes and further 2 minutes to rest. Finally, concretes were mixed again for 2 minutes in order to complete the sequence of mixing process. In this regard, all concretes produced in this study were designed to correspond a slump flow diameter of 680±30 mm proposed by EFNARC (2005). For this, trial batches were prepared for each mix using different amounts of HRWRA until reach out the desired slump diameter.

Table 3.4 Mix proportions in kg/m3

Mix series	Mix Code	Volume fraction (%)				w/b	Binder	Coarse aggregate		Fine aggregate		HRWRA (%)
		Coarse aggregate		Fine aggregate								
		NCAs	RCAs	NFAs	RFAs			NCAs	RCAs	NFAs	RFAs	
Series I	0.3RCA0RFA0SF0	100	0	100	0	0.30	570	859.8	0.0	765.0	0.0	7.1
	0.3RCA0RFA0SF10	100	0	100	0	0.30	570	851.4	0.0	757.5	0.0	5.9
	0.43RCA0RFA0SF0	100	0	100	0	0.43	480	869.3	0.0	773.4	0.0	5.4
	0.43RCA0RFA0SF10	100	0	100	0	0.43	480	862.3	0.0	767.2	0.0	4.4
Series II	0.3RCA100RFA0SF0	0	100	100	0	0.30	570	0.0	749.2	765.0	0.0	4
	0.3RCA100RFA0SF10	0	100	100	0	0.30	570	0.0	741.9	757.5	0.0	4
	0.43RCA100RFA0SF0	0	100	100	0	0.43	480	0.0	757.5	773.4	0.0	6.1
	0.43RCA100RFA0SF10	0	100	100	0	0.43	480	0.0	751.3	767.2	0.0	5.3
Series III	0.3RCA0RFA100SF0	100	0	0	100	0.30	570	859.8	0.0	0.0	667.0	4
	0.3RCA0RFA100SF10	100	0	0	100	0.30	570	851.4	0.0	0.0	660.5	3.3
	0.43RCA0RFA100SF0	100	0	0	100	0.43	480	869.3	0.0	0.0	674.4	3.1
	0.43RCA0RFA100SF10	100	0	0	100	0.43	480	862.3	0.0	0.0	668.9	5.9
Series IV	0.3RCA100RFA100SF0	0	100	0	100	0.30	570	0.0	749.2	0.0	667.0	4.7
	0.3RCA100RFA100SF10	0	100	0	100	0.30	570	0.0	741.9	0.0	660.5	4.5
	0.43RCA100RFA100SF0	0	100	0	100	0.43	480	0.0	757.5	0.0	674.4	4.1
	0.43RCA100RFA100SF10	0	100	0	100	0.43	480	0.0	751.3	0.0	668.9	3.9

3.4 Test Specimens and Curing

The fresh property tests of produced concretes conducted directly after complete the procedure of mixing. Tests such as slump flow diameter, T_{500} time, V-funnel, L-Box and ICAR rheology were conducted to recognize the key of fresh properties of SCCs. The segregation and bleeding of concrete were checked visually during the test of slump flow conducted. The mechanical aspects such as strengths of compressive and tensile as well as modulus of elasticity of SCCs were also determined in the hardened state. Furthermore, fracture parameters tests had been conducted to provide more descriptions for the potential load-carrying capacity and post-peak behavior of the material in a given structural system.

For typical mixture casting, specimens mainly consisted of:

- Three 150 mm cubes for compressive strength test.
- Three 150 mm cubes for static modulus of elasticity test.
- Three 100x200 mm cylinders for splitting tensile strength test.
- Three 100x100x500 mm notched prisms for fracture parameters test.

It is worth mentioning that all concrete specimens were casted with no need to vibrate and/or compacted. Moreover, the specimens were covered with a plastic sheet to prevent the surface evaporation and it saved inside the casting room for 24 hr. Then, they were demolded and fully saturated cured in water till the testing age of 56 days.

3.5 Tests for Fresh Properties

In general, slump flow defines the filling ability of fresh concrete in unconfined conditions. In the absence of obstructions, slump flow test assess the horizontal flow of concrete. In effect, the diameter of the concrete circle is measure to evaluate the filling ability of the concrete. However, slump test can’t give an indication to the ability of the concrete to pass through reinforcement bars without blocking; but it may refer to the level of segregation resistance. Thus, to measure the slump flow, an ordinary slump flow cone is filled with SCRACs without any consolidating and leveled. The cone is lifted and average diameter of the resulting concrete spread is measured as shown in Figure 3.4.

In this study, slump flow value ranging from 650 mm to 800 mm refers to compacted concrete. In the present study, the diameter of slump flow for all mixtures was kept constant at 680±3 mm; T_{500} time was also measured. Indeed, T_{500} test represent the time taken by concrete to reach 500 mm spread circle; where the lower time indicates greater flowability. EFNARC (2005) specification suggests 2 to 5 sec as T_{500} for SCCs.

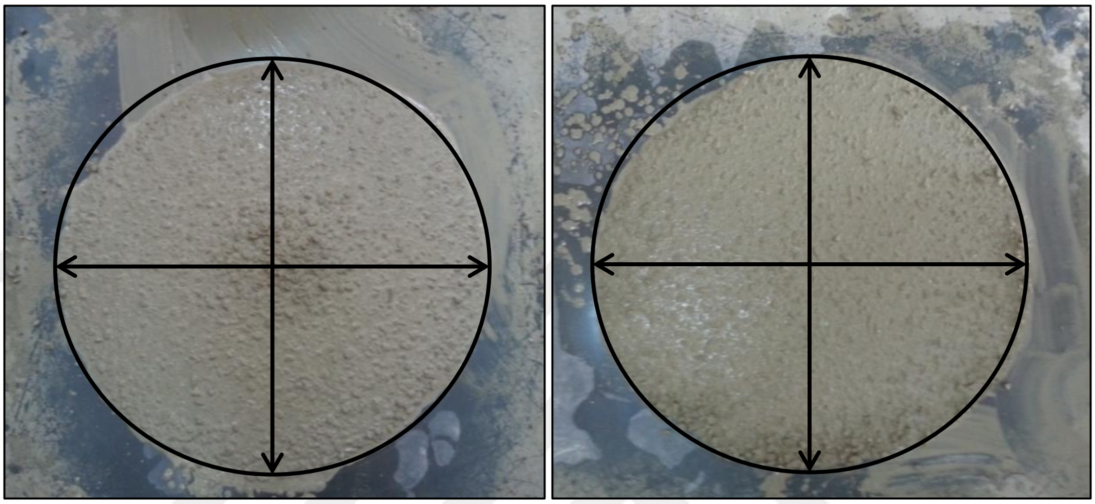

(a) 0.3RCA100RFA100SF0 **(b) 0.43RCA100RFA100SF0**

Figure 0.4 Typical slump flow of SCCs (a) 100% RCAs (b) 100% RCAs

In this regard, Figure 3.5 depicted the schematic representation of the test where the flow time calculated using a simple procedure. Firstly, 12 liter in volume V-shape funnel had been filled by fresh concrete; then the time of flowing is measured as the time between the opening of orifice plate and complete passing of fresh concrete from the funnel. In effect, the concrete can be classified as stable and good flowable concrete when it flows out in short time. In this regard, EFNARC (2005) ranging this time between 6-12 sec for adequate for SCCs. Further, Khayat et al. (1997) recommended flow time less than 6 sec for good qualify of SCCs.

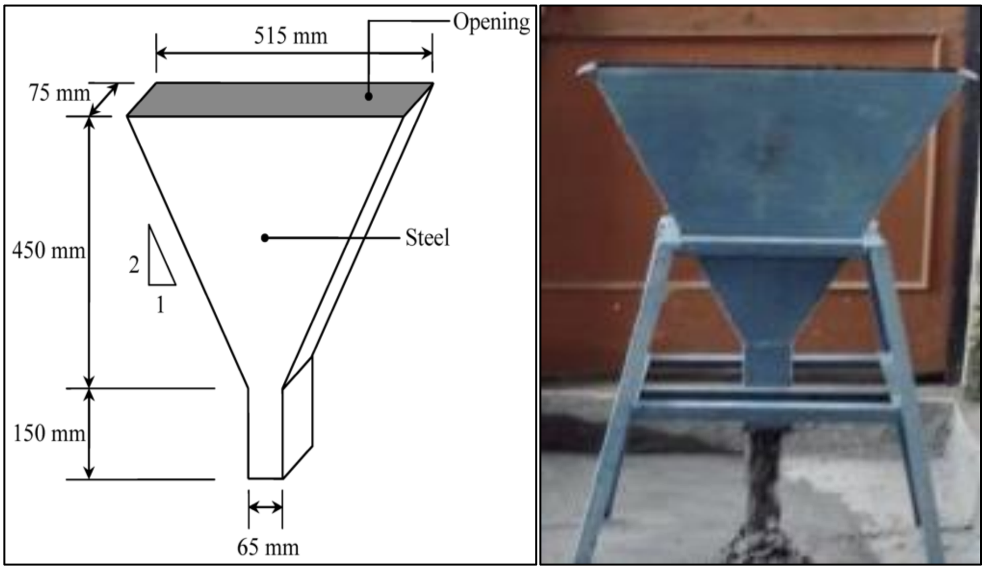

(a) (b)

Figure 0.5 Photographic view of V-funnel test a) Measurement of V-funnel flow time and b) V-funnel tool after it filled by concrete

The test of L-box is employed to assess the flowability of fresh concrete; hence evaluate the filling and passing ability of SCCs. In this test, the lack of stability or segregation can be visually detected as well as the blockage occurred due to presence of reinforcement. In effect, segregation can be observed via subsequently examining fresh concrete in the horizontal section. The test apparatus mainly consists of ‘L’ shape rectangular-section box. Likewise, movable gate are installed in front of rebars of the test tool (Figure 3.6). Moreover, the horizontal part of test box is marked at the distance of 200mm and 400mm from the gate; so, the times that concrete need to reach these points is measured (T200 and T400). Indeed, these times indicate the filling ability of fresh concrete. In this regard, EFNARC (2005) specify the ratio of (H2/H1) as “blocking ratio” and proposed a typical acceptance values in the range of 0.8 to 1.0. In effect, any value closer to 1.0 refers that the concrete can more easily flow than low values.

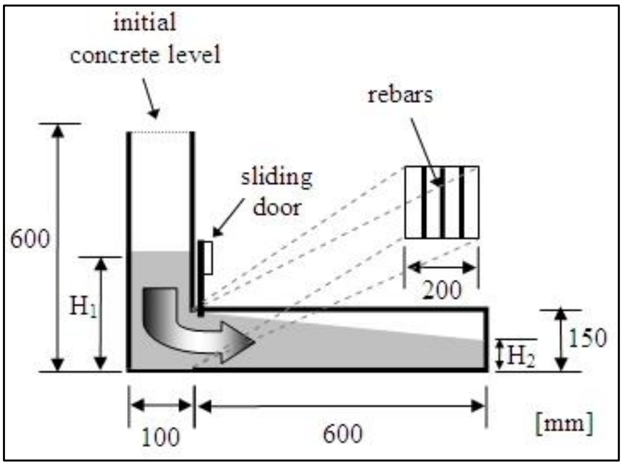

(a) (b)

Figure 0.6 Photographic view of the L-box test a) Measurement of the L-box flow time and b) Schematic representation of the L-box

To perform the rheology test and to calculate its parameters, ICAR rheometer device, of which the schematic details are depicted in Figure 3.7, is employed. Firstly, 30 cm of height and diameter container is filled by fresh concrete. The container includes a series of vertical ribs along the circumference to prevent slippage between the container wall and the fresh concrete during the test (Saak et al., 2001). Due to the ribs presented on the wall, the fresh concrete has the same speed at the surface of cylinder and all other parts of container. Thereby, laminar flow occurs and no slip condition takes place on the walls (Koehler and Fowler, 2004; Wallevik, 2003). Firstly, fresh concrete is placed inside the container and then four-bladed vane of 127 mm height and diameter is positioned in the center of containers. It is assumed that concrete will flow as Bingham fluid where the lateral effects are ignored. Indeed, Bingham model, which is the simplest form of a non-Newtonian model, is satisfying for describing the behavior of fresh concrete.

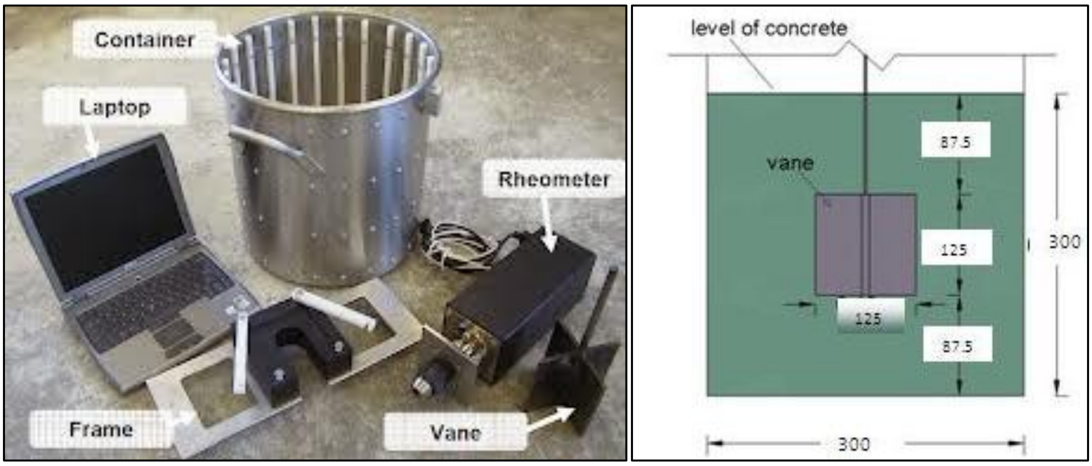

Figure 3.7 ICAR rheometer device including vane and principal dimensions (All dimensions are in mm)

3.6 Tests for Mechanical Properties

In this study, compressive strength of SCCs was tested in accordance with BS 1881-116 (1983) via 2000 kN capacity testing machine. For this, three 150x150x150 mm cubes specimens were employed for each mix. The value of compressive strength was adopted by averaging three tested samples at the ages of 56 days. The test of splitting tensile strength of SCCs conducted in the present study follow the procedures of ASTM C496 (2012); thus, the tensile strength value adopted via averaging three 100x200 mm cylindrical samples of at 56 days.

Static modulus of elasticity was determined in accordance with BSI 1881-121 (1983); in which the specimens was loaded three times to about 30% - 40% of the ultimate load. In effect, the peak load value specified based on the compressive strength results for each mixtures. Further, the modulus was computed as the average of the second two sets of readings to reach more accurate reading. For this, three samples were used for each of the mentioned tests. It is worth mentioning that the load rate used in this test was 1 kN/sec.

In general, the term “fracture parameters” refer to; crack initiation and propagation of small cracks, pattern of load-displacement graphs or crack mouth opening displacement (CMOD), critical stress intensity factor (kic), fracture toughness, fracture energy (G_F) and characteristics length (l_{ch}). In this study, work-of-fracture method (WFM) is employed to evaluate the fracture parameters of produced concrete which is agree with Hillerborg's method in conformity with RILEM recommendations. Hence, fracture energy termed as work of fracture is an indirect surface energy measure of cementitious materials (Hillerborg, 1983). The recommendation of RILEM Technical Committee 50-FMC (1985) had been followed to determine fracture energy. At mid-span of specimens, displacement simultaneously measured via linear variable displacement transducer (LVDT). As shown in Figure 3.18(a), Instron 5500R testing machine with capacity of 250 kN were used to applied the load. Moreover, Figure 3.18(b) shows the prepared beam for the fracture energy tests. The opening notch was achieved through reducing the effective cross section to 60x100 mm via a diamond saw. The notch to depth (a/W) ratio for all specimens was 0.4. Hence, in a single edge notched beams when three points bending tests are performed, fracture energy of specimens can be calculated as (RILEM, 1985):

$$G_F = \frac{W_0 + mg\delta_s \frac{S}{U}}{B(W-a)} \tag{3.1}$$

Where :W_0 is the area under load-deflection curve, m is the mass of the beam, g is the acceleration due to gravity, δs is the specified deflection of the beam, while, S, U, B, W and a are span, length, width, depth, and notch depth of the beam, respectively. For each mix at least five specimens were tested at the age of 56 days; in which the load applies at 0.02 mm/minute rate.

Assuming no notch sensitivity, the net flexural strength, f_{flex}, was calculated by the following formulation (P_{max} is the ultimate load):

$$f_{flex} = \frac{3P_{max}S}{2B(W-a)^2} \tag{3.2}$$

The brittleness of materials in terms of characteristic length, l_{ch}, was determined according to the following expression (Hillerborg, 1983):

$$l_{ch} = \frac{EG_F}{f_{st}^2} \tag{3.3}$$

In which, E and f_{st} are representing static modulus of elasticity and splitting tensile strength, respectively.

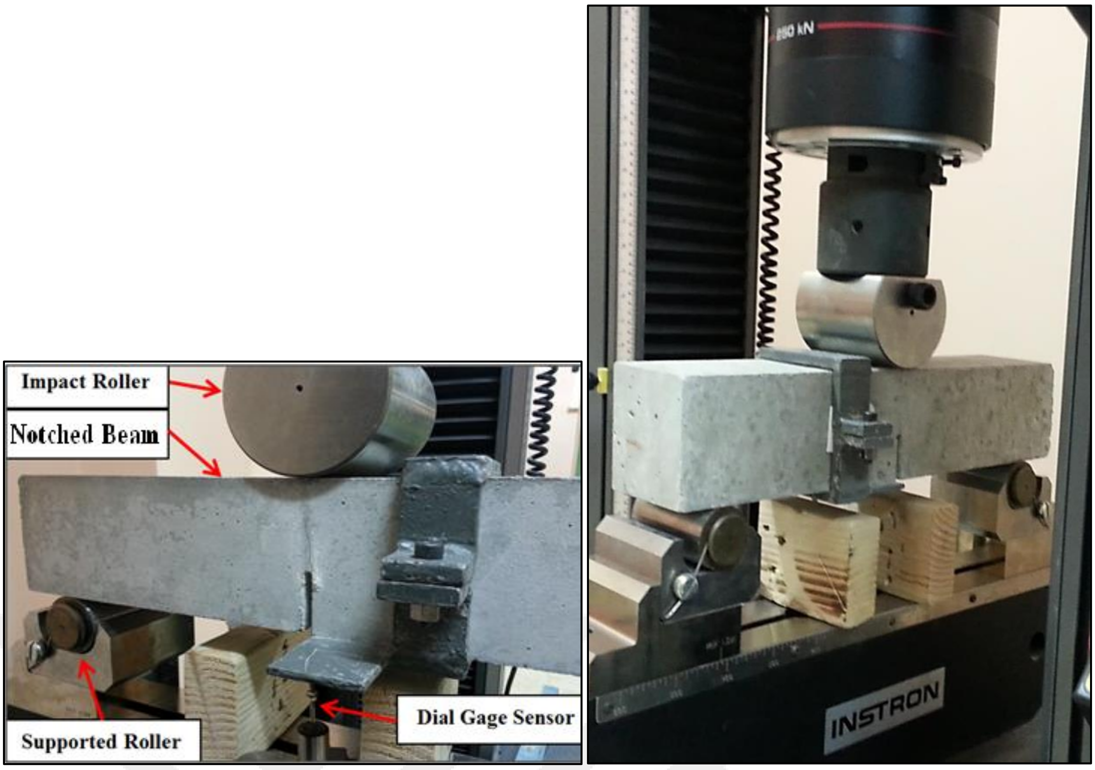

(a) (b)

Figure 0.8 Photographic views of universal testing devices and three point flexural testing machine (a) Schematic for flexural strength and fracture tests, (b) Beam testing

3.7. Computational Study on CFST Columns

In this part, the structural behavior of the composite columns, namely concrete filled steel tube (CFST) columns were studied under the effect of axial compression. Benefiting from a set of experimental data, a total of 400 axial load carring capacity (Pu) test results of the composite columns were calculated via 5 different yield strengths of steel tube (185, 235, 275, 355, 450 MPa) and five different D/t ratios (20, 40, 60, 80, 100). Basically, the test of ultimate axial load considered several important geometric and material properties taken as predictive parameters such as D/t ratio, length of columns (L), the nominal strengths of the concrete (f_{ck}) and steel tube (f_y). The compression test of CFST columns is schematically depicted in Figure 3.9 in which the steel tube was loaded simultaneously with the concrete core. For each investigated code, the test specimens had 3 mm in thickness of circular steel tube and length to diameter ratio (L/D) of 3. The parameters of CFST columns applied in design codes are listed in Table 3.5 below.

Table 3.5 Parameters of CFST columns applied in design codes

Diameter of steel tube	**Diameter of concrete**	**Length of CFST**	**D/t**	**Area of concrete (Ac)** (mm^2)	**Area of steel (As)** (mm^2)	**Concrete moment of inertia (Ic)**(mm^4)	**Steel moment of inertia (Is)** (mm^4)
60	54	180	20	2290	537.2	417393	218780
120	114	360	40	10207	1102.7	8290664	1888096
180	174	540	60	23778	1668.2	44995273	6534700
240	234	720	80	43005	2233.6	147174757	15685406
300	294	900	100	121922	2799.2	1182918397	30867027

The details of mix proportion as well as compressive strength of concrete were imported from Table 3.4; in which totally 16 self-compacting concrete (SCC) mixtures were manufactured and the concrete specimens were 150 mm cubic. The concretes were produced by utilizing NA and/or RA at specific proportions. Moreover, the concrete properties were enhanced by adding silica fume (SF) as mineral admixture for half of mixtures to clarify the effect of this material in concretes. In this regard, the concretes were mixed via two different water/binder ratios (w/b); 0.30 and 0.43. The effect of abovementioned parameters on the Pu results would be observed, compared and discussed in detail.

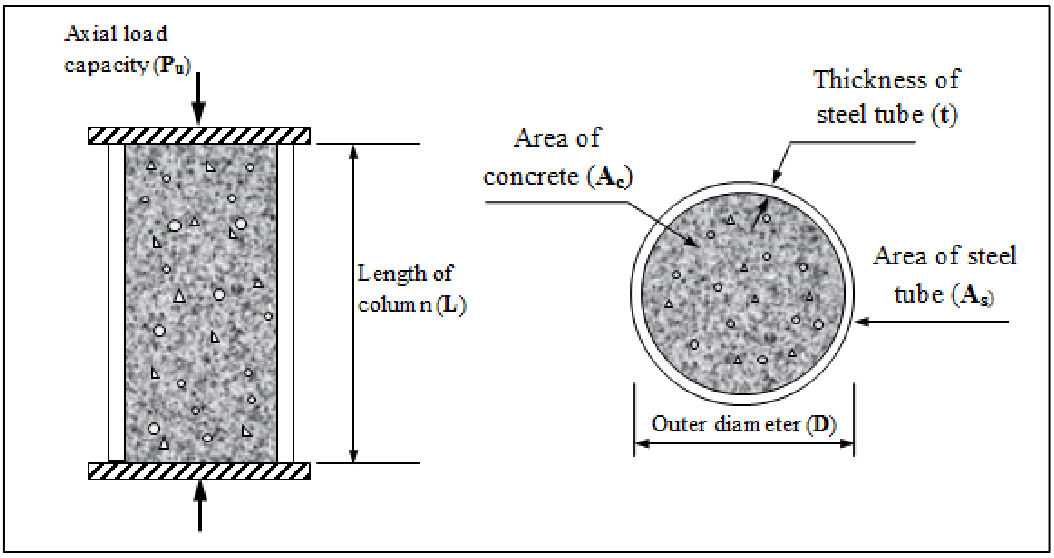

Figure 3.9 Test clarification of load applied to cross section of circular CFST columns

In order to achieve good comparison of the database of circular CFST columns with various codes, the compressive strength of tested concrete (fc') used in codes was generally measured for 150*200 mm cylindrical specimens. However, the results of compressive strength of RASCC were obtained through 150 mm cube test; thus, significant effects on the predicted results would occur. For this, conversion factors proposed by BS EN 206-1 (2000) and DL/T (1999) were yielded to convert these results. It is worth mentioning that BS EN 206 specifies the conversion factors according to classes and weight of concrete; while, DL/T, (1999) specifies 0.67 as a conversion factor regardless of other considerations. The details as well as the conversion factor applied in design codes are listed in Table 3.6 below.

Table 3.6 Characteristics and standard compressive strength of concrete applied in design codes

Mix Code	**Strength of 150 mm cubes (f_c')** (MPa)	**Conversion factor**		**Characteristic strength (f_{ck})** (MPa)		**Modulus of elasticity (Ecm)** (GPa)
		BS EN 206	**DL/T**	**BS EN 206**	**DL/T**	
0.3RCA0RFA0SF0	77.96	0.82	0.67	64.20	52.23	39.81
0.3RCA0RFA0SF10	81.4	0.82	0.67	67.03	54.54	40.27
0.3RCA100RFA0SF0	68.67	0.80	0.67	54.94	46.01	38.20
0.3RCA100RFA0SF10	70.39	0.80	0.67	56.31	47.16	38.45
0.3RCA0RFA100SF0	61.97	0.82	0.67	50.87	41.52	37.44
0.3RCA0RFA100SF10	64.61	0.82	0.67	53.04	43.29	37.85
0.3RCA100RFA100SF0	55.76	0.83	0.67	46.47	37.36	36.58
0.3RCA100RFA100SF10	57.41	0.83	0.67	47.85	38.46	36.86
0.43RCA0RFA0SF0	66.63	0.82	0.67	54.70	44.64	38.16
0.43RCA0RFA0SF10	72.47	0.80	0.67	57.98	48.55	38.75
0.43RCA100RFA0SF0	55.38	0.83	0.67	46.15	37.10	36.52
0.43RCA100RFA0SF10	63.89	0.82	0.67	52.45	42.81	37.74
0.43RCA0RFA100SF0	48.69	0.80	0.67	38.95	32.62	34.99
0.43RCA0RFA100SF10	61.04	0.82	0.67	50.11	40.90	37.30
0.43RCA100RFA100SF0	46.04	0.80	0.67	36.83	30.85	34.51
0.43RCA100RFA100SF10	52.92	0.82	0.67	43.29	35.46	35.93

3.7.1. Calculation of Axial Capacity of Circular CFST Columns Recommended by Design Codes

In order to evaluate the axial load carrying capacity (Pu) results and make a good comparison, a brief review of related standards would be given. The details of relations would also be presented for each design codes. In different codes, several limitation such as yield strength of steel tube (f_y), f_c', D/t, steel ratio and confining coefficient (ξ) are prescribed. Moreover, multiple approaches and design philosophies have been adopted in these design codes.

3.7.1.1. Eurocode 4 (EC 4)

In all design codes, there are circular, square, rectangular and circular hollow CFST structure design regulations. In these regulations, the design methods are different. Moreover, the code must be combining the design approach of both reinforced concrete columns and structural steelwork in order to dedicate the composite construction. In the present study, the formula was designated as EC 4. In Eurocode4, (2004) code, the strength capacity of circular CFST column was calculated through taking in account the contribution of the concrete core and steel tube as well as the confinement effect of steel tube. Indeed, the strength of concrete core increases for circular cross-section CFST columns due to concrete confinement coefficients (ηc) and to the occurrence of a tri-axial state of stress condition. Conversely, the yield strength of steel decreases by the confinement coefficients of steel (ηa) since the hoop stresses cause a reduction in the effective yield stress of the steel. Hence, the axial load capacity of circular CFST columns can be calculated by:

$$P_u = \left(1 + \eta_c \frac{t}{D} \frac{f_y}{f_c'}\right) f_c' A_c + \eta_a f_y A_s \tag{3.4}$$

Because the eccentricity of loading (e) is equal to zero,

$$\eta_a = \eta_{a0} \quad \text{and} \quad \eta_c = \eta_{c0} \tag{3.4-a}$$

For this,

$$\eta_{a0} = 0.25\ (3+ 2\ \bar{\lambda}) \qquad \leq 1 \tag{3.4-b}$$

$$\eta c_0 = 4.9- 18.5\ \bar{\lambda} + 17\ \bar{\lambda}^2 \qquad \geq 0 \tag{3.4-c}$$

$$\bar{\lambda} = \sqrt{\frac{N_{PIR}}{N_{cr}}} \tag{3.4-d}$$

$$N_{P^{IR}} = f_y A_s + f_c' A_c \tag{3.4-e}$$

$$N_{cr} = \frac{\pi\ (EI)_{eff2}}{L^2} \tag{3.4-f}$$

$$(EI)_{eff2} = E_s\ I_s + K_e\ E_{cm}\ I_c \tag{3.4-g}$$

Where:

f_c' is the compressive strength of 150×300 mm cylinder specimens in MPa

f_y is the yield strength of steel tube

A_c , A_s is cross section area of concrete and steel tube, respectively.

$\bar{\lambda}$ is the relative slenderness

$N_{P^{IR}}$ is characteristic value of the plastic resistance

N_{cr} is the elastic critical force for the relevant buckling mode

Ke is correction factor equal to 0.6

I_s , I_c is the second moment of inertia of steel and concrete, respectively.

L is the length of CFT column

E_s is the modulus of elasticity of steel ≈ 200 MPa

It is worth mentioning that the elastic modulus of steel was assumed as 200 GPa, while the modulus for concrete was used as secant modulus of elasticity (E_{cm}) calculated via Eq. (3.7) proposed by Eurocode 2 and 4, (2004)

$$E_{cm} = 22000\ ([fc'+8)/10]^{0.3}) \tag{3.5}$$

3.7.1.2. ACI-318R

Unlike similar codes, American Concrete Institute (ACI-318R, 2005) underestimated the effectiveness of concrete confinement and the interaction between the concrete core and steel tube. For this, the predictive results of axial load capacity are expected to be smaller than comparative codes. The ultimate axial capacity of circular CFST columns can be calculated by

$$P_u = 0.85\, f_c'\, A_c + f_y\, A_s \tag{3.6}$$

3.7.1.3. AIJ (1997; 2001)

In the equation proposed by Architectural Institute of Japan (AIJ, 1997; 2001), the design code adopted a simple method of superposition assumption; where it used the allowable stresses of the materials or working stress method. In effect, the standard classified the composite columns according to the effective length (l_k) to diameter (D) ratio of CFT column (l_k/D); if it was less or more than 4. Moreover, the code took into consideration the confinement factor (η) for the columns, which was independent of the strength of the materials and the dimensions of the columns. For this, the ultimate compressive strength of an axially loaded circular CFST column could be expressed via Eq. (4) for $\frac{l_k}{D} \leq 4$

$$P_u = 0.85\, f_c'\, A_c + (1+ \eta\,)\, f_y\, A_s \tag{3.7}$$

In which

η is equal to 0.27 for a circular CFST column

l_k is the effective length of a CFST column

3.7.1.4. DL/T (1999)

The Chinese code (DL/T, 1999) also used either the allowable stresses of the concrete and steel or the working stress method. In effect, DL/T (1999) code assumes that the composite column is made of one material with a total area of composite columns (A_{sc}) and nominal yielding strength (f_{scy}). Moreover, the confinement factor (ξ) is employed in the standard to describe the superposition composition between steel tube and concrete core. The code introduced the ultimate compressive strength of concrete-filled steel circular hollow-section columns by Eq. (5) as shown below

$$P_u = f_{scy}\ A_{sc} \tag{3.8}$$

In which

$$A_{sc} = (A_s + A_c) \tag{3.8-a}$$

$$f_{scy} = (1.212 + B\,\xi + C\,\xi^2)\, f_{ck} \tag{3.8-b}$$

$$B = 0.1759\ \frac{f_y}{235} + 0.974 \tag{3.8-c}$$

$$C = -0.1038\ \frac{f_{ck}}{20} + 0.0309 \tag{3.8-d}$$

$$\xi = \frac{A_s\, f_y}{A_c\, f_{ck}} \tag{3.8-e}$$

$$f_{ck} = 0.67\, f_{cu} \tag{3.8-f}$$

Where:

f_{ck} is the characteristic concrete strength.

f_{cu} is the compressive strength of 150 mm cubic specimens

ξ is the confinement factor

f_{scy} is the nominal yielding strength of the composite section

A_{sc} is the area of composite section

CHAPTER IV

RESULT AND DISCUSSIONS

4.1. Fresh Properties

It is crucial to maintain high flowability and good segregation resistance of concretes to ensure readily flowability around obstacles as well as to achieve good filling capacity (Khayat and Mitchell, 2008). For a given application, the fresh requirements of SCCs can be chosen from one or more of the aforesaid characteristics and then specified by class or target value. In the same regard, it was observed that almost all mixes showed no bleeding and segregation even for the 0.3RCA100RFA100SF0 and 0.43RCA100RFA100SF0 mixture containing 100% RAs for w/b of 0.3 and 0.43, respectively (Figure 3.4). In this study, all SCCs mixes designed to target slump equal to 680±30mm, which agree with EFNARC standard specification for SCCs. In EFNARC (2005), at least 650 mm slump flow diameter is required to consider the concrete as SCCs. In effect, high value of slump flow indicates that concrete have a good ability to fill formwork with no need to vibration and compaction. As shown in Figure 4.1, all SCCs produced in this study were in SF2 region, which refers to the moderate slump flow value.

In general, SCCs with RAs needed less HRWRA than control mixes (when NAs were used) for a given target slump flow diameter. For example, 8.02% of HRWRA was used in a control mix (0.3RCA0RFA0SF0) to get a slump flow diameter of 670 mm whereas the mix 0.3RCA100RFA100SF0 (when both RFAs and RCAs were used) gave approximately the same slump with 4.39% of HRWRA (Table 3.4). T_{500} slump flow time and V-funnel time of produced SCCs were presented in Figure 4.2. These parameters can be used to evaluate the filling ability of SCCs (Koehler and Fowler, 2004). Slump flow time of all produced concretes was less than 4 sec. It was obvious that the increase in w/b ratio lead to less viscose concretes; thus, these concretes had low flow times. For instance, T_{500} slump flow time and V-funnel flow time for the control mix (RCA0RFA0SF0) for w/b of 0.3 were 3.05 and 14.34 sec. respectively, compared with 2.45 and 9.74 sec. for the same mix with w/b of 0.43. These results are in agreement with those that many researchers have observed (Safiuddin et al., 2011-b; Khayat, 1999; Alam et al., 2013; Kou and Poon, 2009; Özbay, 2007).

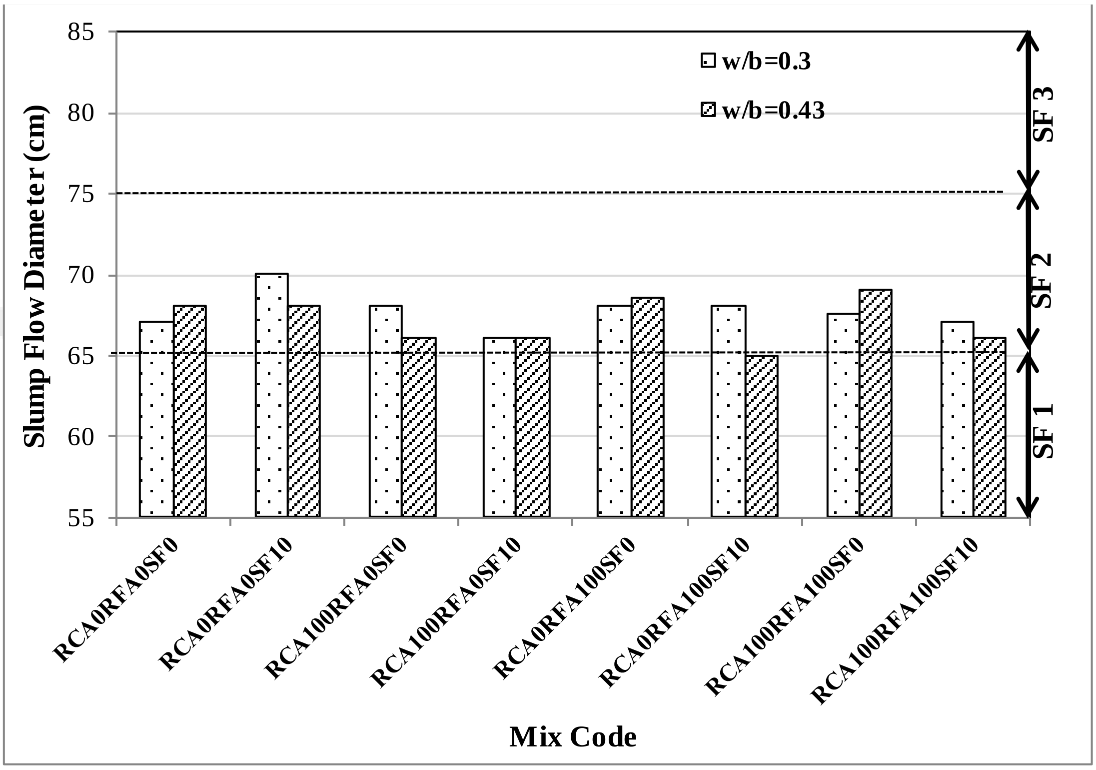

Figure 4.1 Slump flow diameter as well as slump flow classes for structural SCCs

In order to compensate high absorption ability of RAs, concerts need to add more mixing water than NAs mixes; therefore, initial slump flow time decreased (Kou and Poon, 2009). In the present study, the use of RCAs had a little effect on the decreasing of T_{500} slump flow and V-funnel flow times which conformity with several researchers result (Grdic et al., 2010; Kamal et al., 2013; Safiuddin et al., 2011-b). The previous literatures reported that there is significant reduction in the filling ability for 100% RCAs mixes because of the increase in the amount of post-mixing fine aggregate.

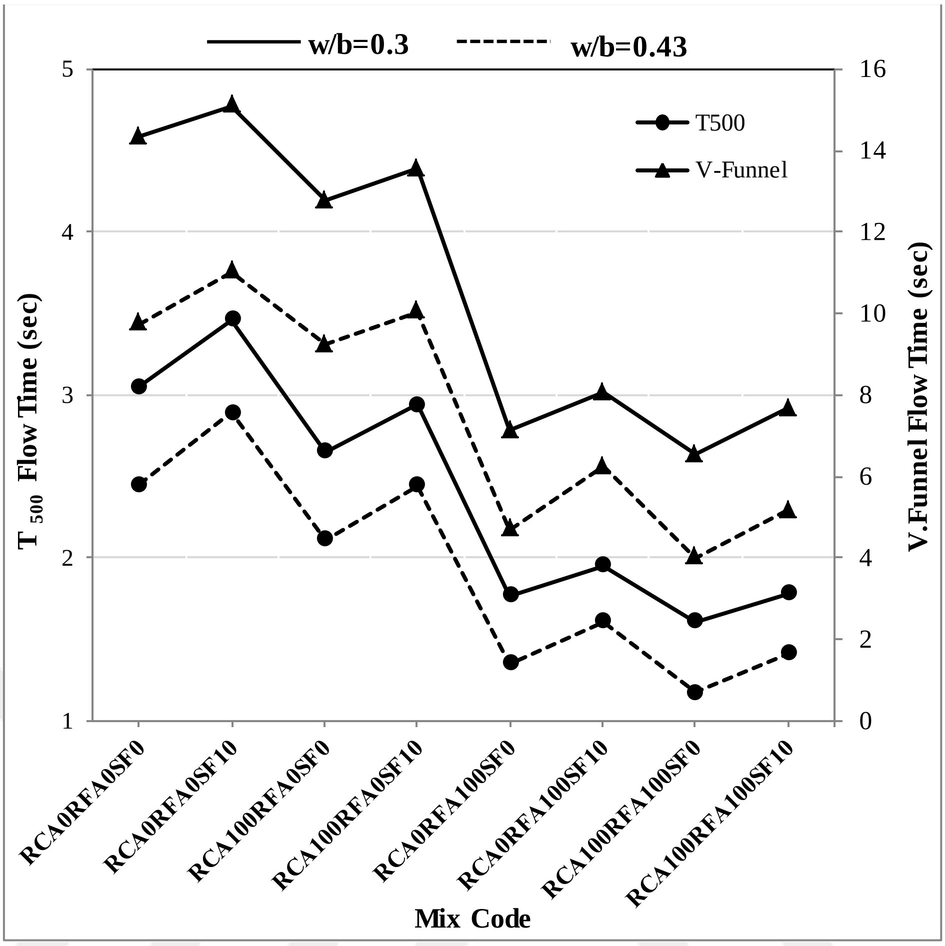

Figure 4.2 Variation of T500 flow time and V-funnel flow time

In this study, 10% SF incorporated with the mixture had effected on the filling ability of SCCs. For example, as compared with the control mix (RCA0RFA0SF0), SF causes an increase in T_{500} time and V-funnel time by 9.86% and 13.4%, respectively. This result was approved by Khayat (1999) which was indicated that the internal resistance to flow increased due to solid-to-solid friction; thereby the deformability and speed of flow of the fresh concrete might be limited. As obviously seen in Figure 4.3, series I and II were classified as VS2/VF2 while the other series (III and IV) were in the category of VS1/VF1. The lack in cohesion resulted from higher water content normally occurred in RA concrete, particularly when RFAs aggregate are used. In effect, EFNARC (2005) consider class VS2/VF2 concretes proper to use for walls/columns and ramps; in which it faced SF2 class in slump flow. Moreover, class VS1/VF1 concretes deemed as suitable for wide span slabs construction.

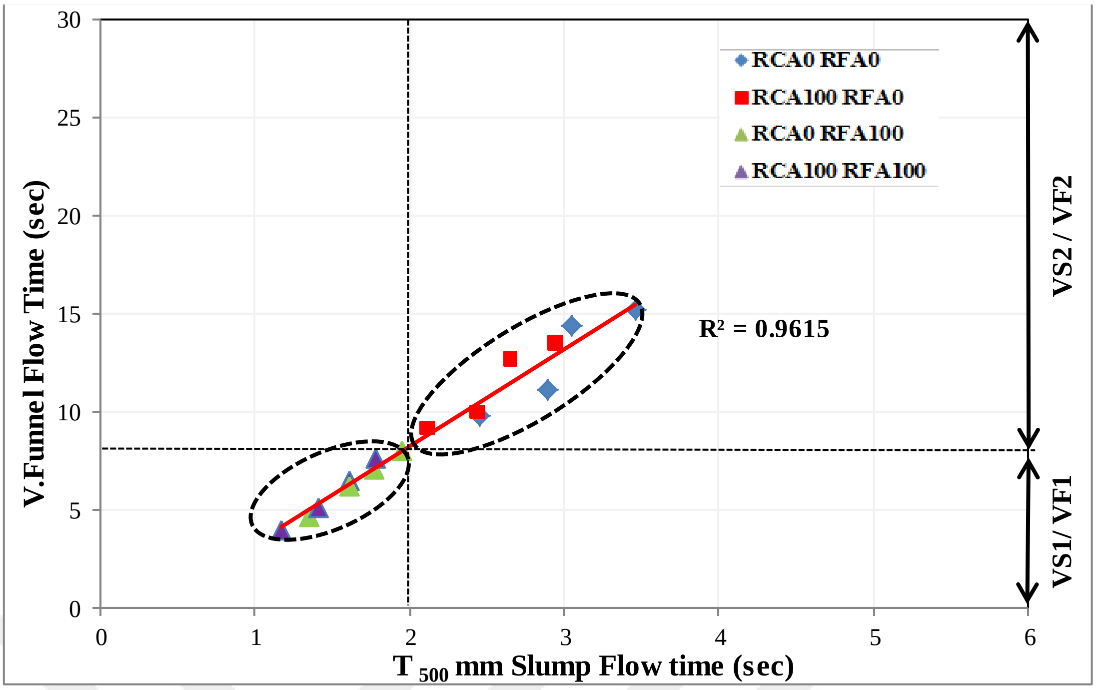

Figure 4.3 Variation of T500 flow vs V-funnel flow times

Passing ability of the SCCs was measured by means of the L-box test. The test provided the parameter of the ratio (H_2/H_1) as flowability measurement of concrete between reinforcing bars. The results of L-box height ratio (H_2/H_1) are presented in Figure 4.4. The H_2/H_1 ratio value mainly varies according to the properties of aggregate used in concrete as well as incorporating of SF and w/b ratio. The ratio of H_2/H_1 was in the range of 0.846 to 0.995 for concretes made with 0.3 w/b ratio, compared with 0.820 to 0.911 for 0.43 w/b ratio. Thus, all SCCs produced in this study were generally satisfying with EFNARC (2005) recommendation for the passing ability in terms of L-box test.

In the present study, the highest value for each series was 0.881, 0.935, 0.995, and 0.990 for series I, II, III and IV, respectively. Indeed, the rising in H_2/H_1 ratio refers to decreasing of viscosity and cohesiveness of concretes (Khayat, 1999; Grdic et al., 2010; Kamal et al., 2013; Safiuddin et al., 2011-b; Özbay, 2007). However, RFAs concrete mixtures were more effective on L-box high ratio than other SCCs.

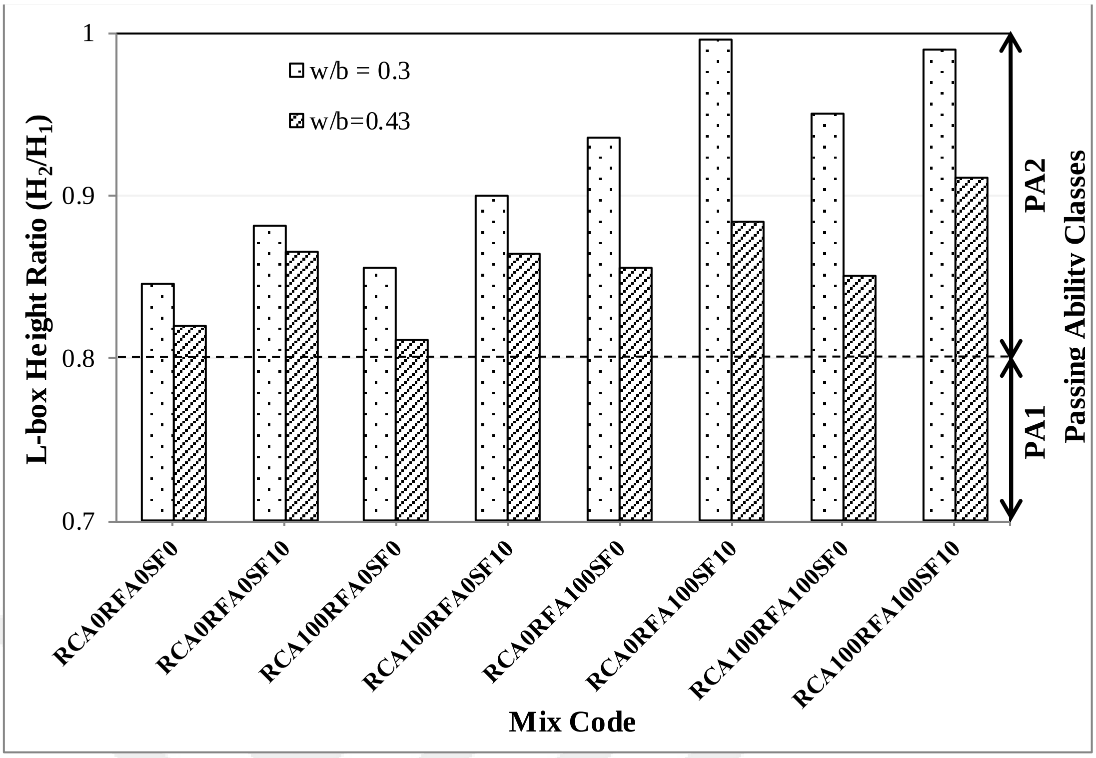

Figure 4.4 Variation of passing ability classes with L-box height ratio

The results of L-box test revealed that whenever SF presented in mixtures, the ratio of H_2/H_1 would be decreased. In this context and for 0.3 w/b mixes, the mixes containing SF recorded constant decrease for all concretes produced in this study. This behavior is due to the fact that utilizing continuously graded cementitious materials fillers like SF make the concrete more cohesive (Wang and Li, 2012). Figure 4.5 (a, b, c and d) represented the rheology behavior for SCC Mixes for series I, II, III and IV, respectively. It was observed that series I mixes showed the highest amount of torque at a constant speed equal to 0.6 (rev/s) compared with other series. Indeed, the torque decreases whenever water content increases. Mix 0.3RCA0RFA0SF0 demonstrated the highest torque value by 1.8 N.m while the minimum torque value was 0.62 N.m for mix 0.43RCA100RFA10SF0 when w/b used was 0.43. Additionally, the presence of SF in the mixture causes an increase in torque (Banfill, 2006; Nielsson and Wallevik, 2003; Koehler and Fowler, 2007; Wang and Li, 2012). A conspicuous example for this case is the increase in torque recorded for mix 0.3RCA0RFA0SF0 and 0.43RCA0RFA0SF0 due to incorporating SF. It was 14.74% and 8.3%, respectively. Aforementioned, the density of the RAs is lower than equivalent of NAs, and the water absorption value also high. If the paste viscosity is so low, the aggregate become more pronounced to migrate towards the surface due to the low density leading to troubles in workability (Tattersall and Banfill, 1983). In the present work, and inasmuch of using an adjusted amount of HRWRA, the slump flow of the SCCs mixtures has been controlled.

It was observed that series I and II behaved as a shear thickening concrete as well as constant reduction in viscosity; while, incorporating RFAs in series III concretes minimize the effect of shear thickening (Figure 4.5-c). Indeed, RAs cause a reduction in plastic viscosity and increase the possibility of concretes to exhibit shear thickening behavior. However, the most significant effect of using RAs in SCCs was observed in Figure 4.5-d for series IV concretes; in which almost all this series concretes showed a Bingham's behavior particularly at high shear rates. In fact, 100% RA concrete behaved as Bingham's material at low and high shear rates. The importance of shear thickening emerge in operations happened at high shear rates like mixing and pumping of concrete.

In the present study, series I concretes showed very low values of yield stress (0.1 Pa) indicating that there is no discernable trend for this parameter. This behavior may be attributing to the constant slump flow diameter which it kept for all concretes. In this regard, Feys et al. (2008) and Nielsson and Wallevik (2003) also approved this conclusion that lower than 10 Pa yield values could be negligible. In this study, all mixes showed yield stress near to zero for series I and II, while yield stress of series III and IV were changed between 6.9-26.3 and 28.3-29.8 Pa, respectively. However, Figure 4.6 displays the plastic viscosity of concretes produced in this study.

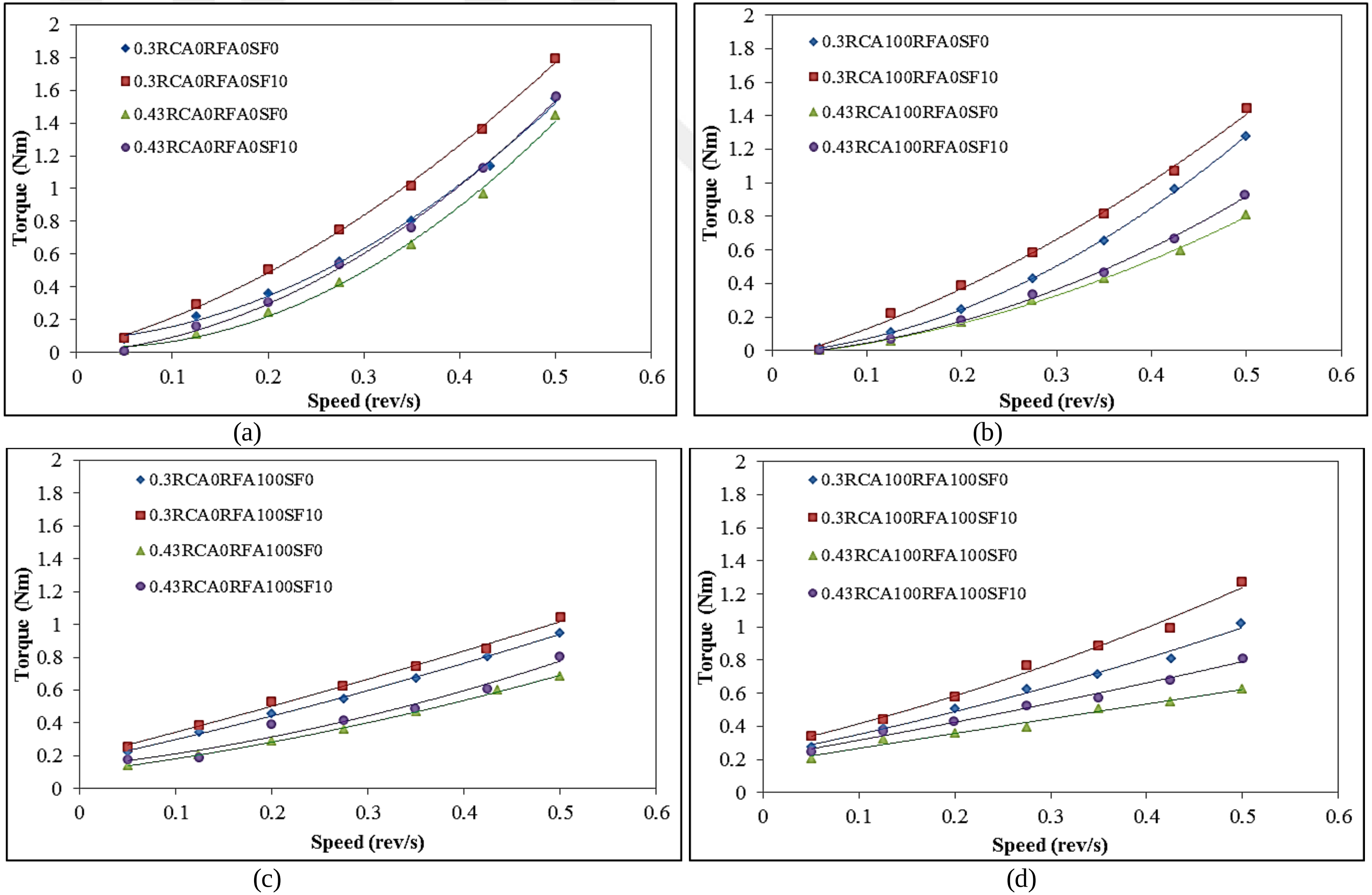

Figure 4.5 Rheology results for SCCs (a) 100% NAs (b) NFAs and RCAs (c) NCAs and RCAs (d) 100% RAs

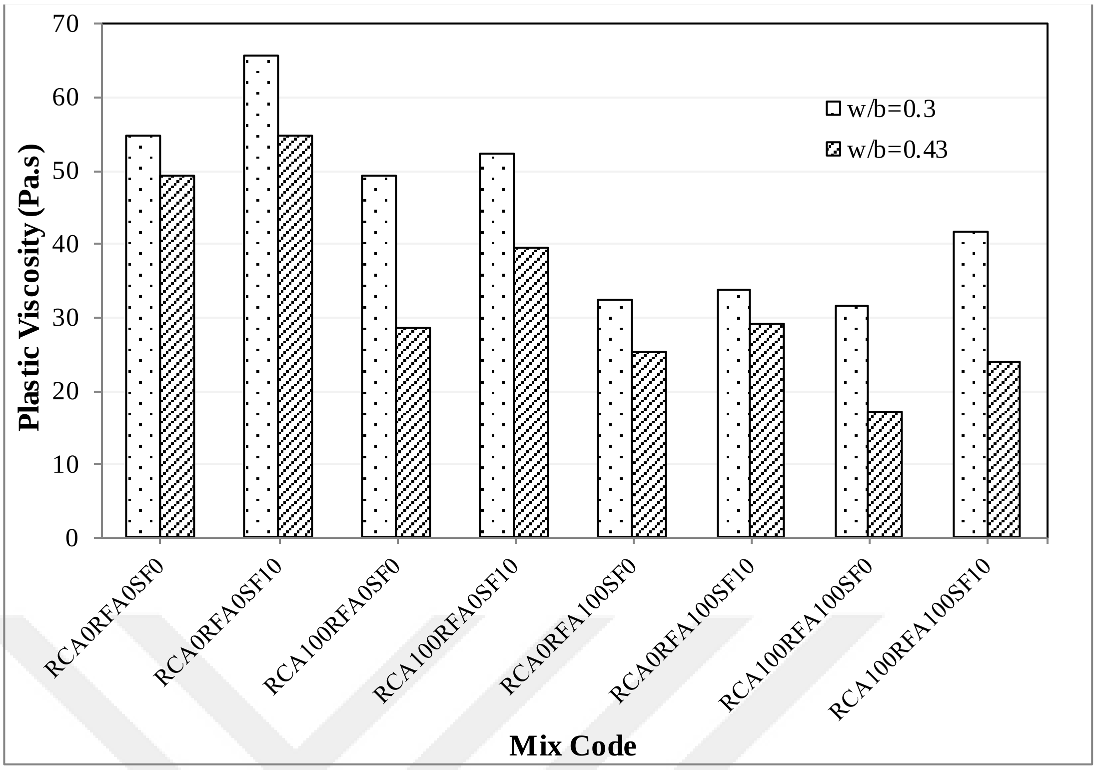

Figure 4.6 Plastic viscosity for all SCCs

4.2 Mechanical Properties

The strengths results of all SCCs are summarized in Table 4.1; also, the effects of aggregate type, increase water content and SF on the 56-day compressive strength of SCCs are demonstrated in Figure 4.7. The incorporation of RAs as a full or partial replacement for NAs adversely affected the compressive strength of SCRACs. The compressive strength of reference series concrete (series I) varied from 66.63 to 81.40 MPa. In addition, compressive strength values of SCRACs recorded 55.38-70.39, 48.69-64.61, and 46.04-57.41 MPa for Series II, III, and IV respectively. In other words, the use of RCAs, RFAs and RCAs+RFAs inversely affected the compressive strength of the corresponding reference concretes by 11.8-16.9, 15.8-26.9, and 27.0-30.9%, respectively.

In series IV concrete, the lowest compressive strength values obvious in this concretes. The reduction in compressive strength due to incorporation of RAs may be attributing to the strength and volume of the aggregate used in production of old concrete. Moreover, the poor quality of the adhered mortar to RAs, which had experienced the crushing process and consequently, were created weak areas in the concrete as well as the weak ITZ (Safiuddin et al., 2011-b; Corinaldesi and Moriconi, 2009; Sagoe-Crentsil et al., 2001). For a given w/b ratio, the strength of RAs deemed as the main factor affecting the SCRACs (Safiuddin et al., 2011-a; Sagoe-Crentsil et al., 2001). Obviously it can be noted that the failure occurred through the hardened cement paste in Series I; whereas in Series IV (as an example) this path passed through the aggregate phase, which was the weakest component of the composite (Figure 4.8 a and b).

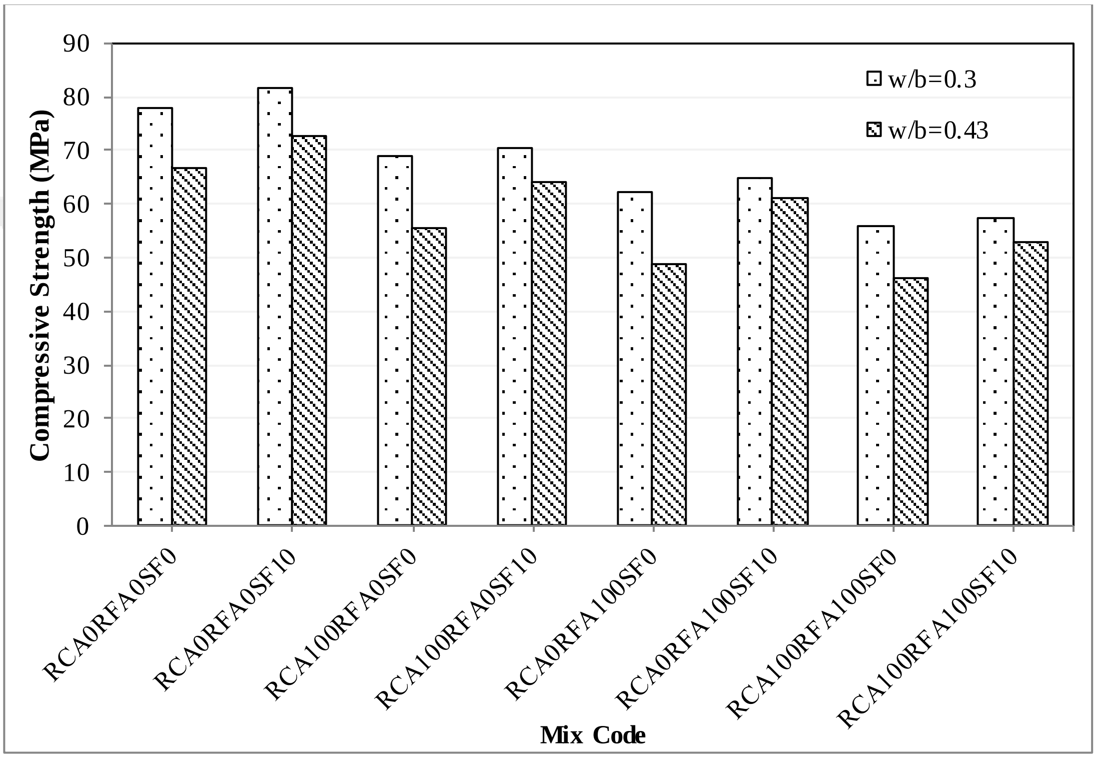

Figure 0.7 Compressive strength results for all structural SCCs

Table 4.1 Strengths properties and fracture characteristics

Series Code	Mix Code	Compressive Strength (MPa)	Splitting Tensile Strength (MPa)	Modulus of Elasticiy (GPa)	Net Flexural Strength (MPa)	Area under load-disp. curve (Wo) (N.mm)	Final disp. at midspan (δs) (mm)	Fracture Energy (N/m)	Characteristic Length (mm)
Series I	0.3RCA0RFA0SF0	77.96	4.25	26.06	5.41	711.25	1.45	141.56	204.59
	0.3RCA0RFA0SF10	81.40	4.46	27.81	6.53	689.10	0.78	127.02	177.69
	0.43RCA0RFA0SF0	66.63	3.50	23.62	4.79	613.13	1.26	121.79	234.98
	0.43RCA0RFA0SF10	72.47	3.75	24.99	6.25	590.78	0.87	111.92	198.78
Series II	0.3RCA100RFA0SF0	68.67	3.50	21.26	4.27	504.24	1.13	101.04	175.12
	0.3RCA100RFA0SF10	70.39	4.13	23.33	5.43	473.25	0.78	90.45	123.68
	0.43RCA100RFA0SF0	55.38	2.89	20.52	4.01	417.87	0.89	82.70	203.10
	0.43RCA100RFA0SF10	63.89	3.24	21.43	4.77	385.45	0.79	75.78	154.54
Series III	0.3RCA0RFA100SF0	61.97	3.15	19.84	4.19	469.97	1.02	93.54	187.26
	0.3RCA0RFA100SF10	64.61	3.59	21.14	4.85	449.55	0.81	86.80	142.21
	0.43RCA0RFA100SF0	48.69	2.53	18.30	3.82	367.29	0.70	71.56	204.90
	0.43RCA0RFA100SF10	61.04	2.81	18.85	4.52	331.87	0.78	66.55	158.76
Series IV	0.3RCA100RFA100SF0	55.76	2.72	17.44	3.58	322.18	0.55	61.56	145.15
	0.3RCA100RFA100SF10	57.41	3.16	18.66	4.25	291.37	0.56	56.35	105.33
	0.43RCA100RFA100SF0	46.04	2.20	15.60	3.26	264.08	0.45	50.20	162.27
	0.43RCA100RFA100SF10	52.92	2.59	16.92	3.77	249.21	0.50	48.28	122.24

Hence, the failure line of control mixes (where NAs were used) located in the ITZ around the aggregate particles and almost NAs did not fracture under the compressive load. Moreover, Series II concrete, which was made with a blend of RCAs and NFAs, performed better than the other two series of SCRACs. This behavior is attributed to a better interfacial bond between cement paste and aggregate in the presence of rough as well as the angular RCAs which can lead to a better interlocking of aggregates. These two factors may contribute to counterbalance the reduction of compressive strength due to the presence of less strong aggregate (Sagoe-Crentsil et al., 2001).

The compressive strength was higher as the w/b ratio decreased irrespective of matrix type and aggregate type. This is due to that the volume of capillary pores and their connectivity significantly declined for mixes with a lower w/b ratio (Safiuddin et al., 2011-a). The incorporation of SF also enhanced the compressive strength despite that the effect of SF was more pronounced with a higher w/b ratio mixes as agreed with the study of (Lam et al., 1998) and others (Wang and Li, 2012; Xie et al., 1995; Elahi et al., 2010). In this study; it was found that incorporating 10% SF results increase in compressive strength values by 2.5-4.4% and 8.8-25.4% for 0.30, 0.43 w/b ratio mixes, respectively (Figure 4.9). Indeed, for a given w/b ratio, the compressive strength values of SCRACs with SF was still lower than that of SCC incorporating NAs with no SF despite that the strength difference became higher as increasing the RAs replacement level. In other words, the further improvement of the matrix caused by the incorporation of SF did not compensate for the reduction in the strength due to the earlier failure of the RAs particles.

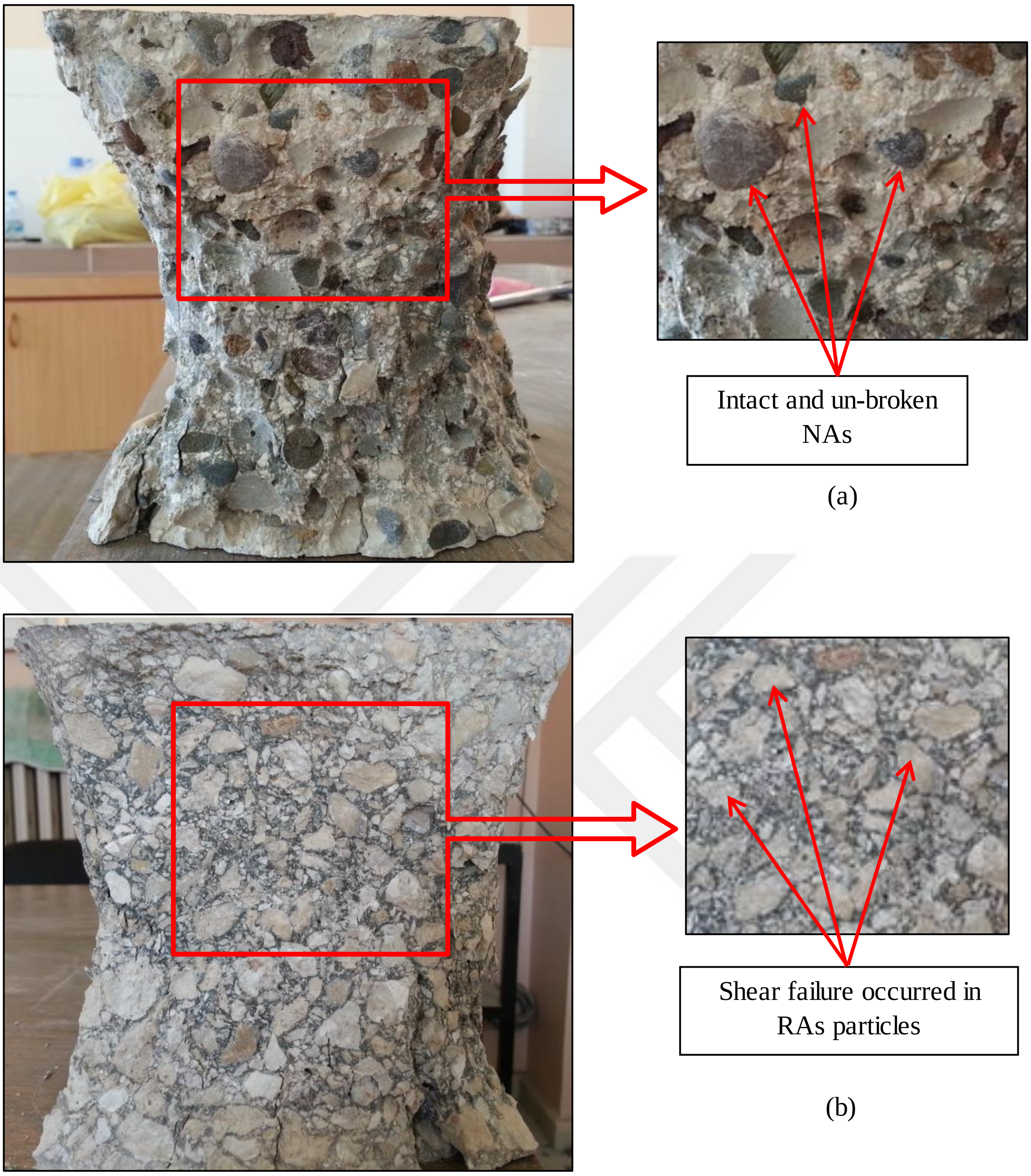

Figure 4.8 Failure shape of test specimens made with (a) 100%NAs, (b) 100%RAs

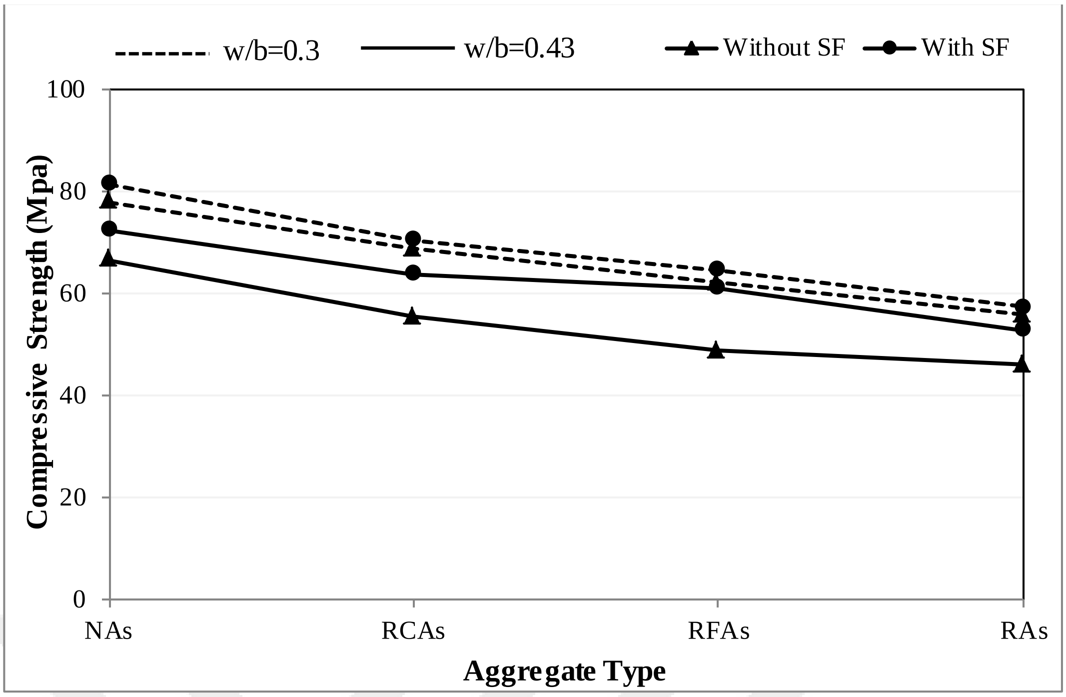

Figure 4.9 Relationship between compressive strength and aggregate type for structural SCCs

The splitting tensile strength and net flexural strength of SCCs at 56 days are depicted in Figure 4.10 and 4.11, respectively. As with the compressive strength, both splitting tensile and flexural strengths decreased due to the presence of RCAs and/or RFAs. Considering the three series of SCRACs, it was found that the best strengths were observed for mixes in Series II where the NCAs were replaced by RCAs. However, small differences in flexural strength were recorded between Series II and III concretes. The mixes containing 100% RAs exhibited the lowest strength among all the concrete mixtures. The SCRACs in Series II, III, and IV showed a reduction in splitting tensile strength of 7.4-17.6%, 19.5-27.7%, and 29.1-37.1%, respectively as compared to the corresponding control mixes in Series I.

As depicted in Figure 4.11, the equivalent reduction in the net flexural strength was 16.3-23.7%, 20.3-27.7%, and 31.9-39.7%, respectively. This is because of the same reasons as discussed in the cases of compressive strength that the strength and volume of the RAs have an important impact on the reduction in the mechanical properties (Tavakoliand Soroushian, 1996-b; Suvash and Gideon, 2013; Safiuddin et al., 2011-a). An equivalent or better splitting tensile or flexure strength can be obtained in the presence of RAs owing to good interfacial bond between aggregate and mortar matrix. As a result, the usage of RAs rather than NAs reduces the splitting tensile or flexural strength of SCCs (Güneyisi et al., 2014; Sagoe-Crentsil et al., 2001). According to (Tavakoliand Soroushian, 1996-b), the splitting tensile strength of RACs can be higher than that of CCs provided that the RAs were derived from a concrete with a higher compressive strength compared to the control concrete. In the present study, the parent concrete for RAs had a compressive strength of almost 20 MPa, which was much lower than that of reference SCCs.

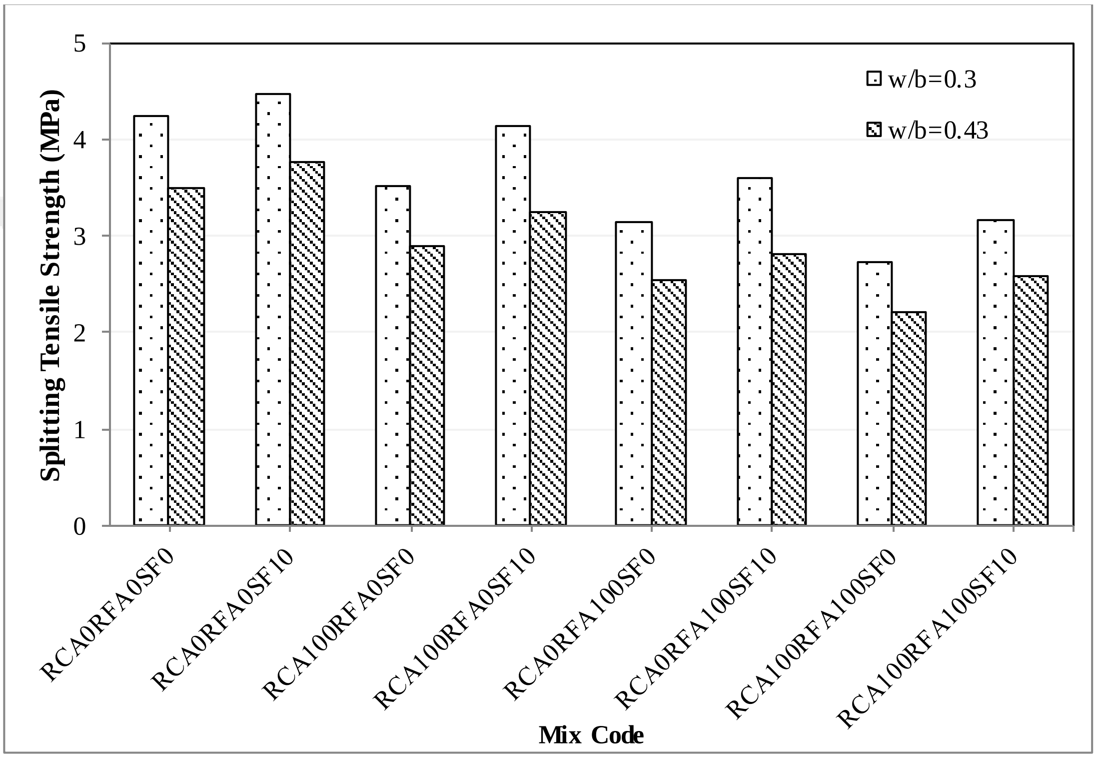

Figure 0.10 Splitting tensile strength results

As expected, for a given series, the concretes with SF and a w/b ratio of 0.30, performed better in terms of both splitting tensile and flexural strengths as compared to those with no SF and a 0.43 w/b (Figures 4.12 and 4.13). Other researchers also found that the splitting tensile strengths increased with the addition of SF though the optimum content of SF was varied depending on the w/b ratio of the mixture (Alam et al., 2013; Wang and Li, 2012; Neville, 2006).

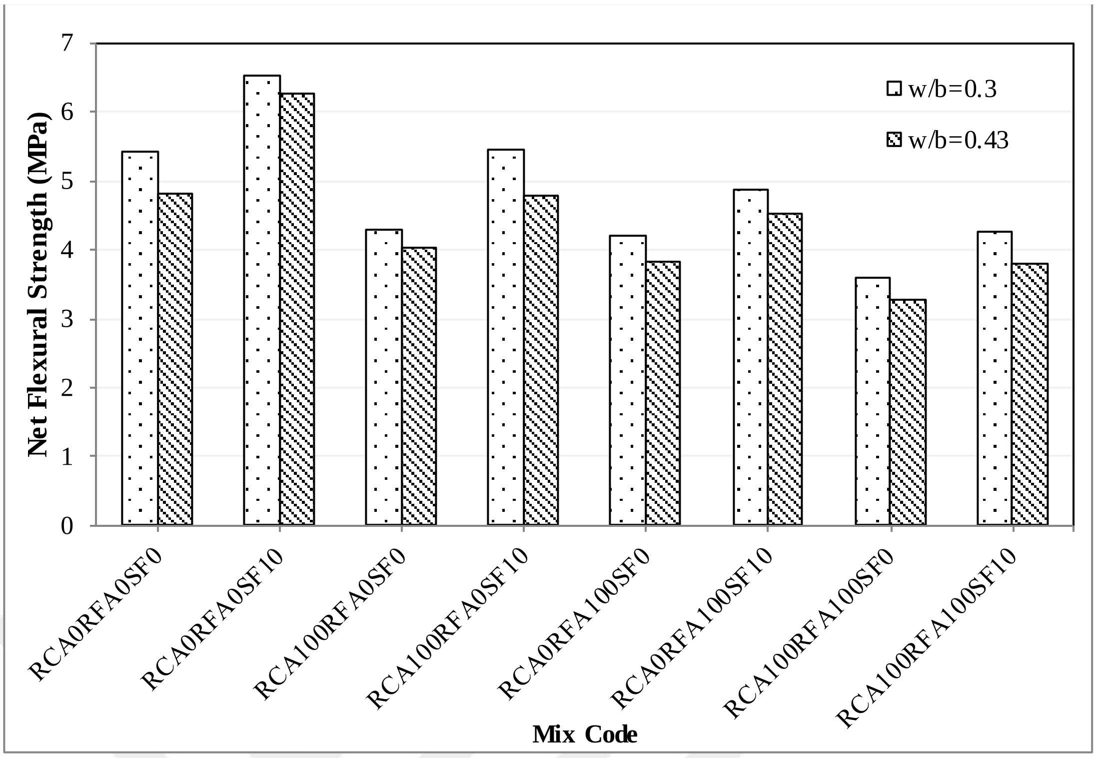

Figure 4.11 Net flexural strength results

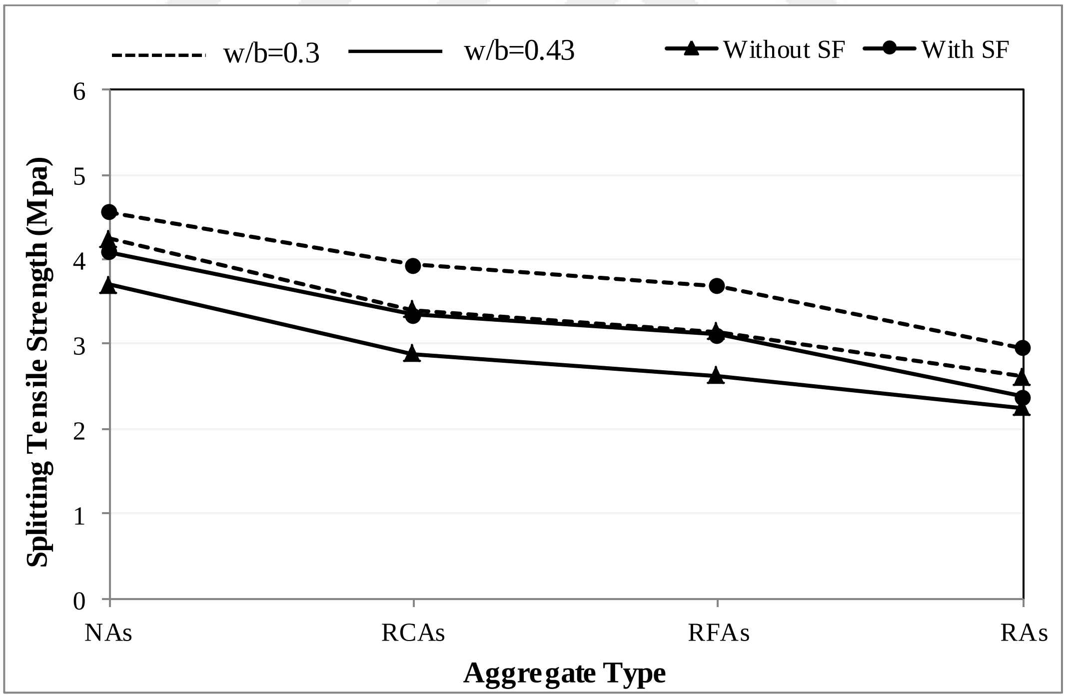

Figure 4.12 Relationship between splitting tensile strength and aggregate type for structural SCCs

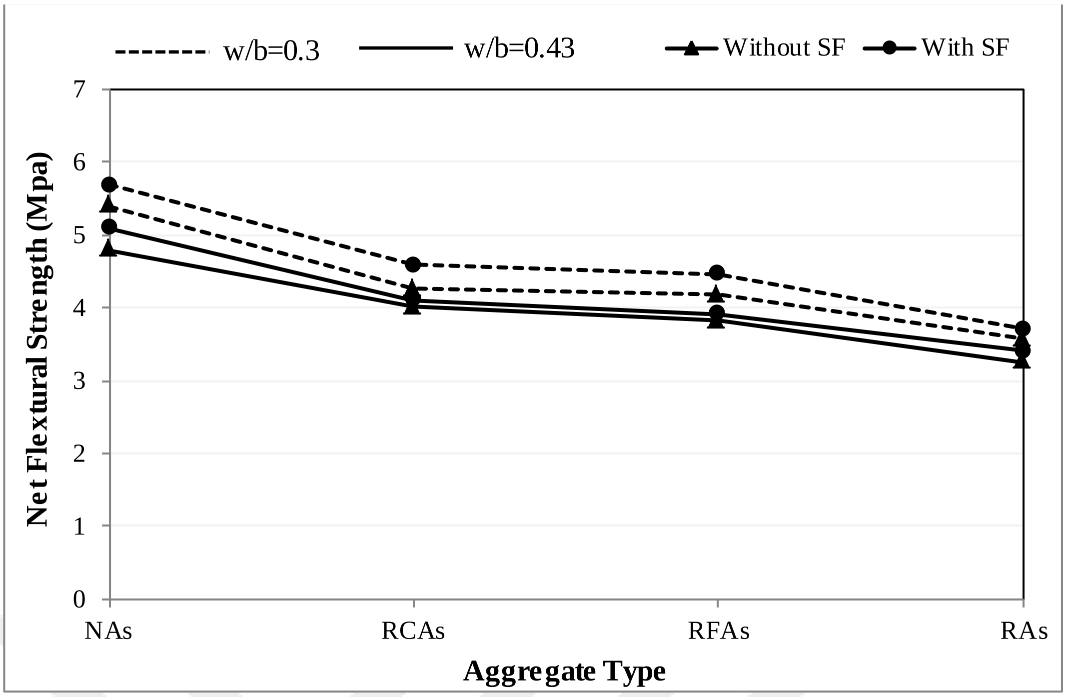

Figure 4.13 Relationship between net flexural strength and aggregate type for structural SCCs

The results of modulus of elasticity of SCCs are graphically represented in Figure 4.14. Obviously, the mixes containing RCAs and/or RFAs gave lower modulus of elasticity as compared to the reference mixes (Series I). Among the three SCRACs series, the highest and lowest values were observed for concretes in Series II and IV, respectively. The earlier studies (Pereira et al., 2012; Safiuddin et al., 2011-a) showed that more porous and less strong RAs adversely affected the modulus elasticity of SCRACs. However, the paste parameters investigated in the present study such as w/b ratio and the presence of SF also had a certain effect on the modulus of elasticity of SCCs. As shown in Figure 4.15, decreasing the w/b ratio to 0.30 enhanced the modulus of elasticity of Series I, II, III, and IV by up to 10.1, 8.1, 10.8, and 10.5%, respectively. Similarly, replacing 10% of the binder by SF resulted in an improvement in the modulus of elasticity of up to 6.3, 8.9, 6.1, and 7.8% for Series I, II, III, and IV, respectively.

In effect, Figure 4.16 shows the variation of splitting tensile strength and net flexural strength with compressive strength. The high value of the coefficient of correlation, R^2, indicated that the compressive strength and the other two phenomena were well correlated despite the use of RFAs and/or RCAs. Moreover, the modulus of elasticity also exhibited a good linear correlation with compressive strength (R^2=0.89). This finding is compatible with that of many other investigators (Grdic et al., 2010; Bordelon et al., 2009; Pereira et al., 2012; Suvash and Gideon, 2013; Safiuddin et al., 2011-a). However, Neville (2006) stated that the incorporation of SF in concrete does not alter significantly the usual relations between compressive strength and flexural strength as well as modulus of elasticity.

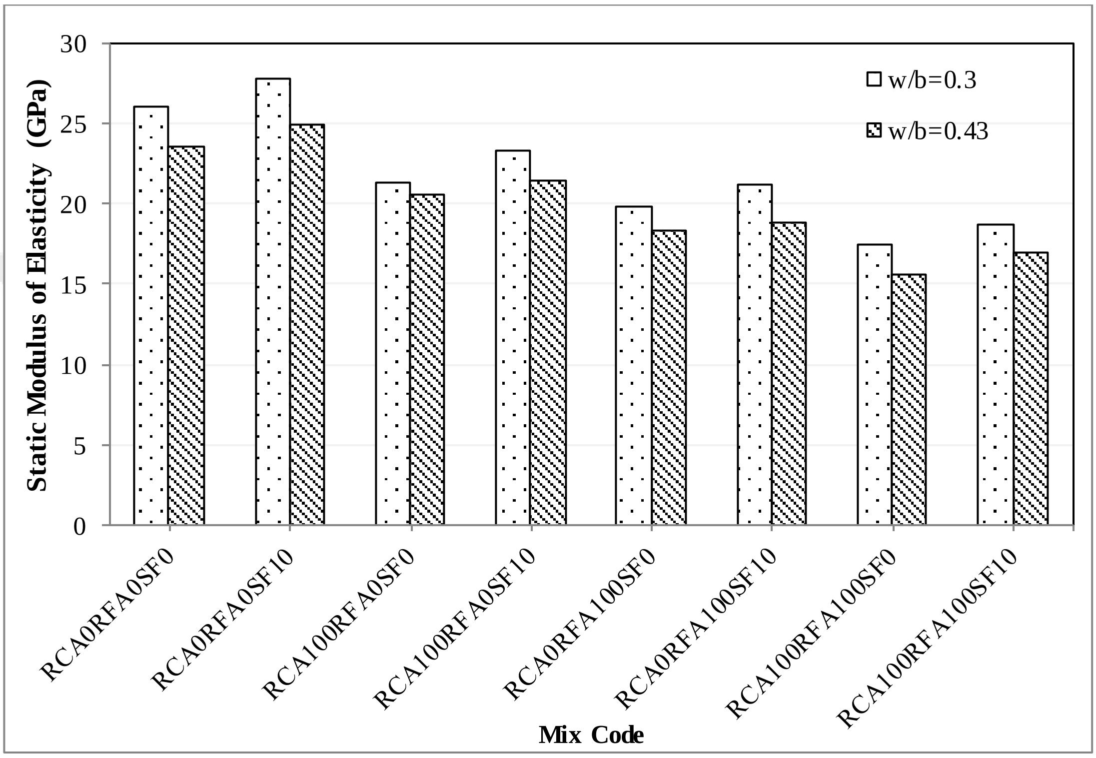

Figure 4.14 Static modulus of elasticity results

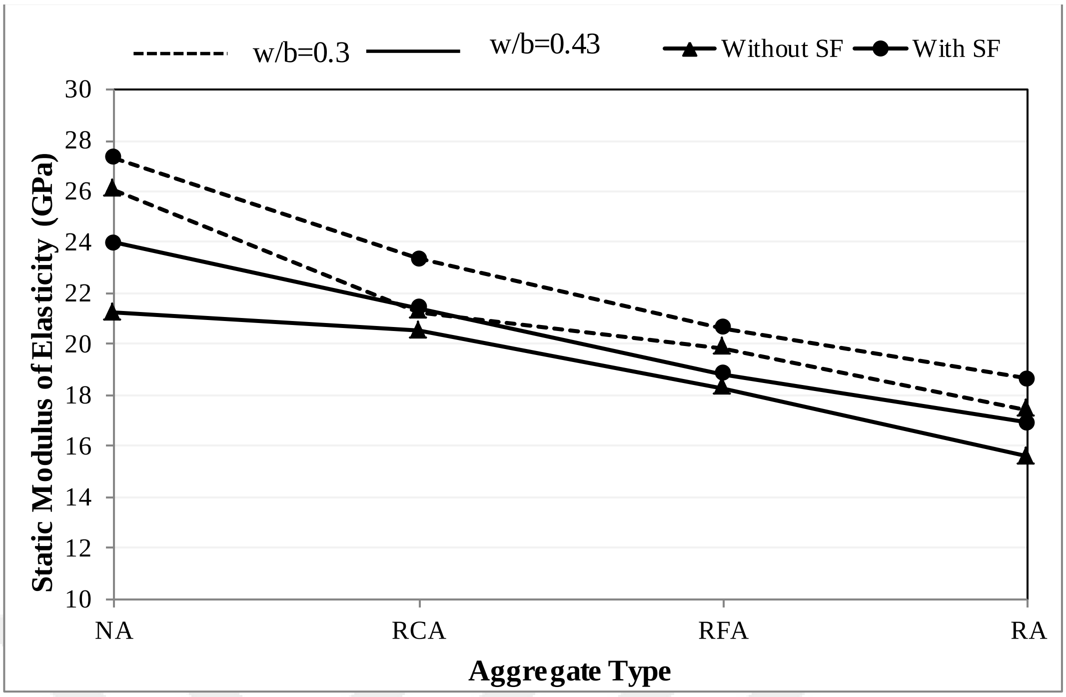

Figure 4.15 Relationship between elastic modulus and aggregate type for structural SCCs

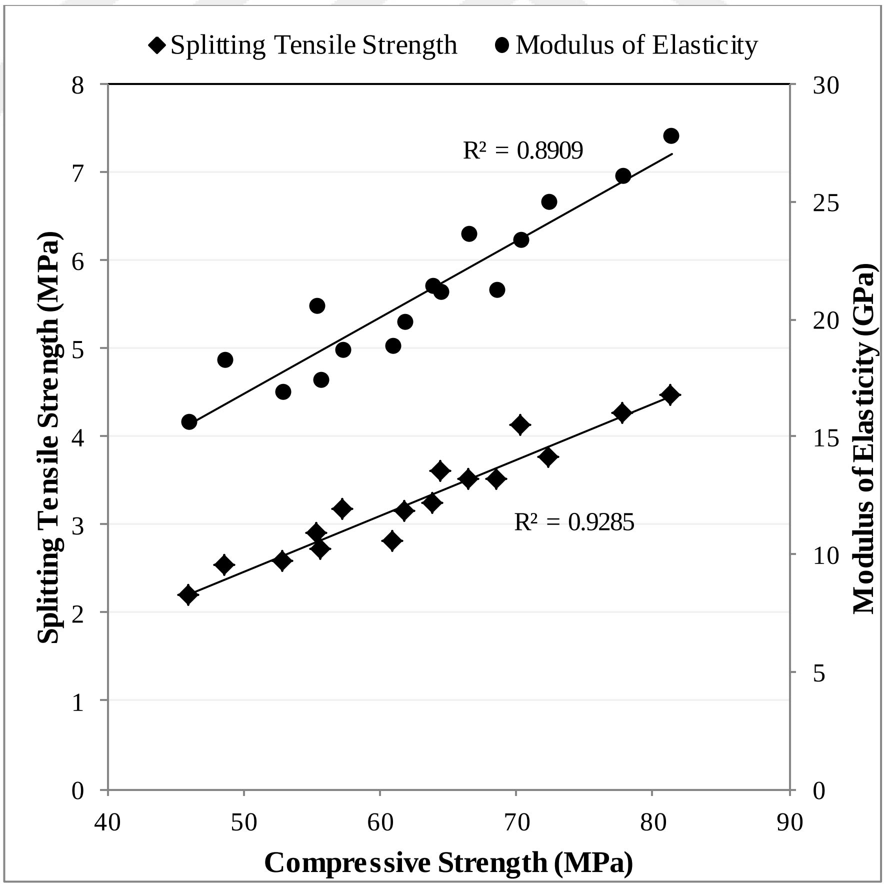

Figure 0.16 Correlation between mechanical properties

4.3 Fracture Properties

In the present study, Figure 4.17 (a), (b), (c) and (d) shows the load-displacement plots for the four series of test beams under three point bending test. However, the test results related to the fracture parameters are summarized in Table 4.1 The inferior specification of RAs for both fine and coarse gradation strongly affected the pre-peak stiffness of the load-displacement curve for the produced SCRACs. For an instant, 0.3RCA100RFA100SF0 and 0.3RCA100RFA100SF10 mixes had peak values of 2147 and 2551 N, respectively; while the peak values of corresponding control mixes, 0.3RCA0RFA0SF0and 0.3RCA0RFA0SF10, were 3244 and 3915 N, respectively.

As depicted in Figure 4.17, it can be noted that the peak load noticeably depends on w/b ratio and incorporating of SF. Furthermore, the slope of the pre-peak region of the curve and early post-peak region, to some extent, related to the presence of SF. Utilizing 10% SF also results in a steeper slope in the declining part of the curve indicating a more brittle behavior in SCC. In the same way, reduction of the w/b ratio, results in a higher ultimate load and less ductility behavior in concrete. Also it was previously, reported that using a small amount of SF and low w/b ratio enhanced the brittleness of concrete (Beygi et al., 2013; Karihaloo et al., 2003). The final displacement for SCRACs was lower than that for SCCs with NAs. In the present study, increasing w/b ratio to 0.43 and utilizing SF in the concrete resulted in a decrease in the value of final displacement. However, as shown in Table 4, except control mixes (Series I), the differences in final displacement values were small between SCCs mixes; especially for SCRACs (Figure 4.17d). Moreover, the variation detected in the tail of the softening branch was small or negligible. Thus, Beygi et al. (2013) reported the same trend for SCCs and CCs. Further, Taşdemir et al. (1999) stated that the incorporation of SF in concrete result steeper gradient of the softening branch as well as greater peak load corresponding lower final displacement values. This performance might be because pre-peak and the early post-peak regions in load–displacement curve are mainly is due to micro-cracks and their expansion. However, the declining slope at the end of the softening branch is highly related with the aggregate interlocking and other frictional effects.

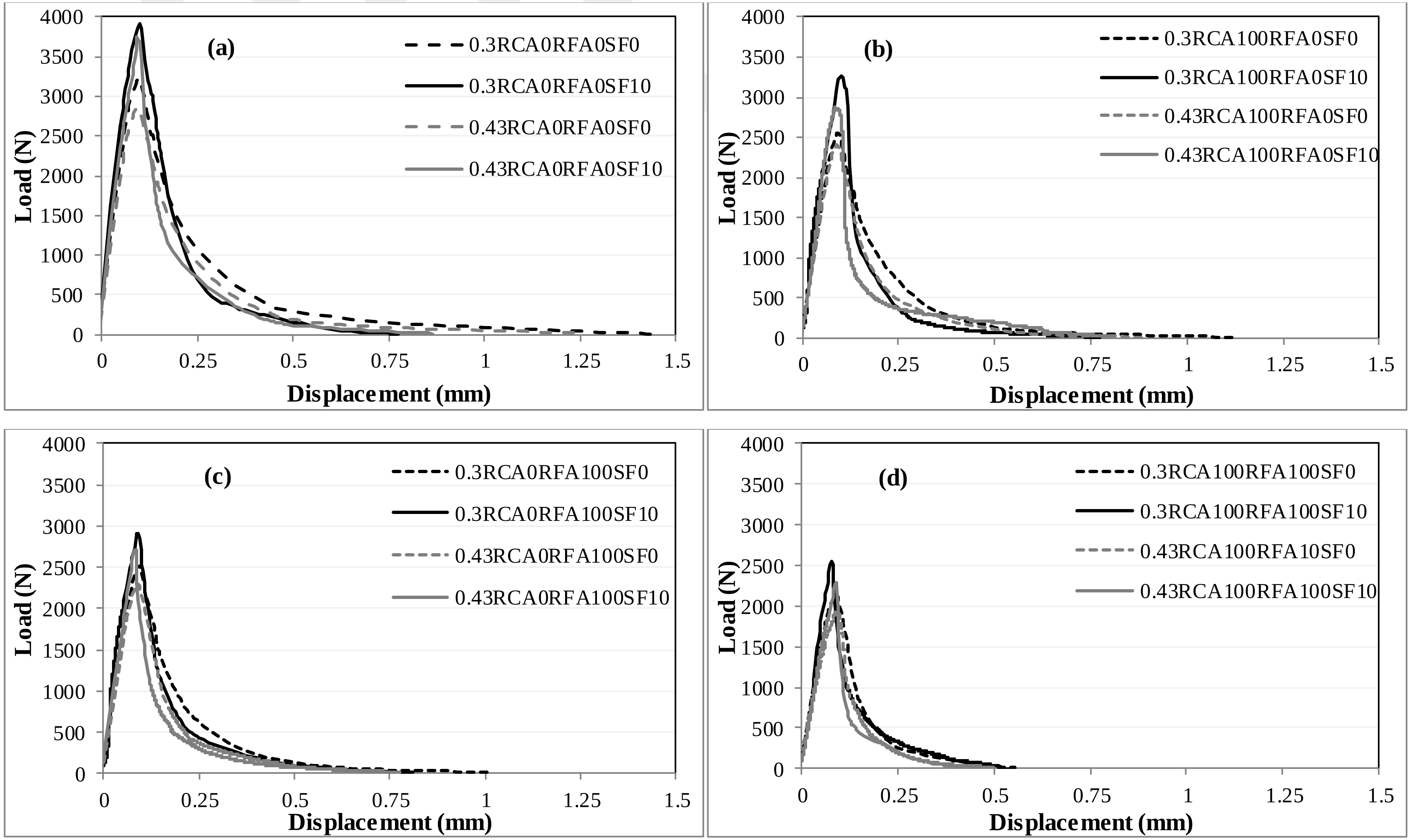

Figure 4.17 Load-displacement behavior of the test beam (a) NAs, (b) RCAs, (c) RFAs and (d) RCAs+RFAs

The area under the load-displacement curve is demonstrated in Table 4.1. It can be observed that the utilization of RAs in SCCs significantly decreased the area under the load-displacement curve. Figure 4.18 illustrates the fracture energy (GF) values of investigated concretes where the effects of aggregate type, w/b ratio and SF content are given. The effect of RAs on GF is important because the crack surface roughness induces aggregate interlock (Taşdemir et al., 1999). It was observed that GF was lower for SCRAC with RAs replacement. The GF of control concretes (Series I) was in the range of 111.9-141.5 N/m and gradually decreased by the range of 28.6-32.3%, 31.6-41.2%, 55.6-58.8% for the mixes with RCA (Series II), RFA (Series III) and RFA+RCA (Series IV), respectively. The inferior properties of RAs make the cracks easily penetrate into the aggregate grains and concrete matrix phases due to the lack of stiffer RAs. Thus, as RAs were utilized, the value of GF decreased (Bordelon et al., 2009; Arezoumandi et al., 2014). Also, as mentioned above, the crushing strength and volume fraction of the aggregate used in production of RAs has an important impact on the reduction of fracture parameters of SCCs especially with 100% replacement level (Sagoe-Crentsil et al., 2001; Tavakoli and Soroushian, 1996).

As in the strength properties, SCCs mixes with less w/b (0.30) recorded the best fracture energy. When all the mixes were considered, the enhancement in the GF due to the decrease of a w/b ratio was in the range of 11.9-23.3%, respectively. For example, in control mixes GF for 0.3RCA0RFA0SF0 was 141.5 N/m, compared with 121.8 N/m for 0.43RCA0RFA0SF0 (Figure 4.19).

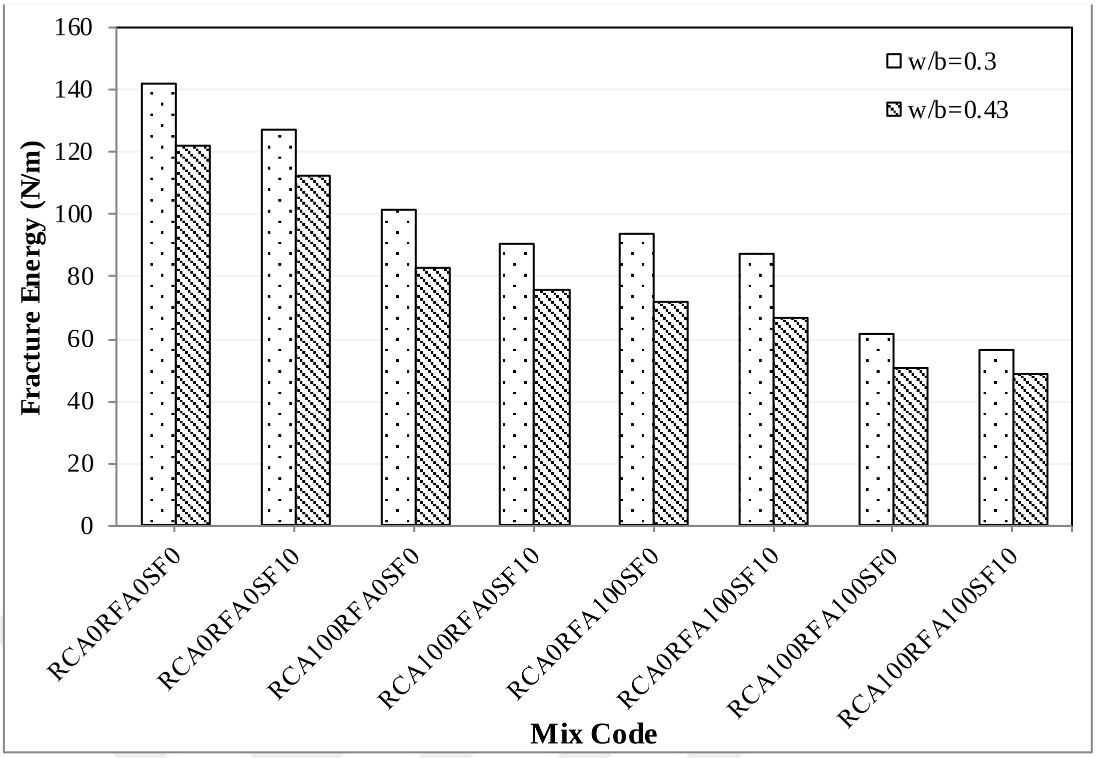

Figure 0.18 Fracture energy calculated on the beam subjected to flexural test

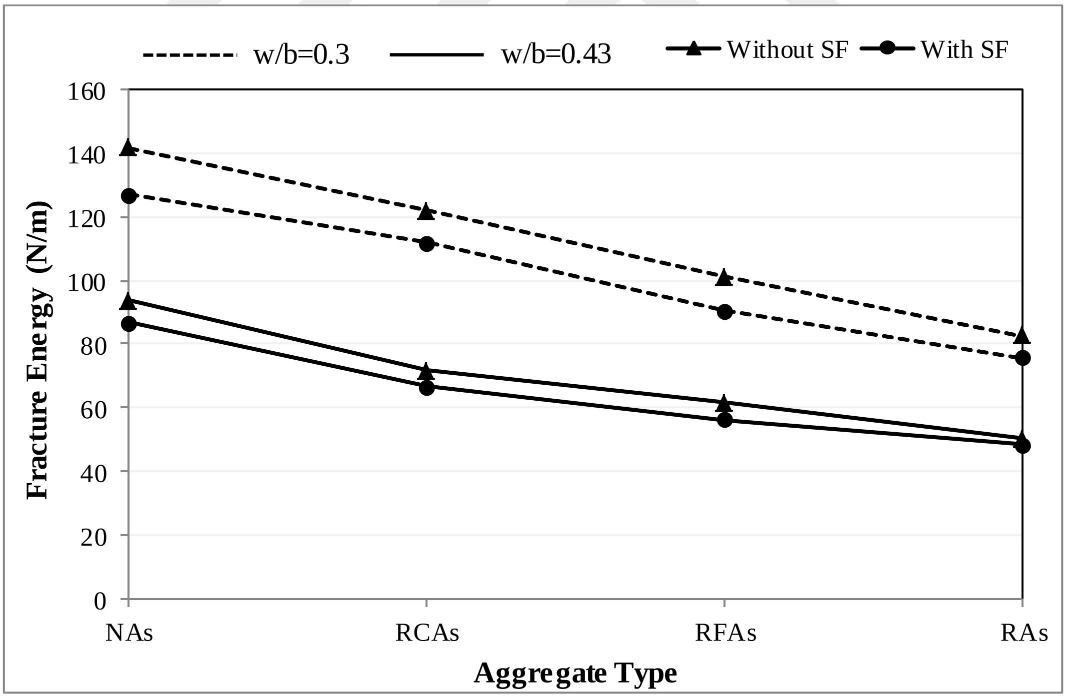

Figure 4.19 Relationship between fracture energy and aggregate type

In the present study, GF increases from 111.9 to 141.6 N/m as compressive strength changes from 72.5 to 78.0 MPa for control mixes (series I). While, for SCRACs (series II), GF was changed from 48.3 to 61.6 N/m corresponding to a compressive strength range from 52.9 to 55.8 MPa. As depicted in Figure 4.20, fracture energy was directly proportional with compressive strength and the variation of fracture energy with compressive strength was presented by regression analysis with the correlation coefficients of 0.73:

$$G_F = 0.059\, f_c^{1.75} \tag{4-1}$$

Where G_F represent the fracture energy (N/m) and f_c is the average compressive strength at 56 days (MPa).

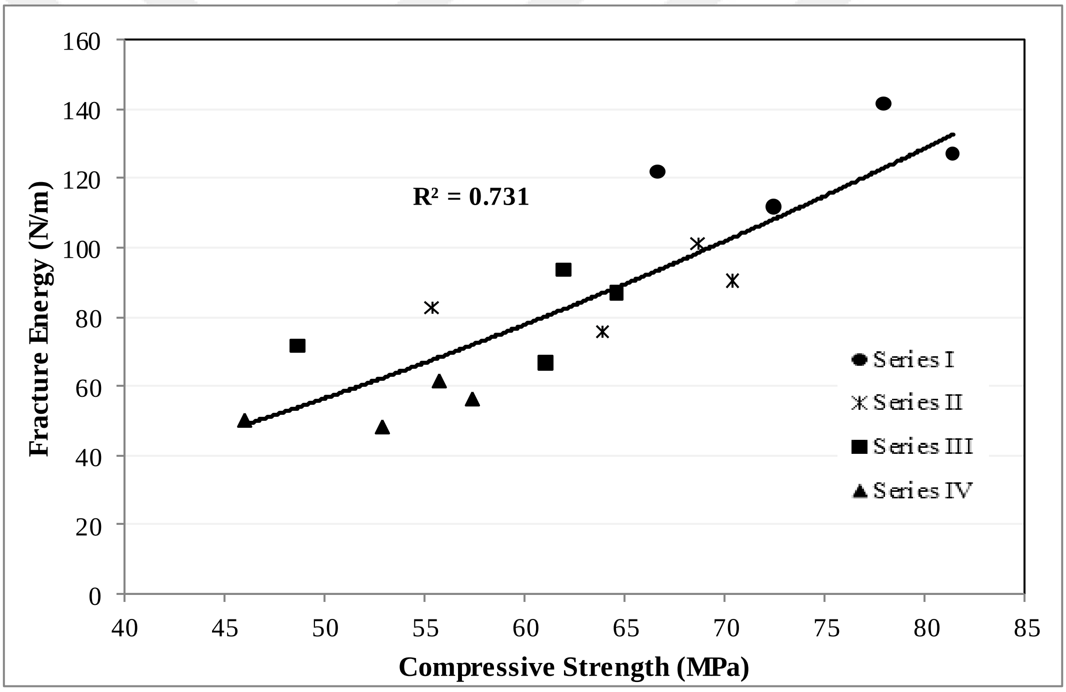

Figure 0.20 Variation of fracture energy with strength

In order to estimate the brittleness of SCCs, the characteristic length (l_{ch}) calculated via Eq. 3.5 is employed. As shown in Figure 4.21, SCRACs with 100% RAs (Series IV) recorded the lower values of l_{ch}; the values were in the range of 29.1-40.7% compared with control mixes. Indeed, the result significantly depends on w/b ratio and the presence of SF in concretes. These findings confirmed that the material became more brittle when the NAs were fully or partially replaced by the RAs due to the fact that the use of RAs decreased the compressive strength. However, in the present study, for the same aggregate type mixes, the increment of compressive strength due to lowering w/b ratio and utilizing SF lead to make the concrete more brittle.

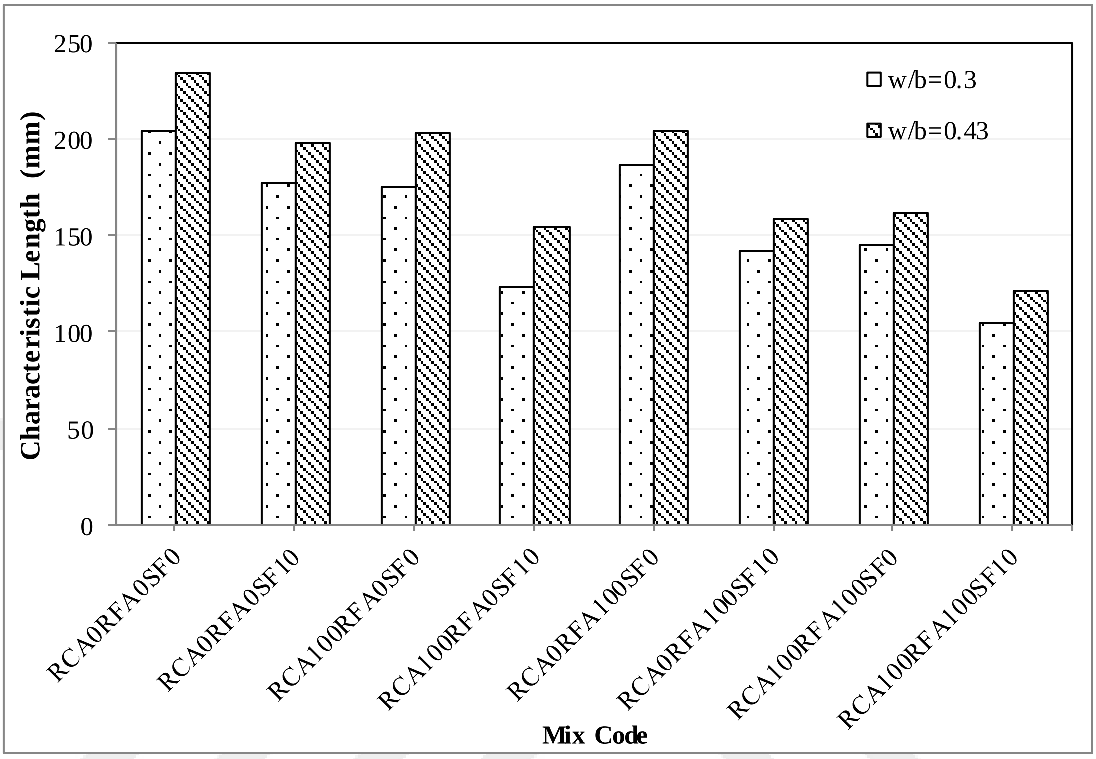

Figure 4.21 Characteristic length results

In the present study, the results calculated could be comparable with the trend proposed by previous researchers (Karihaloo et al., 2003; Arezoumandi et al., 2014; Bordelon et al., 2009). Accordingly, (Beygi et al., 2013) reported that enhancing the compressive strength from 26.0 to 75.5 MPa caused a decrease in the l_{ch} from 427.0 to 251.1 mm, respectively. In fact, due to the strength enhancement of cement paste and ITZ due to decreasing w/b ratio, cracks developed through aggregates which led to contraction of the FPZ at the tip of the crack. In effect, high rupture ability in aggregate phase made the concrete more brittle behavior (Beygi et al., 2013). As a result, l_{ch} increased with a higher w/b ratio, and the brittleness of concrete decreased. Indeed, this trend can be observed in the present study to explain the effect of the w/b ratio. For control mixes, series I, increasing w/b from 0.30 to 0.43 enhanced l_{ch} by the range of 10.6-12.9 %. Moreover, all SCCs series showed the same performance of brittleness when the w/b ratio changed. For an instant, l_{ch} for Series IV enhanced from 10.5 to 13.9% as the w/b ratio increased from 0.30 to 0.43.

As shown in Figure 4.22, for control mixes (series I), the decrease in l_{ch} due to the incorporation of SF was in the range of 13.1 to 15.4%. Moreover, the trend of brittleness was valid for the other series. For an example, in series IV, mix 0.3RCA100RFA100SF0 was more brittle than mix 0.3RCA100RFA100SF10 by 27.4%.

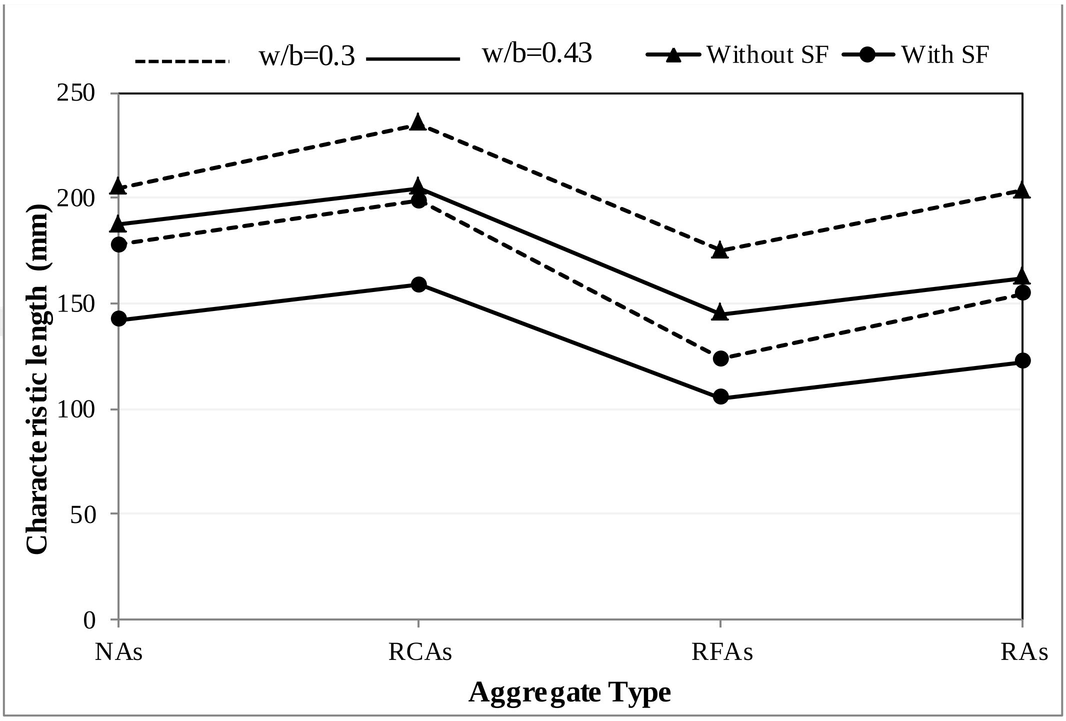

Figure 0.22 Relationship between characteristic length and aggregate type

4.4 Statistical Evaluation

The primary visual inspection of variance (GLM-ANOVA) was performed by using Minitab software to assess the statistical significance of the experimental test parameters and to reach a better understand the quantitative effects of the RAs, utilizing of SF and increasing w/b ratio on the characteristics of SCRACs. The properties in the term of mechanical and fracture parameters had conducted and examined by a variance of GLM-ANOVA at a 0.05 level of significance (Güneyisi et al., 2010).

Obviously, it could be seen from Table 4.2 that all independent variables were statistically significance on all tested mechanical parameters because p-value was less than the critical value (0.05). Thereby, the independent variable considered as significant factor on the test results; also the dependent variables explained significance less than 0.05. This analysis result revealed that the variability of hardened properties must be explained in terms of RAs replacement and adding of SF. Moreover, the use of higher w/b appeared to be effective on the mechanical properties of SCCs. Likewise, all independent variables used in the production of SCCs are statistically significant at 95% confidence level. Hence, the use of RAs appeared to be the most effective independent variables on the mechanical properties of SCRACs. The analysis of results also revealed that the contribution of utilizing RAs was the highest factor affected the variation of properties compare to other factors. Examples include 67.41, 60.83, 86.98 and 67.45% for compressive, splitting tensile, modulus of elasticity and net flexural strength respectively, referred that the RAs factor have a high degree of effectiveness on the hardened properties. In addition, the effect of these factors on that particular response is high. Actually, the other independent variable was effect on the properties results but not in the same quantitative of the factor of RAs replacing. As revealed from the results, the increase of w/b ratio from 0.30 to 0.43 has less contribute on the effectiveness of hardened properties than RAs. However, the percentages had been higher than factor of SF utilization. For instant, when the test results of compressive strength were examined in more detail, it was observed that the most effective factor on the compressive strength of the produced SCCs was the use of RAs with a contribution of 67%, while the increase in the w/b ratio contribute by 21%.

From Table 4.3, the percentages revealed that the use of RAs rather than NAs cause the plurality contributions on the fracture parameters compare with other factors. For example, the contribution percentage induced by the use of RAs was 88% for G_F variable, compare with 2% and 9% for factors of utilize SF and increase w/b ratio, respectively. The other fracture properties revealed similar performance in this regard. Hence, the ANOVA analysis proved that the factor of RAs was the most significant variable on the properties of the SCRACs. Indeed, the difference between the properties of NAs and RAs might cause this effect on the property of any type of concrete.

Table 0.2 The variance of linear model analysis for mechanical properties

Dependent Variable	Independent Variable	Statistical Parameters					Significance	Contribution (%)
		Degree of freedom	Sequential Sum of Squares	Adjusted Mean Square	F	P- value		
Compressive Strength	Replacing RAs Effect	3	1008.12	336.040	60.37	0.000	Yes	67.41
	Incorporating of SF	1	115.72	115.724	20.79	0.001	Yes	7.74
	Increasing w/b	1	316.04	316.040	56.78	0.000	Yes	21.13
	Error	10	55.66	5.566	-	-	-	3.72
Splitting Tensile Strength	Replacing RAs Effect	3	3.88982	1.29661	145.50	0.000	Yes	60.83
	Incorporating of SF	1	0.55876	0.55876	62.70	0.000	Yes	8.74
	Increasing w/b	1	1.85641	1.85641	208.32	0.000	Yes	29.03
	Error	10	0.08911	0.00891	-	-	-	1.39
Modulus of Elasticity	Replacing RAs Effect	3	154.738	51.5792	314.27	0.000	Yes	86.98
	Incorporating of SF	1	6.878	6.8775	41.91	0.000	Yes	3.87
	Increasing w/b	1	14.650	14.6498	89.26	0.000	Yes	8.23
	Error	10	1.641	0.1641	-	-	-	0.92
Net Flexural Strength	Replacing RAs Effect	3	8.6381	2.87936	75.38	0.000	Yes	67.45
	Incorporating of SF	1	3.0976	3.09760	81.09	0.000	Yes	24.19
	Increasing w/b	1	0.6889	0.68890	18.03	0.002	Yes	5.38
	Error	10	0.3820	0.03820	-	-	-	2.98

Table 4.3 The variance of linear model analysis for fracture properties

Dependent Variable	Independent Variable	Statistical Parameters					Significance	Contribution (%)
		Degree of freedom	Sequential Sum of Squares	Adjusted Mean Square	F	P- value		
Area under load-disp.	Replacing RAs Effect	3	283005	94334.9	428.48	0.000	Yes	89.05
	Incorporating of SF	1	2741	2741.3	12.45	0.005	Yes	0.86
	Increasing w/b	1	29862	29862.4	135.64	0.000	Yes	9.40
	Error	10	2202	220.2	-	-	-	0.69
Maximum load ($P_{max.}$)	Replacing RAs Effect	3	3103653	1034551	77.31	0.000	Yes	67.47
	Incorporating of SF	1	1117249	1117249	83.49	0.000	Yes	24.29
	Increasing w/b	1	245520	245520	18.35	0.002	Yes	5.34
	Error	10	133816	13382	-	-	-	2.91
Fracture Energy	Replacing RAs Effect	3	10499.4	10499.81	287.10	0.000	Yes	88.22
	Incorporating of SF	1	231.0	231.04	18.95	0.001	Yes	1.94
	Increasing w/b	1	1048.8	1048.79	86.04	0.000	Yes	8.81
	Error	10	121.9	12.19	-	-	-	1.02
Characteristic Length	Replacing RAs Effect	3	10042.0	3347.35	100.89	0.000	Yes	51.91
	Incorporating of SF	1	6978.1	6978.10	210.33	0.000	Yes	36.07
	Increasing w/b	1	1992.3	1992.28	60.05	0.000	Yes	10.30
	Error	10	331.8	33.18	-	-	-	1.72

4.8 Axial Capacity of CFST Columns According to Design Codes

In order to prepare a logic comparison between the axial load capacity of CFST columns for the tested mixtures themselves and/or between the codes followed to calculate the strengths, the predicted ultimate axial strength of circular CFST was depicted for each code. Actually, Figures 4.23–4.26 represents the variation of ultimate load for various D/t ratios calculated via formulas produced by Eurocode 4 (2004), ACI-318R (2005), AIJ (1997; 2001) and DL/T (1999) design codes, respectively. In each figure, the predicted strengths were classified into w/b ratio of concrete mixtures as well as the yield strength of steel tube. Indeed, the concrete mixtures were also scheduled depending on the type of utilized aggregate. The mixtures started with NA and then followed by recycle coarse aggregate (RCA), recycle fine aggregate (RFA) and finally for both grade of recycle aggregate (RCA+RFA). Moreover, the nomenclature (SF) denoted to silica fume, which was incorporated into half of mixtures at 10% of total binder content. For instant, the nomenclature (RCA100RFA100SF10) means that the mixtures are manufactured by using 100% RCA and 100% RFA as well as utilizing 10% SF; or it can be simply named as RASCC.

The predicted Pu results calculated via EC 4 ranged from 259 to 6946 kN (Figure4.23). Indeed, the ultimate strength increased whenever the diameter of columns and/or the yield strength of steel increased. The trend of load capacity increment was similar and comparable for the four codes tested in this study, which will be discussed later in detail. When all design codes considered, the lowest values of Pu were recorded by using the formulas of ACI code depending on D/t ratio and the hardening of steel tube. In this code, the predicted Pu ranged from 171 to 5127 kN compared with 259-6946 kN recorded for equivalent EC 4 code. In effect, the conserved results of Pu calculated by ACI code were attributed to the underestimation of concrete confinement factor as well as steel, unlike EC 4 code. As shown in Figures 4.24–4.26 and compared with EC 4 code results, the reduction percentages in the predicted Pu were 26-34%, 21-23% and 9.6-15% for ACI, AIJ and DL/T codes, respectively. Indeed, AIJ and DL/T code took into account the composite action between steel tube and filled concrete. For this, Pu results calculated via these codes were the closest to EC 4 results unlike ACI code. The trend of findings agreed with plenty of previous literatures stressing the trend of

CFST columns (Lu and Zhao, 2010; Lin, 1998; Saisho et al., 1999; Giakoumelis and Lam, 2004; Sakino and Hayashi, 1991; Lin and Guo, 2004; Luksha and Nesterovich, 1991; Kato, 1995; Yamamoto et al., 2002; Yu et al., 2002). In this regard, O'Shea and Bridge (1994) reported that the Pu recorded between 1350–3360 kN when the diameter of columns and yield strength of steel increased from 165-190 mm and 186-363 kN, respectively. Further, Han et al. (2005) presented similar trend of Pu results in which it ranged from 312 to 4800 kN for columns with 60-250 mm in diameter and 282-404 kN steel yield strength.

The utilization of SF slightly enhanced the strength performance of mixtures; thus increased the ultimate strength of composite columns. Actually, the known effect of SF is the improvement of bond between the paste and aggregate as well as strengthening the transition zone (the thin layer between aggregate and cement past) (Safiuddin et al., 2011-a; Suvash and Gideon, 2013). Hence, the compressive strength of SF mixtures was higher than others by 2.5-4.4% and 8.8-25.4% for mixes with a w/b ratio of 0.30 and 0.43, respectively. The effect of SF was more pronounced with a 0.43 w/b ratio mixes as agreed with the study of Wang and Li (2012) and others (Lam et al., 1998; Xie et al., 1995; Elahi et al., 2010). The Figures 4.23–4.26 also indicated that Pu was higher as the w/b ratio decreased irrespective of matrix and aggregate type. This behavior was attributed to the highest strength revealed by 0.30 w/b ratio mixes. Indeed, the volume of capillary pores and their connectivity significantly declined for low w/b ratio mixes (Safiuddin et al., 2011-a).

Beside steel strength and dimensions effect of columns, the type and strength of concrete core play a significant role in the Pu results. In this paper, the highest value was recorded for NA mixtures prepared by using 0.30 w/b ratio; while, the lowest value was obtained from RACs prepared by using 0.43 w/b ratio. Indeed, the incorporation of RA causes a decrease in the strengths of produced concrete due to the inferior quality of these aggregates (Kou and Poon, 2009; Gesoglu et al., 2015; Khatib, 2005). The incorporation of RAs (as a full or partial replacement for NAs) adversely affects the mechanical properties of tested concretes. The reduction in strength might be attributed to the low strength and volume of RA. Moreover, there is an adhered mortar attached to RA which creates weak areas inside the concrete as well as weak transition zone (Safiuddin et al., 2011-b; Lin and Guo, 2004; Sagoe-Crentsil et al., 2011; Corinaldesi and Moriconi, 2009). The reduction in the strength of concrete reflects on the results of axial capacity of CFST columns causing equivalent decrease in predicted Pu. Similar trend of results can be observed for other tested codes but at lower values of Pu (Figures 4.23–4.26). Further, the details of the databases for prediction axial capacities were presented in "Appendix A" for all design codes tested in this study.

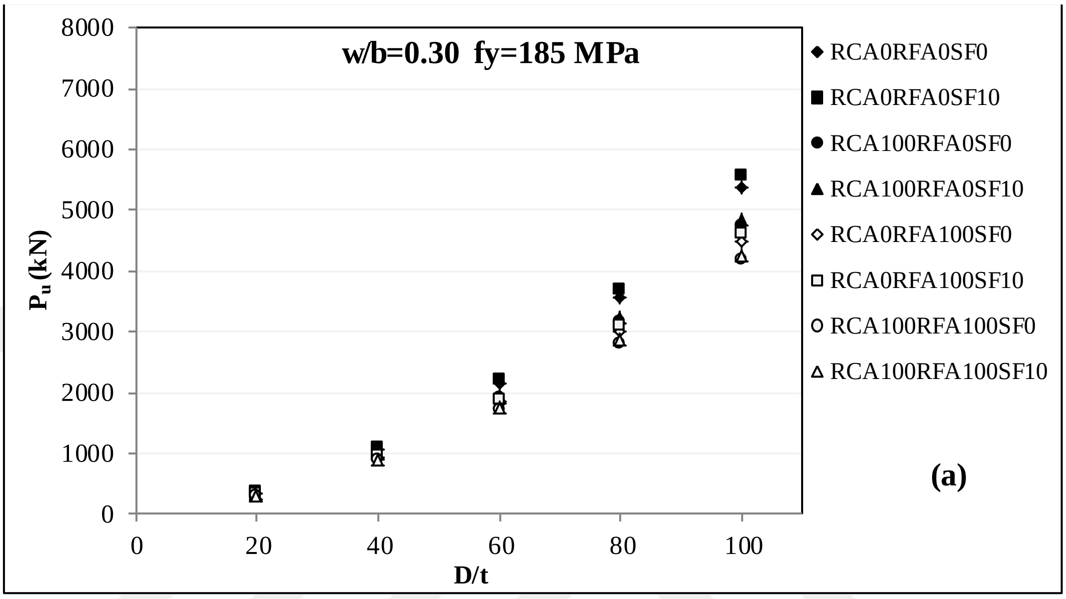

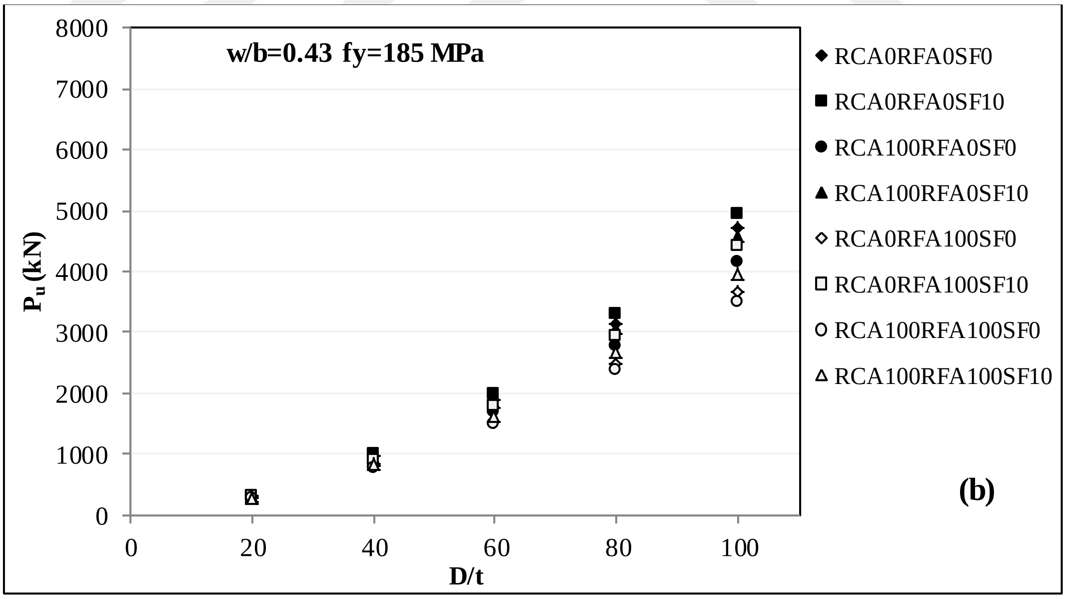

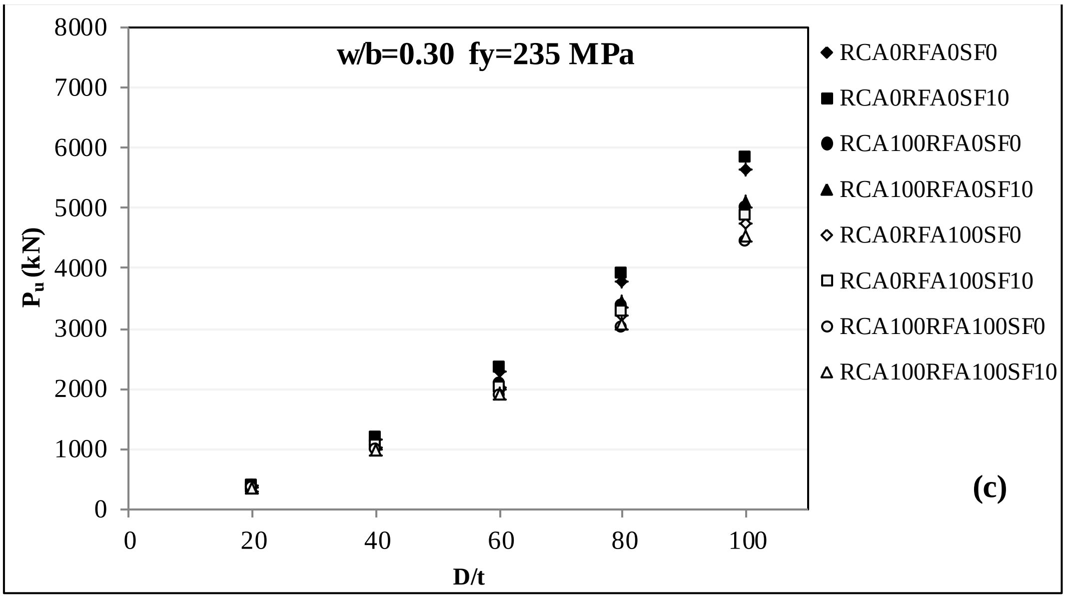
w/b=0.30 fy=235 MPa
Pu (kN)
D/t
RCA0RFA0SF0
RCA0RFA0SF10
RCA100RFA0SF0
RCA100RFA0SF10
RCA0RFA100SF0
RCA0RFA100SF10
RCA100RFA100SF0
RCA100RFA100SF10
(c)

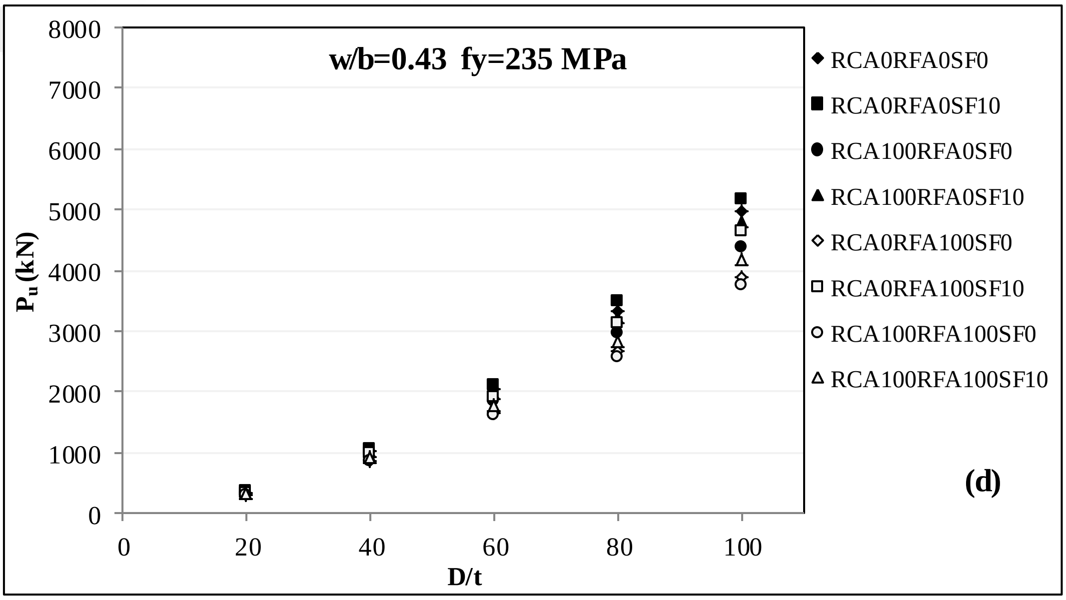
w/b=0.43 fy=235 MPa
Pu (kN)
D/t
RCA0RFA0SF0
RCA0RFA0SF10
RCA100RFA0SF0
RCA100RFA0SF10
RCA0RFA100SF0
RCA0RFA100SF10
RCA100RFA100SF0
RCA100RFA100SF10
(d)

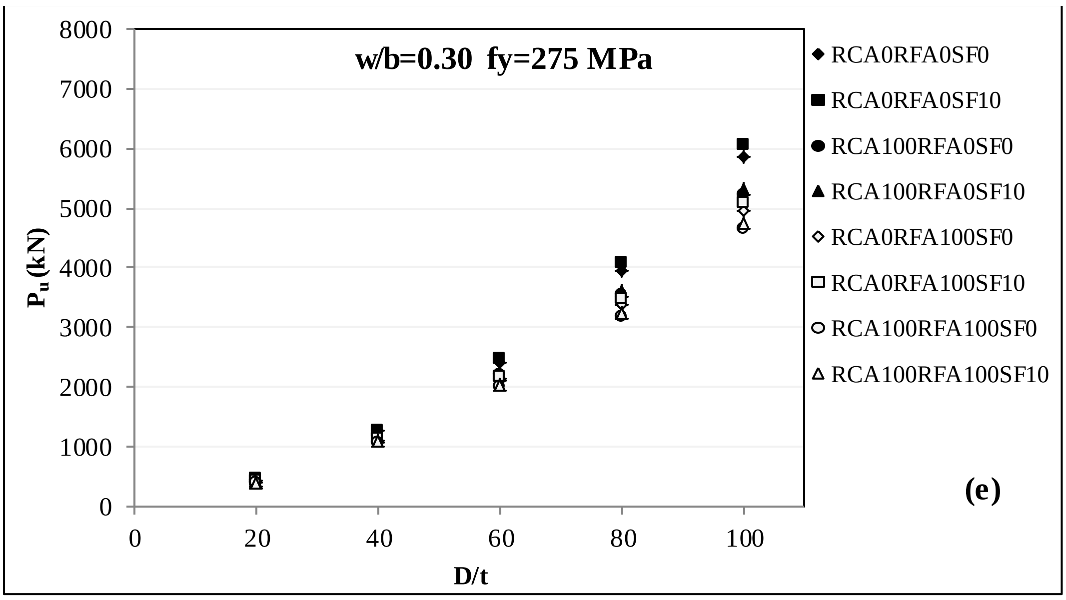
w/b=0.30 fy=275 MPa
Pu (kN)
D/t
RCA0RFA0SF0
RCA0RFA0SF10
RCA100RFA0SF0
RCA100RFA0SF10
RCA0RFA100SF0
RCA0RFA100SF10
RCA100RFA100SF0
RCA100RFA100SF10
(e)

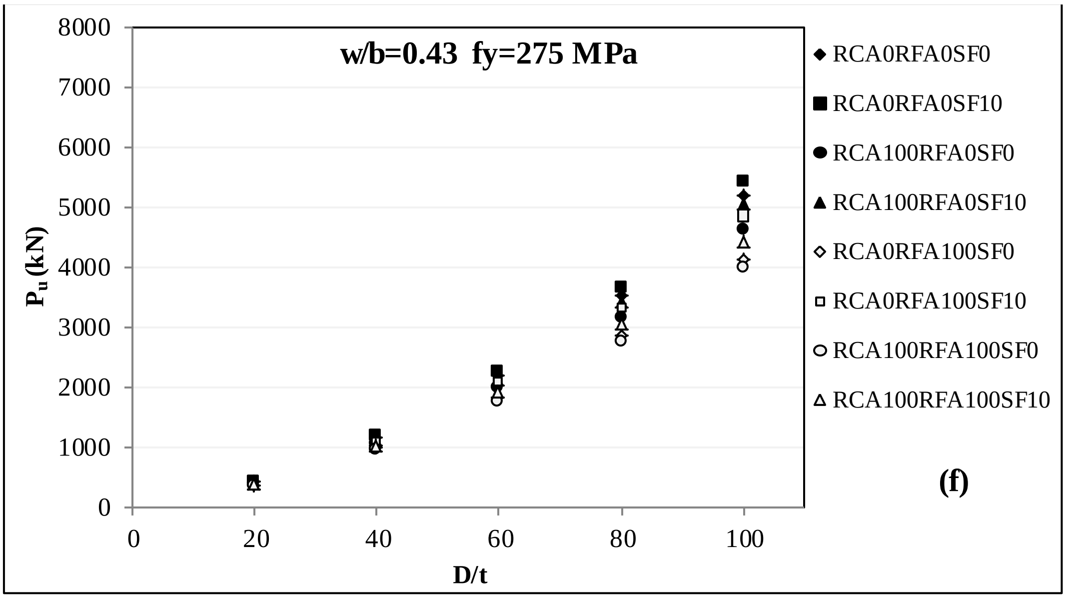
w/b=0.43 fy=275 MPa
Pu (kN)
D/t
RCA0RFA0SF0
RCA0RFA0SF10
RCA100RFA0SF0
RCA100RFA0SF10
RCA0RFA100SF0
RCA0RFA100SF10
RCA100RFA100SF0
RCA100RFA100SF10
(f)

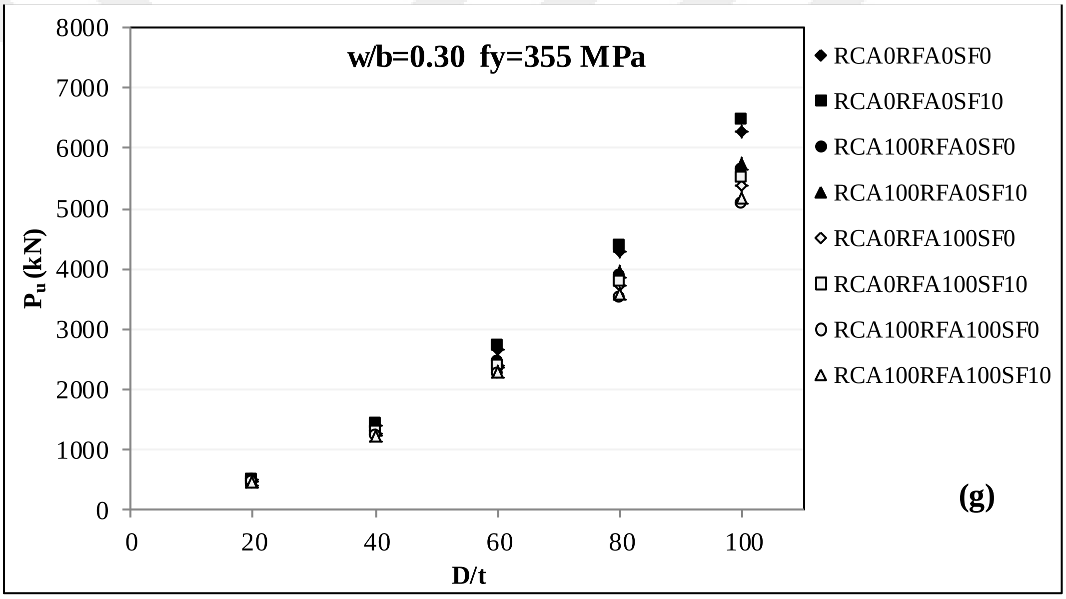
w/b=0.30 fy=355 MPa
Pu (kN)
D/t
RCA0RFA0SF0
RCA0RFA0SF10
RCA100RFA0SF0
RCA100RFA0SF10
RCA0RFA100SF0
RCA0RFA100SF10
RCA100RFA100SF0
RCA100RFA100SF10
(g)

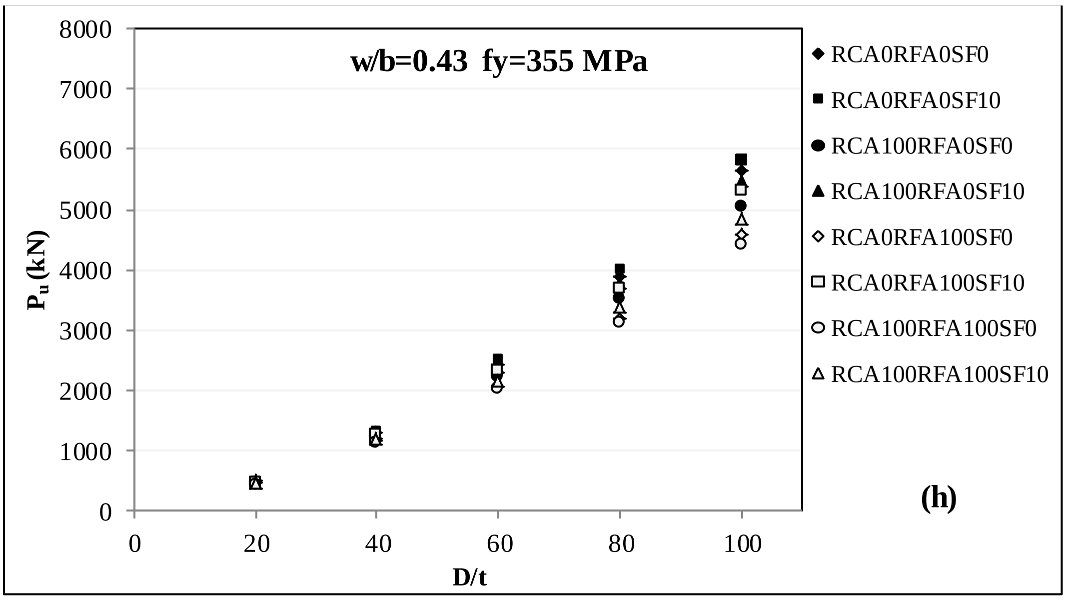
w/b=0.43 fy=355 MPa
Pu (kN)
D/t
RCA0RFA0SF0
RCA0RFA0SF10
RCA100RFA0SF0
RCA100RFA0SF10
RCA0RFA100SF0
RCA0RFA100SF10
RCA100RFA100SF0
RCA100RFA100SF10
(h)

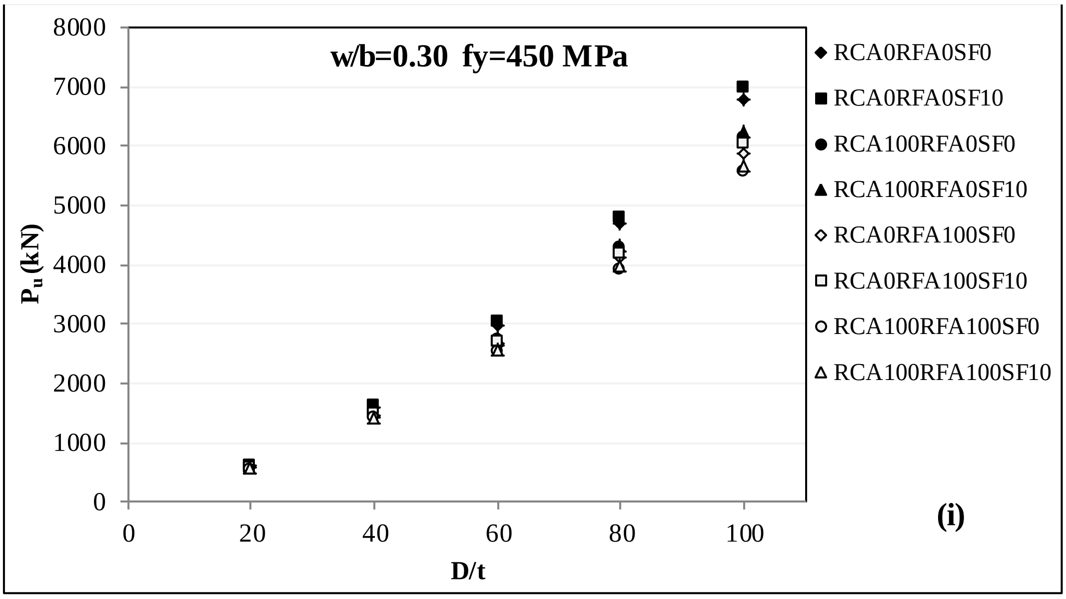

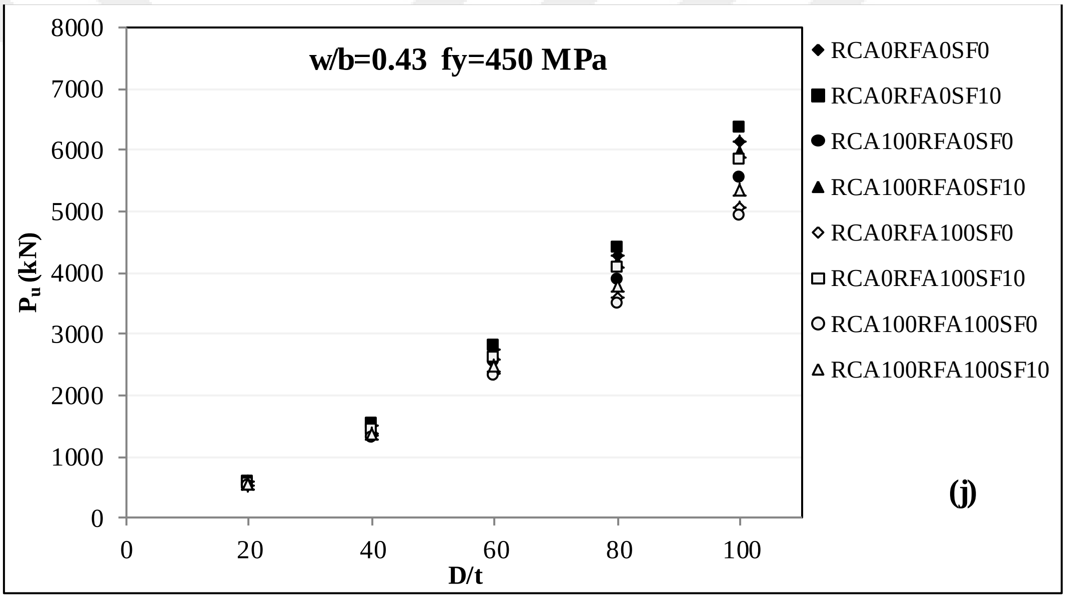

Figure 4.23 The variation of ultimate load vs. D/t ratio of the composite columns according to Eurocode 4 (2004)

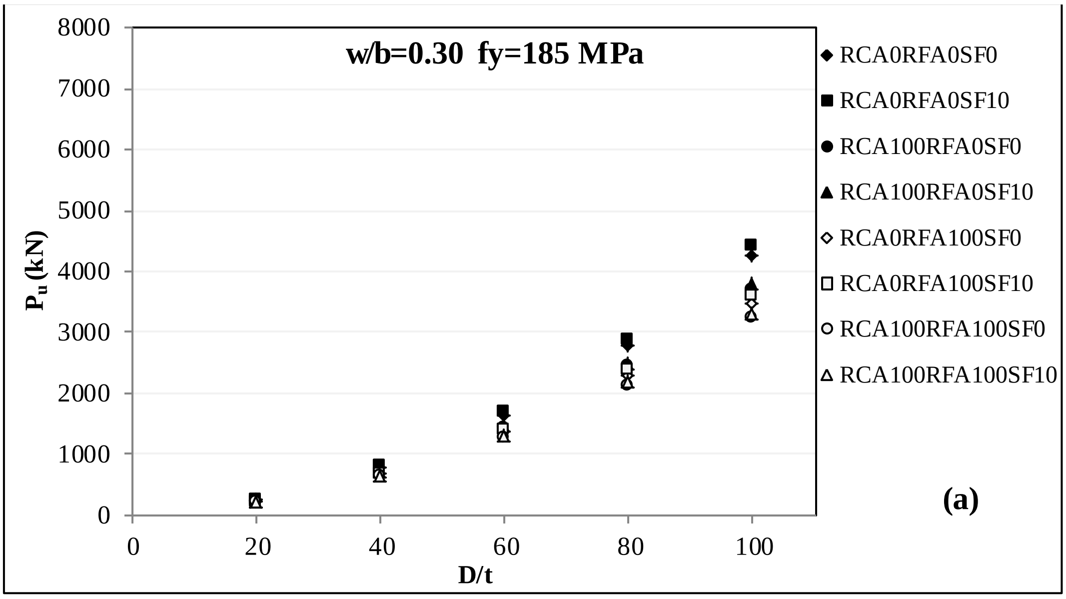
w/b=0.30 fy=185 MPa
RCA0RFA0SF0
RCA0RFA0SF10
RCA100RFA0SF0
RCA100RFA0SF10
RCA0RFA100SF0
RCA0RFA100SF10
RCA100RFA100SF0
RCA100RFA100SF10
P_u (kN)
D/t
0
1000
2000
3000
4000
5000
6000
7000
8000
20
40
60
80
100
(a)

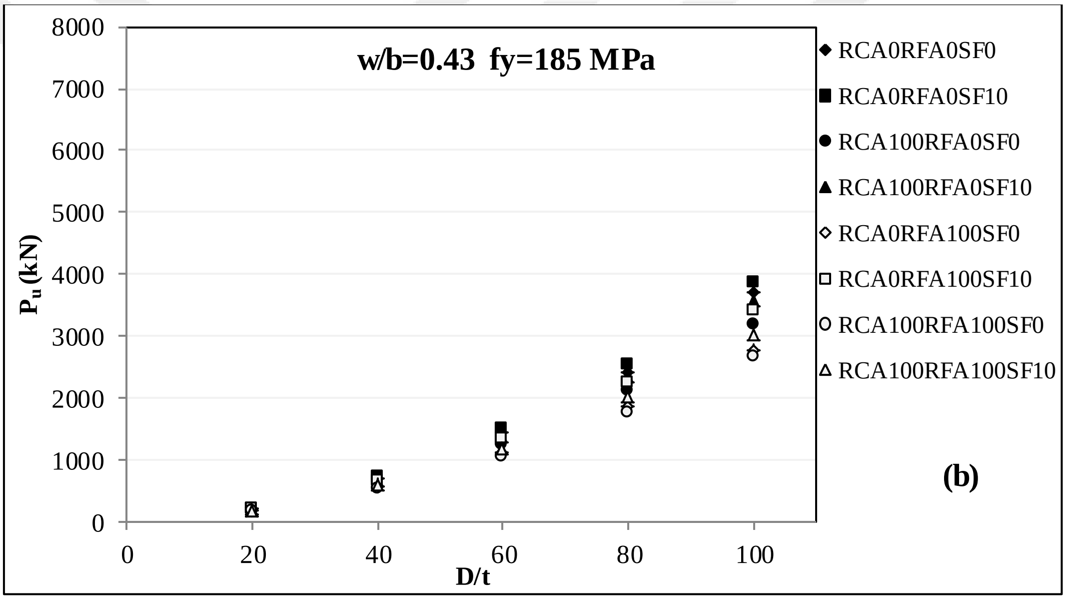
w/b=0.43 fy=185 MPa
RCA0RFA0SF0
RCA0RFA0SF10
RCA100RFA0SF0
RCA100RFA0SF10
RCA0RFA100SF0
RCA0RFA100SF10
RCA100RFA100SF0
RCA100RFA100SF10
P_u (kN)
D/t
0
1000
2000
3000
4000
5000
6000
7000
8000
20
40
60
80
100
(b)

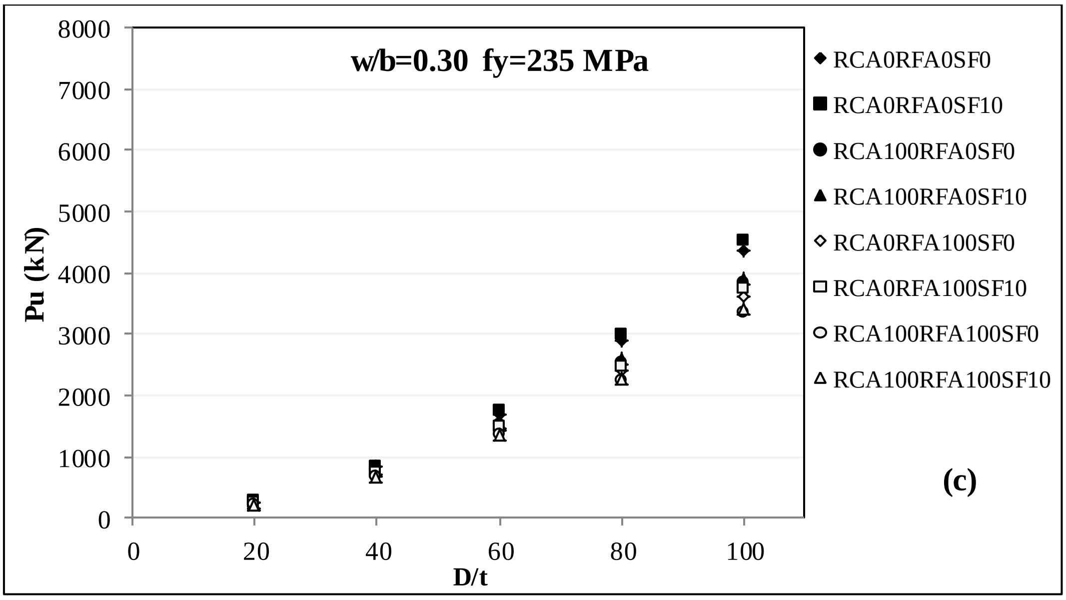
w/b=0.30 fy=235 MPa
RCA0RFA0SF0
RCA0RFA0SF10
RCA100RFA0SF0
RCA100RFA0SF10
RCA0RFA100SF0
RCA0RFA100SF10
RCA100RFA100SF0
RCA100RFA100SF10
Pu (kN)
D/t
0
1000
2000
3000
4000
5000
6000
7000
8000
20
40
60
80
100
(c)

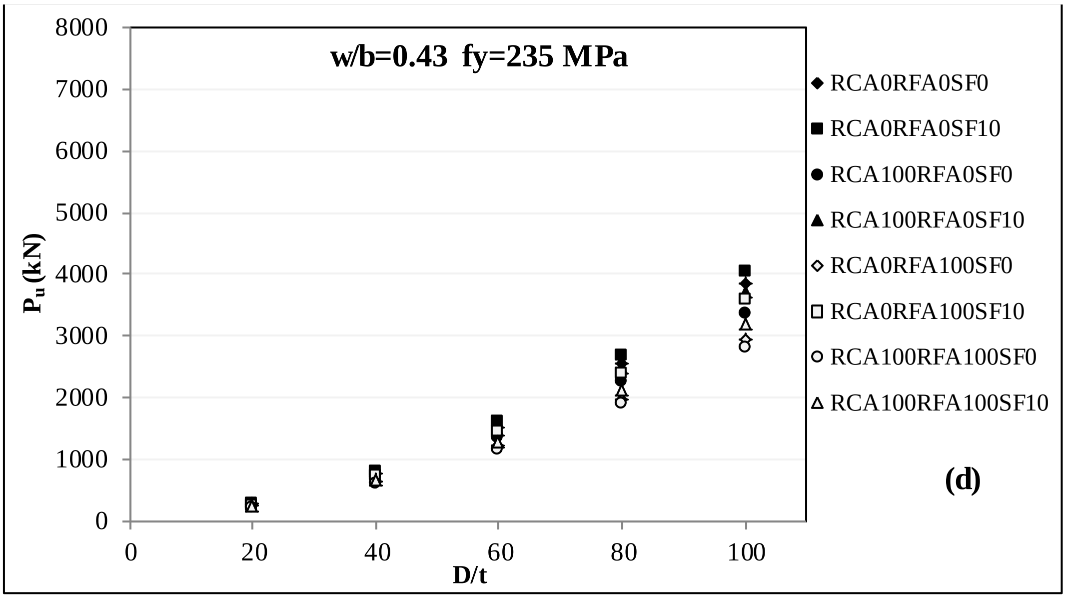

w/b=0.43 fy=235 MPa
RCA0RFA0SF0
RCA0RFA0SF10
RCA100RFA0SF0
RCA100RFA0SF10
RCA0RFA100SF0
RCA0RFA100SF10
RCA100RFA100SF0
RCA100RFA100SF10
(d)
Pu (kN)
D/t
0
1000
2000
3000
4000
5000
6000
7000
8000
0
20
40
60
80
100

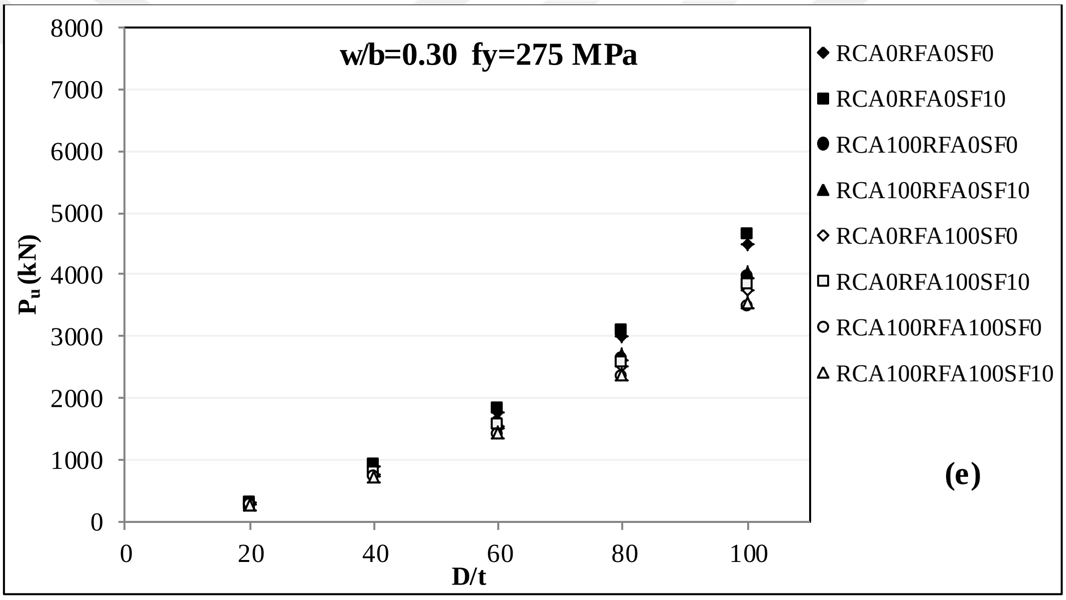

w/b=0.30 fy=275 MPa
RCA0RFA0SF0
RCA0RFA0SF10
RCA100RFA0SF0
RCA100RFA0SF10
RCA0RFA100SF0
RCA0RFA100SF10
RCA100RFA100SF0
RCA100RFA100SF10
(e)
Pu (kN)
D/t
0
1000
2000
3000
4000
5000
6000
7000
8000
0
20
40
60
80
100

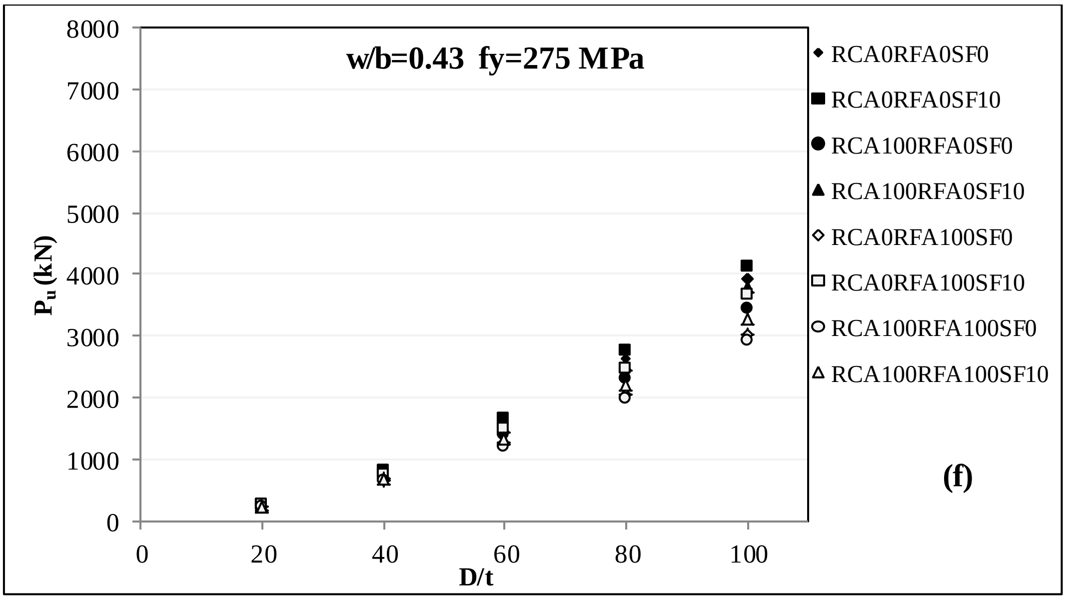

w/b=0.43 fy=275 MPa
RCA0RFA0SF0
RCA0RFA0SF10
RCA100RFA0SF0
RCA100RFA0SF10
RCA0RFA100SF0
RCA0RFA100SF10
RCA100RFA100SF0
RCA100RFA100SF10
(f)
Pu (kN)
D/t
0
1000
2000
3000
4000
5000
6000
7000
8000
0
20
40
60
80
100

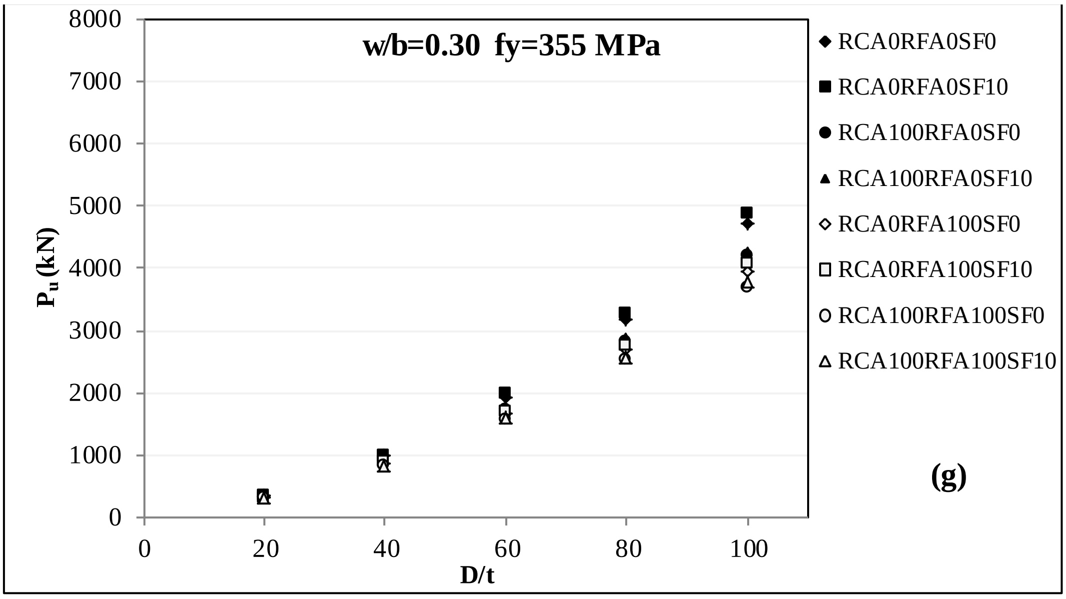
w/b=0.30 fy=355 MPa
P_u (kN)
D/t
RCA0RFA0SF0
RCA0RFA0SF10
RCA100RFA0SF0
RCA100RFA0SF10
RCA0RFA100SF0
RCA0RFA100SF10
RCA100RFA100SF0
RCA100RFA100SF10
(g)

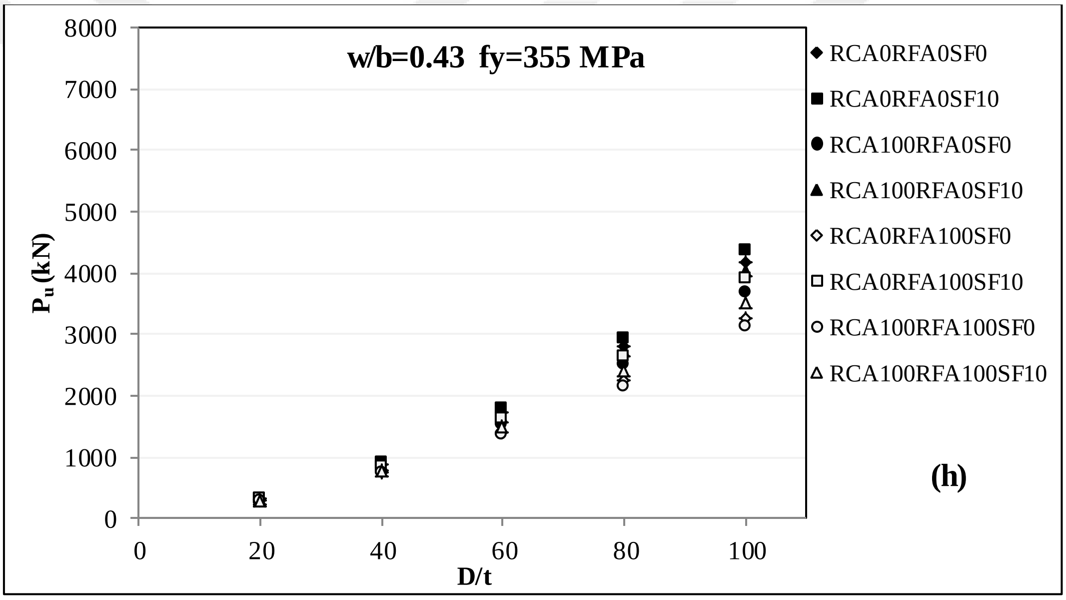
w/b=0.43 fy=355 MPa
P_u (kN)
D/t
RCA0RFA0SF0
RCA0RFA0SF10
RCA100RFA0SF0
RCA100RFA0SF10
RCA0RFA100SF0
RCA0RFA100SF10
RCA100RFA100SF0
RCA100RFA100SF10
(h)

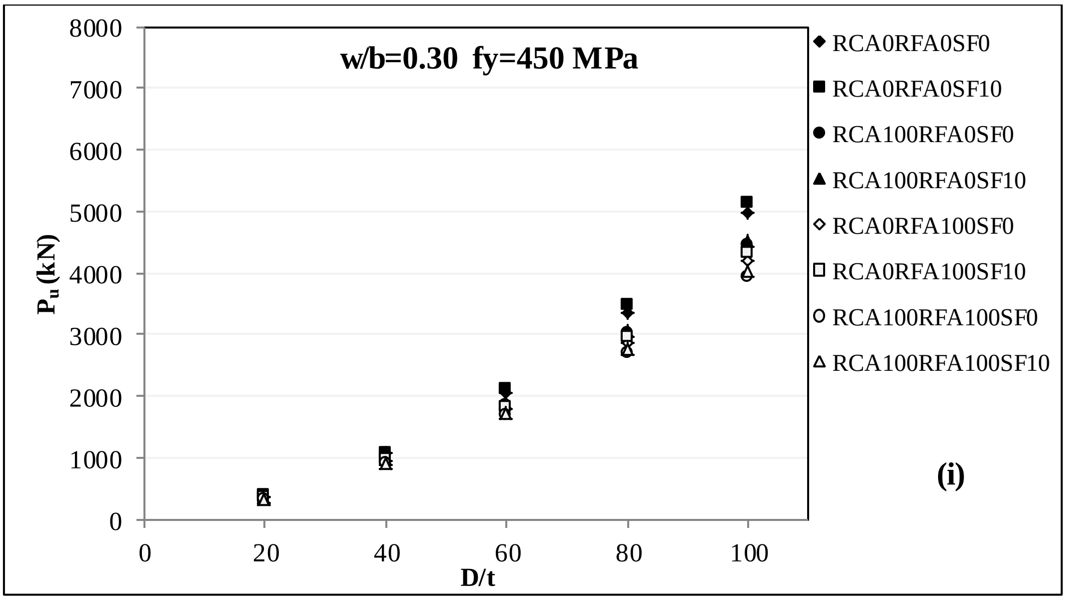
w/b=0.30 fy=450 MPa
P_u (kN)
D/t
RCA0RFA0SF0
RCA0RFA0SF10
RCA100RFA0SF0
RCA100RFA0SF10
RCA0RFA100SF0
RCA0RFA100SF10
RCA100RFA100SF0
RCA100RFA100SF10
(i)

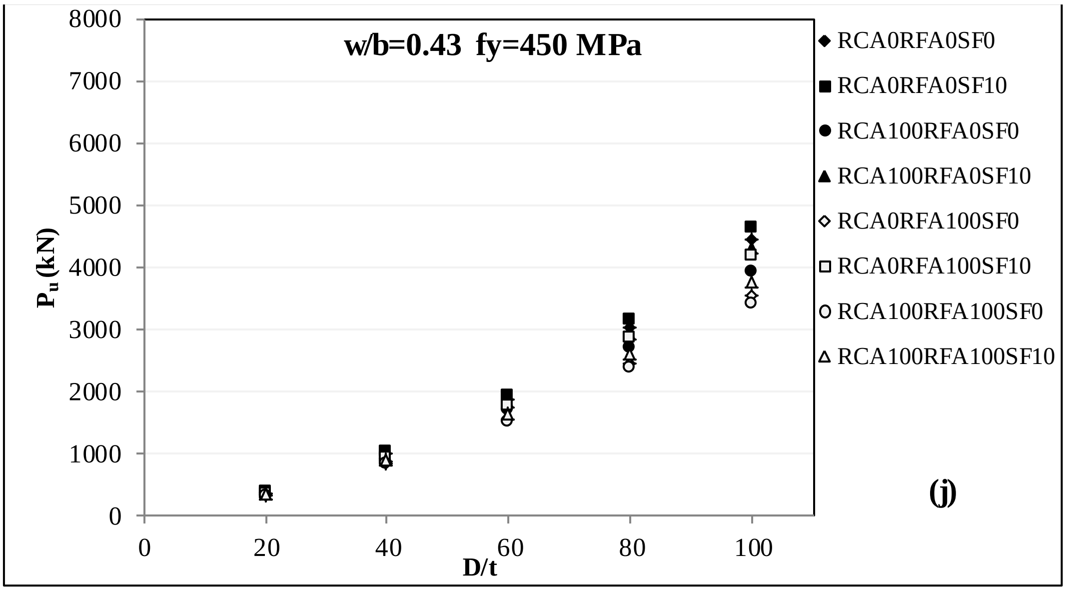

Figure 4.24 The variation of ultimate load vs. D/t ratio of the composite columns calculated according to ACI (2005)

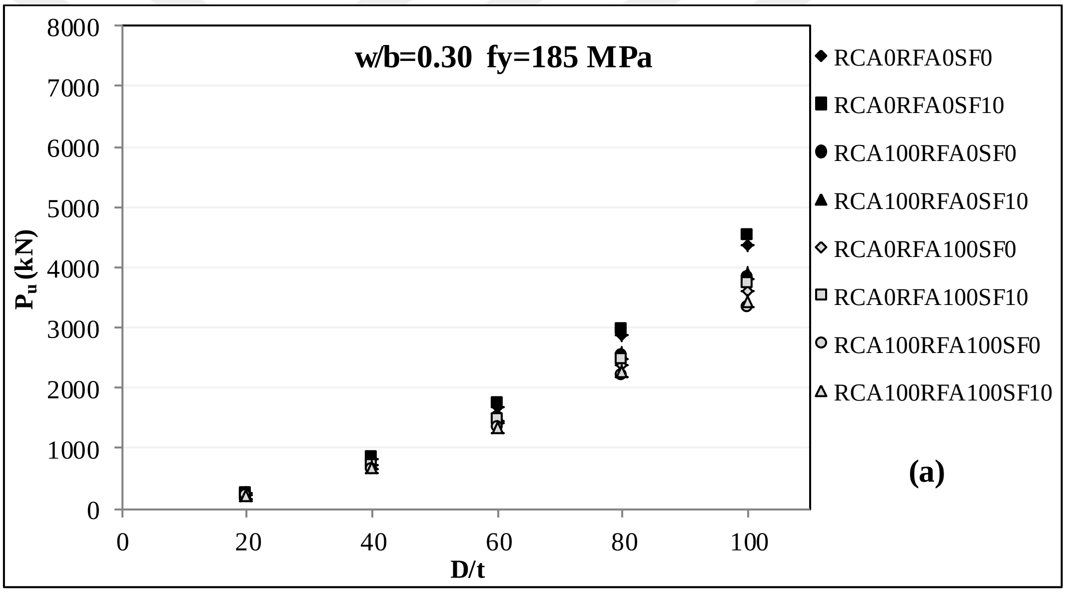

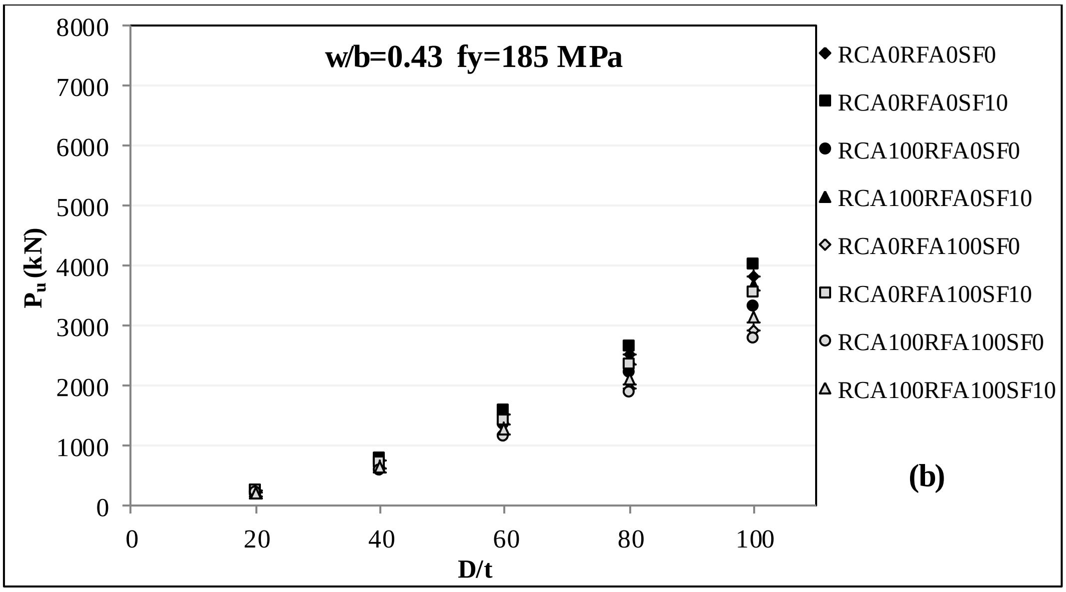

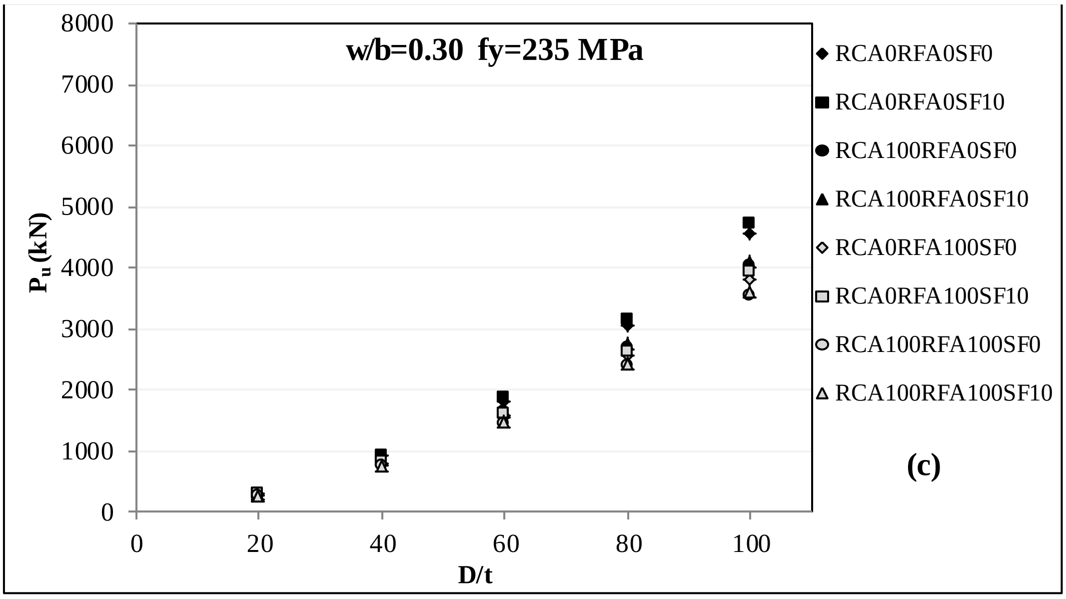
w/b=0.30 fy=235 MPa
Pu (kN)
D/t
RCA0RFA0SF0
RCA0RFA0SF10
RCA100RFA0SF0
RCA100RFA0SF10
RCA0RFA100SF0
RCA0RFA100SF10
RCA100RFA100SF0
RCA100RFA100SF10
(c)

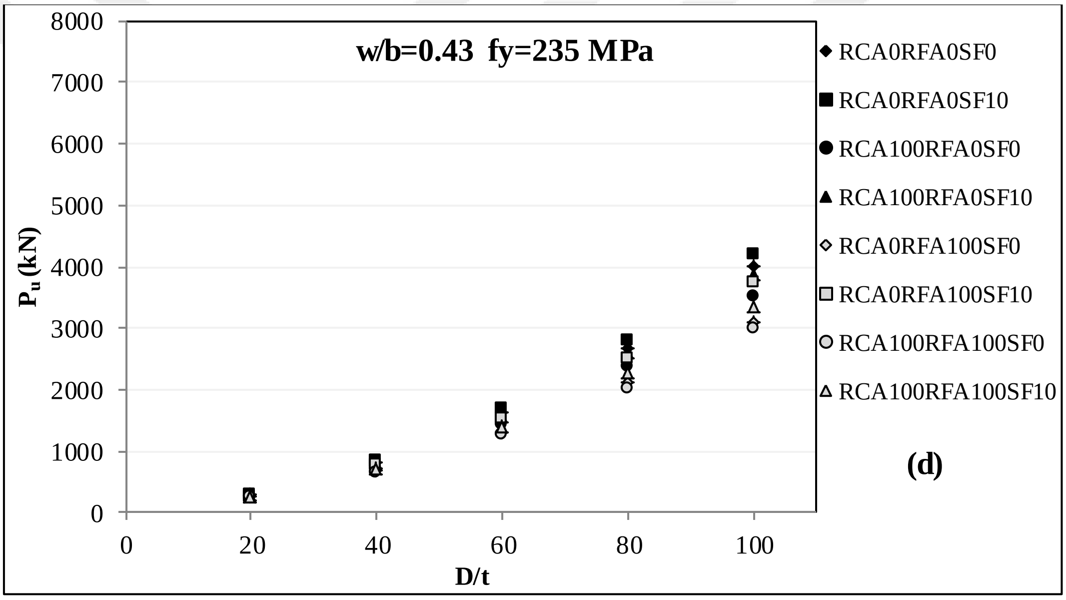
w/b=0.43 fy=235 MPa
Pu (kN)
D/t
RCA0RFA0SF0
RCA0RFA0SF10
RCA100RFA0SF0
RCA100RFA0SF10
RCA0RFA100SF0
RCA0RFA100SF10
RCA100RFA100SF0
RCA100RFA100SF10
(d)

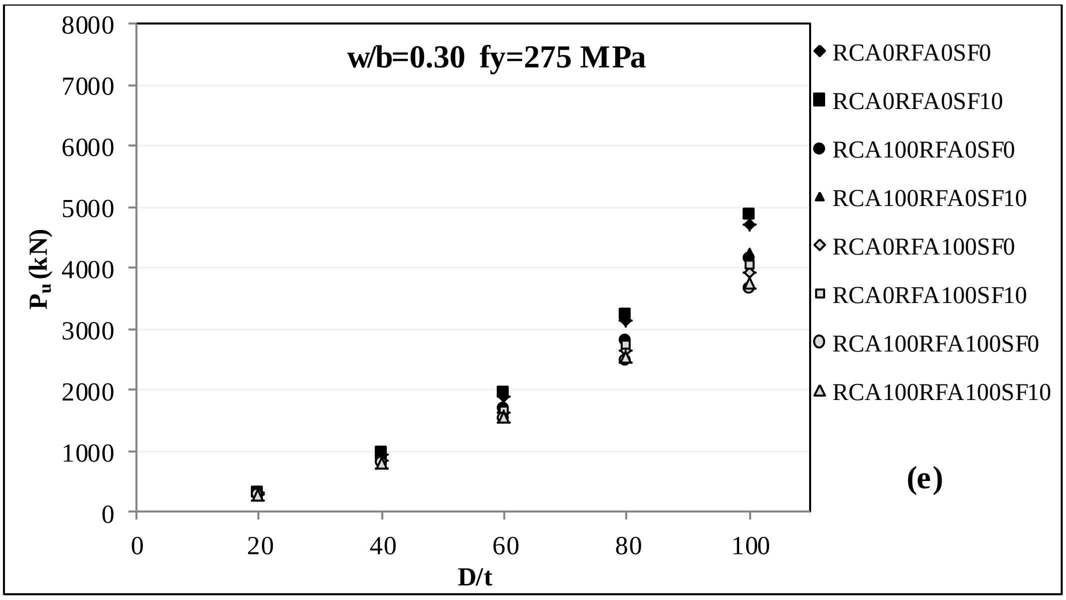
w/b=0.30 fy=275 MPa
Pu (kN)
D/t
RCA0RFA0SF0
RCA0RFA0SF10
RCA100RFA0SF0
RCA100RFA0SF10
RCA0RFA100SF0
RCA0RFA100SF10
RCA100RFA100SF0
RCA100RFA100SF10
(e)

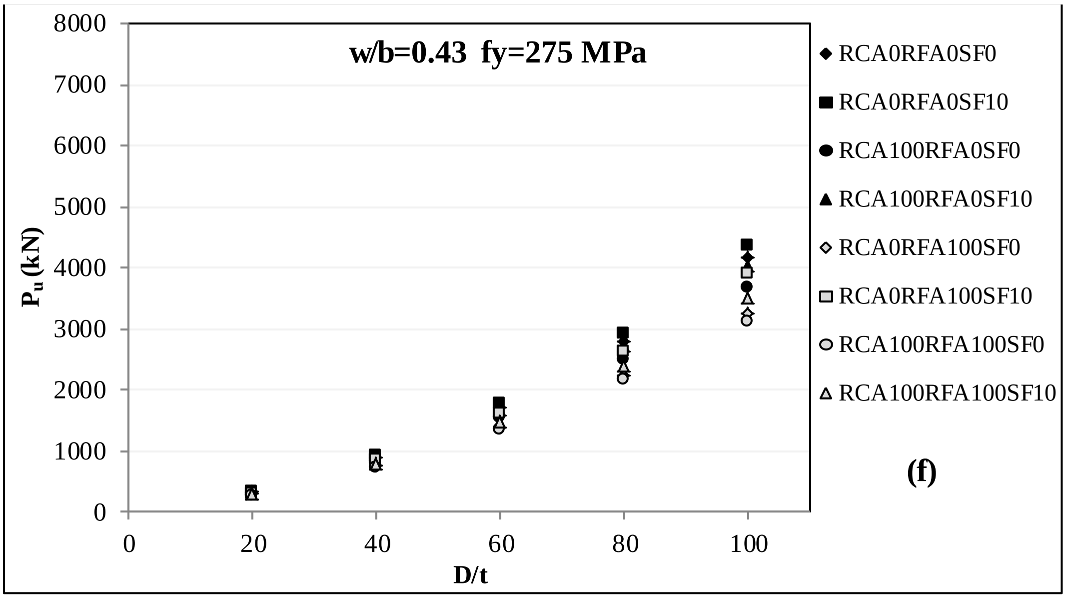

w/b=0.43 fy=275 MPa
P_u (kN)
D/t
RCA0RFA0SF0
RCA0RFA0SF10
RCA100RFA0SF0
RCA100RFA0SF10
RCA0RFA100SF0
RCA0RFA100SF10
RCA100RFA100SF0
RCA100RFA100SF10
(f)

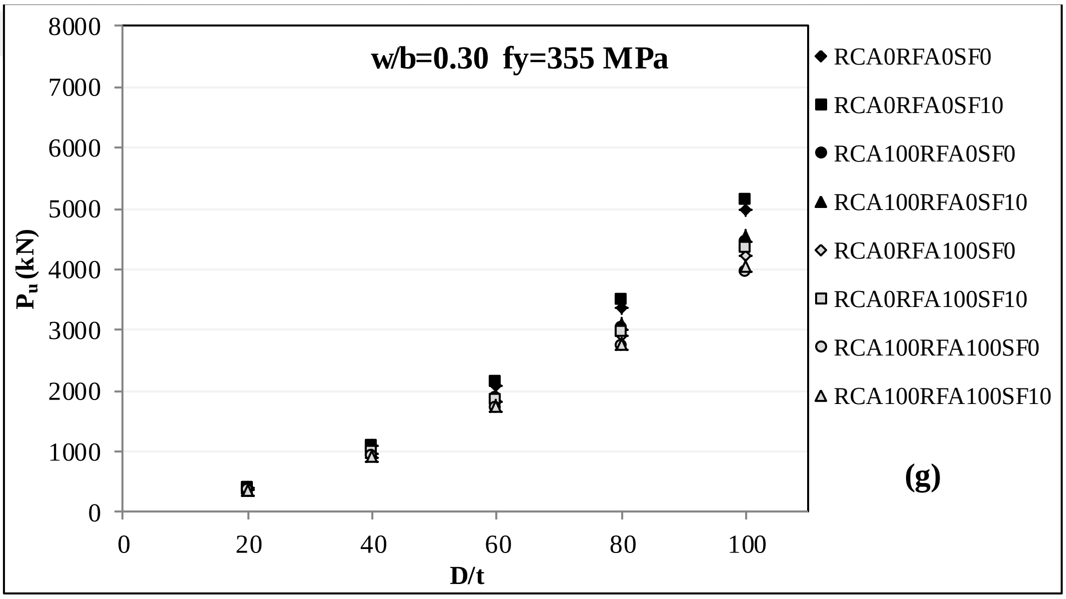

w/b=0.30 fy=355 MPa
P_u (kN)
D/t
RCA0RFA0SF0
RCA0RFA0SF10
RCA100RFA0SF0
RCA100RFA0SF10
RCA0RFA100SF0
RCA0RFA100SF10
RCA100RFA100SF0
RCA100RFA100SF10
(g)

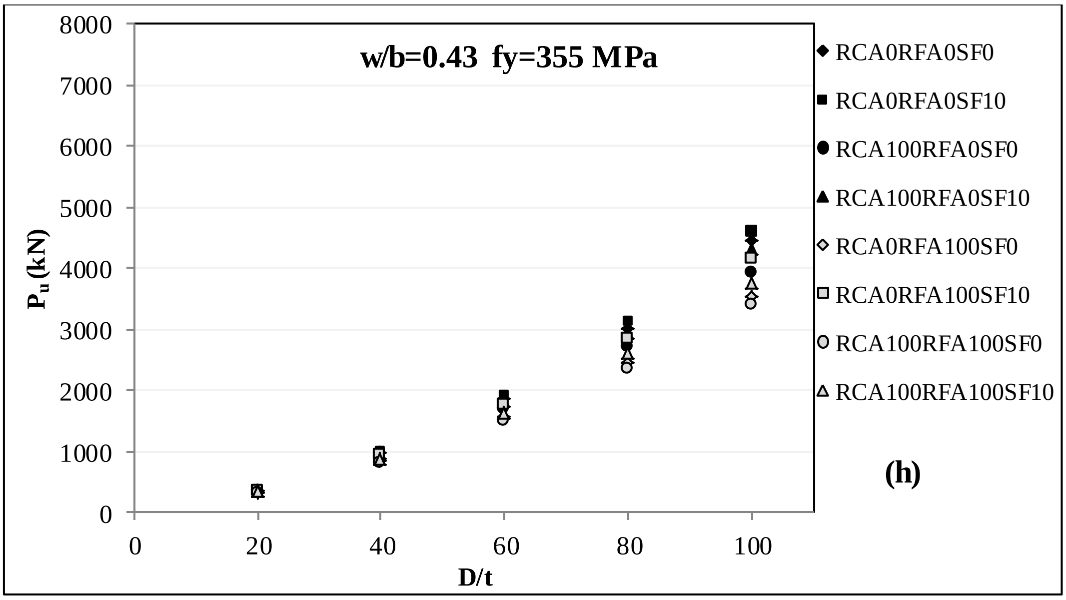

w/b=0.43 fy=355 MPa
P_u (kN)
D/t
RCA0RFA0SF0
RCA0RFA0SF10
RCA100RFA0SF0
RCA100RFA0SF10
RCA0RFA100SF0
RCA0RFA100SF10
RCA100RFA100SF0
RCA100RFA100SF10
(h)

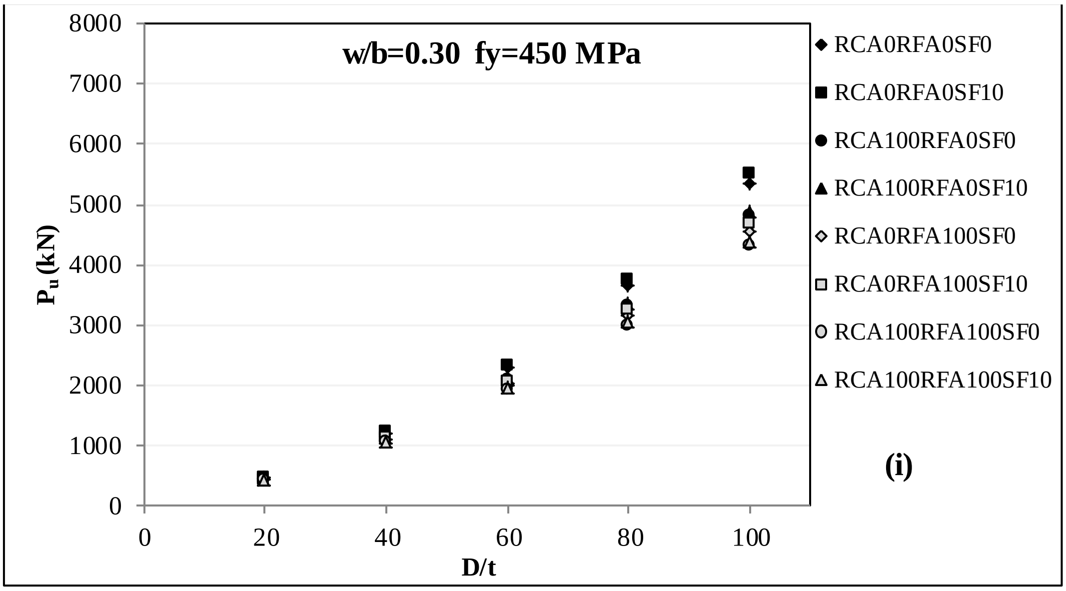

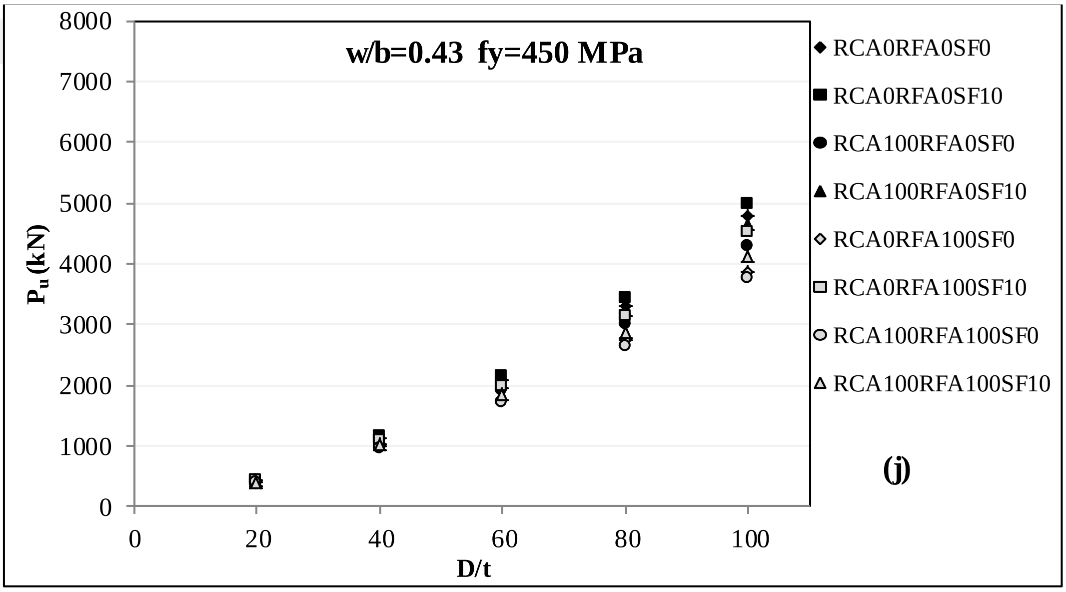

Figure 4.25 The variation of ultimate load vs. D/t ratio of the composite columns calculated according to AIJ (1997; 2001)

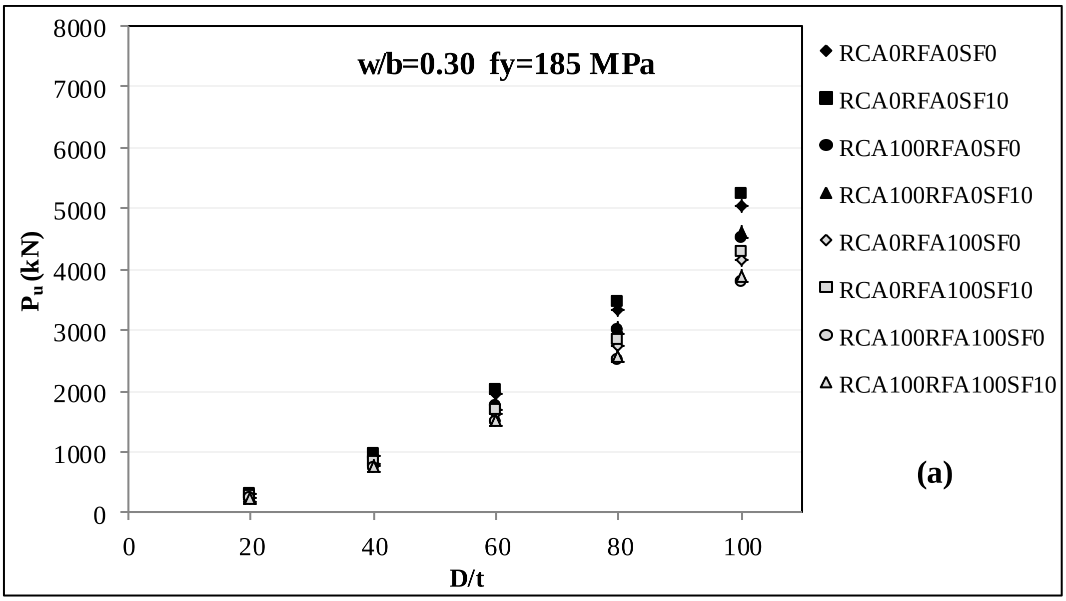

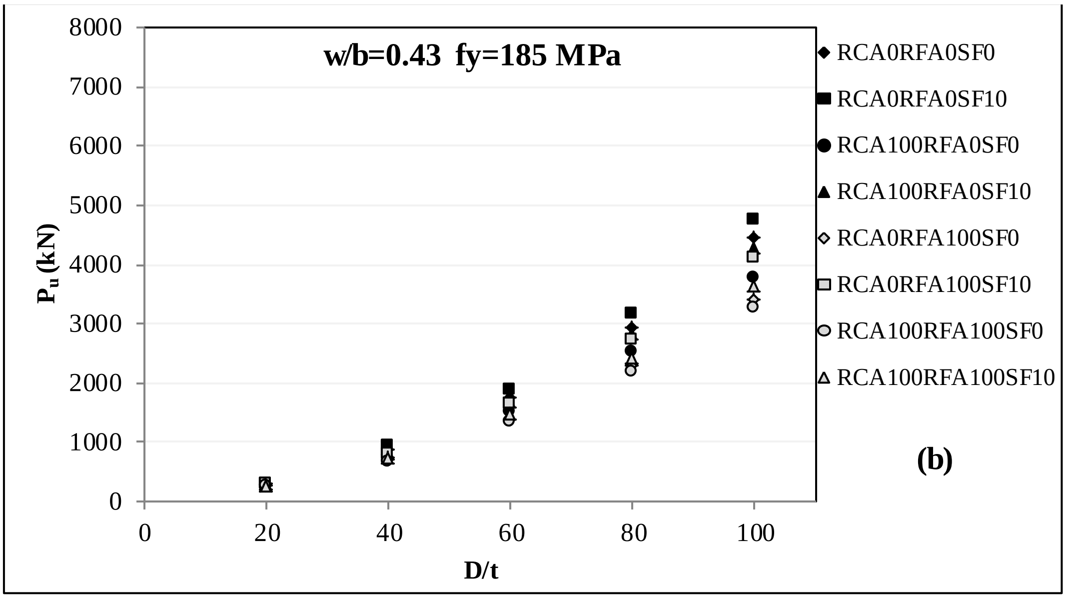
w/b=0.43 fy=185 MPa
RCA0RFA0SF0
RCA0RFA0SF10
RCA100RFA0SF0
RCA100RFA0SF10
RCA0RFA100SF0
RCA0RFA100SF10
RCA100RFA100SF0
RCA100RFA100SF10
(b)
Pu (kN)
D/t

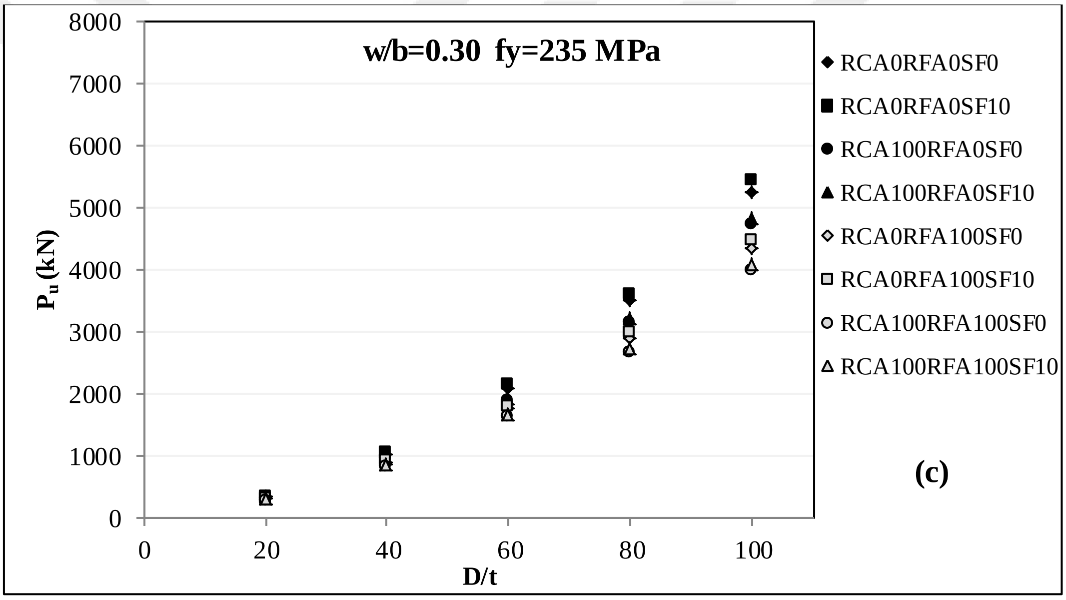
w/b=0.30 fy=235 MPa
RCA0RFA0SF0
RCA0RFA0SF10
RCA100RFA0SF0
RCA100RFA0SF10
RCA0RFA100SF0
RCA0RFA100SF10
RCA100RFA100SF0
RCA100RFA100SF10
(c)
Pu (kN)
D/t

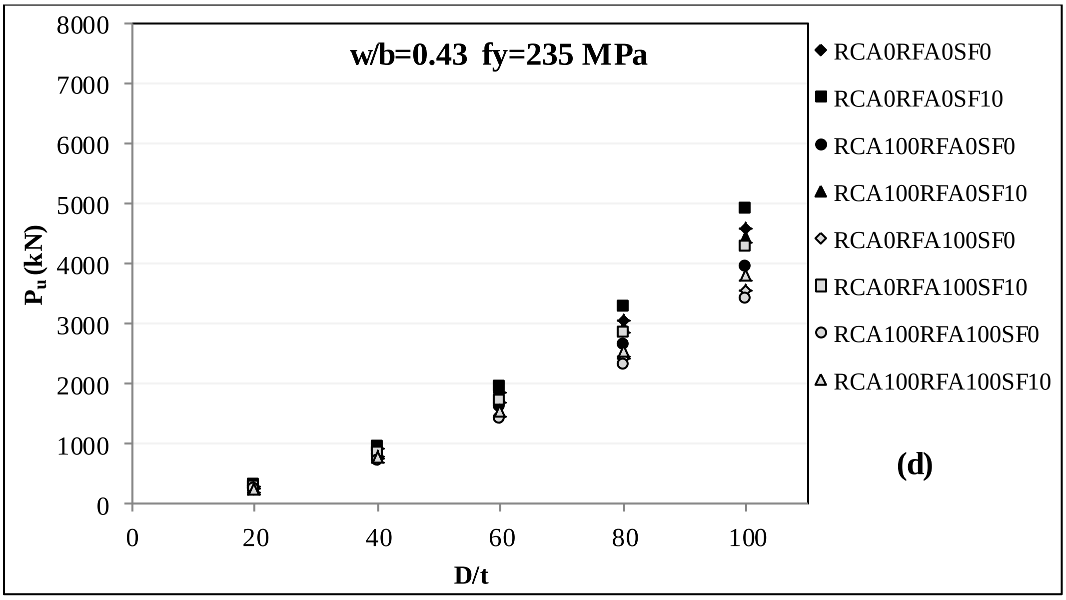
w/b=0.43 fy=235 MPa
RCA0RFA0SF0
RCA0RFA0SF10
RCA100RFA0SF0
RCA100RFA0SF10
RCA0RFA100SF0
RCA0RFA100SF10
RCA100RFA100SF0
RCA100RFA100SF10
(d)
Pu (kN)
D/t

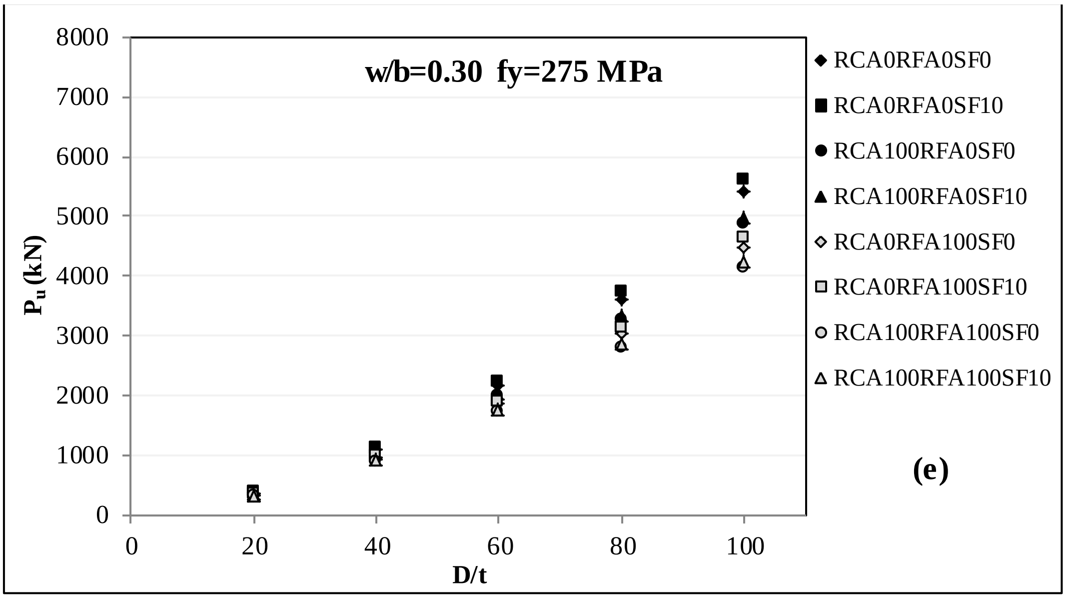

w/b=0.30 fy=275 MPa
P_u (kN)
D/t
RCA0RFA0SF0
RCA0RFA0SF10
RCA100RFA0SF0
RCA100RFA0SF10
RCA0RFA100SF0
RCA0RFA100SF10
RCA100RFA100SF0
RCA100RFA100SF10
(e)

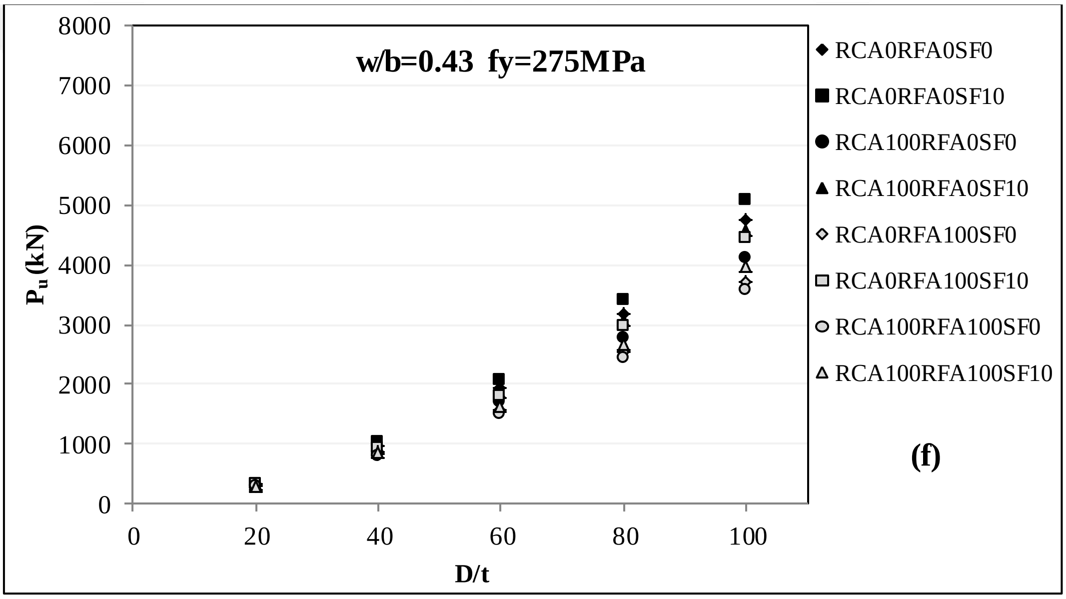

w/b=0.43 fy=275MPa
P_u (kN)
D/t
RCA0RFA0SF0
RCA0RFA0SF10
RCA100RFA0SF0
RCA100RFA0SF10
RCA0RFA100SF0
RCA0RFA100SF10
RCA100RFA100SF0
RCA100RFA100SF10
(f)

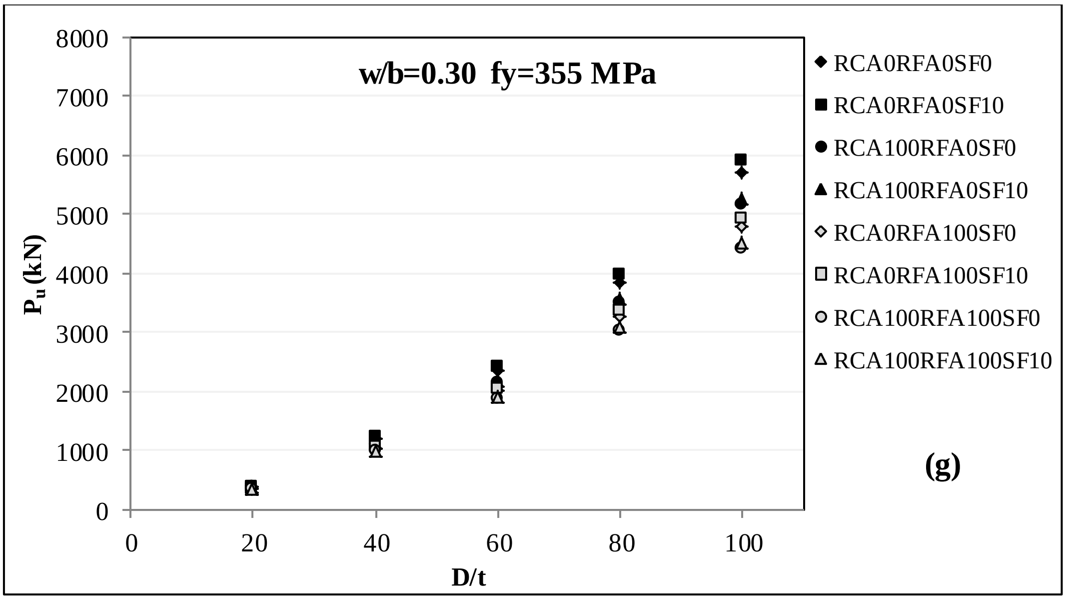

w/b=0.30 fy=355 MPa
P_u (kN)
D/t
RCA0RFA0SF0
RCA0RFA0SF10
RCA100RFA0SF0
RCA100RFA0SF10
RCA0RFA100SF0
RCA0RFA100SF10
RCA100RFA100SF0
RCA100RFA100SF10
(g)

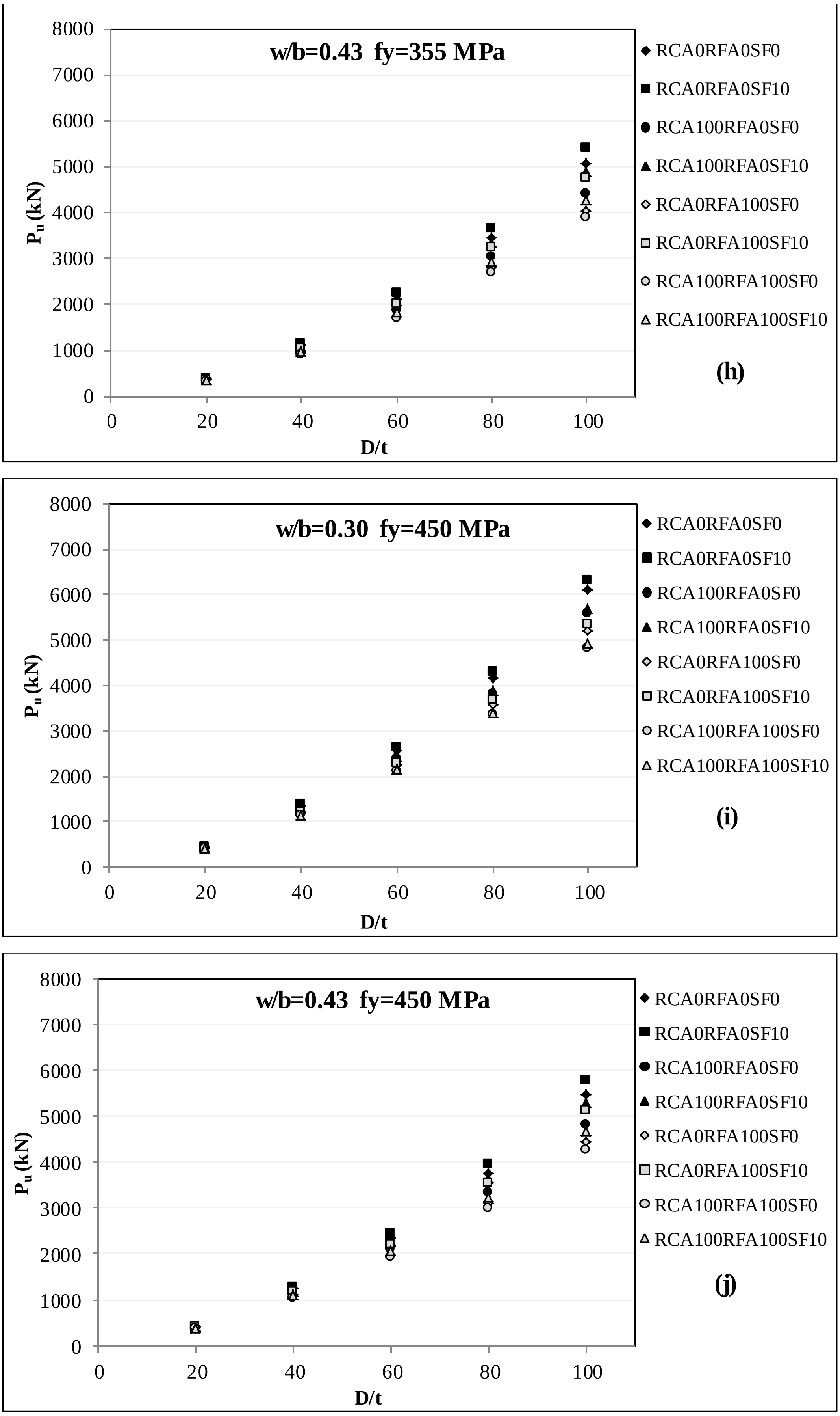

Figure 4.26 The variation of ultimate load vs. D/t ratio of the composite columns calculated according to DL/T (1999)

The effect of utilizing RA on the Pu results is also depicted in Figure 4.27 where the effect of using RA instead of NA on the axial capacity of the composite columns calculated via EC 4 is presented. In similar way, Figures 4.28, 4.29 and 4.30 represent the ratio of axial load for RA mixes to axial load for NA for ACI, AIJ and DL/T codes, respectively. In aforesaid figures, the mixtures were divided according to type of aggregate into three main groups, RCA, RFA and (RCA+RFA) group. The mixes classification was conducted in order to compare each group with NA group. In spite of the difference in amount, the same trend could be observed in all figures; where the difference in the predicted Pu value between NA and RA mixes was minor at low D/t ratio. However, the difference was more pronounced whenever D/t ratio and yield strength of steel had increased. Indeed, Figures 4.28-4.30 revealed that there was a significant effect of aggregate type on the predicted ultimate axial strength of circular CFST columns using EC 4 provisions as well as other design codes. When the comparison with NA mixes was considered, RCA, RFA and (RCA+RFA) groups showed the highest ratio respectively. Indeed, these findings agreed with the aforesaid explanation that the compressive strength constantly decreased by this sequence due to the nature and properties of RA which in-turn decreased the strength of produced concrete. The use of RCA, RFA, and (RCA + RFA) decreased the compressive strength of the corresponding NA concretes by 11.8-16.9%, 15.8-26.9%, and 27.0-30.9%, respectively. For a given w/b ratio, the strength of RAs is the primary factor affecting the strength of the RASCC (Kou and Poon, 2009; Safiuddin et al., 2011-a; Safiuddin et al., 2011-b; Grdic et al., 2010; Sagoe-Crentsil et al., 2001). It is worth mentioning that the predicted Pu ratios were closer to 1.0 in high w/b ratio mixtures (0.43). Moreover, this trend repeated for other tested design codes. For instant, the ($Pu,_{RA}/Pu,_{NA}$) ratio recorded 0.978 for (fy=450 RCA) at 0.43 w/b ratio mixture compared with 0.963 for the same group at 0.30 w/b ratio mixture (Figure 4.27).

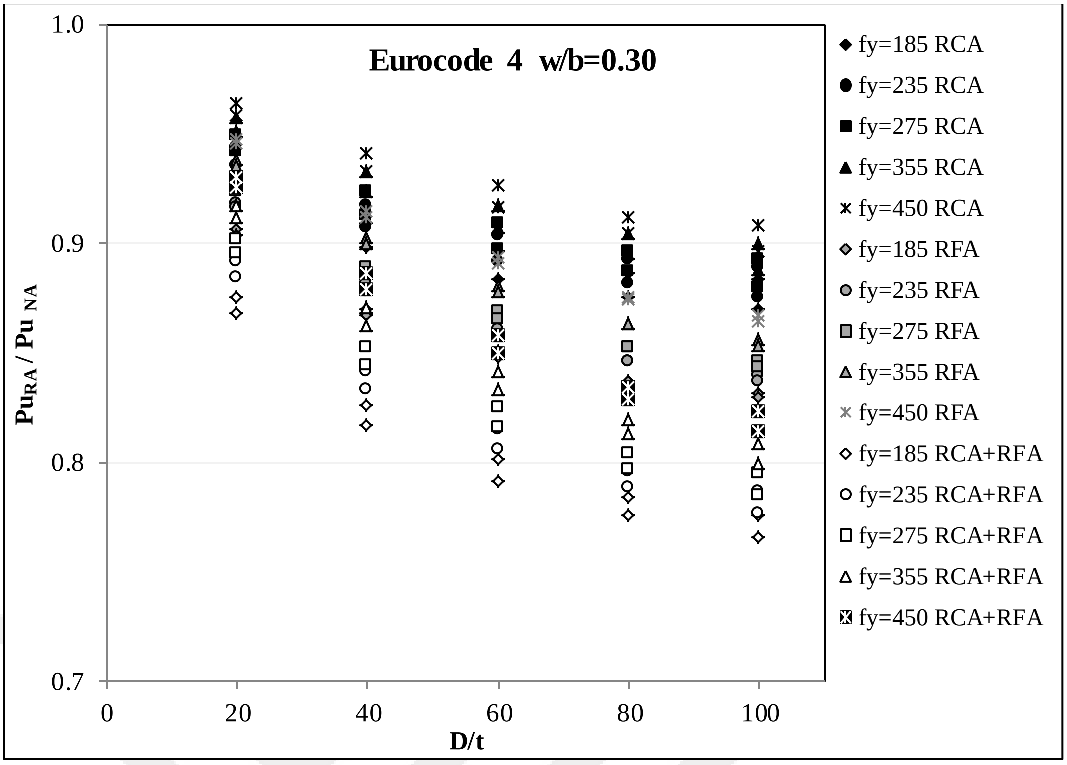

(a)

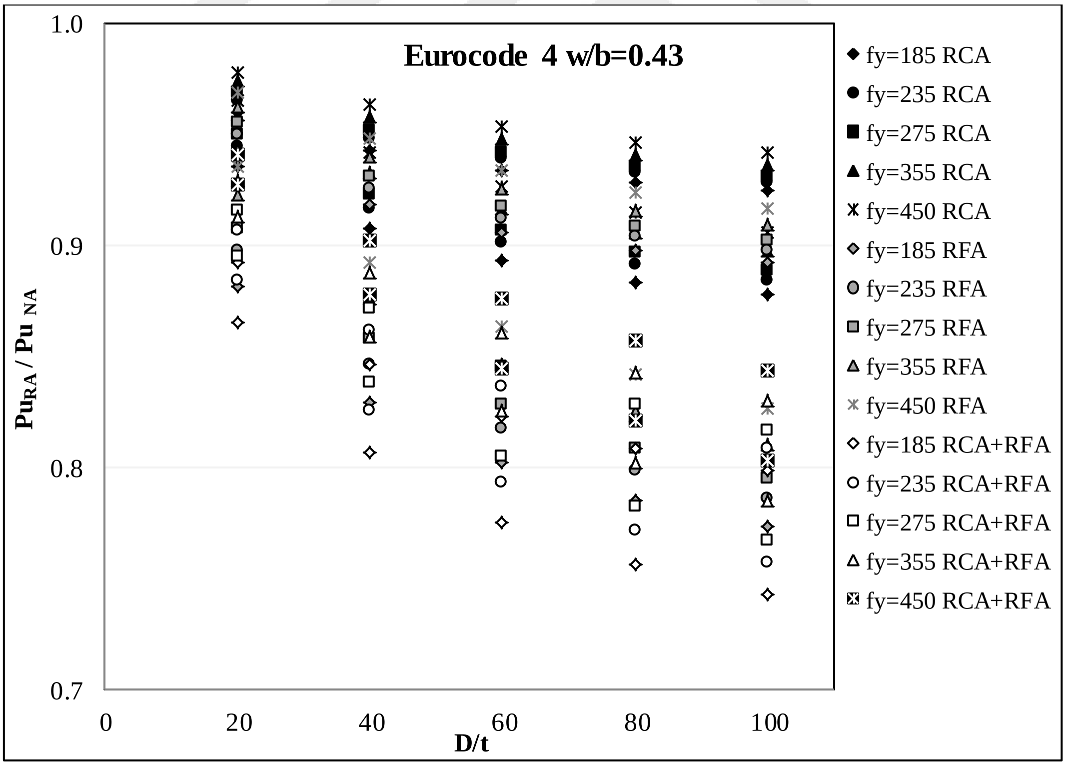

(b)

Figure 0.27 Effect of using RA instead of NA on the axial capacity of the composite columns calculated via Eurocode 4 (2004)

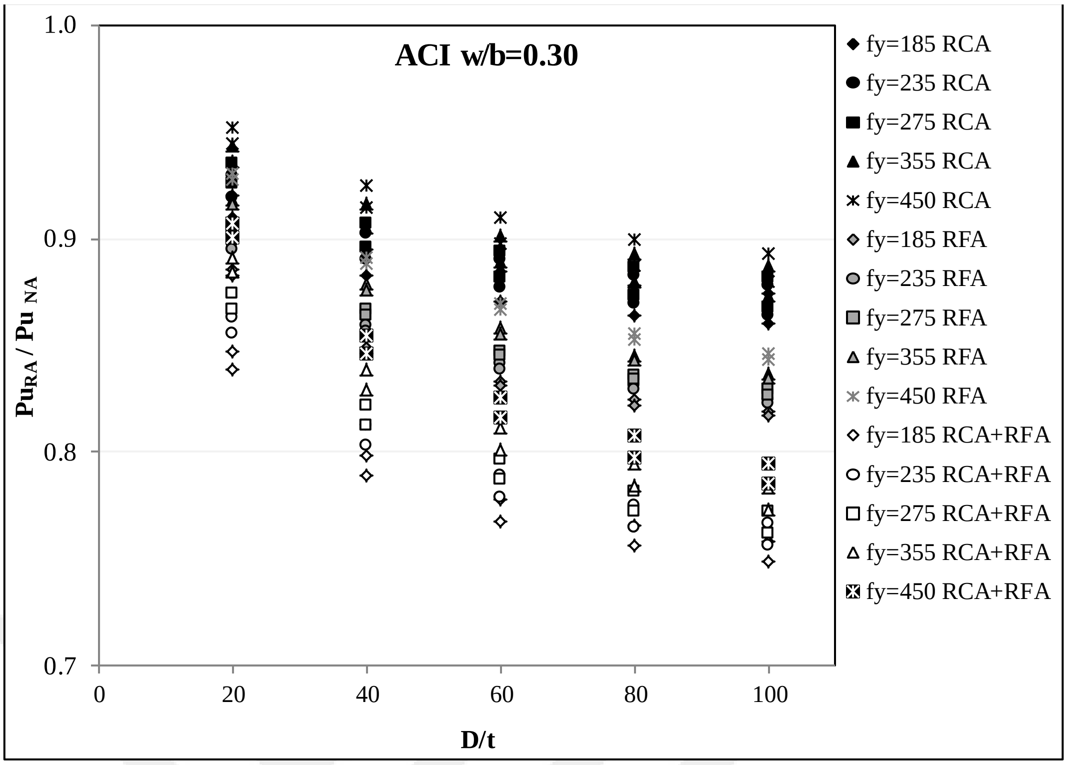

(a)

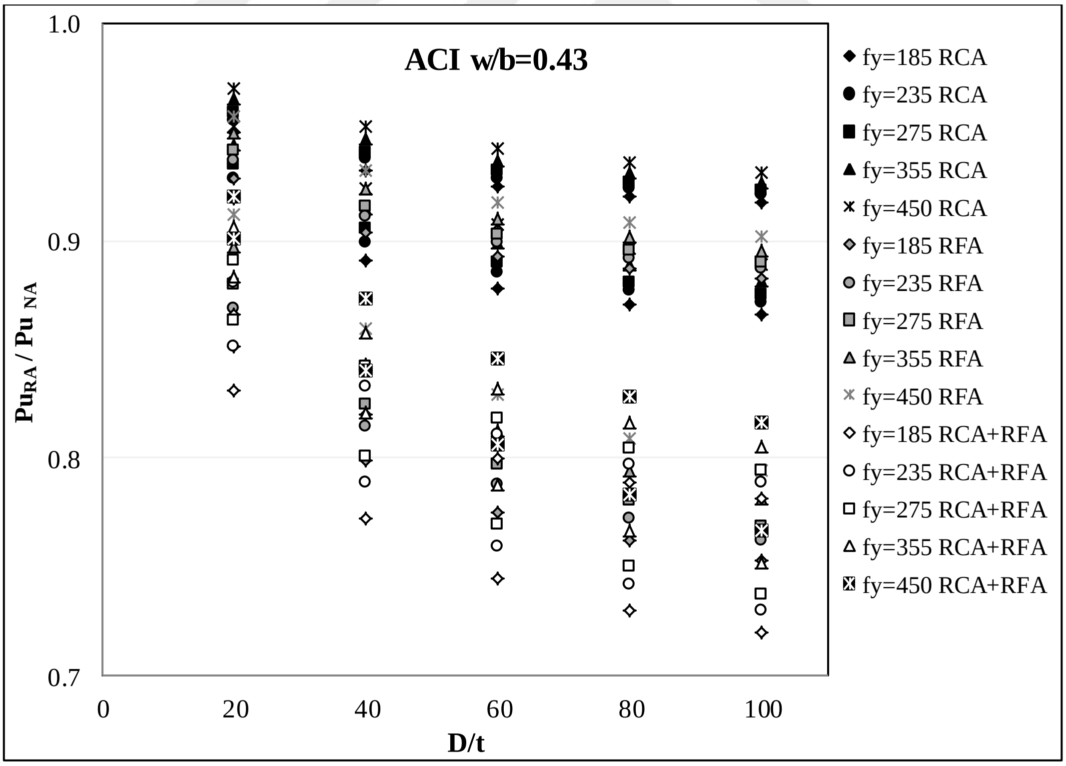

(b)

Figure 0.28 Effect of using RA instead of NA on the axial capacity of the composite columns calculated via ACI (2005)

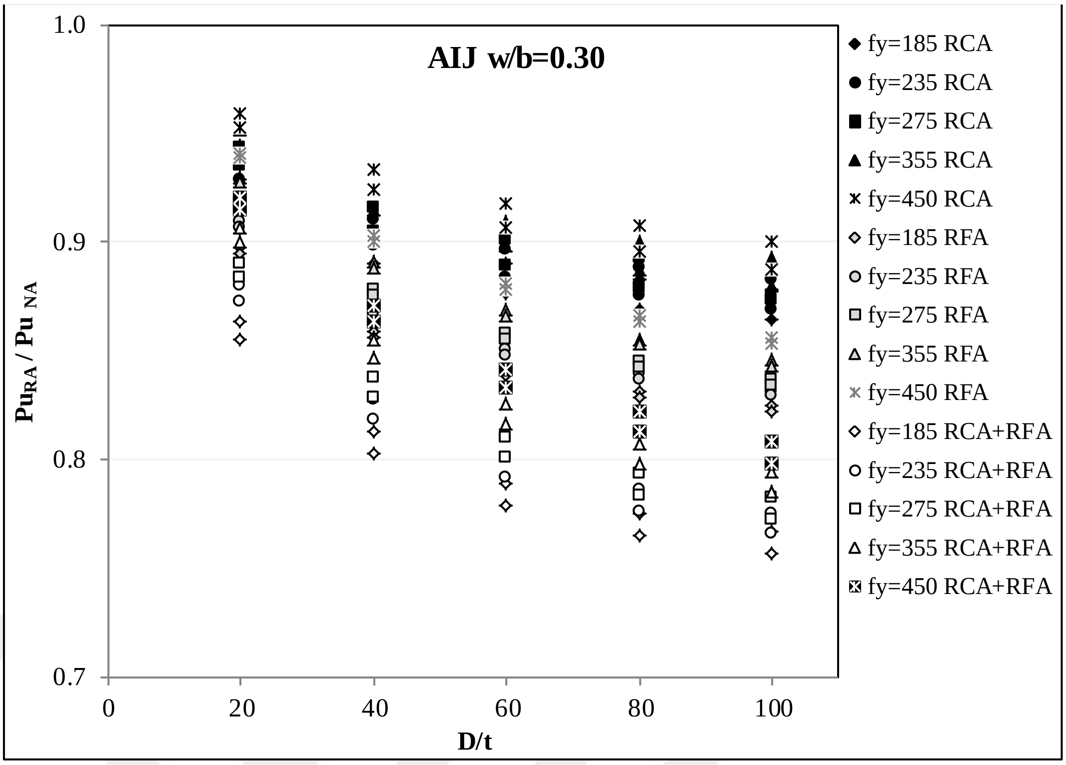

(a)

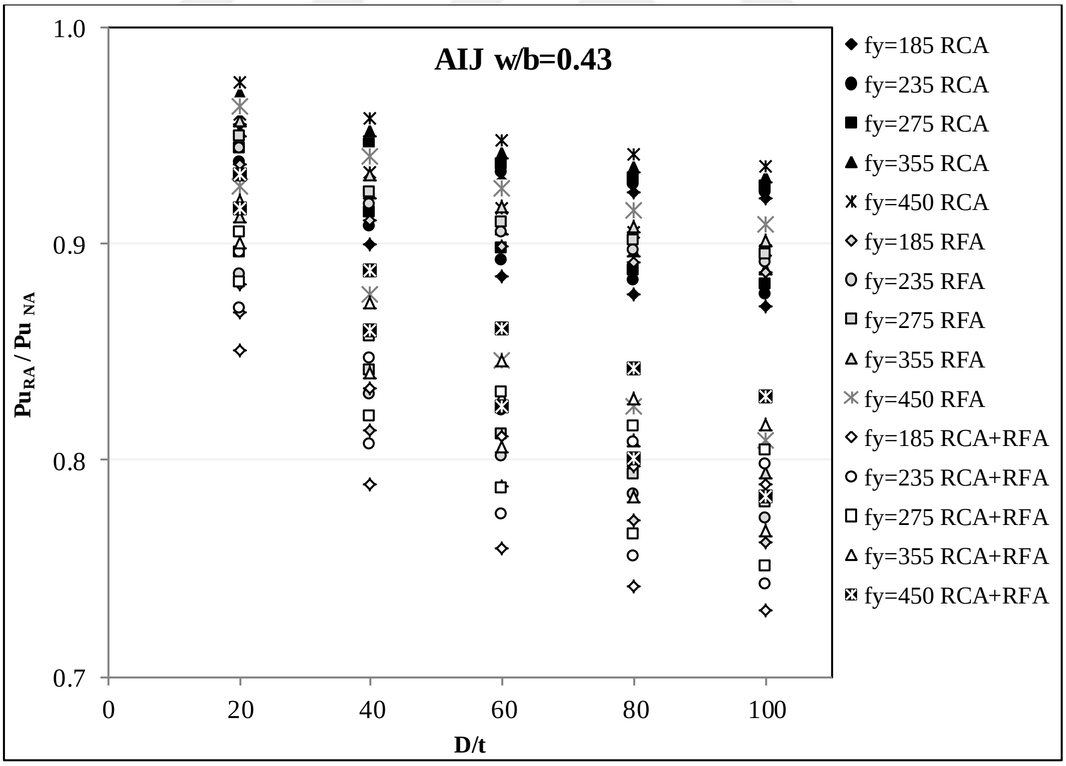

(b)

Figure 0.29 Effect of using RA instead of NA on the axial capacity of the composite columns calculated via AIJ (1997; 2001)

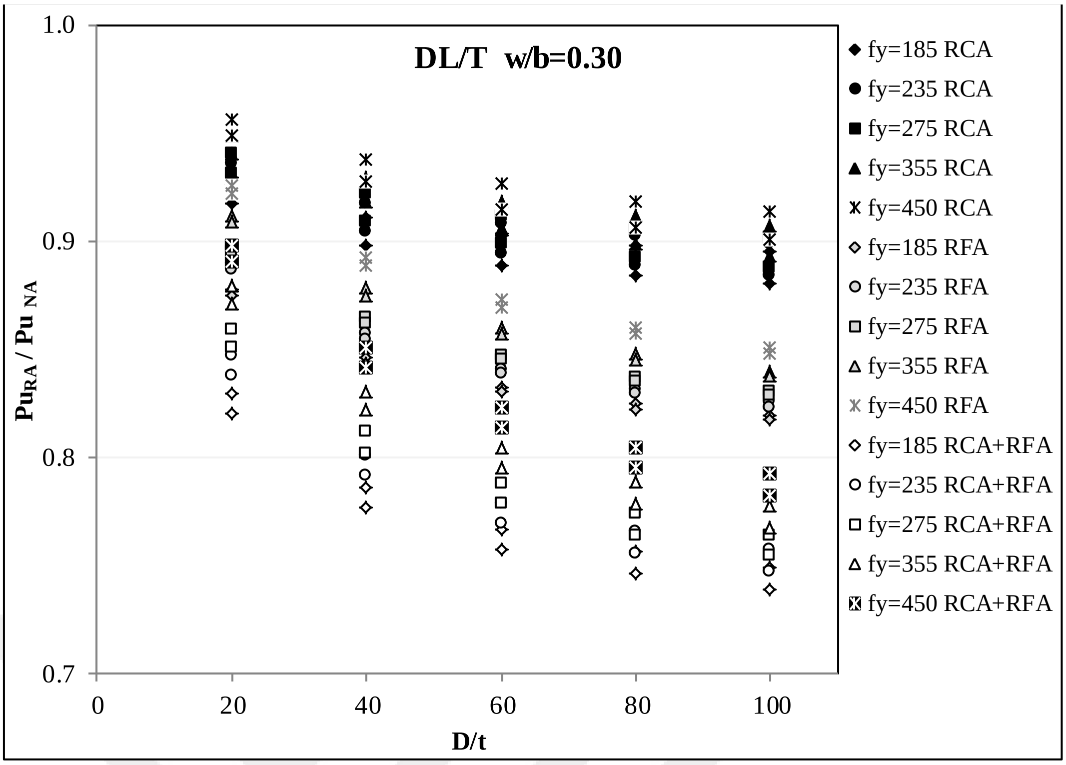

(a)

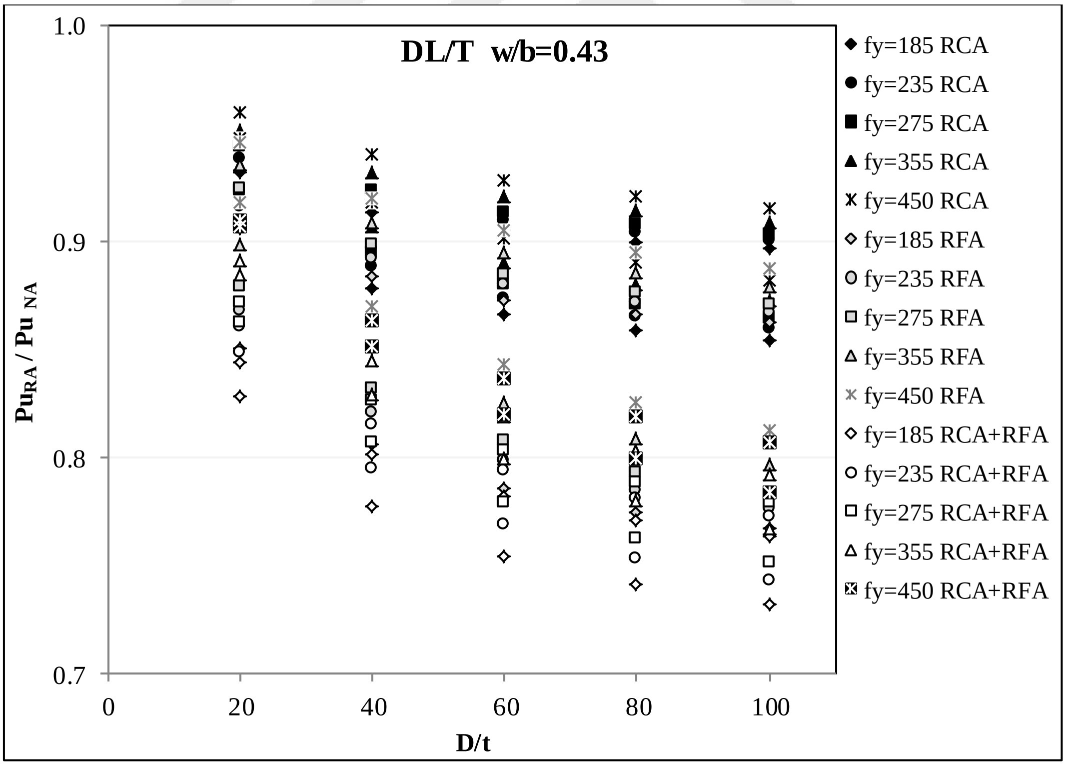

(b)

Figure 0.30 Effect of using RA instead of NA on the axial capacity of the composite columns calculated via DL/T (1999)

In order to estimate the performance of each design codes, the predicted Pu calculated via EC 4 was compared with ACI, AIJ and DL/T codes respectively. The comparison is conducted and depicted in Figure 4.31 a-f. In effect, the comparisons were divided according to w/b ratio of concretes, type of aggregate and yield strength of steel tube. In the term of D/t ratio, the design codes preserved the same trend of decreasing at high D/t ratios with respect to predicted EC 4 axial capacity. In other word, the difference between Pu calculated via EC 4 and other codes were approaching whenever D/t ratios of columns increased. This performance means that the main factors controlling the predicted Pu results are the type and hardening of steel tube; whereas the strength and properties of concrete control the results at low ratios of D/t.

The ratios of Pu results calculated via EC 4 and other codes recorded high values whenever ACI code was considered as compared with other codes (Figure 4.31-a and b). Depending on D/t ratio, the ratios of (EC4/ACI) ranged from 1.26 to 1.62; whilst in the comparisons of AIJ and DL/T codes, ratios decreased to 1.22-1.37 and 1.04-1.39, respectively. Indeed, these results indicated shortage results recorded for axial capacity calculated via ACI code and better performance for AIJ and DL/T codes when the amount of axial load was considered.

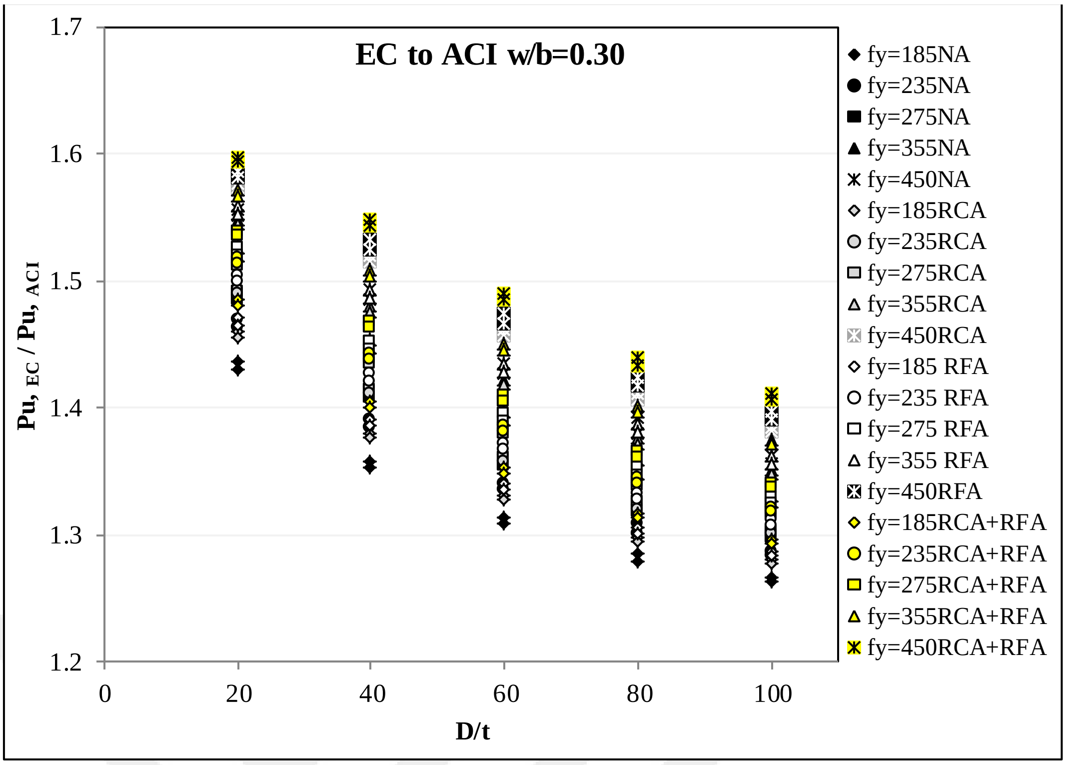
EC to ACI w/b=0.30
Pu, EC / Pu, ACI
D/t
1.7
1.6
1.5
1.4
1.3
1.2
0
20
40
60
80
100
fy=185NA
fy=235NA
fy=275NA
fy=355NA
fy=450NA
fy=185RCA
fy=235RCA
fy=275RCA
fy=355RCA
fy=450RCA
fy=185 RFA
fy=235 RFA
fy=275 RFA
fy=355 RFA
fy=450RFA
fy=185RCA+RFA
fy=235RCA+RFA
fy=275RCA+RFA
fy=355RCA+RFA
fy=450RCA+RFA

(a)

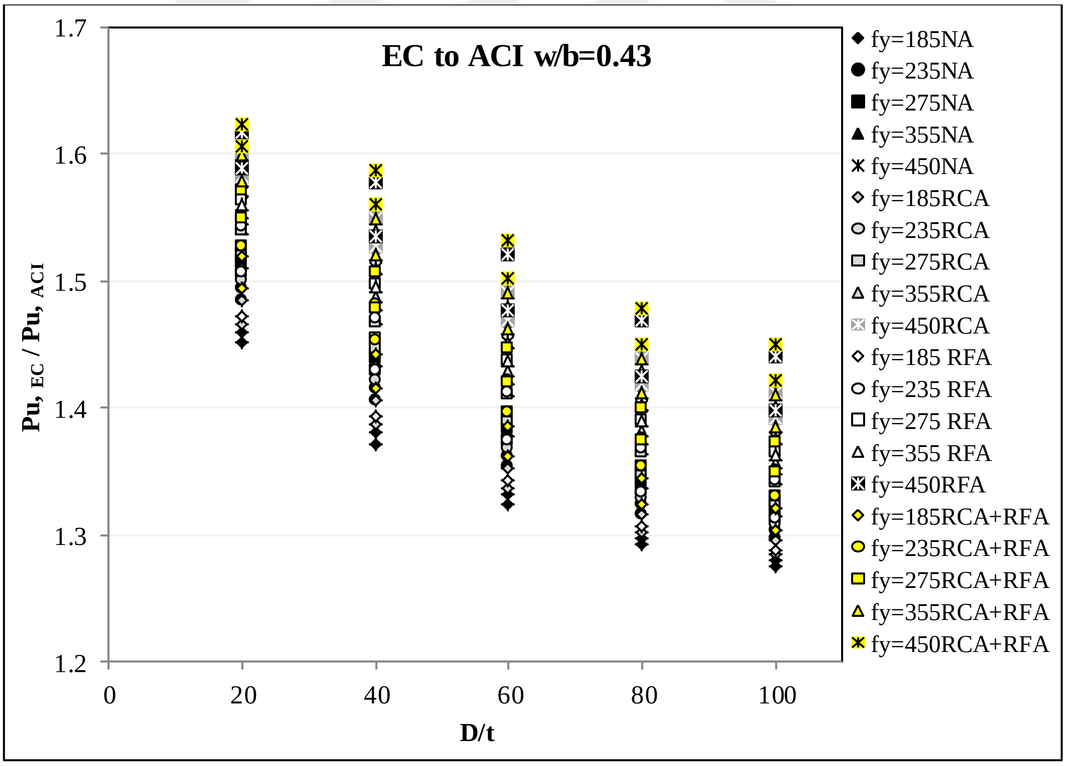
EC to ACI w/b=0.43
Pu, EC / Pu, ACI
D/t
1.7
1.6
1.5
1.4
1.3
1.2
0
20
40
60
80
100
fy=185NA
fy=235NA
fy=275NA
fy=355NA
fy=450NA
fy=185RCA
fy=235RCA
fy=275RCA
fy=355RCA
fy=450RCA
fy=185 RFA
fy=235 RFA
fy=275 RFA
fy=355 RFA
fy=450RFA
fy=185RCA+RFA
fy=235RCA+RFA
fy=275RCA+RFA
fy=355RCA+RFA
fy=450RCA+RFA

(b)

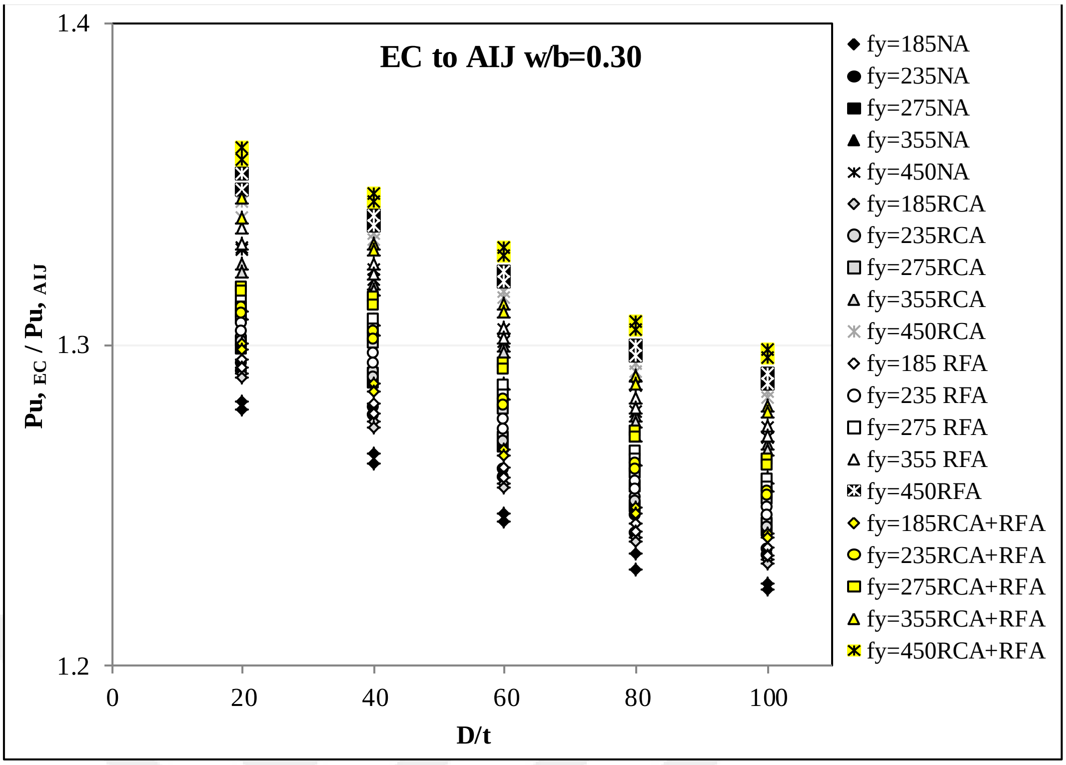

EC to AIJ w/b=0.30
Pu, EC / Pu, AIJ
D/t
1.4
1.3
1.2
0
20
40
60
80
100
fy=185NA
fy=235NA
fy=275NA
fy=355NA
fy=450NA
fy=185RCA
fy=235RCA
fy=275RCA
fy=355RCA
fy=450RCA
fy=185 RFA
fy=235 RFA
fy=275 RFA
fy=355 RFA
fy=450RFA
fy=185RCA+RFA
fy=235RCA+RFA
fy=275RCA+RFA
fy=355RCA+RFA
fy=450RCA+RFA

(c)

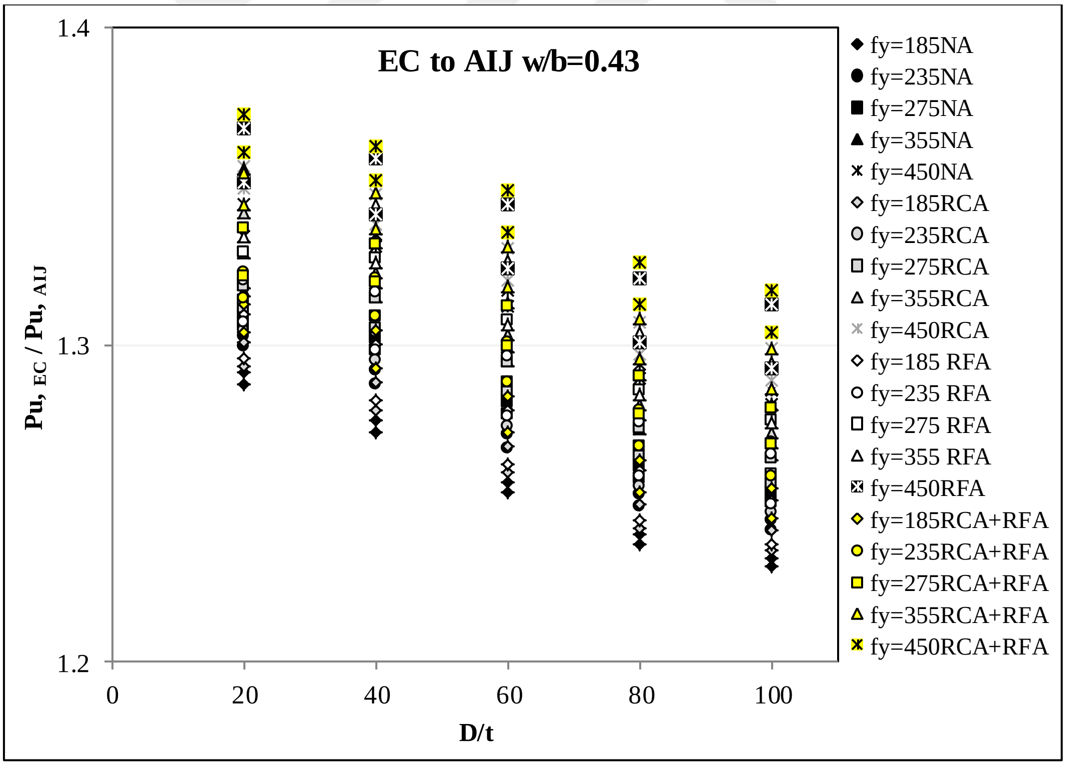

EC to AIJ w/b=0.43
Pu, EC / Pu, AIJ
D/t
1.4
1.3
1.2
0
20
40
60
80
100
fy=185NA
fy=235NA
fy=275NA
fy=355NA
fy=450NA
fy=185RCA
fy=235RCA
fy=275RCA
fy=355RCA
fy=450RCA
fy=185 RFA
fy=235 RFA
fy=275 RFA
fy=355 RFA
fy=450RFA
fy=185RCA+RFA
fy=235RCA+RFA
fy=275RCA+RFA
fy=355RCA+RFA
fy=450RCA+RFA

(d)

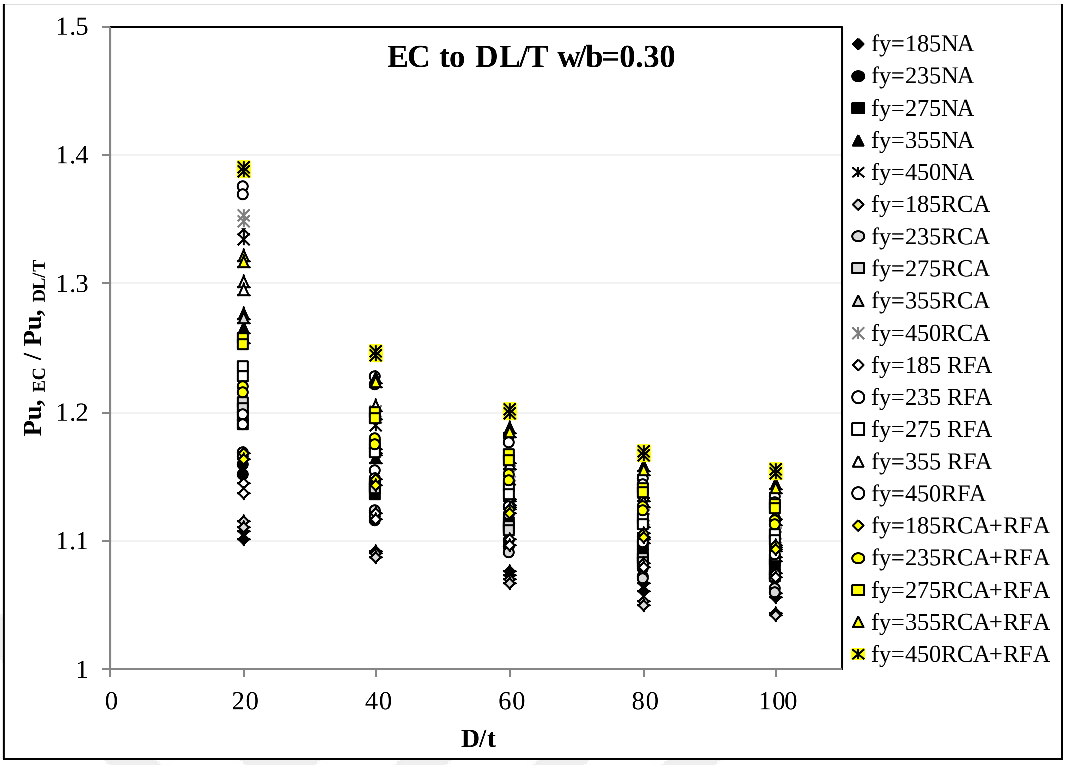

(e)

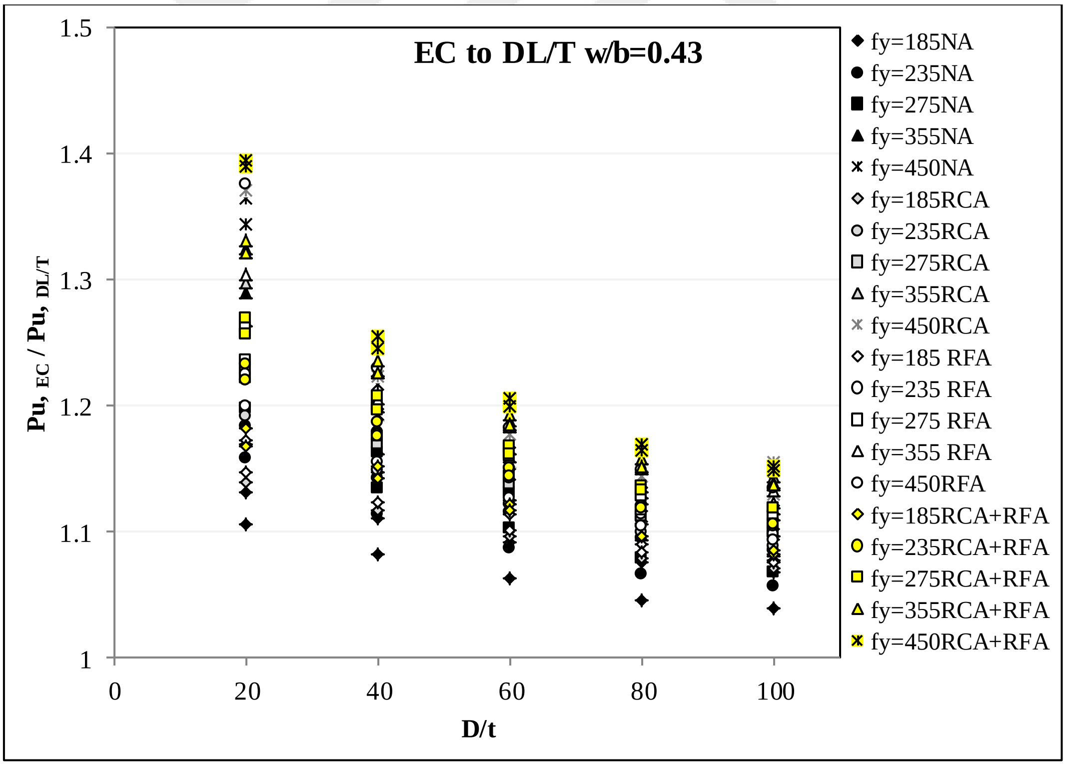

(f)

Figure 0.31 Comparison of prediction capability of different codes with respect to Eurocode 4 in the terms of D/t ratio, steel yield strength and aggregate type

In all tested codes, the prediction capability ratio constantly increased at high-strength steel tube; this trend can be observed even for 0.43 w/b ratio mixtures. However, slightly high ratios were recorded for 0.43 w/b ratio mixtures compared to the corresponding 0.30 mixes. In addition, steel tube controlled the performance of CFST columns rather than concrete core strength whenever steel strength increased; thus, the difference in ratios became more pronounced at high fy value. However, the difference in ratios was relatively small, which means that the effects of steel yield strength in this case were less significant. Moreover, when considering the type of aggregate, the ratios were in the following sequence, (RCA+RFA), RFA, RCA and NA concretes respectively. This trend indicated that the differences between codes were going to enlarge at low concrete strengths, for instant (RCA+RFA) concrete. However, the aforesaid differences were modest in general and unnoticeable (Figure 4.32 a-c).

In the DL/T code, the conversion factor used to convert the strength of 150 mm cubic specimens into 150*200 mm cylinder (0.67) leads to a decrease in the produced results of Pu. However, only for D/t=20 the ratio of (Pu_{EC4}/ $Pu_{DL/T}$) revealed the highest values unlike other ratios, which seems to be a shortcoming in the DL/T equations (Figure 4.31-e and f). This behavior may be attributed to the large randomness occurred in high yield strength steel; also, the effects of steel hardening may exist in low D/t ratio (Lu and Zhao, 2010). Similar behavior is clearly observed in Figure 4.32-c, in which the ratios extremely scatter at high yield strength of D/t =20 ratio causing large variance in the predicted results where the ratios are larger than 1.25. The difference between the lower limit and upper limit of ratios recorded 0.35 for DL/T codes; however, it decreased to 0.21 by eliminating high yield strength (fy=450) of D/t =20. In the comparison of Pu calculated via EC 4 and ACI, the highest randomness in the predicted Pu can be noticed (Figure 4.32-a). The difference between the lower limit and upper limit of ratios recorded 0.36 for ACI; compared with 0.15 for AIJ code. In effect, the ratios slightly increased through the following sequence: NA, RCA, RFA and (RCA+RFA) respectively; similar trend was also observed in other codes. However, these results indicate that CFST columns filled by RASCC give comparable compressive and flexural behavior to the ones filled with NA concrete; which agree with previous studies (Dong et al., 2013; Yang and Han, 2006; Chen et al., 2010; Yang and Ma, 2013). Thus, the difference between these concretes in term of Pu values is minor, particularly at low D/t ratios.

When the EC4 was considered, AIJ code showed the lowest scatter in the predicted Pu values in comparison with other codes. This trend is clearly observed in Figure 4.32-b, where the ratios range from 1.23 to 1.37 depending on the type of aggregate. In effect, the uniformity and non-randomness of results may be due to the lock-buckling effect considered in AIJ code, where the limits mentioned in code are convenient (Lu and Zhao, 2010; AIJ, 1997; AIJ 2001). Although the confining effect had been taken into account in the AIJ code design, the results were more conservative (about 21.6% lower than Pu mean results of EC4 code). However, the highest conservative results were recorded for predicted Pu calculated via ACI code (about 27.1% lower than mean results of EC4 code).

The aforementioned results denoted defects in ACI and DL/T equations compared to other tested codes. In effect, Lu and Zhao (2010) also indicated a shortcoming in the DL/T equations and conservative results in ACI code due to disregarding the effect of the composite action between the concrete core and steel tube of columns. The randomness in Pu results calculated via ACI and DL/T codes could also be noticed through the statistical parameters listed in Table 4.4, where the highest coefficient of variations (COV) was recorded for these codes; 0.732 and 0.728 respectively.

Table 4.4 Statistical evaluation of predicted axial load capacity of circular CFST columns

Design codes	**Pu (kN)**					
	Min	**Max**	**Difference**	**Mean**	**SD**	**COV**
Eurocode 4	259.73	6946.25	6686.52	2450.12	1732.09	0.707
ACI (2005)	171.08	5127.63	4956.55	1784.46	1306.85	0.732
AIJ (1997; 2001)	197.92	5467.71	5269.79	1919.58	1375.85	0.717
DL/T (1999)	219.90	6279.00	6059.10	2183.51	1589.63	0.728

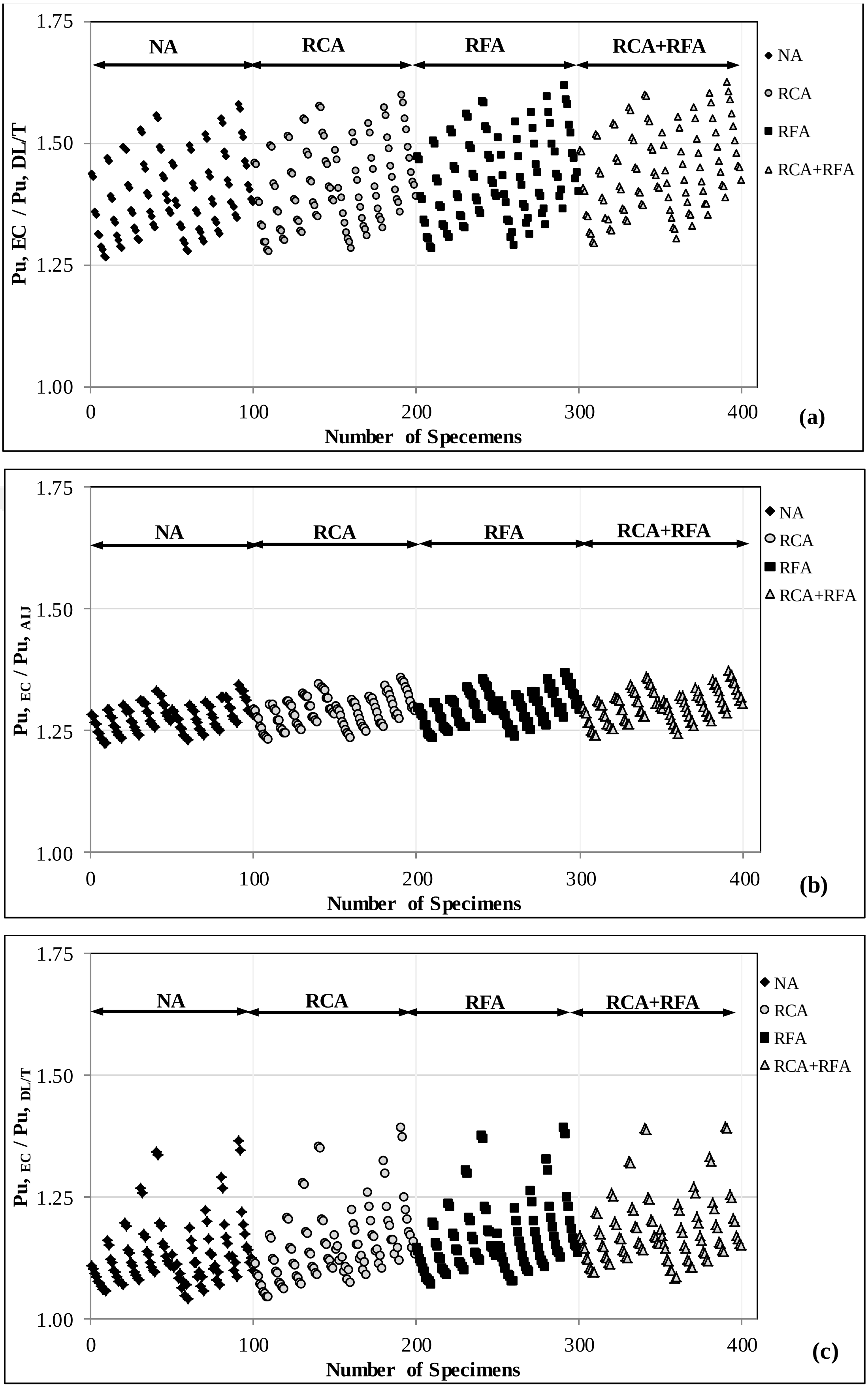

Figure 4.32 Illustration of the influence of aggregate type on the calculated axial load capacity by various codes

Indeed, COV is deemed as a measure of the dispersion or scattering probability distribution as well as frequency distribution. Therefore, the efficiency of code results can be evaluated in term of data scattering. In spite of high difference between maximum and minimum Pu value recorded in EC 4, this code showed the best performance relating to scatter and COV results. Actually, EC 4 can be used with confidence for the design of CFST columns (Goode, 2007). For this, EC4 was selected to compare the predicted sectional capacity calculated by other codes with it. This comparison is obviously depicted in Figure 4.33 a-c; where the relationship can be linearly expressed. The term "Line of equality" represents the evenness between EC4 and other codes results. In effect, the tested codes revealed high correlation coefficient (R), describing the fit of codes results as well as indicating better approximation capability of results. The highest correlation factor was recorded for the relationship between EC 4 and AIJ code results (Figure 4.33- b); compatible with aforesaid approaches. However, other codes relations also showed good correlations with EC4. Moreover, the predicted Pu results calculated via DL/T codes were deemed as the closest results to EC 4 as depicted in Figure 4.33- c.

When considering the overall tendency of the design codes, the highest values of predicted axial capacity were recorded in the sequence of EC 4, DL/T, AIJ and ACI respectively. The tendency is clearly depicted in Figure 4.34; where the results of Pu are represented with respect to D/t ratios. The randomness of results increased at high D/t ratios indicating that the hardening of steel tube was not important at low D/t ratio; where the difference in Pu results was the closest for all calculated codes. Thus, the difference was gradually bigger at higher D/t ratios. For instant, the variance between results recorded about 406 kN at D/t=20 compared with 4360 kN at D/t=100. For this, the estimation of steel tube strength is much more important at high diameter CFST columns; thus a proper design is required.

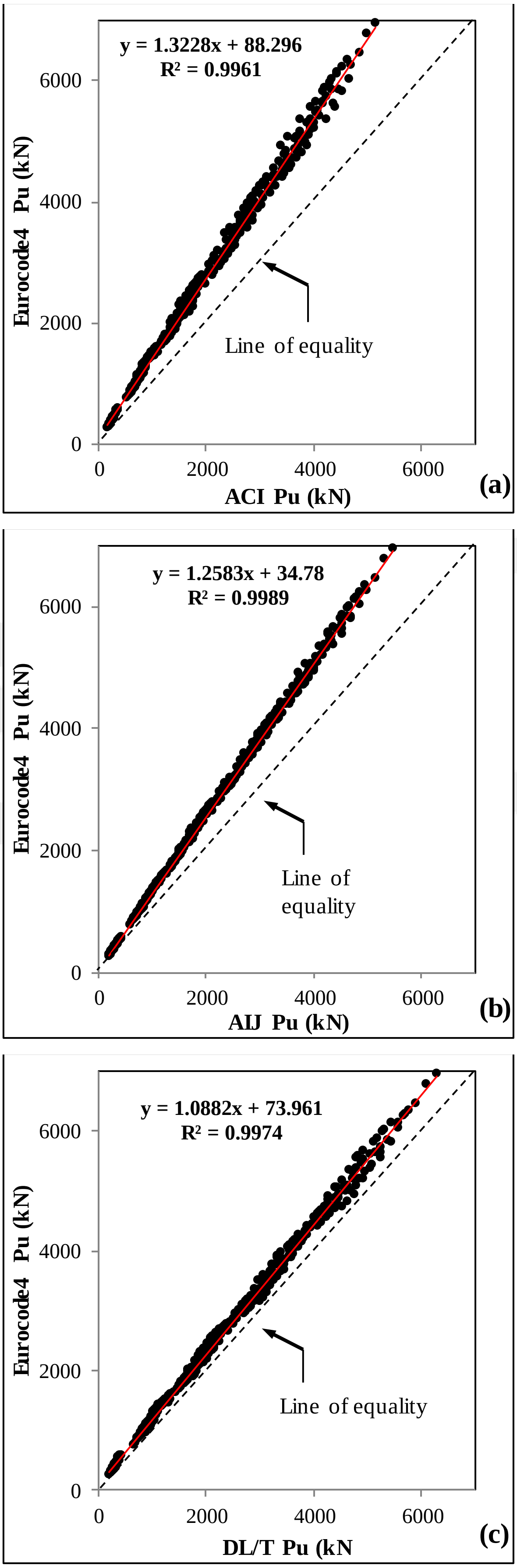

Figure 4.33 Relationship between Eurocode 4 and the other codes

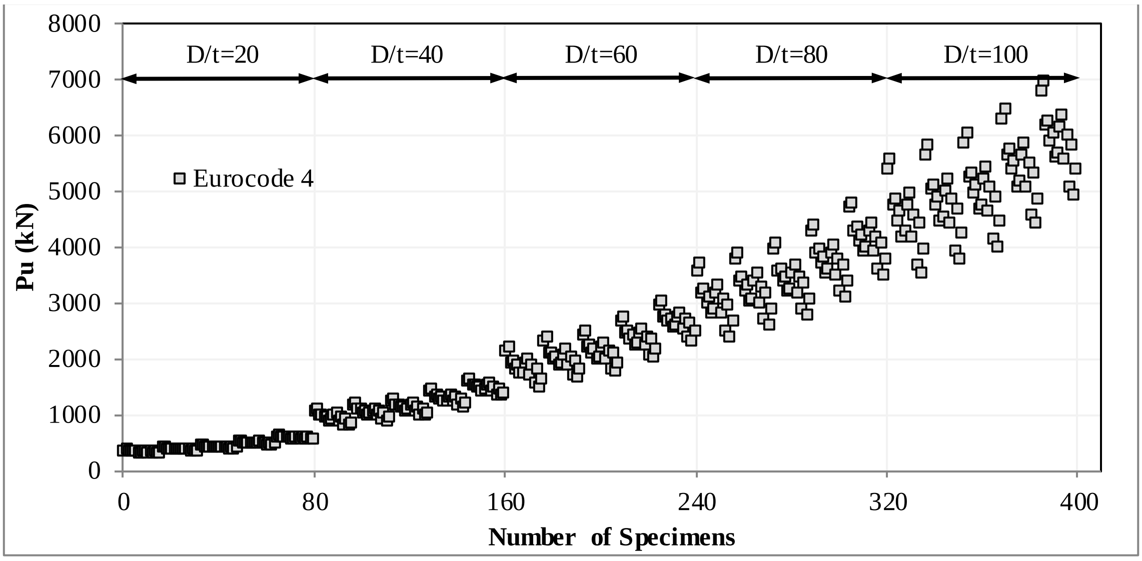
8000
7000
6000
5000
4000
3000
2000
1000
0
D/t=20
D/t=40
D/t=60
D/t=80
D/t=100
Eurocode 4
Pu (kN)
0
80
160
240
320
400
Number of Specimens

(a)

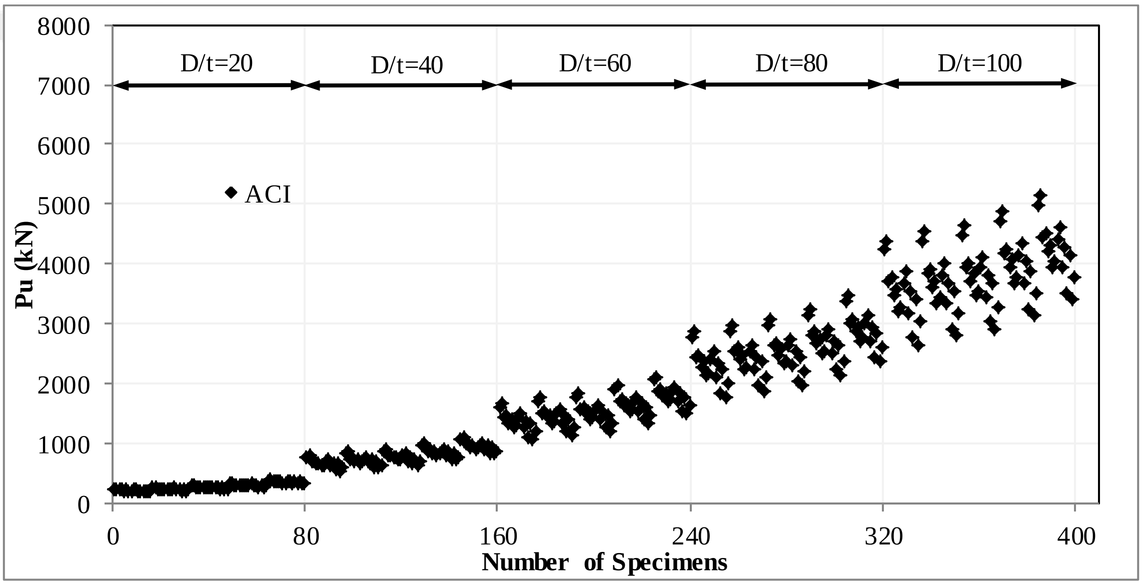
8000
7000
6000
5000
4000
3000
2000
1000
0
D/t=20
D/t=40
D/t=60
D/t=80
D/t=100
ACI
Pu (kN)
0
80
160
240
320
400
Number of Specimens

(b)

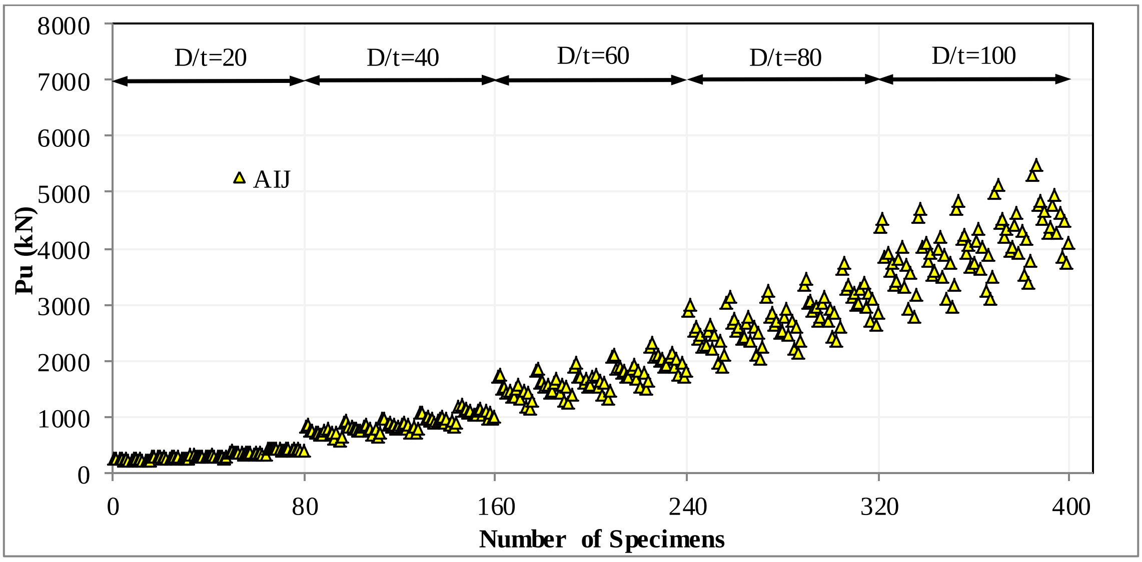
8000
7000
6000
5000
4000
3000
2000
1000
0
D/t=20
D/t=40
D/t=60
D/t=80
D/t=100
AIJ
Pu (kN)
0
80
160
240
320
400
Number of Specimens

(c)

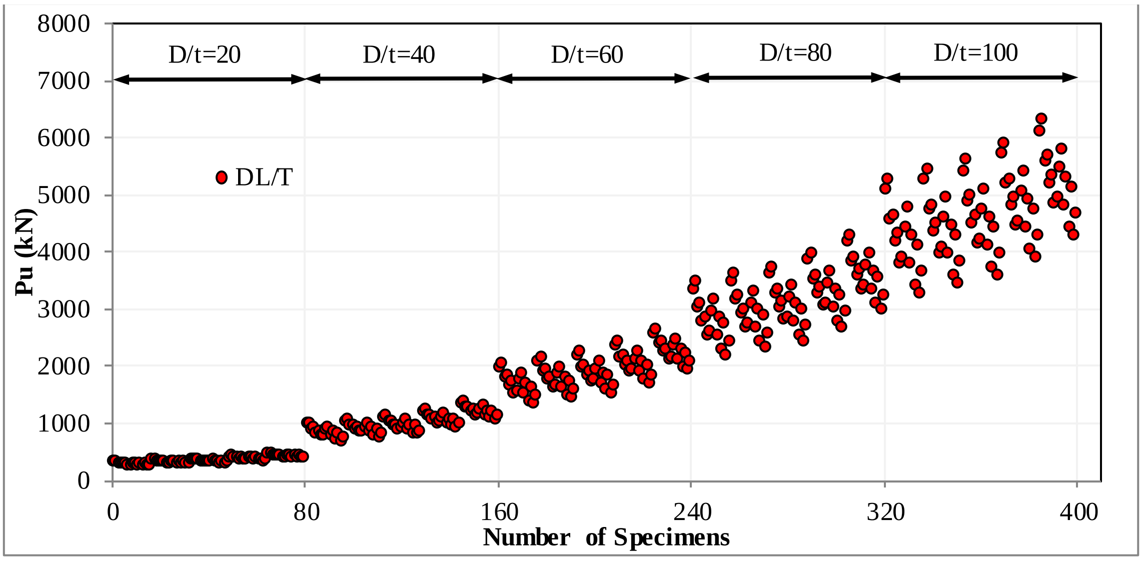

(d)

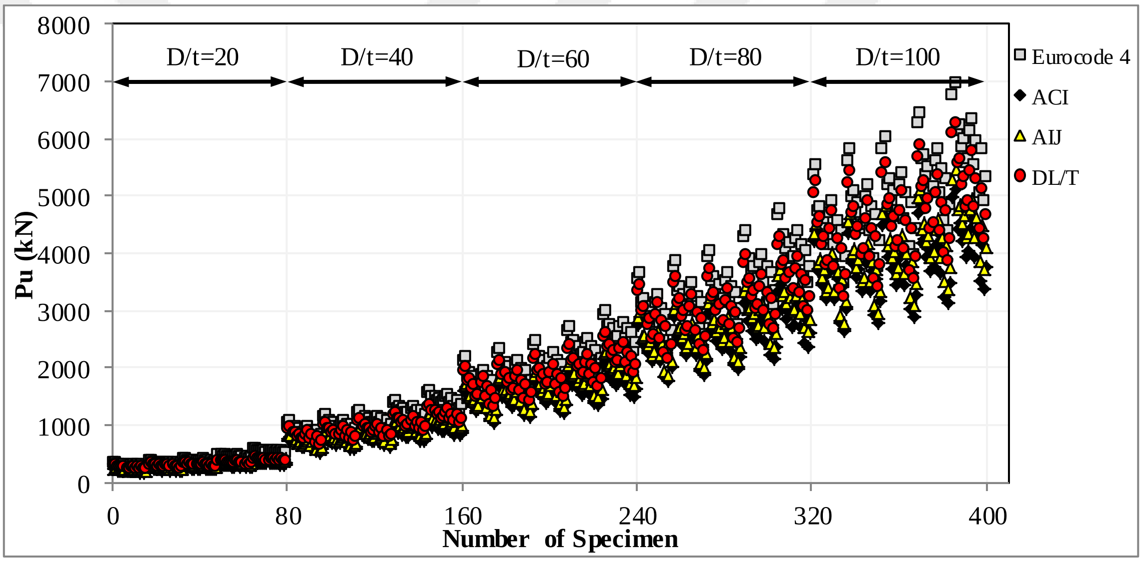

(e)

Figure 0.34 Overall tendency of the design codes in accordance with D/t ratio to predict the axial capacity of the composite columns

CHAPTER V

CONCLUSIONS

The following conclusions were drawn from the results of presented study:

- Usage of recycled aggregate in SCCs needs less HRWRA than those with natural aggregate. This may be attributed to using RAs in SSD condition and the characteristics of RAs that mixes reached to the desired slump with lower viscosity.

- The slump flow time and V-funnel flow time decreased when the RAs were used. This behavior attributed to the high water absorption capacity of RAs compared to NAs; as well as using this aggregate in SSD condition.

- It was obvious that the increases of w/b lead to descend the viscosity of concretes via decrease the slump flow times. Moreover, incorporate SF in the concrete matrix generally make concretes more cohesive, so that these concretes had higher flow times.

- All SCCs produced in this study were satisfying the EFNARC recommendation for the passing ability in terms of L-box test. The values were ranged from 0.811 to 0.995 depending mainly on the type of aggregate used in SCCs, incorporating of SF and w/b ratio.

- The compressive strength of the SCRACs was adversely affected by the incorporation of RCAs and/or RFAs and caused a strength reduction up to 30.9%. However, it is possible to produce the structural SCRACs with a compressive strength varying from 46 to 70 MPa. Other strength characteristics such as splitting tensile strength, net flexural strength and modulus of elasticity revealed similar trend of compressive strength performance.

- Due to the inferior properties of RAs, the post-peak stiffness, final displacement, area under the load- displacement curve, fracture energy and characteristic length for the test beam with SCRACs were less than those for the beams with SCCs having NAs. This indicated that the SCRACs became more brittle behavior.

- Almost all strength properties and fracture parameters of RCAs concrete were higher than RFAs concrete except the brittleness was lower. At all events, the maximum values of these parameters were recorded for NAs concrete; moreover, the minimums were for mixes contained both graded RAs.

- The predicted axial load (Pu) of the composite columns having NA and RA concrete calculated via EC4 revealed the highest values compared with other tested codes followed by the values calculated via DL/T, AIJ and ACI codes, respectively. Indeed, the lowest Pu values were recorded in ACI code formula due to underestimating. Since, this design code does not consider the composite action between confined concrete and steel tube.

- When the standards were considered, the incorporation of RA (as partial or full replacement aggregate) caused a reduction in the strength of concrete; thus, significantly affected the predicted axial load capacity of CFST columns. This behavior was attributed to the inferior properties of this aggregate.

- In high w/b ratio mixtures, the reduction in concrete strength significantly affected the results of axial capacity of CFST columns; decreasing the predicted Pu values. In similar way, excluding SF from the mixes also produced lack in Pu results.

- Compared with NA, the predicted Pu constantly decreased via RCA, RFA and (RCA+RFA) sequence, respectively. Indeed, the reductions occurred due to the nature and properties of RA which in-turn decreased the strength of concrete core; thereby, decreasing composite column strength.

- At high D/t ratios, the main factor that controlled the predicted Pu results was the strength of steel tube rather than the strength and properties of concrete. For this, the difference between Pu calculated via EC 4 and other codes approached at these ratios. Moreover, at high yield strength of steel, the differences between codes results became more pronounced denoting that the type of steel dominated the performance of CFST columns.

- In DL/T code, the effects of steel hardening were clearly observed at low D/t ratios denoting larger randomness of Pu results and shortcoming of the DL/T equations; hence large scatter occurred in the predicted results of Pu. The predicted results also revealed defects in ACI formulas, where the data showed the highest randomness as well as highest conservative results (about 37%) compared with the mean value of EC4 code.

- Due to the lock-buckling effect considered in AIJ code, the best performance in the term of scatter and randomness of results was observed in this code. However, the mean value of Pu results was 28 % lower than that of EC4 code; in spite of taking the confining effect into account.

- In the evenness measurement between EC4 and other codes, the closest results to EC 4 were recorded for DL/t code; however, other codes revealed good correlation between Pu results.

- The best performance relating to scatter and COV values was recorded for the results calculated via EC 4.

- The overall tendency of results revealed that the capacity of steel tube columns became more significant at high D/t ratios than low ratios because the randomness of results was more pronounced at high ratios.

REFERENCES

Aïtcin, P.C., Mehta, P.K. (1990). Effect of coarse-aggregate characteristics on mechanical properties of high-strength concrete, *ACI Materials Journal*, **87**, 103-107.

ACI-318R (2005). Building code requirements for structural concrete and commentary, Farmington Hills, *American Concrete Institute*, MI, USA.

AIJ. Architecture Institute of Japan. (1997). Recommendations for design and construction of concrete filled steel tubular structures, *Architectural Institute of Japan*, Tokyo, Japan (in Japanese).

AIJ. Architecture Institute of Japan. (2001). Standards for structural calculation of steel reinforced concrete structures. *5th ed.*, *Architectural Institute of Japan*, Tokyo, Japan (in Japanese).

Ajdukiewicz, A., Kliszczewicz, A. (2002). Influence of recycled aggregates on mechanical properties of HS/HPC, *Cement Concrete Composites*, **24**, 269-279.

Akçay, B. (2007). Effects of Lightweight Aggregates on Autogenous Deformation and Fracture of High Performance Concrete, *PhD Thesis*, İstanbul Technical University.

Alam, M., Singh, G., Bahaa, B., Sahar, M. (2013). Acceptability of demolished concrete waste aggregate in making high strength self-compacting concrete, *International Journal of Civil Engineering (IJCE)*, **2,** 1–12.

Alaee, F.J. (2002). Retrofitting of concrete structures using high performance fiber reinforced cementitious composite, *PhD Thesis*, Department of Civil Engineering, Cardiff University, Cardiff.

Andreas, B., Rühl, M. (1989). The influence of recycled aggregate on the compressive strength and the elastic modulus of concrete, *Darmstadt Concrete*, **13**, 131-141.

Angelakos, D., Bentz, E.C., Collins, M.P. (2001). Effect of concrete strength and minimum stirrups on shear strength of large members, *ACI Structural Journal*, **98**, 290-300.

Akash, R., Kumar, J.H., Misra, S. (2007). Use of aggregates from recycled construction and demolition waste in concrete, *Resources, Conservation and Recycling*, **50**, 78-81.

Amnon, K. (2003). Properties of concrete made with recycled aggregate from partially hydrated old concrete, *Cement and Concrete Research*, **33**, 703-711.

Amnon, K. (2004). Treatments for the improvement of recycled aggregate, *Proceedings of American Society of Civil Engineering, Journal of Materials in Civil Engineering*, **16,** 597-603.

Arezoumandi, M., Drury, J., Volz, J.S. (2014). Effect of Recycled Concrete Aggregate Replacement Level on the Fracture Behavior of Concrete. *Journal of Frontiers in Construction Engineering*, **3**, 1-8.

ASTM C127. American Society for Testing and Materials. (2007). Standard test method for specific gravity and absorption of coarse aggregate, *Annual Book of ASTM Standards*.

ASTM C192. American Society for Testing and Materials. (2007).Standard practice for making and curing concrete test specimens in the laboratory, *Annual Book of ASTM Standards*.

ASTM C496. American Society for Testing and Materials. (2012). Standard test method for splitting tensile strength of cylindrical concrete specimens, *Annual book of ASTM standards*.

Bairagi, N.K., Kishore, R. (1993). Behaviour of concrete with different proportions of natural and recycled aggregates, *Resource Conservation and Recycling*, **9,** 109-126.

Banfill, P.F. (2006). Rheology of fresh cement and concrete, *The British Society of Rheology, Rheology Reviews, Heriot-Watt University, UK*, 61-130.

Bažant, Z.P. (1984). Size Effect in Blunt Fracture- Concrete. Rock. Metal, *ASCE Engineering Mechanics*, **110**, 518-535.

Bažant, Z.P. (1998). Fracture and Size Effect in Concrete and other quasi Brittle Materials, *CRC Press.*

Bažant, Z.P. (2002). Concrete fracture model: testing and practice, *Engineering Fracture Mechanics*. **69**: 165–205.

Bažant, Z. P., Oh, B. H. (1983). Crack band theory for fracture of concrete, *Materials and Structures*, **16**, 155-157.

Bažant, Z. P., Planas, J. (1998). Fracture and Size Effect in Concrete and Other Quasibrittle Materials, *CRCP Press*, New York, NY.

B.C.S.J. Building Contractor Society of Japan. (1978). Study on Recycle Aggregate and Recycle Aggregate Concrete, *Committee on Disposal and Reuse of Concrete construction Waste*, *Summery in concrete Journal*, **16**, 18-31.

Beygi, H., Kazemi, M., Nikbin, I., Amiri, J. (2013). The effect of water to cement ratio on fracture parameters and brittleness of self-compacting concrete, *Materials and Design*, **50**, 267–276.

Bordelon, A., Cervantes, V., Roesler, R. (2009). Fracture properties of concrete containing recycled concrete aggregates, *Magazine and Concrete Research*; **61,** 665–670.

BRE. Building Research Establishment. (1992). Design of normal concrete mixes, *Department of the Environment*, UK.

BS 1881: Part 116. British Standard Institution. (1983). Testing concrete method for determination of compressive strength of concrete cubes, *BSI*, London.

BS 1881: Part 121. British Standard Institution. (1983). Recommendations for the measurement of static modulus of elasticity, *BSI*. London.

BS EN 206-1. British Standards Institution. (2000). Concrete - Part 1: Specification, performance, production and conformity, British Standard, 68, *BSI*. London.

BS 8500-2. British Standards Institution. (2002). Concrete, Complementary British Standard to BS EN 206-1, Specification for constituent materials and concrete, *BSI*. London.

BS EN 12620. British Standards Institution. (2002). Aggregates for concrete. Specification for constituent materials and concrete, *BSI*. London.

Buck, A.D. (1973). Recycled concrete, Highway (Transportation), *Highway Research Record*, **430**, 1-8.

Chen, W., Chen, C. (1973). Analysis of concrete-filled steel tubular beam-columns, *International Association for Bridge and Structural Engineering Publications*, **33**, 37-52.

Chen, Z., Liu, F., Zheng, H., Xue, J. (2010). Research on the bearing capacity of recycled aggregate concrete-filled circle steel tube column under axial compression loading.

Collins, R.J. (1993). Reuse of demolition materials in relation to specifications in the UK. Demolition and reuse of concrete and masonry: guidelines for demolition and reuse of concrete and masonry, *In: Proceedings of the third international RILEM symposium on demolition and reuse of concrete masonry*, 49–56.

Corinaldesi, V., Moriconi, G. (2009). Influence of mineral additions on the performance of 100% recycled aggregate concrete, *Construction and Building Materials*; **23**, 2869–2876.

Crawford, T. (2007). A study by Tim Crawford Group Economist, *Halifax Bank of Scotland*, now Lloyds Banking Group.

Dae, J.M., Han, Y.M. (2002). Effect of pore size distribution on the qualities of recycled aggregate concrete, *KSCE Journal of Civil Engineering*, **6,** 289-295.

Darshika, K., Shah, Merool D., Vakil, M., Patel, N. (2014). Behavior of concrete filled steel tube column, *International Journal of Engineering Development and Research*, **2**, 325-8.

DEFRA. Department for Environment Food and Rural Affairs. (2008). Waste Strategy for England 2007. Presented to Parliament by the Secretary of State for Environment, *Crown Copyright*. 127.

DeVenny, A. (1999). Recycling of demolished masonry rubble, *PhD thesis*, Napier University, Edinburgh.

DeVries, P. (1996). Concrete recycled: crushed concrete aggregate, *In: Proceedings of the International Conference: Concrete in the Service of Mankind. I, Concrete for Environmental Enhancement and Protection*, 121-131.

Dhir, R. K. (1998). Recycled concrete aggregate for use in BS 5328 designated mixes, *Concrete Technology Unit, University of Dundee*, CTU/498.

Dhir, R. K. (2001). Resolving application issues with the use of recycled concrete aggregate, *Concrete Technology Unit, University of Dundee,* CTU/1601.

Dhir, R. K., Zhu, W.Z., McCarthy, M.J. (1998). Use of Portland PFA cement in combination with superplasticizer admixtures, *Cement and Concrete Research*, **28**, 1209-1216.

Dhir, R. K., Limbachiya, C., Leelawat, T. (1999).Suitability of recycled concrete aggregate for use in BS 5328 designated mixes, *Proceedings of the Institution of Civil Engineers - Structures and Buildings*; **134**, 257-274.

DL/T. Chinese Design Code for Steel-Concrete Composite Structures (1999). In: DL/T 5085-1999, *Chinese Electricity Press,* Beijing, China (in Chinese).

Domone, P., Illston, J. (2010). Construction materials, their nature and behaviour, *Spon Press,* 4th Edition.

Dong, J., Wang, Q., Guan, Z. (2013). Structural behaviour of recycled aggregate concrete filled steel tube columns strengthened by CFRP, *Engineering Structures*, **48**, 532−542.

Duan, K., Hu, X.Z., Wittmann, F.H. (2003). Boundary effect on concrete fracture and non-constant fracture energy distribution, *Engineering Fracture Mechanics*, **70**, 2257-2268.

Dugdale, D.S. (1960). Yielding of steel sheets containing slits, *Journal of the Mechanics and Physics of Solids*, **8**, 100-104.

EFNARC. European Guidelines for Self-Compacting Concrete. (2005). Specification and Production and Use, *Association House*, UK.

Elahi, A., Basheer, P., Nanukuttan, S., Khan, Q. (2010). Mechanical and durability properties of high performance concretes containing supplementary cementitious materials, *Construction and Building Materials*, **24**, 292–9.

Etxeberria, M., Vázquez, E., Marí, A., Barra, M. (2007). Influence of amount of recycled coarse aggregates and production process on properties of recycled aggregate concrete, *Cement and Concrete Research*, **37**, 735-742.

Eurocode 2. European Standards. (2004). Design of concrete structures - Part 1- 1: General rules and rules for buildings, *European Committee for Standardization*, British Standards Institution.

Eurocode 4. European Standards. (2004). Design of composite steel and concrete structures. Part 1.1, General rules and rules for buildings, *European Committee for Standardization*: British Standards Institution.

ECR. European Commission Report. (1999). Construction and demolition waste management practices and their economic impacts, *Symonds, in association with ARGUS, COWI and PRC Bouwcentrum*, **43**.

UEPG. European Aggregates Association. (2008). A Sustainable Industry for a Sustainable Europe, Annual review 2008-2009, *UEPG aisbl, Rued Arlon 21I1050, Brussels I Belgium*, 30.

UEPG. European Aggregates Association. (2013) A Sustainable Industry for a Sustainable Europe, Annual review 2013-2014. *UEPG aisbl, Rued Arlon 21I1050, Brussels I Belgium*, 38.

Evangelista, L., De Brito, J. (2007). Mechanical behaviour of concrete made with fine recycled concrete aggregates, *Cement and Concrete Composites*; **29**, 397–401.

Evangelista, L., De Brito, J. (2010). Durability performance of concrete made with fine recycled concrete aggregates, *Cement and Concrete Composites*; **32**, 9–14.

Feys, D., Verhoeven, R., Schutter, G. (2008). Fresh self-compacting concrete, a shear thickening material, *Cement and Concrete Research*; **38**, 920–929.

Fong, W.F, Jaime, S.K. (2002). Production and application of recycled aggregates, *In: Proceedings of International Conference on Innovation and Sustainable Development of Civil Engineering in the 21st century*, China.

Fong, W.F., Yeung, J.S., Poon, C.S. (2004). Hong Kong Experience of Using Recycled Aggregates from Construction and Demolition Materials in Ready Mix Concrete, *Proceedings of the International Workshop on Sustainable Development and Concrete Technology*, China, 267-275.

Fonseca, N., Brito, J.D., Evangelista, L. (2011). The influence of curing conditions on the mechanical performance of concrete made with recycled concrete waste, *Cement and Concrete Composites*, **33**, 637-643.

Frondistou-Yannas, S. (1977). Waste Concrete as aggregate for New Concrete. *ACI Journal*, **74**, 373–376.

Gagne, R., Pigeon, M., Aitcin, P.C. (1989). Decier salt scaling resistance of high performance concrete, *Paul Klieger Symposium on Performance of Concrete*, SP-122, ACI.

Ghasemian, M., Schmidt, L. (1999). Curved circular hollow (CHS) steel struts infilled with high-strength concrete, *American Concrete Institute Structural Journal*; 275-281.

Gerardu, J.J., Hendriks C.F. (1985). Recycling of road pavement material in The Netherlands, *Rijkswaterstaat Communication*, **38**, The Hague.

Gesoğlu, M. (2004). Effects of lightweight aggregate properties on mechanical, fracture, and physical behavior of lightweight concretes, *PhD thesis*, Boğaziçi University, Istanbul.

Gesoğlu, M., Özturan, T., Güneyisi E. (2004). Shrinkage cracking of lightweight concrete made with cold-bonded fly ash aggregates, *Cement and Concrete Research*. **34**, 1121-1130.

Gesoğlu, M., Özturan, T., Güneyisi, E. (2007). Effects of fly ash properties on characteristics of cold-bonded fly ash lightweight aggregates, *Construction and Building Materials*, **21**, 1869-1878.

Gesoğlu, M., Güneyisi, E. Öz, H. (2012). Properties of lightweight aggregates produced with cold-bonding pelletization of fly ash and ground granulated blast furnace slag, *Materials and Structures*, **45**:1535-1546.

Gesoğlu, M., Güneyisi, E., Öz, H., Taha, I., Yasemin, M. (2015). Failure Characteristics of Self-Compacting Concretes Made with Recycled Aggregates. Construction and Building Materials, **98**, 334−344.

Giakoumelis, G., Lam, D. (2004). Axial capacity of circular concrete-filled tube columns, *Journal of Constructional Steel Research*, **60**, 1049-1068.

Gilpin, R., Menzie, W., David, H.H. (2004). Recycling of construction debris as aggregate in the mid-Atlantic region, USA, *Resources, Construction and Recycling*, **42**, 275-294.

Gómez-Soberón, J.M. (2002). Shrinkage of Concrete with Replacement of Aggregate with Recycled Concrete Aggregate, Innovations in Design with Emphasis on Seismic, Wind and Environmental Loading; Quality Control and Innovations in Materials/Hot-Weather Concreting, *Proceedings of the 5th ACI International Conference*. Cancun, México, 475–495.

Gonzalez, B.F., Martinez, A. (2008). Concretes with aggregates from demolishing waste and silica fume: materials and mechanical properties, *Building and Environment*, **43**, 429-437.

Goode, C. (2007). ASCCS database of concrete-filled steel tube columns, Available at: http://web.ukonline.co.uk/asccs2/. Accessed by 03/01/2017.

Goode, C., Narayanan, R. (1997). Design of concrete filled steel tubes to EC4: Concrete Filled Steel Tubes: A Comparison of International Codes and Practices, *Seminar of Association for International Cooperation and Research in Steel-Concrete Composite Structures*, Innsbruck, Austria.

Gore, V., Kumbhar, P. (2014). Performance of Concrete Filled Steel Tube (CFST) Section: A Review. International Journal of Science and Research (IJSR), 4, 645-647.

Grdic, Z.J., Toplicic-Curcic, G.A., Despotovic, I.M., Ristic, N.S. (2010). Properties of self-compacting concrete prepared with coarse recycled concrete aggregate, *Construction and Building Materials,* **24**, 1129–1133.

Griffith, A. (1921). The phenomena of rupture and flow in solids. *Philosophical Transactions of the Royal Society of London,* **221**, 163–198.

Güneyisi, E. M., Gültekin, A., Mermerdaş, K. (2016). Ultimate capacity prediction of axially loaded CFST short columns, *International Journal of Steel Structures*, **16**, 99-114.

Güneyisi, E., Gesoğlu, M., Özbey, E. (2010). Strength and drying shrinkage properties of self-compacting concretes incorporating multi-system blended mineral admixtures, *Construction and Building Materials,* **24**, 1878–1887.

Güneyisi, E., Gesoğlu, M., Algın, Z., Yazıcı, H. (2014). Effect of surface treatment methods on the properties of self-compacting concrete with recycled aggregates, *Construction and Building Material*; **64**, 172–83.

Han, L., Yao, G., Zhao, X. (2005). Tests and calculations for hollow structural steel (HSS) stub columns filled with self-consolidating concrete (SCC), *Journal of Constructional Steel Research*, **61**, 1241-1269.

Han, L., Li W., Bjorhovde R. (2014). Developments and advanced applications of concrete-filled steel tubular (CFST) structures: Members, *Journal of Constructional Steel Research*,**100**, 211–228.

Hansen, T.C. (1985). Elasticity and drying shrinkage of recycled aggregate concrete. *ACI Materials Journal*, **82**, 82-52.

Hansen, T.C. (1986). Physical structure of hardened cement pastes, A classical approach, *Materials and Structures*, **19**, 423-436.

Hansen, T.C. (1996). Recycled aggregate and recycled aggregate concrete, Second state-of-the-art report developments 1945-1985. *Materials and Structures*, **111**, 201-246.

Hansen, T.C., Narud, H. (1983). Strength of recycled concrete made from crushed concrete coarse aggregate, *Concrete International Design and Construction*, **5**, 79–83.

Hansen, T.C., Narud, H. (1992). Recycling of Demolished Concrete and Masonry, *RILEM*, E and FN Spon. London

Hassan, K.E., Cabrera, J.G., Maliehe, R.S. (2000). The effect of mineral admixtures of the properties of high-performance concrete, *Cement and Concrete Composites*, **22**, 267-271.

Hillerborg, A., Modeer, M., Peterson, P.E. (1976). Analysis of crack formation and crack growth in concrete by means of fracture mechanics and finite elements, *Cement and Concrete Research*, **6**, 773-782.

Hillerborg, A. (1983). Concrete fracture energy tests performed by 9 different laboratories according to a draft RILEM recommendation, *Report to RILEM TC50-FMC*, Report TVMB-3015.

Hu, X. Z., Wittman, F. H. (2000). Size effect on toughness induced by crack close to free surface, *Engineering Fracture Mechanics*, **65**, 209-211.

Huang, W. L., Lin, D. H., Chang, N.B., Lin, K. S. (2002). Recycling of construction and demolition waste via a mechanical sorting process, *Resources, conservation and recycling*, **37**, 23–37.

Irwin, G.R. (1957). Analysis of stresses and strains near the end of a crack transversing a plate, *Journal of Applied Mechanics*, **24**, 361-364.

Ishiguro, S., Stanzl-Tschegg, S.E. (1995). Mode I, Fracture Behaviour of Recycled Concrete. *Fracture Mechanics of Concrete Structures, Proceedings FRAMCOS-2*, 145-154.

Jegadesh, S., Jayalekshmi, S. (2015). Application of artificial neural network for calculation of axial capacity of circular concrete filled steel tubular columns, *International Journal of Earth Sciences and Engineering*, **8**, 35–42.

Jenq, Y., Shah, S. P. (1985). Two parameter fracture model for concrete, *ASCE Journal of Engineering Mechanics*, **11**, 1227-1241.

Jianzhuang, X., Jiabin, L., Zhang, C. (2005). Mechanical properties of recycled aggregate concrete under uniaxial loading, *Cement and Concrete Research*, **35**, 1187-1194.

Kamal, M. M., Safan, M. A., Etman, Z. A., Eldaboly, E. A. (2013). Evaluating the Prolonged Properties of Fresh Self-Compacting Concrete Incorporating Recycled Aggregates, *International Journal of Current Engineering and Technology*, **3**, 436-446.

Kaplan, M. E. (1961). Crack Propagation and Fracture of Concrete, *Journal of American Concrete Institute*. **58**, 591–610.

Karihaloo, B. L. (1995). Fracture Mechanics and Structural Concrete, *Longman Group Ltd*. Essex, England.

Karihaloo, B., Abdalla, H., Imjai, T. (2003). A simple method for determining the true specific fracture energy of concrete, *Magazine and Concrete Research*; **55**, 471–81.

Katharina, K. (1997). Bearing and deformation of concrete with recycled aggregate, *Darmstadt Concrete*, **97**, 97-105.

Kato, B. (1995). Compressive strength and deformation capacity of concrete-filled tubular stub columns. Part I: Strength and rotation capacity of concrete-filled tubular columns, *Journal of Structural and Construction Engineering*, **468**, 183-191 (in Japanese).

Katz, A. (2003). Properties of concrete made with recycled aggregate from partially hydrated old concrete, *Cement and Concrete Research*, **33**, 703–711.

Ketema, E. (2005). Design aid for composite columns. *Master's Thesis*, Addis Ababa University, Ethiopia.

Khatib, M. (2005). Properties of concrete incorporating fine recycled aggregate. *Cement and Concrete Research*, **35**, 763–769.

Khalaf, F.M., DeVenny, A.S. (2004). Recycling of demolished masonry rubble as coarse aggregate in concrete: a review, *Journal of Materials in Civil Engineering*, **16**, 331-340.

Khaldoun, R. (2007). Mechanical properties of concrete with recycled coarse aggregate, *Building and Environment*, **42**, 407–415.

Khayat, K.H. (1999). Workability, testing, and performance of self-consolidating concrete, *ACI Materials Journal, Technical paper*, **96**, 346-354.

Khayat, K.H., Manai, K., Trudel, A. (1997). In situ mechanical properties of wall elements cast using self-consolidating concrete, *ACI Materials Journal,* **94**, 492-500.

Khayat, K.H., Mitchell, D. (2008). Self-Consolidating Concrete for Precast, Prestressed Concrete Bridge Elements, *Final Report for NCHRP Project,* 392

Klee, H. (2009). Recycling Concrete, World Business Council for Sustainable Development (WBCSD), Chemin de Conches Conches-Geneva Switzerland, www.wbcsd.org. Accessed by 11.10.2015.

Koehler, E. P. (2004). Development of a portable rheometer for Portland cement concrete, *MSc. Thesis*, The University of Texas at Austin.

Koehler, E.P., Fowler, D.W. (2004). Development of a portable rheometer for fresh Portland cement concrete, Aggregates foundation for technology research and education (AFTRE), *Research Report ICAR –105-3F*, 306.

Koehler, E.P., Fowler, D.W. (2007). Aggregates in self-consolidating concrete, International Center for Aggregates Research (ICAR), *Final Report ICAR Project 108*.

Konno, K., Sato, Y., Kakuta, Y., Ohira, M. (1997). Property of recycled concrete column encased by steel tube subjected to axial compression. *Transactions of the Japan Concrete Institute*, **19**, 231–238.

Konno, K., Sato, Y., Ueda, T., Onaga, M. (1998). Mechanical property of recycled concrete under lateral confinement, Transactions of the Japan Concrete Institute, **20**, 287–292.

Kou, S.C., Poon, C.S. (2009). Properties of self-compacting concrete prepared with coarse and fine recycled concrete aggregates, *Cement and Concrete Composites*, **31**, 622-627.

Kou, S.C., Poon, C.S., Etxeberria, M. (2011-a). Influence of recycled aggregates on long term mechanical properties and pore size distribution of concrete, *Cement and Concrete Composites*, **33**, 286-291.

Kou, S.C., Poon, C.S., Agrela F. (2011-b). Comparisons of Natural and recycle aggregate concretes prepared with the addition of different mineral admixtures, *Cement Concrete Composites*, **33**, 788-795.

Lam, L., Wong, Y., Poon, C. (1998). Effect of fly ash and silica fume on compressive and fracture behaviors of concrete, *Cement and Concrete Research;* **28**, 271–283.

Li, J., Xiao, H., Zhou, Y. (2009). Influence of coating recycled aggregate surface with pozzolanic powder on properties of recycled aggregate concrete, *Construction and Building Materials*, **23**, 1287-1291.

Limbachiya, M.C. (2004). Coarse Recycled Aggregates for Use in New Concrete, *Proceedings of the Institution of Civil Engineers, Engineering Sustainability*, 157.

Lin C. (1998). Axial capacity of concrete infilled cold-formed steel columns, *Proc. of Ninth International Specialty Conference on Cold-Formed Steel Structures*, St. Louis, Missouri, USA.

Lin-Hai, H., Guo-Huang, Y. (2004). Experimental behaviour of thin-walled hollow structural steel (HSS) columns filled with self-consolidating concrete (SCC), *Thin-Walled Structures*, **42**: 1357-1377.

Liu, B., Xie, Y., Zhou, S., Yuan, Q. (2000). Influence of ultrafine fly ash composite on the fluidity and compressive strength of concrete. *Cement and Concrete Research*, **30**, 1489-1493.

Lu, H., Zhao, Y. (2010). Suggested empirical models for the axial capacity of circular CFT stub column. *Journal of Constructional Steel Research*, **66**, 850-862.

Luksha, L., Nesterovich, A. (1991). Strength testing of larger-diameter concrete filled steel tubular members, *Proc. 3rd International Conference on Steel-concrete Composite Structures*.

Malhotra, V.M. (1978). Use of recycled concrete as a new aggregate, *Proceedings of Symposium on Energy Ad Resource Conservation in the Cement and Concrete Industry*, **76,** Ottawa.

Malhotra, V.M. (1997). Innovative applications of superplasticizers in concrete: a review. *In: Proceedings of the 5th CANMET/ACI International Conference on Superplasticizers and other Chemical Admixtures*, Italy, 271-314.

Margarido, F. (2015). Environmental impact and Life Cycle Evaluation of Materials, *Materials for Construction and Civil Engineering - Science, Processing, and Design, Springer Publishing International*, 799-835

Mazloom, M., Ramezanianpour, A.A., Brooks, J.J. (2004). Effect of silica fume on mechanical properties of high-strength concrete, *Cement and Concrete Composites*, **26**, 347-357.

Mehta, P.K. (2002). High-performance high-volume fly ash concrete for sustainable development, *International Workshop on Sustainable Development and Concrete Technology, Concrete International*, **24**, 30-34.

Mindess, S., Diamond, S. (1982). The cracking and fracture of mortar, *Materials and Structures*, **15**, 107-113.

Ministry of Environment and Urbanization, (MEU). (2013). Turkey's fifth national communication under UNFCCC, *General Directorate of Environmental Management*, Ankara, 290.

Modani, P.O., Mohitkar, N.M, (2014). Self-compacting concrete with recycled aggregate: A solution for sustainable development, *International Journal of Civil and Structural Engineering*, **4**, 430-440.

Montgomery, D.G. (1998). Workability and compressive strength of concrete containing recycled concrete aggregate, Proceedings, Sustainable construction: Use of recycled concrete aggregate, *Thomas Telford*, 289-296.

Mulheron, M. (1988). The recycling of demolition debris: current practice, products and standards in the United Kingdom, *In: Proceedings of the Second International Symposium on Demolition and Reuse of Concrete and Masonry*, Tokyo, Japan, 510-519.

Murthy, A., Palani, G., Riyer, N. (2009). State-of-the-art review on fracture analysis of concrete structural components, *Sadhana*, **34**, 345–367.

Nallathambi, P., Karihaloo, B.L. (1990). Fracture of concrete: Application of effective crack model, *9th International Conference on Experimental Mechanics*, **4**, 1413-1422.

Neville, A.M. (2003). Neville on concrete, *Farmington Hills, Michigan, ACI International*, 531.

Neville, A.M. (2006).Concrete Neville′s Insights and Issues, *Thomas Telford Publishing, Thomas Telford Ltd*.

Nielsson, I, Wallevik, O. (2003). Rheological evaluation of some empirical test methods preliminary results, *Third International Symposium on Self Compacting Concrete*. RILEM Publications S.A.R.L..

Nik, D.O. (2005). Recycled aggregate concrete, *Cement and Concrete Composites*, **27**, 315-318.

Niro, G.D., Dolara, E., Cairns, R. (1998). Properties of hardened RAC for structural purposes, *In: Proceedings of Conference on Sustainable Construction*, Dundee, Scotland, UK, 177-187.

Nishio, A.H., Tamura, M., Ohashi. (1998). Self-compacting concrete with high-volume crushed rock fines, in: V.M. Malhotra (Ed.), *Fourth CANMET/ACI/JCI International Symposium on Advances in Concrete Technology*, 617-630.

Okamura, H., Ouchi, M. (2003). Self-compacting concrete, *Journal of Advanced Concrete Technology*, **1**, 5-15.

O'Shea, M., Bridge, R. (1994). Tests of thin-walled concrete filled steel tubes. *Proc. Twelfth International Specialty Conference on Cold-Formed Steel Structures*, St. Louis, Missouri, USA.

Otsuki, N., Miyazato, S., Yodsudjai, W. (2003). Influence of recycled aggregate on interfacial transition zone, strength, chloride penetration and carbonation of concrete, *Journal of Materials in Civil Engineering*, **15**, 443–451.

Ozawa, K., Maekawa, K., Kunishima, M., Okamura, H. (1989). Development of high performance concrete based on the durability design of concrete structures:

Proceedings of the second East-Asia and Pacific Conference on Structural Engineering and Construction (EASEC-2), **1**, 445-450.

Özbay E. (2007). Effects of mineral admixtures on the fresh and hardened properties of self-compacting concretes: binary, ternary and quaternary systems. *PhD Thesis*, University of Gaziantep.

Öztürk, M. (2005). Construction / Demolition Waste Management, *Ministry of Environment and Forests*, Ankara, **26**.

Öztürk, M. (2009). Construction / Demolition Waste, *Ministry of Environment and Forests*, Ankara, **44**.

Öztürk, Ö., Çelikkol, M., Erkan, M. (2007). Turkey, Aggregate Sector Report. *Ready Mixed Concrete Journal*, **84**, 52-56.

Padmini, A. K., Ramamurthy, K., Mathews, M.S. (2009). Influence of Parent Concrete on the Properties of Recycled Aggregate Concrete, *Construction and Building Materials*, **23**, 829-836.

Panda, K.C, Bal, P.K. (2013).Properties of self-compacting concrete using recycled coarse aggregate. *Procedia Engineering*, **51**,159–164.

Pereira, P., Evangelista, L., de Brito, J. (2012). The effect of superplasticizers on the mechanical performance of concrete made with fine recycled concrete aggregates, *Cement and Concrete Composites*; **34**, 1044–1052.

Poon, C.S. (2004). Influence of moisture state of natural and recycled aggregates on the slump and compressive strength of concrete, *Cement and Concrete Research*, **34**, 31-36.

Poon, C., Kou, S., Lam, L. (2007). Influence of recycled aggregate on slump and bleeding of fresh concrete, *Materials and Structures*, **40**, 981-988.

Raoa, A., Jha, K.N., Misra, S. (2007). Use of aggregates from recycled construction and demolition waste in concrete, *Resources, Conservation and Recycling*, **50**, 71–81.

Ravindrarajah, R.S., Tam, T.C. (1985). Properties of concrete made with crushed concrete as coarse aggregate, *Magazine and Concrete Research*, **37**, 29–38.

Ravindrarajah, R.S., Collins, J. (1998). Temperature development in mass concrete containing polystyrene aggregate concrete, *Journal of the Australian Ceramic Society*, **34**, 226-241.

Reis J.M., Jurumenha, M.A. (2011). Experimental investigation on the effects of recycled aggregate on fracture behavior of polymer concrete, *Materials Research*. **14**, 326-330.

Reddy, C.S., Sai, K.V., Kumar, P.R. (2013). Mechanical and durability properties of self-compacting concrete with recycled concrete aggregates, *International Journal of Scientific and Engineering Research* (IJSER), **4**, 260-264.

RILEM, 50-FMC. (1985). Draft Recommendation: Determination of the fracture energy of mortar and concrete by means of three-point bend test on notched beams, *Materials and Structures*, **18**, 287-291.

RILEM, TC 121 DRG Recommendations. (1994). Specification for concrete with recycled aggregates, *Materials and Structures*, **27**, 557-559.

RILEM, TC Final Report 188-CSC. (2006). Casting of self- compacting concrete, *Materials and Structure*s, **39**, 937–954.

RILEM, (1992). Recycling of demolished concrete and masonry, *London, E and FN Spon*.

Saak, A. Jennings, H. Shah, S. (2001). The influence of wall slip on yield stress and viscoelastic measurements of cement paste, *Cement and Concrete Research*, **31**, 205-212.

Safiuddin, M.D., Alengaram, U.J. Salam M.D., Jumaat M.Z., Jaafar F., Saad, H.B. (2011-a). Properties of High-Workability Concrete with Recycled Concrete Aggregate, *Materials Research*. **14**, 248-255.

Safiuddin, D., Salam, A., Jumaat, Z. (2011-b). Effects of recycled concrete aggregate on the fresh properties of self-consolidating concrete, *Archives of Civil and Mechanical Engineering.***11**, 1023–1041.

Salkhordeh, S., Golbazi, P., Amini, H. (2011). The Improvement of 28-day Compressive Strength of Self Compacting Concrete Made by Different Percentages of Recycled Concrete Aggregates using Nano-Silica, *World Academy of Science, Engineering and Technology*, **59**, 874-877.

Sagoe, C.K., Brown, T., Taylor, A.H. (2001). Performance of concrete made with commercially produced coarse recycled concrete aggregate, *Cement and Concrete Research*, **31**, 707-712.

Saisho, M., Abe, T., Nakaya, K. (1999). Ultimate bending strength of high-strength concrete filled steel tube column. Journal of Structural and Construction behaviour of concrete-filled steel tubular columns. *Journal of Constructional Steel Research*, **61**, 53-66.

Sakino, K., Hayashi, H. (1991). Behavior of concrete filled steel tubular stub columns under concentric loading, *Proc. 3rd International Conference on Steel-concrete Composite Structures*.

Schneider S., Kramer D., Sarkkinen D. (2004). The Design and Construction of Concrete-Filled Steel Tube Column Frames, *13th World Conference on Earthquake Engineering Vancouver*, Canada, pp 252.

Shah, S.P., Swartz, S.E., Ouyang, C. (1995). Fracture Mechanics of Concrete: Applications of Fracture Mechanics to Concrete, Rock, and Other Quasi- Brittle Materials, *John Wiley and Sons, Inc.*, New York.

Sherwood, P.T. (1995). The use of waste and recycled materials in roads, *Proceedings of the Institution of Civil Engineers, Transport*, **111**, 116-124.

Solyman, M. (2005). Classification of recycled sands and their applications as fine aggregates for concrete and bituminous mixtures, *PhD thesis*, Kassel.

Speare, R.S. (1995). Recycling of structural materials, *The Structural Engineer*, **73**, 220-222.

Suvash, P, Gideon, Z. (2013). Mechanical and durability properties of recycled concrete aggregate for normal strength structural concrete, *International Journal of Sustainable Construction Engineering and Technology*; **4**, 89-103.

Tabsh, S., Abdelfalah, A. (2009). Influence of recycled concrete aggregate on strength properties of concrete, *Construction and Building Materials*, **23**, 1163–1167.

Tam, V.W.Y, Cao, X.F., Tam, C.M. (2005). Microstructural analysis of recycled aggregate concrete produced from two-stage mixing approach, *Cement Concrete Research*, **35**, 1195-203.

Tam, V.W.Y., Cao, X.F., Tam, C.M. (2006). Environmental enhancement through use of recycled aggregate concrete in a two-stage mixing approach, *Human Ecological Risk Assess*, **12**, 277-288.

Tam, V.W.Y., Tam, C.M. (2007). Crushed aggregate production from centralized combined and individual waste sources in Hong Kong, *Construction and Building Materials*, **21**, 879–886.

Tam, V.W.Y., Tam, C.M. (2008). Diversifying two-stage mixing approach (TSMA) for recycled aggregate concrete: TSMAs and TSMAsc, *Construction and Building Materials*, **22**, 2068-2077.

Taşdemir, C., Taşdemir, M., Mills, N., Barr, B. I., Lydon, F.D. (1999). Combined effects of silica fume, aggregate type, and size on postpeak response of concrete in bending, *ACI Materials Journal*, **96**, 74–83.

Taşdemir, M.A., Karihaloo, B.L. (2001). Effect of aggregate volume fraction on the parameters of concrete: A meso-mechanical approach, *Magazine of Concrete Research*, **53**, 405-415.

Tattersall, G.H., Banfill, P.F. (1983). The rheology of fresh concrete, *Pitman Advanced Publishing*, Boston (USA).

Tavakoli, M., Soroushian, P. (1996-a). Drying shrinkage behavior of recycled aggregate concrete, *ACI Materials Journal*, **18**, 58–61.

Tavakoli, M. Soroushian, P. (1996-b).Strengths of recycled aggregate concrete made using field-demolished concrete as aggregate, *ACI Materials Journal*, **93**, 182–90.

Thomas, S., Setién, J., Polanco, J.A., Alaejos, P., Sánchez, M. (2013). Durability of recycled aggregate concrete, *Construction and Building Materials,* **40**, 1054–1065.

Topçu, I. B, Günçan N.F. (1995). Using Waste Concrete as Aggregate, *Cement and Concrete Research*, **25**, 1385-1390.

Topçu, I. B., Şengel, S. (2004). Properties of Concretes Produced with Waste Concrete Aggregates, *Cement and Concrete Research*, **34**, 1307-1312.

TS EN 197-1. (2002). Cement- Part 1: Composition, specifications and conformity criteria for common cements, *Institute of Turkish Standards*, Ankara, Turkey.

TS 706 EN 12620-A1. (2009). Aggregates for Concrete, *Institute of Turkish Standards*, Ankara, Turkey.

Tsuda K., Matsui, C., Ishibashi, Y. (1995). Stability design of slender concrete filled steel tubular columns, *Proc. Fifth Asia-Pacific Conference on Structural Engineering and Construction*; EASEC-5.

Tsung, Y.T., Yuen, Y., Chen, L.H. (2006). Properties of HPC with recycled aggregates, *Cement and Concrete Research*, **36**, 943-950.

Van Mier, J.G.M (1997). Fracture Process of Concrete, Assessment of Material Parameters for Fracture Model, *CRC Press.*

Vivian, W.Y.T., Tam, C.M. (2007). Crushed aggregate production from centralized combined and individual waste sources in Hong Kong, *Construction and Building Materials*, **21**, 879-886.

Wang, F., Li, S. (2012). Effect of silica fume on workability and water impermeability of concrete, *Applied Mechanics and Materials*, **238**, 157–60.

Wang, W., Kou, S., Xing, F. (2013). Deformation properties and direct shear of medium strength concrete prepared with 100 % recycled coarse aggregates, *Construction and Building Materials*, **48**, 187–193.

Wang Y., Chen J., Geng Y. (2015). Testing and analysis of axially loaded normal-strength recycled aggregate concrete filled steel tubular stub columns; *Engineering Structures*, **86**, 192–212.

Webb, C. (1999). Roll out the waste heaps, *Surveyor*, **176**, 51-60.

Wittmann, F.H. (1983). Structure of concrete with respect to crack formation, in Fracture Mechanics of Concrete, *Elsevier Applied Science Publishers*, 43-74.

Wrap, (2007). Performance related approach to use of recycled aggregate, *Waste and Resources and Action Programme*, 75.

Xiao, J., Li, J., Zhang, C.h. (2005). Mechanical properties of recycled aggregate concrete under uniaxial loading, *Cement and Concrete Research*, **35**, 1187-1194.

Xiao, J.Z., Li, J.B., Zhang, C. (2006). On relationship between the mechanical properties of recycled aggregate concrete: an overview, *Materials and Structures*, **39**, 655-664.

Xie, J., Elwi, A.E., MacGregor, J. (1995). Mechanical properties of three high strength concrete containing silica fume, *ACI Materials Journal*; **92**, 135–45.

Yamamoto, T., Kawaguchi, J., Morino, S. (2002). Experimental study of the size effect on the behaviour of concrete filled circular steel tube columns under axial compression, *Journal of Structural and Construction Engineering*, **561**, 237-244 (in Japanese).

Yamato, T., Soeda, M., Emoto, Y. (2000).Physical properties of recycled aggregate and the utilization as concrete aggregate, *International Seminar on Recycled Concrete*, 59-68.

Yang, Y., Han, L. (2006). Experimental behaviour of recycled aggregate concrete filled steel tubular columns, *Journal of Constructional Steel Research*, **62**, 1310−1324.

Yang, Y., Ma, G. (2013). Experimental behaviour of recycled aggregate concrete filled stainless steel tube stub columns and beams, *Thin-Walled Structures*, **66**, 62–75.

Yu, Z., Ding, F., Lin, S. (2002). Researches on behavior of high-performance concrete filled tubular steel short columns, *Journal of Building Structure*, **23**, 41-47 (in Chinese).

Zega, C., DiMaio, A. (2011). Use of recycled fine aggregate in concrete with durable requirements, *Waste Management*, **31**, 2336–2340.

Zeghiche J., Chaoui K. (2005). An experimental behaviour of concrete-filled steel tubular columns, *Journal of Constructional Steel Research*, **61**, 53-66.

APPENDIX A. Ultimate capacities of CFST columns for different design codes

Design Code	Sample No.	Name of mixture	(D/t)	Ultimate Load, Pu (kN)				
				Yield stress of steel tube, fy (MPa)				
				185	**235**	**275**	**355**	**450**
EC 4	1	0.3RCA0RFA0SF0	20	321.9	369.0	406.6	481.6	570.4
	2	0.3RCA0RFA0SF10	20	328.4	375.4	413.0	488.0	576.8
	3	0.3RCA100RFA0SF0	20	300.9	348.0	385.6	460.6	549.5
	4	0.3RCA100RFA0SF10	20	304.0	351.1	388.7	463.7	552.6
	5	0.3RCA0RFA100SF0	20	291.6	338.7	376.3	451.4	540.3
	6	0.3RCA0RFA100SF10	20	296.6	343.6	381.2	456.3	545.2
	7	0.3RCA100RFA100SF0	20	281.6	328.7	366.4	441.4	530.3
	8	0.3RCA100RFA100SF10	20	284.8	331.9	369.5	444.5	533.4
	9	0.43RCA0RFA0SF0	20	300.3	347.4	385.0	460.0	548.9
	10	0.43RCA0RFA0SF10	20	307.8	354.9	392.4	467.5	556.3
	11	0.43RCA100RFA0SF0	20	280.9	328.0	365.6	440.7	529.6
	12	0.43RCA100RFA0SF10	20	295.2	342.3	379.9	455.0	543.8
	13	0.43RCA0RFA100SF0	20	264.5	311.7	349.3	424.4	513.4
	14	0.43RCA0RFA100SF10	20	289.9	337.0	374.6	449.7	538.5
	15	0.43RCA100RFA100SF0	20	259.7	306.9	344.5	419.6	508.6
	16	0.43RCA100RFA100SF10	20	274.4	321.5	359.2	434.2	523.2
	17	0.3RCA0RFA0SF0	40	1032.6	1134.4	1215.7	1378.0	1570.5
	18	0.3RCA0RFA0SF10	40	1061.4	1163.1	1244.4	1406.8	1599.2
	19	0.3RCA100RFA0SF0	40	938.5	1040.3	1121.6	1284.2	1476.8
	20	0.3RCA100RFA0SF10	40	952.5	1054.3	1135.6	1298.1	1490.7
	21	0.3RCA0RFA100SF0	40	897.2	999.0	1080.4	1243.0	1435.7
	22	0.3RCA0RFA100SF10	40	919.2	1021.0	1102.4	1264.9	1457.6
	23	0.3RCA100RFA100SF0	40	852.5	954.3	1035.8	1198.4	1391.2
	24	0.3RCA100RFA100SF10	40	866.4	968.3	1049.7	1212.3	1405.1
	25	0.43RCA0RFA0SF0	40	936.0	1037.8	1119.2	1281.7	1474.4
	26	0.43RCA0RFA0SF10	40	969.4	1071.2	1152.5	1315.0	1507.6
	27	0.43RCA100RFA0SF0	40	849.2	951.1	1032.5	1195.2	1388.0
	28	0.43RCA100RFA0SF10	40	913.2	1015.0	1096.4	1258.9	1451.6
	29	0.43RCA0RFA100SF0	40	776.1	878.0	959.5	1122.3	1315.1
	30	0.43RCA0RFA100SF10	40	889.4	991.3	1072.7	1235.2	1428.0

31	0.43RCA100RFA100SF0	40	754.5	856.5	938.0	1100.8	1293.7
32	0.43RCA100RFA100SF10	40	820.2	922.1	1003.5	1166.2	1359.0
33	0.3RCA0RFA0SF0	60	2106.9	2263.4	2388.6	2638.6	2935.2
34	0.3RCA0RFA0SF10	60	2174.0	2330.5	2455.6	2705.6	3002.2
35	0.3RCA100RFA0SF0	60	1887.2	2043.9	2169.2	2419.5	2716.3
36	0.3RCA100RFA0SF10	60	1919.8	2076.5	2201.8	2452.0	2748.8
37	0.3RCA0RFA100SF0	60	1790.9	1947.6	2072.9	2323.3	2620.3
38	0.3RCA0RFA100SF10	60	1842.2	1999.0	2124.2	2374.6	2671.5
39	0.3RCA100RFA100SF0	60	1686.6	1843.4	1968.8	2219.3	2516.3
40	0.3RCA100RFA100SF10	60	1719.1	1876.0	2001.3	2251.8	2548.8
41	0.43RCA0RFA0SF0	60	1881.5	2038.2	2163.5	2413.8	2710.7
42	0.43RCA0RFA0SF10	60	1959.3	2115.9	2241.2	2491.4	2788.1
43	0.43RCA100RFA0SF0	60	1679.0	1835.9	1961.3	2211.8	2508.9
44	0.43RCA100RFA0SF10	60	1828.2	1985.0	2110.3	2360.6	2657.5
45	0.43RCA0RFA100SF0	60	1508.4	1665.3	1790.8	2041.5	2338.8
46	0.43RCA0RFA100SF10	60	1772.8	1929.5	2054.9	2305.3	2602.3
47	0.43RCA100RFA100SF0	60	1458.1	1615.1	1740.7	1991.4	2288.8
48	0.43RCA100RFA100SF10	60	1611.3	1768.2	1893.6	2144.2	2441.3
49	0.3RCA0RFA0SF0	80	3544.3	3755.7	3924.7	4262.5	4663.3
50	0.3RCA0RFA0SF10	80	3658.2	3867.3	4034.4	4368.4	4764.3
51	0.3RCA100RFA0SF0	80	3139.7	3349.2	3516.7	3851.3	4248.0
52	0.3RCA100RFA0SF10	80	3198.7	3408.2	3575.6	3910.1	4306.8
53	0.3RCA0RFA100SF0	80	2965.5	3175.2	3342.8	3677.7	4074.6
54	0.3RCA0RFA100SF10	80	3058.4	3268.0	3435.5	3770.2	4167.1
55	0.3RCA100RFA100SF0	80	2777.0	2986.8	3154.6	3489.7	3886.9
56	0.3RCA100RFA100SF10	80	2835.9	3045.7	3213.4	3548.4	3945.6
57	0.43RCA0RFA0SF0	80	3129.4	3339.0	3506.5	3841.1	4237.8
58	0.43RCA0RFA0SF10	80	3270.0	3479.4	3646.8	3981.2	4377.8
59	0.43RCA100RFA0SF0	80	2763.4	2973.3	3141.0	3476.1	3873.4
60	0.43RCA100RFA0SF10	80	3033.1	3242.7	3410.3	3745.0	4141.9
61	0.43RCA0RFA100SF0	80	2454.9	2665.1	2833.1	3168.6	3566.4
62	0.43RCA0RFA100SF10	80	2932.8	3142.5	3310.2	3645.0	4042.1
63	0.43RCA100RFA100SF0	80	2364.1	2574.4	2742.4	3078.1	3476.0
64	0.43RCA100RFA100SF10	80	2640.9	2850.9	3018.7	3354.0	3751.5
65	0.3RCA0RFA0SF0	100	5344.8	5611.1	5824.0	6249.6	6754.7
66	0.3RCA0RFA0SF10	100	5536.7	5803.0	6015.8	6441.3	6946.3
67	0.3RCA100RFA0SF0	100	4717.0	4983.6	5196.8	5622.8	6128.4

	68	0.3RCA100RFA0SF10	100	4810.2	5076.8	5289.9	5715.9	6221.4
	69	0.3RCA0RFA100SF0	100	4441.6	4708.3	4921.6	5347.8	5853.6
	70	0.3RCA0RFA100SF10	100	4588.4	4855.1	5068.3	5494.5	6000.1
	71	0.3RCA100RFA100SF0	100	4143.4	4410.3	4623.7	5050.2	5556.2
	72	0.3RCA100RFA100SF10	100	4236.6	4503.4	4716.8	5143.2	5649.1
	73	0.43RCA0RFA0SF0	100	4700.8	4967.4	5180.5	5606.6	6112.2
	74	0.43RCA0RFA0SF10	100	4923.0	5189.5	5402.6	5828.5	6333.9
	75	0.43RCA100RFA0SF0	100	4122.0	4388.8	4602.2	5028.7	5534.8
	76	0.43RCA100RFA0SF10	100	4548.4	4815.0	5028.3	5454.5	5960.1
	77	0.43RCA0RFA100SF0	100	3634.1	3901.2	4114.8	4541.7	5048.2
	78	0.43RCA0RFA100SF10	100	4389.9	4656.6	4869.9	5296.2	5802.0
	79	0.43RCA100RFA100SF0	100	3490.5	3757.7	3971.4	4398.4	4904.9
	80	0.43RCA100RFA100SF10	100	3928.2	4195.2	4408.7	4835.3	5341.5
ACI-318	81	0.3RCA0RFA0SF0	20	224.4	251.2	272.7	315.7	366.7
	82	0.3RCA0RFA0SF10	20	229.9	256.7	278.2	321.2	372.2
	83	0.3RCA100RFA0SF0	20	206.3	233.2	254.7	297.7	348.7
	84	0.3RCA100RFA0SF10	20	209.0	235.9	257.4	300.3	351.4
	85	0.3RCA0RFA100SF0	20	198.4	225.3	246.8	289.7	340.8
	86	0.3RCA0RFA100SF10	20	202.6	229.5	251.0	294.0	345.0
	87	0.3RCA100RFA100SF0	20	189.8	216.7	238.2	281.2	332.2
	88	0.3RCA100RFA100SF10	20	192.5	219.4	240.9	283.8	334.9
	89	0.43RCA0RFA0SF0	20	205.9	232.7	254.2	297.2	348.2
	90	0.43RCA0RFA0SF10	20	212.2	239.1	260.6	303.6	354.6
	91	0.43RCA100RFA0SF0	20	189.2	216.1	237.6	280.6	331.6
	92	0.43RCA100RFA0SF10	20	201.5	228.3	249.8	292.8	343.8
	93	0.43RCA0RFA100SF0	20	175.2	202.1	223.6	266.5	317.6
	94	0.43RCA0RFA100SF10	20	196.9	223.8	245.3	288.3	339.3
	95	0.43RCA100RFA100SF0	20	171.1	197.9	219.4	262.4	313.4
	96	0.43RCA100RFA100SF10	20	183.7	210.5	232.0	275.0	326.0
	97	0.3RCA0RFA0SF0	40	761.0	816.1	860.2	948.4	1053.2
	98	0.3RCA0RFA0SF10	40	785.6	840.7	884.8	973.0	1077.8
	99	0.3RCA100RFA0SF0	40	680.6	735.8	779.9	868.1	972.8
	100	0.3RCA100RFA0SF10	40	692.6	747.7	791.8	880.0	984.8
	101	0.3RCA0RFA100SF0	40	645.4	700.5	744.6	832.8	937.6
	102	0.3RCA0RFA100SF10	40	664.2	719.3	763.4	851.6	956.4
	103	0.3RCA100RFA100SF0	40	607.2	662.3	706.4	794.6	899.4
	104	0.3RCA100RFA100SF10	40	619.1	674.2	718.3	806.6	911.3

105	0.43RCA0RFA0SF0	40	678.5	733.7	777.8	866.0	970.8
106	0.43RCA0RFA0SF10	40	707.0	762.1	806.2	894.4	999.2
107	0.43RCA100RFA0SF0	40	604.4	659.6	703.7	791.9	896.6
108	0.43RCA100RFA0SF10	40	659.0	714.2	758.3	846.5	951.2
109	0.43RCA0RFA100SF0	40	541.9	597.1	641.2	729.4	834.2
110	0.43RCA0RFA100SF10	40	638.7	693.9	738.0	826.2	930.9
111	0.43RCA100RFA100SF0	40	523.6	578.7	622.8	711.0	815.8
112	0.43RCA100RFA100SF10	40	579.6	634.7	678.9	767.1	871.8
113	0.3RCA0RFA0SF0	60	1606.2	1689.6	1756.3	1889.8	2048.3
114	0.3RCA0RFA0SF10	60	1663.5	1746.9	1813.6	1947.1	2105.5
115	0.3RCA100RFA0SF0	60	1419.0	1502.4	1569.1	1702.6	1861.0
116	0.3RCA100RFA0SF10	60	1446.8	1530.2	1596.9	1730.4	1888.8
117	0.3RCA0RFA100SF0	60	1336.8	1420.2	1486.9	1620.4	1778.9
118	0.3RCA0RFA100SF10	60	1380.6	1464.0	1530.7	1664.2	1822.7
119	0.3RCA100RFA100SF0	60	1247.9	1331.3	1398.0	1531.4	1689.9
120	0.3RCA100RFA100SF10	60	1275.7	1359.1	1425.8	1559.2	1717.7
121	0.43RCA0RFA0SF0	60	1414.1	1497.5	1564.3	1697.7	1856.2
122	0.43RCA0RFA0SF10	60	1480.4	1563.8	1630.5	1764.0	1922.5
123	0.43RCA100RFA0SF0	60	1241.5	1324.9	1391.6	1525.0	1683.5
124	0.43RCA100RFA0SF10	60	1368.7	1452.1	1518.8	1652.3	1810.7
125	0.43RCA0RFA100SF0	60	1095.9	1179.3	1246.0	1379.5	1538.0
126	0.43RCA0RFA100SF10	60	1321.4	1404.8	1471.5	1605.0	1763.4
127	0.43RCA100RFA100SF0	60	1053.1	1136.5	1203.2	1336.6	1495.1
128	0.43RCA100RFA100SF10	60	1183.7	1267.1	1333.8	1467.2	1625.7
129	0.3RCA0RFA0SF0	80	2760.0	2871.7	2961.0	3139.7	3351.9
130	0.3RCA0RFA0SF10	80	2863.6	2975.3	3064.6	3243.3	3455.5
131	0.3RCA100RFA0SF0	80	2421.4	2533.1	2622.4	2801.1	3013.3
132	0.3RCA100RFA0SF10	80	2471.7	2583.4	2672.7	2851.4	3063.6
133	0.3RCA0RFA100SF0	80	2272.8	2384.5	2473.8	2652.5	2864.7
134	0.3RCA0RFA100SF10	80	2352.0	2463.7	2553.0	2731.7	2943.9
135	0.3RCA100RFA100SF0	80	2111.9	2223.6	2312.9	2491.6	2703.8
136	0.3RCA100RFA100SF10	80	2162.2	2273.9	2363.2	2541.9	2754.1
137	0.43RCA0RFA0SF0	80	2412.6	2524.3	2613.6	2792.3	3004.5
138	0.43RCA0RFA0SF10	80	2532.5	2644.2	2733.5	2912.2	3124.4
139	0.43RCA100RFA0SF0	80	2100.3	2212.0	2301.4	2480.1	2692.3
140	0.43RCA100RFA0SF10	80	2330.4	2442.1	2531.4	2710.1	2922.3
141	0.43RCA0RFA100SF0	80	1837.1	1948.8	2038.1	2216.8	2429.0

	142	0.43RCA0RFA100SF10	80	2244.9	2356.6	2445.9	2624.6	2836.8
	143	0.43RCA100RFA100SF0	80	1759.6	1871.3	1960.6	2139.3	2351.5
	144	0.43RCA100RFA100SF10	80	1995.8	2107.5	2196.8	2375.5	2587.7
	145	0.3RCA0RFA0SF0	100	4222.4	4362.4	4474.3	4698.3	4964.2
	146	0.3RCA0RFA0SF10	100	4385.9	4525.8	4637.8	4861.7	5127.6
	147	0.3RCA100RFA0SF0	100	3687.8	3827.8	3939.8	4163.7	4429.6
	148	0.3RCA100RFA0SF10	100	3767.2	3907.2	4019.2	4243.1	4509.0
	149	0.3RCA0RFA100SF0	100	3453.3	3593.2	3705.2	3929.1	4195.0
	150	0.3RCA0RFA100SF10	100	3578.3	3718.3	3830.3	4054.2	4320.1
	151	0.3RCA100RFA100SF0	100	3199.3	3339.3	3451.3	3675.2	3941.1
	152	0.3RCA100RFA100SF10	100	3278.7	3418.6	3530.6	3754.5	4020.4
	153	0.43RCA0RFA0SF0	100	3674.0	3814.0	3925.9	4149.9	4415.8
	154	0.43RCA0RFA0SF10	100	3863.3	4003.2	4115.2	4339.1	4605.0
	155	0.43RCA100RFA0SF0	100	3181.1	3321.0	3433.0	3656.9	3922.8
	156	0.43RCA100RFA0SF10	100	3544.2	3684.2	3796.2	4020.1	4286.0
	157	0.43RCA0RFA100SF0	100	2765.5	2905.5	3017.4	3241.3	3507.3
	158	0.43RCA0RFA100SF10	100	3409.2	3549.2	3661.1	3885.1	4151.0
	159	0.43RCA100RFA100SF0	100	2643.2	2783.1	2895.1	3119.0	3384.9
	160	0.43RCA100RFA100SF10	100	3016.0	3156.0	3268.0	3491.9	3757.8
AIJ, 1999	161	0.3RCA0RFA0SF0	20	251.2	285.3	312.6	367.2	432.0
	162	0.3RCA0RFA0SF10	20	256.7	290.8	318.1	372.7	437.5
	163	0.3RCA100RFA0SF0	20	233.2	267.3	294.6	349.1	414.0
	164	0.3RCA100RFA0SF10	20	235.8	270.0	297.2	351.8	416.6
	165	0.3RCA0RFA100SF0	20	225.2	259.4	286.7	341.2	406.0
	166	0.3RCA0RFA100SF10	20	229.5	263.6	290.9	345.4	410.3
	167	0.3RCA100RFA100SF0	20	216.7	250.8	278.1	332.7	397.5
	168	0.3RCA100RFA100SF10	20	219.4	253.5	280.8	335.3	400.2
	169	0.43RCA0RFA0SF0	20	232.7	266.8	294.1	348.7	413.5
	170	0.43RCA0RFA0SF10	20	239.1	273.2	300.5	355.1	419.9
	171	0.43RCA100RFA0SF0	20	216.1	250.2	277.5	332.0	396.9
	172	0.43RCA100RFA0SF10	20	228.3	262.4	289.7	344.3	409.1
	173	0.43RCA0RFA100SF0	20	202.0	236.2	263.4	318.0	382.8
	174	0.43RCA0RFA100SF10	20	223.8	257.9	285.2	339.7	404.6
	175	0.43RCA100RFA100SF0	20	197.9	232.0	259.3	313.9	378.7
	176	0.43RCA100RFA100SF10	20	210.5	244.6	271.9	326.5	391.3
	177	0.3RCA0RFA0SF0	40	816.1	886.1	942.1	1054.1	1187.2
	178	0.3RCA0RFA0SF10	40	840.7	910.7	966.7	1078.7	1211.8

179	0.3RCA100RFA0SF0	40	735.7	805.7	861.7	973.8	1106.8
180	0.3RCA100RFA0SF10	40	747.6	817.7	873.7	985.7	1118.7
181	0.3RCA0RFA100SF0	40	700.4	770.5	826.5	938.5	1071.5
182	0.3RCA0RFA100SF10	40	719.2	789.3	845.3	957.3	1090.3
183	0.3RCA100RFA100SF0	40	662.3	732.3	788.3	900.3	1033.4
184	0.3RCA100RFA100SF10	40	674.2	744.2	800.2	912.2	1045.3
185	0.43RCA0RFA0SF0	40	733.6	803.6	859.7	971.7	1104.7
186	0.43RCA0RFA0SF10	40	762.1	832.1	888.1	1000.1	1133.2
187	0.43RCA100RFA0SF0	40	659.5	729.5	785.5	897.6	1030.6
188	0.43RCA100RFA0SF10	40	714.1	784.1	840.1	952.2	1085.2
189	0.43RCA0RFA100SF0	40	597.0	667.0	723.1	835.1	968.1
190	0.43RCA0RFA100SF10	40	693.8	763.8	819.8	931.9	1064.9
191	0.43RCA100RFA100SF0	40	578.6	648.6	704.7	816.7	949.7
192	0.43RCA100RFA100SF10	40	634.7	704.7	760.7	872.8	1005.8
193	0.3RCA0RFA0SF0	60	1689.5	1795.5	1880.2	2049.7	2250.9
194	0.3RCA0RFA0SF10	60	1746.8	1852.7	1937.5	2106.9	2308.2
195	0.3RCA100RFA0SF0	60	1502.3	1608.2	1693.0	1862.4	2063.7
196	0.3RCA100RFA0SF10	60	1530.1	1636.0	1720.8	1890.3	2091.5
197	0.3RCA0RFA100SF0	60	1420.1	1526.1	1610.8	1780.3	1981.5
198	0.3RCA0RFA100SF10	60	1463.9	1569.9	1654.6	1824.1	2025.4
199	0.3RCA100RFA100SF0	60	1331.2	1437.1	1521.9	1691.3	1892.6
200	0.3RCA100RFA100SF10	60	1359.0	1464.9	1549.6	1719.1	1920.4
201	0.43RCA0RFA0SF0	60	1497.5	1603.4	1688.1	1857.6	2058.9
202	0.43RCA0RFA0SF10	60	1563.7	1669.7	1754.4	1923.9	2125.1
203	0.43RCA100RFA0SF0	60	1324.8	1430.7	1515.5	1684.9	1886.2
204	0.43RCA100RFA0SF10	60	1452.0	1557.9	1642.7	1812.1	2013.4
205	0.43RCA0RFA100SF0	60	1179.2	1285.2	1369.9	1539.4	1740.6
206	0.43RCA0RFA100SF10	60	1404.7	1510.6	1595.4	1764.9	1966.1
207	0.43RCA100RFA100SF0	60	1136.4	1242.3	1327.0	1496.5	1697.8
208	0.43RCA100RFA100SF10	60	1267.0	1372.9	1457.7	1627.1	1828.4
209	0.3RCA0RFA0SF0	80	2871.6	3013.4	3126.9	3353.8	3623.3
210	0.3RCA0RFA0SF10	80	2975.1	3117.0	3230.4	3457.4	3726.9
211	0.3RCA100RFA0SF0	80	2532.9	2674.8	2788.2	3015.2	3284.7
212	0.3RCA100RFA0SF10	80	2583.2	2725.1	2838.5	3065.5	3335.0
213	0.3RCA0RFA100SF0	80	2384.4	2526.2	2639.7	2866.6	3136.1
214	0.3RCA0RFA100SF10	80	2463.6	2605.4	2718.9	2945.8	3215.3
215	0.3RCA100RFA100SF0	80	2223.5	2365.3	2478.8	2705.7	2975.2

	216	0.3RCA100RFA100SF10	80	2273.8	2415.6	2529.1	2756.0	3025.5
	217	0.43RCA0RFA0SF0	80	2524.2	2666.0	2779.5	3006.4	3275.9
	218	0.43RCA0RFA0SF10	80	2644.1	2785.9	2899.4	3126.3	3395.8
	219	0.43RCA100RFA0SF0	80	2211.9	2353.7	2467.2	2694.1	2963.6
	220	0.43RCA100RFA0SF10	80	2442.0	2583.8	2697.3	2924.2	3193.7
	221	0.43RCA0RFA100SF0	80	1948.7	2090.5	2204.0	2430.9	2700.4
	222	0.43RCA0RFA100SF10	80	2356.5	2498.3	2611.8	2838.7	3108.2
	223	0.43RCA100RFA100SF0	80	1871.2	2013.0	2126.5	2353.4	2622.9
	224	0.43RCA100RFA100SF10	80	2107.4	2249.2	2362.7	2589.6	2859.1
	225	0.3RCA0RFA0SF0	100	4362.2	4540.0	4682.2	4966.5	5304.3
	226	0.3RCA0RFA0SF10	100	4525.7	4703.4	4845.6	5130.0	5467.7
	227	0.3RCA100RFA0SF0	100	3827.7	4005.4	4147.6	4432.0	4769.7
	228	0.3RCA100RFA0SF10	100	3907.1	4084.8	4227.0	4511.4	4849.1
	229	0.3RCA0RFA100SF0	100	3593.1	3770.8	3913.0	4197.4	4535.1
	230	0.3RCA0RFA100SF10	100	3718.2	3895.9	4038.1	4322.5	4660.2
	231	0.3RCA100RFA100SF0	100	3339.2	3516.9	3659.1	3943.5	4281.2
	232	0.3RCA100RFA100SF10	100	3418.5	3596.2	3738.4	4022.8	4360.5
	233	0.43RCA0RFA0SF0	100	3813.8	3991.6	4133.8	4418.2	4755.9
	234	0.43RCA0RFA0SF10	100	4003.1	4180.8	4323.0	4607.4	4945.1
	235	0.43RCA100RFA0SF0	100	3320.9	3498.6	3640.8	3925.2	4262.9
	236	0.43RCA100RFA0SF10	100	3684.0	3861.8	4004.0	4288.4	4626.1
	237	0.43RCA0RFA100SF0	100	2905.3	3083.1	3225.3	3509.6	3847.3
	238	0.43RCA0RFA100SF10	100	3549.0	3726.8	3869.0	4153.4	4491.1
	239	0.43RCA100RFA100SF0	100	2783.0	2960.7	3102.9	3387.3	3725.0
	240	0.43RCA100RFA100SF10	100	3155.9	3333.6	3475.8	3760.2	4097.9
DL/T	241	0.3RCA0RFA0SF0	20	291.0	318.7	340.1	380.7	425.3
	242	0.3RCA0RFA0SF10	20	298.8	326.4	347.7	388.1	432.5
	243	0.3RCA100RFA0SF0	20	270.1	298.1	319.7	361.0	406.5
	244	0.3RCA100RFA0SF10	20	274.0	301.9	323.4	364.6	410.0
	245	0.3RCA0RFA100SF0	20	255.1	283.3	305.2	347.0	393.4
	246	0.3RCA0RFA100SF10	20	261.0	289.1	310.9	352.5	398.5
	247	0.3RCA100RFA100SF0	20	241.3	269.8	291.9	334.4	381.8
	248	0.3RCA100RFA100SF10	20	245.0	273.3	295.4	337.7	384.8
	249	0.43RCA0RFA0SF0	20	265.5	293.6	315.3	356.7	402.5
	250	0.43RCA0RFA0SF10	20	278.6	306.5	328.0	369.0	414.2
	251	0.43RCA100RFA0SF0	20	240.4	268.9	291.1	333.6	381.1
	252	0.43RCA100RFA0SF10	20	259.4	287.5	309.3	351.0	397.1

253	0.43RCA0RFA100SF0	20	225.7	254.6	277.1	320.5	369.3
254	0.43RCA0RFA100SF10	20	253.0	281.3	303.2	345.1	391.7
255	0.43RCA100RFA100SF0	20	219.9	248.9	271.6	315.5	365.0
256	0.43RCA100RFA100SF10	20	235.0	263.6	285.9	328.7	376.7
257	0.3RCA0RFA0SF0	40	946.7	1012.6	1066.5	1177.2	1313.8
258	0.3RCA0RFA0SF10	40	978.1	1044.0	1097.8	1208.4	1344.7
259	0.3RCA100RFA0SF0	40	861.7	927.9	982.0	1093.2	1230.6
260	0.3RCA100RFA0SF10	40	877.4	943.6	997.6	1108.7	1246.0
261	0.3RCA0RFA100SF0	40	800.5	866.9	921.2	1032.9	1171.0
262	0.3RCA0RFA100SF10	40	824.6	890.9	945.1	1056.6	1194.4
263	0.3RCA100RFA100SF0	40	743.8	810.5	865.0	977.2	1116.2
264	0.3RCA100RFA100SF10	40	758.9	825.4	879.9	992.0	1130.7
265	0.43RCA0RFA0SF0	40	843.1	909.3	963.5	1074.8	1212.4
266	0.43RCA0RFA0SF10	40	896.4	962.5	1016.5	1127.5	1264.6
267	0.43RCA100RFA0SF0	40	740.4	807.0	861.5	973.8	1112.9
268	0.43RCA100RFA0SF10	40	818.0	884.4	938.6	1050.2	1188.0
269	0.43RCA0RFA100SF0	40	679.5	746.4	801.2	914.3	1054.5
270	0.43RCA0RFA100SF10	40	792.0	858.4	912.7	1024.5	1162.8
271	0.43RCA100RFA100SF0	40	655.4	722.5	777.4	890.9	1031.6
272	0.43RCA100RFA100SF10	40	718.0	784.7	839.3	951.9	1091.3
273	0.3RCA0RFA0SF0	60	1958.6	2061.6	2146.6	2324.0	2547.4
274	0.3RCA0RFA0SF10	60	2029.6	2132.5	2217.5	2394.7	2617.8
275	0.3RCA100RFA0SF0	60	1767.0	1870.1	1955.4	2133.3	2357.4
276	0.3RCA100RFA0SF10	60	1802.5	1905.6	1990.8	2168.6	2392.6
277	0.3RCA0RFA100SF0	60	1628.9	1732.2	1817.6	1996.0	2220.8
278	0.3RCA0RFA100SF10	60	1683.3	1786.5	1871.9	2050.1	2274.6
279	0.3RCA100RFA100SF0	60	1500.9	1604.4	1690.1	1869.0	2094.6
280	0.3RCA100RFA100SF10	60	1534.9	1638.4	1724.0	1902.7	2128.1
281	0.43RCA0RFA0SF0	60	1725.0	1828.1	1913.4	2091.5	2315.8
282	0.43RCA0RFA0SF10	60	1845.4	1948.4	2033.6	2211.3	2435.1
283	0.43RCA100RFA0SF0	60	1493.1	1596.6	1682.3	1861.3	2086.9
284	0.43RCA100RFA0SF10	60	1668.5	1771.7	1857.1	2035.4	2259.9
285	0.43RCA0RFA100SF0	60	1355.3	1459.2	1545.2	1724.8	1951.5
286	0.43RCA0RFA100SF10	60	1609.7	1713.1	1798.5	1977.0	2201.9
287	0.43RCA100RFA100SF0	60	1300.8	1404.8	1490.9	1670.9	1898.2
288	0.43RCA100RFA100SF10	60	1442.4	1546.1	1631.8	1811.0	2037.0
289	0.3RCA0RFA0SF0	80	3328.3	3467.9	3583.8	3827.3	4136.3

290	0.3RCA0RFA0SF10	80	3454.6	3594.1	3710.0	3953.3	4262.0
291	0.3RCA100RFA0SF0	80	2987.3	3127.1	3243.3	3487.2	3797.0
292	0.3RCA100RFA0SF10	80	3050.5	3190.2	3306.3	3550.2	3859.7
293	0.3RCA0RFA100SF0	80	2741.5	2881.5	2997.8	3242.2	3552.6
294	0.3RCA0RFA100SF10	80	2838.4	2978.3	3094.5	3338.7	3648.9
295	0.3RCA100RFA100SF0	80	2513.7	2653.9	2770.5	3015.4	3326.5
296	0.3RCA100RFA100SF10	80	2574.3	2714.4	2830.9	3075.6	3386.6
297	0.43RCA0RFA0SF0	80	2912.5	3052.3	3168.5	3412.6	3722.5
298	0.43RCA0RFA0SF10	80	3126.8	3266.5	3382.6	3626.3	3935.7
299	0.43RCA100RFA0SF0	80	2499.8	2640.0	2756.6	3001.5	3312.7
300	0.43RCA100RFA0SF10	80	2812.0	2951.9	3068.2	3312.4	3622.6
301	0.43RCA0RFA100SF0	80	2254.5	2395.0	2511.9	2757.5	3069.8
302	0.43RCA0RFA100SF10	80	2707.4	2847.4	2963.8	3208.2	3518.7
303	0.43RCA100RFA100SF0	80	2157.4	2298.0	2415.0	2661.0	2973.8
304	0.43RCA100RFA100SF10	80	2409.6	2549.9	2666.6	2911.7	3223.3
305	0.3RCA0RFA0SF0	100	5055.8	5231.9	5378.7	5687.9	6082.2
306	0.3RCA0RFA0SF10	100	5253.1	5429.2	5575.9	5885.0	6279.0
307	0.3RCA100RFA0SF0	100	4522.9	4699.2	4846.2	5155.9	5550.9
308	0.3RCA100RFA0SF10	100	4621.5	4797.8	4944.8	5254.4	5649.2
309	0.3RCA0RFA100SF0	100	4138.6	4315.1	4462.3	4772.4	5168.1
310	0.3RCA0RFA100SF10	100	4290.0	4466.5	4613.5	4923.5	5318.8
311	0.3RCA100RFA100SF0	100	3782.5	3959.2	4106.6	4417.2	4813.6
312	0.3RCA100RFA100SF10	100	3877.1	4053.8	4201.1	4511.6	4907.7
313	0.43RCA0RFA0SF0	100	4405.9	4582.3	4729.3	5039.1	5434.3
314	0.43RCA0RFA0SF10	100	4740.9	4917.1	5064.0	5373.5	5768.1
315	0.43RCA100RFA0SF0	100	3760.7	3937.5	4084.8	4395.5	4791.9
316	0.43RCA100RFA0SF10	100	4248.7	4425.2	4572.3	4882.3	5277.7
317	0.43RCA0RFA100SF0	100	3377.2	3554.2	3701.9	4013.2	4410.7
318	0.43RCA0RFA100SF10	100	4085.3	4261.8	4409.0	4719.2	5114.9
319	0.43RCA100RFA100SF0	100	3225.3	3402.5	3550.2	3861.9	4259.9
320	0.43RCA100RFA100SF10	100	3619.7	3796.5	3944.0	4254.9	4651.7

PERSONAL INFORMATION

Name, Middle, Surname	Ihsan Taha KADHIM
Academic Degree	Assistant Researcher
Department	Department of Civil Engineering
Institution	Gaziantep University, Gaziantep, Turkey University of Technology, Baghdad, Iraq
Nationality	Iraqi
Birth place and date	Baghdad/1974
Social status	Married
Mobile number	+90 5432001916 in Turkey
E-mail	ihsantahak@yahoo.com ihsantahak@gmail.com

HIGH EDUCATION

Degree	**Graduate School**	**Year**
Master Degree	University of technology/ Baghdad	2007
High Diploma	University of technology/ Baghdad	2000
Bachelor of Science	University of technology/ Baghdad	1996
High School	Al-Ameen High School / Baghdad	1991

LANGUAGES

Language	**Level**
Arabic	Native language
English	Advance
Turkish	Moderate

SKILLS and EXPERIENCE

Year	**Place**	**Enrollment**
2001-2012	Baghdad Municipality	Head of engineering department
2000-2001	Free Business	Civil engineer in construction field
1997-1999	Military projects Authority	Civil engineer in construction field

PUBLICATIONS and SCIENTIFIC EFFORTS

A. Journals

Gesoglu, M. Güneyisi, E. Öz, H. Yasemin, M. **Taha I**., Durability and Shrinkage Characteristics of Self-Compacting Concretes Containing Recycled Coarse and/or Fine Aggregates- Advances in Materials Science and Engineering Volume 2015, Article ID 278296, 18 pages.

Gesoglu, M. Güneyisi, E. Öz, H. Yasemin, M. **Taha I**., Failure characteristics of self-compacting concretes made with recycled aggregates- Construction and Building Materials 98 (2015) 334–344.

Güneyisi, E., Gesoglu, M., Ghanim H., Ipek S., **Taha I**., Influence of the artificial lightweight aggregate on fresh properties and compressive strength of the self-compacting mortars- Construction and Building Materials 116 (2016) 151–158.

B. Educational Thesis

Taha I. (2007) Using of crushed brick waste to produce paving units for Baghdad municipality projects- MSc Thesis. University of technology Baghdad- Iraq.

C. Conference and Symposium

Taha I. (2012). Using of building waste to produce paving units for Baghdad municipality projects. Comprehensive Engineering Conference for university thesis Researches. AL-Mustansiriyah University , Baghdad- Iraq.

D. Workshops

Training program of Housing and Urban Services Maintenance Workshop (2005). Nations Human Settlements Programme (UN-HABITAT), Sharm El Sheikh, Egypt.